Tampere University

SANNA-KAISA HARJULA

Zebrafish as a Genetic Model to Study Tuberculosis

Tampere University Dissertations 265

Tampere University Dissertations 265

SANNA-KAISA HARJULA

Zebrafish as a Genetic Model to Study Tuberculosis

ACADEMIC DISSERTATION
To be presented, with the permission of
the Faculty of Medicine and Health Technology
of Tampere University,
for public discussion in the auditorium F114
of the Arvo building, Arvo Ylpön katu 34, Tampere,
on 9 October 2020, at 12 o'clock.

ACADEMIC DISSERTATION
Tampere University, Faculty of Medicine and Health Technology
Finland

Responsible supervisor and Custos	Professor Mika Rämet Tampere University Finland	
Supervisor	Docent Mataleena Parikka Tampere University Finland	
Pre-examiners	Docent Maija Hollmén University of Turku Finland	Docent Eliisa Kekäläinen University of Helsinki Finland
Opponent	Professor Annemarie Meijer Leiden University The Netherlands	

The originality of this thesis has been checked using the Turnitin OriginalityCheck service.

Cover design: Roihu Inc.

ISBN 978-952-03-1588-7 (print)
ISBN 978-952-03-1589-4 (pdf)
ISSN 2489-9860 (print)
ISSN 2490-0028 (pdf)
http://urn.fi/URN:ISBN:978-952-03-1589-4

PunaMusta Oy – Yliopistopaino
Tampere 2020

ACKNOWLEDGEMENTS

This Doctoral thesis was carried out in the Experimental Immunology Research Group in the Faculty of Medicine and Health Technology at the Tampere University.

First, I would like to express my greatest gratitude to my supervisors Professor Mika Rämet and Docent Mataleena Parikka. I would like to thank you Mika for taking me to work as a summer student in your lab and for giving me the possibility to do this thesis during all these years, for all the guidance you have given but also for encouraging me to gain independence as a researcher by trusting my decisions. Thank you Mataleena for your help, enthusiasm, and expertise during this thesis work, especially during the writing process.

I want to thank the pre-examiners of this thesis, Docent Maija Hollmén from the University of Turku and Docent Eliisa Kekäläinen from the University of Helsinki, for their valuable comments and positive feedback. I also acknowledge Professor Annemarie Meijer from the Leiden University for acting as my opponent in the future dissertation. I thank my thesis committee members, Professor Marko Pesu and Docent Olli Lohi for their comments, ideas and encouraging words during these years. Eloise Mikkonen is acknowledged for proof-reading this thesis and Heini Huhtala for all the statistical advice she has given me during the years.

Next, I want to express my deepest gratitude to all the former and present members of the Experimental Immunology Research Group. I would like to thank Dr. Anni Saralahti for working with me as a fellow PhD student all these years with our large project with enthusiasm and for being such a great friend and colleague. I would also like to thank Dr. Markus Ojanen, another fellow PhD student, especially for his help with manuscripts and never-ending optimism. I would also like to thank all the other PhD students and post-docs of our lab for their help and for sharing the ups and downs of the research work: Dr. Leena-Maija Vanha-aho, Mirja Niskanen, Meri Uusi-Mäkelä, Mirva Järvelä-Stölting, Kaisa Oksanen, Dr. Carina Bäuerlein, Dr. Henna Myllymäki and Dr. Laura Vesala. Special thanks go to Dr. Susanna Valanne for being my first supervisor in the lab. I would especially like to thank Leena Mäkinen, Hannaleena Piippo, Jenna Ilomäki, Tuula Myllymäki, Matilda Salminen and Annemari Uusimäki for all their work for this project as well as several students, especially Heather Baird and Nicholas Halfpenny who were always ready

to do any work that needed to be done. I would also like to acknowledge the colleagues in Mataleena's group, especially Dr. Milka Hammarén for her work with the *Mycobacterium marinum* zebrafish model and Hanna Luukinen for all the discussions over the lunches and lab work.

Next, I would like to thank all my other co-authors. Special thanks to Marika Koivisto (nèe Lahtinen) for her work with histology and for being such a great person to work with and to Professor Matti Nykter's Group, to Tommi Rantapero for extensive data analysis during this project and to Sinja Taavitsainen for helping on such a short notice with sequencing data analysis. Thank you also all the other people in our faculty that I have had the honor to work with and who have been helping me along the way. I would also like to thank all the people working in the Tampere Zebrafish Laboratory at the BioMediTech, Tampere University, partly funded by Biocenter Finland, for making zebrafish research possible in our university. Tampere Imaging, NGS & Sanger Sequencing, Fragment Analyzer and Histology Facilities at the BioMediTech are also acknowledged for their services.

Next I want to acknowledge the following organizations for supporting this thesis project financially: the Tampere Tuberculosis Foundation, the University of Tampere Foundation, the Emil Aaltonen Foundation, Foundation of the Finnish Anti-Tuberculosis Association, the City of Tampere Science Foundation, the Väinö and Laina Kivi Foundation, the Finnish Cultural Foundation, the Central Fund, the Finnish Concordia Fund, Orion Research Foundation, the Academy of Finland (PROFI4-project at the University of Tampere) and the Finnish Society for Study of Infectious Diseases. I would also like to acknowledge Tampere University Doctoral Programme in Medicine and Life Sciences for financing conference trips and for providing such a good setting for postgraduate studies.

Last but not the least I would like to express my warmest gratitude to my family and friends for reminding me about the life outside the lab. Kiitokset vanhemmilleni Riitta-Liisa ja Antti Harjulalle kaikesta avusta ja loppumattomasta kannustuksesta ja kiinnostuksesta työhöni. Kiitokset siskolleni Riikka Koholle sekä siskontytöille Suville ja Sonjalle kaikesta tuesta ja hyvästä seurasta. Kiitokset Terhi Hakalalle "maailmaaparantavista" (lenkki)kahveista sekä Marjatta ja Esko Nikkilälle ystävällisyydestänne. Suuri kiitos puolisolleni Antti-Juhani Nikkilälle kaikesta avusta, kärsivällisyydestä ja kannustuksesta näiden vuosien aikana sekä pojallemme Onnille.

Tampere, April 2020

Sanna-Kaisa Harjula

ABSTRACT

Tuberculosis is still a major global health issue, with 10 million new cases and over one million casualties each year. Tuberculosis is caused by *M. tuberculosis*, which spreads via airways. This infection may result in a wide spectrum of outcomes, from an asymptomatic latent state to active disease. Due to the insufficiency of current treatments, new approaches to combat tuberculosis are needed. Host genetics has been shown to affect the outcome of *M. tuberculosis* infection. Therefore, screening the effect of different genetic variations of the host on the progression of mycobacterial infection provides information useful for developing new treatments. Moreover, the research on tuberculosis has been impeded by the lack of good animal models that mimic the progression of tuberculosis and are still feasible to use whilst meeting ethical challenges.

The zebrafish has become more and more popular as an immunological research model. There are various tools available to carry out both forward and reverse genetic modifications in the zebrafish. Moreover, *Mycobacterium marinum* is a close relative of *M. tuberculosis* and a natural zebrafish pathogen. It causes a systemic infection in zebrafish. The *M. marinum* infection in zebrafish larvae is an especially well-established tuberculosis model. Thus our group considered the *M. marinum* infection in adult zebrafish as an advantageous tuberculosis model. The first aim of this thesis was to study the progression of *M. marinum* infection in adult zebrafish with histological methods and transcriptional analysis. The second aim was to study the role of *interleukin 10* (*il10*) during this infection. The final aim was to perform a forward genetic screen to identify host genes having a role in the defense against mycobacterial infection in zebrafish.

To reach the first aim, we used Ziehl-Neelsen staining to identify *M. marinum* in longitudinal tissue sections taken from adult zebrafish at different time-points of the infection. Importantly, analysis showed that in low-dose *M. marinum* infection, the number of granulomas and affected organs remained stable from four weeks post infection onwards, whereas in a high-dose infection the number of affected organs was higher and granuloma numbers kept rising along the course of infection. To further characterize the immune response to *M. marinum*, we did a whole genome-level transcriptome analysis from the kidney (the main hematopoietic organ of fish)

samples. Analysis revealed that at 14 days post infection (dpi), innate immune response related processes were enriched among the upregulated genes and many lipid metabolism-related processes were enriched among the downregulated genes.

To study the role of *il10* during *M. marinum* infection in zebrafish, we used a mutant zebrafish line, $il10^{e46}$, having a non-sense mutation resulting in a truncated protein product. We showed that these homozygous mutated fish had improved survival during *M. marinum* infection compared to wild type (WT) control fish and decreased bacterial burden at 8/9 weeks post low-dose infection, indicating improved resistance against *M. marinum*. In addition, $il10^{e46/e46}$ mutants had decreased expression of the pro-inflammatory cytokines *tnfb* and *il1b* possibly reflecting a slower progression of infection. Most importantly however, $il10^{e46/e46}$ mutants showed improved *interferon gamma 1* (*ifng1*) expression and a shift towards a T helper 1 (Th1) cell response, which provides a potential explanation for the improved resistance.

In order to identify genes participating in the immune defense against mycobacterial infection in adult zebrafish, we performed a forward genetic screen. We identified ten mutant zebrafish lines with impaired survival and one line with improved survival following low-dose infection with *M. marinum*. The most susceptible line, mutant463, showed a significantly higher bacterial burden compared to WT control fish at 14 dpi, indicating impaired resistance rather than tolerance against *M. marinum*. We also included mutant463 in the transcriptome analysis we performed. The results showed impaired expression of 27 genes in zebrafish kidney cells at 14 dpi compared to WT. These included seven genes with known or predicted immunological roles.

In the first original publication, we showed that the histological features of *M. marinum* infection in adult zebrafish are similar to tuberculosis. Results from the experiments with *il10* mutants in the second original publication are in line with earlier literature highlighting the role of the Th1 response in resistance against mycobacterial infection. This further validates the feasibility of our model in studying tuberculosis infection. Moreover, in the third original communication we found genes potentially required for defense against mycobacterial infection. Further studies are warranted to confirm and characterize the roles of these genes in more detail.

TIIVISTELMÄ

Tuberkuloosi on yhä maailmanlaajuinen terveysongelma, sillä joka vuosi siihen sairastuu 10 miljoonaa ihmistä ja yli miljoona kuolee. Tuberkuloosin aiheuttaa *Mycobacterium tuberculosis*, joka leviää ilmateiden kautta. Tartunta voi johtaa erilaisiin tuloksiin oireettomasta latentista tilasta aktiiviseen tautiin. Koska tämänhetkiset hoitomuodot ovat riittämättömiä, taistelussa tuberkuloosia vastaan tarvitaan uusia lähestymistapoja. On näytetty, että isännän geneettinen tausta vaikuttaa *M. tuberculosis* -tartunnan lopputulokseen. Siksi seulomalla isännän geneettisten vaihteluiden vaikutusta mykobakteeri-infektion taudinkulkuun saadaan uutta tietoa, joka on hyödyllistä uusia hoitomuotoja kehitettäessä. Tuberkuloositutkimusta on hidastanut hyvien eläinmallien puute. Hyvä malli jäljittelisi tuberkuloosin taudinkulkua, mutta olisi silti sujuva käyttää ja huomioisi myös eettiset näkökohdat.

Seeprakala on kasvattanut suosiotaan immunologisena tutkimusmallina. On myös olemassa monenlaisia menetelmiä tuottaa seeprakalalle sekä satunnaisia että kohdennettuja mutaatioita. Seeprakalan luontainen taudinaiheuttaja, *Mycobacterium marinum*, on *M. tuberculosis* -bakteerin läheinen sukulainen. Se aiheuttaa seeprakalassa koko elimistöön vaikuttavan taudin. Erityisesti *M. marinum* -infektio seeprakalan poikasessa on vakiintunut tuberkuloosimalli. Väitöskirjatutkimuksessa selvitettiin aikuisen seeprakalan *M. marinum* -infektion käytettävyyttä tuberkuloosimallina. Tämän väitöskirjan ensimmäinen tavoite oli tutkia kyseisen infektion kulkua aikuisessa seeprakalassa histologisilla menetelmillä ja transkriptiotason tutkimuksella. Toinen tavoite oli tutkia *interleukiini 10* (*il10*) -geenin tehtäviä *M. marinum* -infektion aikana. Lopullinen tavoite oli tehdä geneettinen seulonta ja tunnistaa isännän geenejä, joilla on tehtävä seeprakalan puolustautuessa mykobakteeri-infektiota vastaan.

Päästäksemme ensimmäiseen tavoitteeseemme värjäsimme *M. marinum* -bakteerin pitkittäisistä kudosleikkeistä, jotka oli otettu aikuisesta seeprakalasta infektion eri vaiheissa. Tutkimus osoitti, että infektoitaessa pienellä *M. marinum* -annoksella granuloomien ja infektoituneiden elinten lukumäärä vakiintui neljännestä viikosta eteenpäin. Suurella annoksella infektoitaessa infektoituneiden elinten lukumäärä oli korkeampi ja granuloomien lukumäärä kasvoi infektion edetessä. Selvittääksemme *M. marinum* -bakteerin aiheuttamaa immuunivastetta tarkemmin teimme koko genomin kattavan transkriptomianalyysin munuaisnäytteistä (seeprakalan

pääasiallinen verta muodostava elin). Tutkimus osoitti, että 14 päivää infektoinnin jälkeen synnynnäiseen immuunivasteeseen liittyvät prosessit olivat rikastuneet positiivisesti säädeltyjen geenien joukossa, kun taas rasva-aineenvaihduntaan liittyvät prosessit olivat rikastuneet negatiivisesti säädeltyjen geenien joukossa.

Käytimme *il10*^{e46} -mutanttiseeprakalalinjaa tutkiaksemme *il10*-geenin tehtäviä *M. marinum* infektion aikana seeprakalassa. Kyseisessä linjassa on mutaatio, joka aiheuttaa toimimattoman proteiinin syntymisen. Näytimme, että kyseisen mutaation suhteen homotsygootit kalat selvisivät villityypin kontrollikaloja paremmin *M. marinum* -infektion aikana ja kantoivat vähemmän bakteeria 8/9 viikon kuluttua pienellä bakteeriannoksella infektoimisesta. Nämä tulokset viittaavat parantuneeseen vastustuskykyyn *M. marinum* -bakteeria vastaan. *il10*$^{e46/e46}$-mutanteilla *tnfb* ja *il1b* tulehdussytokiinien ilmentyminen oli lisäksi vähentynyt mahdollisesti kuvastaen infektion hitaampaa etenemistä. *interferoni gamma 1* -geenin ilmentyminen oli lisääntynyt ja T-auttajasolu 1 (Th1) -vaste vahvistunut *il10*$^{e46/e46}$-mutanteilla mahdollisesti selittäen parantuneen vastustuskyvyn.

Suoritimme geneettisen seulonnan tunnistaaksemme geenejä, joilla on merkitystä aikuisen seeprakalan puolustautuessa mykobakteeri-infektiota vastaan. Tunnistimme 10 mutanttiseeprakalalinjaa, jotka selviytyivät huonommin ja yhden linjan, joka selviytyi paremmin pienen *M. marinum* -bakteeriannoksen aiheuttaman infektion aikana. Herkin linja, jonka tunnistimme, mutant463, kantoi 14 päivää infektoinnin jälkeen merkittävästi enemmän bakteeria verrattuna villityypin kaloihin. Tämä viittaa ennemmin heikentyneeseen vastustuskykyyn kuin heikentyneeseen sietokykyyn *M. marinum* -bakteeria kohtaan. Teimme myös mutant463-linjalle transkriptomianalyysin. Tulokset osoittivat, että mutant463-seeprakaloilla oli 27 geenin ilmentyminen heikentynyt munuaissoluissa villityypin kaloihin verrattuna 14 päivää infektoinnin jälkeen. Näiden geenien joukossa on seitsemän geeniä, joilla on tunnettu tai ennustettu immunologinen tehtävä.

Ensimmäisessä osatyössä näytimme, että seeprakalan *M. marinum* -infektion histologiset piirteet muistuttavat tuberkuloosin piirteitä. Toisen osatyön tulokset *il10*-geenin tehtävistä sopivat yhteen aiemman kirjallisuuden kanssa, sillä ne korostavat Th1-vasteen osuutta vastustuskyvyssä mykobakteeria kohtaan. Nämä tulokset vahvistavat käyttämäämme tuberkuloosimallia. Lisäksi kolmannessa osatyössä tunnistimme geenejä, joilla on mahdollisesti tehtävä immuunipuolustuksessa mykobakteeri-infektiota vastaan. Näiden geenien tehtävien varmentamiseksi ja tarkentamiseksi on tarpeen tehdä lisätutkimuksia.

CONTENTS

List of Figures

List of Tables

ABBREVIATIONS

ALOX5	Arachidonate 5-lipoxygenase
BCG	Bacillus Calmette-Guérin
Cas	CRISPR-associated
CD	Cluster of differentiation
CFU	Colony forming unit
CRISPR/Cas	Clustered Regularly Interspaced Short Palindromic Repeats
CTS	Cathepsin
CXCL	Chemokine (C-X-C motif)
CXCR	CXC motif chemokine receptor
dpf	Days post fertilization
dpi	Days post infection
EGFP	Enhanced green fluorescent protein
EGR	Early growth response
ENU	N-ethyl-N-nirosurea
FABP	Fatty acid binding protein
fosab	*V-fos FBJ murine osteosarcoma viral oncogene homolog Ab*
FOXP	Forkhead box P
GWAS	Genome-wide association study
GWLS	Genome-wide linkage study
HAMP	Hepcidin antimicrobial peptide
hpf	Hours post fertilization
HIV	Human immunodeficiency virus
IFNG	Interferon gamma
IG	Immunoglobulin
Ighv	Immunoglobulin heavy variable
Ighm, IgM	Immunoglobulin heavy constant mu
IGRA	Interferon gamma release assay
IL	Interleukin
JAK	Janus kinase
LCK	Lymphocyte-specific protein tyrosine kinase

LEAP2	Liver expressed antimicrobial peptide 2
LTA4H	Leukotriene A4 hydrolase
LTB_4	Leukotriene B_4
Lygl2	Lysozyme g-like 2
MHC	Major histocompatibility complex
MyD88	Myeloid differentiation primary response 88
NGS	Next generation sequencing
NK	Natural killer
NOD	Nucleotide-binding oligomerization domain
PCR	Polymerase chain reaction
PBS	Phosphate buffered saline
RAG	Recombination activating gene
RT	Room temperature
siRNA	Small interfering RNA
sgRNA	Single-guide RNA
STAT	Signal transducer and activator of transcription
TBX21	T-box 21
TCR	T cell receptor
Th	T helper
TILLING	Targeting induced local lesions in genomes
TL	Tüpfel long fin
TLR	Toll-like receptor
TMEM	Transmembrane proetein
tricaine	3-aminobenzoic acid ethyl ester
TST	Tuberculin skin test
UNC119	Unc-119 lipid binding chaperone
UV	Ultraviolet
WHO	World Health Organization
wpi	Weeks post infection
WT	Wild type

ORIGINAL PUBLICATIONS

This thesis is based on the following original publications, which are referred to in the text by their Roman numerals. The publications are reproduced with the permission of the copyright holders.

Publication I Parikka M[1], Hammarén[1] MM, **Harjula S-KE**, Halfpenny NJA, Oksanen KE, Lahtinen MJ, Pajula ET, Iivanainen A, Pesu M, Rämet M. *Mycobacterium marinum* causes a latent infection that can be reactivated by gamma irradiation in adult zebrafish. PLoS Pathogens. 2012. 8(9):e1002944.[2]

Publication II **Harjula S-KE**, Ojanen MJT, Taavitsainen S, Nykter M, Rämet M. *Interleukin 10* mutant zebrafish have an enhanced *interferon gamma* response and improved survival against a *Mycobacterium marinum* infection. Scientific Reports. 2018. 8(1):10360.

Publication III **Harjula S-KE**, Saralahti AK, Ojanen MJT, Rantapero T, Uusi-Mäkelä MIE, Nykter M, Lohi O, Parikka M, Rämet M. Characterization of immune response against *Mycobacterium marinum* infection in zebrafish (*Danio rerio*). Developmental and Comparative Immunology. 2020. 103:103523.

[1]) Equal contribution

[2]) The original publication I was in part used in the doctoral thesis of Milka Hammarén (University of Tampere, 2017)

1 INTRODUCTION

Tuberculosis is caused by *Mycobacterium tuberculosis*. Throughout the centuries of co-existence with man this bacterium has developed ways to hide from host defenses and also to rewire host mechanisms in order to benefit its own survival and spread (reviewed in Korb et al., 2016; Cambier et al., 2014; Goldberg et al., 2014). It has succeeded well in this, since each year there are circa 10 million new tuberculosis cases, over one million tuberculosis deaths and circa 22% of the world's population is estimated to carry tuberculosis (WHO, Global Tuberculosis Report, 2019). *M. tuberculosis* is transmitted via the airway in aerosols and migrates into the lungs of the new host (Corleis and Dorhoi, 2020; Jones-López et al., 2013; Fennelly et al., 2012). The outcomes of infection are diverse, ranging from clearance to active disease or asymptomatic, non-transmissible latent disease, which may reactivate (reviewed in Furin et al., 2019; Kaipilyawar and Salgame, 2019; Sia and Wieland, 2011; Barry et al., 2009). The current treatments against tuberculosis are not effective against all stages of the tuberculosis disease spectrum and have fallen behind constantly developing *M. tuberculosis* (Furin et al., 2019).

It is not only bacterial characteristics but also the genetic diversity of the host that affects tuberculosis outcome. The key to developing new treatments could be in understanding this diversity and the effect of different genetic variations on the host immune response against *M. tuberculosis*. To understand the role of host genetics in the outcome of *M. tuberculosis* infection and to develop new treatments, feasible animal research models are needed. Over the past few decades, the zebrafish (*Danio rerio*) has established its position as a useful research model organism (reviewed in Myllymäki et al., 2016; Myllymäki et al., 2015; Lieschke and Currie, 2007). Used initially as a model in developmental biology, it has made its way to a model for infectious diseases, as it has both innate and adaptive immunity (reviewed in Gomes and Mostowy, 2020; Meeker and Trede, 2008; Lieschke and Currie, 2007; van der Sar et al., 2004a). The immune system of the zebrafish includes both the main cellular and humoral components, which suggests evolutionary conservation between zebrafish and humans (reviewed in Meeker and Trede, 2008). *Mycobacterium marinum* infection in zebrafish has established a position as a tuberculosis research model,

since *M. marinum* is a close relative of *M. tuberculosis* and a natural pathogen of zebrafish (Myllymäki et al., 2016; Stinear et al., 2008; Tobin and Ramakrishnan, 2008) causing systemic disease with similar progression compared to tuberculosis (Benard et al., 2016; Ramakrishnan et al., 2006; Prouty et al., 2003, Davis et al., 2002). Furthermore, a wide variety of tools for genetic manipulation is available for zebrafish, including chemical or insertional mutagenesis methods for forward genetic screens and, for example, the Clustered Regularly Interspaced Short Palindromic Repeats (CRISPR)/ CRISPR-associated (Cas) system for reverse genetics (Parant and Yeh, 2016). Moreover, the relatively simple and cost-effective maintenance of zebrafish allows for large-scale experiments such as genetic screens.

Interleukin 10 (IL10) is an anti-inflammatory cytokine that is produced, for example, by T helper 2 (Th2) cells and inhibits T helper 1 (Th1) cells from producing cytokines (Fiorentino et al., 1989; Fiorentino et al., 1991). IL10 is known for maintaining homeostasis and preventing autoinflammation in mouse intestine (Gomes-Santos et al., 2012; Paul et al., 2012). The role of IL10 in *M. tuberculosis* infection has been widely studied in mice and humans. The results are contradictory, but the lack of IL10 during mycobacterial infection has been linked to an improved Th1 response (Harling et al., 2019; Redford et al., 2010; Higgins et al., 2009; Zhang et al., 1994), enhanced production of interferon gamma (IFNG) (Beamer et al., 2008), and the formation of more organized granulomas (Cyktor et al., 2013). On the other hand, challenge with *M. tuberculosis* has also been shown to eventually lead to uncontrollable inflammation and death in IL10 deficient mice (Higgins et al., 2009).

We have developed a research model for studying *M. marinum* infection in adult zebrafish. In this thesis, we studied the progression of this infection with histological methods. The developed model was then used to study the role of *il10* during *M. marinum* infection in zebrafish but also to find new candidate genes underlying defense mechanisms against mycobacterial infection. For the latter, a transposon-based forward genetic screen was performed to identify mutant zebrafish lines with impaired or improved survival. This study provides basic information about the progression of mycobacterial infection. This information can be used in the future when developing new treatments and preventive methods for tuberculosis.

2 REVIEW OF THE LITERATURE

2.1 Overview of tuberculosis

Each year over 10 million new tuberculosis infections emerge worldwide, resulting in over one million deaths (WHO, Global Tuberculosis Report, 2019). However, the distribution of tuberculosis infections is uneven, with most cases occurring in Southern Africa and South-Eastern Asia (WHO, Global Tuberculosis Report, 2019). The causative agent in tuberculosis, *Mycobacterium tuberculosis*, spreads in aerosols through airways and migrates into the lungs of the host (Corleis and Dorhoi, 2020; Jones-López et al., 2013; Fennelly et al., 2012).

M. tuberculosis infection can lead to a wide spectrum of various disease states (Figure 1). Some infected individuals are better able to clear the infection (reviewed in Kaipilyawar and Salgame, 2019) whilst in 5–15% infected individuals an active state of disease develops (Pai et al., 2016; Vynnycky and Fine, 1997). The rest, estimated at 22% of the world's population, develop and carry a latent state of tuberculosis infection, with life-long risk of reactivation (WHO, Global Tuberculosis Report, 2019; Barry et al., 2009). Compared to active disease, during the latent state the host is asymptomatic and does not infect others (Singer-Leshinsky, 2016; Barry et al., 2009; Young et al., 2009). Young or old age, alcohol abuse, malnutrition, smoking or indoor air pollution increases the risk of active tuberculosis (Saunders et al., 2017; Rehm et al., 2009; Lönnroth et al., 2008; Lin et al., 2007; Slama et al., 2007). Human immunodeficiency virus (HIV) positive people also have an increased risk of developing active tuberculosis (Daley et al., 1992; Selwyn et al., 1989). This is reflected in the uneven tuberculosis distribution since most infected areas are also rich in HIV cases (WHO, Global Tuberculosis Report, 2019).

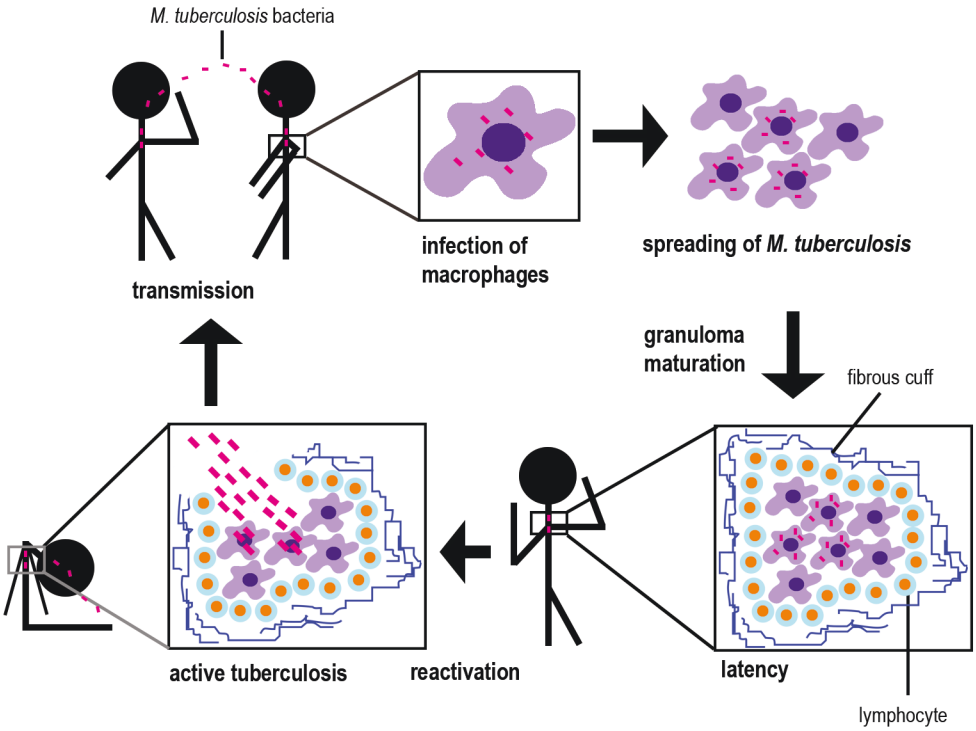

Figure 1. The different phases of tuberculosis infection. *M. tuberculosis* bacilli are transmitted via airways from an individual with the active disease to a new host. *M. tuberculosis* bacteria are first encountered by alveolar macrophages and phagocytosed by them. If the infection is not cleared, the bacteria spread to other macrophages and eventually lymphocytes are recruited to the site. This results in granuloma maturation and the infection can be restricted, that is, latency can be reached. The changes in the immunological status of the host can lead to granuloma eruption and reactivation of the disease after which the host is symptomatic and infectious to other individuals.

There are several tools for diagnosing TB, but they are only effective to a certain extent and at certain phases of the tuberculosis disease spectrum. Latent tuberculosis infection can be detected with either the tuberculin skin test (TST) or interferon gamma release assay (IGRA) (WHO, Latent tuberculosis infection, 2018). TST, however, has specificity limitations (Farhat et al., 2006) and neither TST nor IGRA predicts the reactivation of latent tuberculosis or is reliable in immunocompromised patients (Rangaka et al., 2012; Cattamanchi et al., 2011). Tools for screening and diagnosing active tuberculosis are divided into four categories: imaging technologies, microscopical studies performed from sputum smears, culturing methods and

molecular tests (Pai et al., 2016). The most commonly used method, sputum smear microscopy, has limitations in accuracy and specificity, whereas more improved methods are not always easy to use in poor conditions (Pai et al., 2016; Walzl et al., 2018). Due to these reasons, new diagnostic tools, like biomarkers to identify the different phases of *M. tuberculosis* infection, are needed (Walzl et al., 2018).

2.2 The different phases of *M. tuberculosis* infection

2.2.1 Innate immune response to *M. tuberculosis*

M. tuberculosis bacilli are first encountered by innate immune responses and, more precisely, phagocytosed by alveolar macrophages (Corleis and Dorhoi, 2020; Mayer-Barber and Barber, 2015; Guilliams et al., 2013; O'Garra et al. 2013). On the one hand, this is a defense response, but on the other hand, this does not eliminate the bacteria instead giving them an environment in which to proliferate (Leemans et al., 2005; Leemans et al., 2001; Denis, 1991). Macrophages have a large selection of pattern recognition receptors like Toll-like receptors (TLR), C type lectin receptors and nucleotide-binding oligomerization domain (Nod)-like receptors to recognize pathogen-associated molecular patterns on the surface of *M. tuberculosis* (Mishra et al., 2017; Mayer-Barber and Barber, 2015; Kleinnijenhuis, 2011; Divangahi et al., 2008; Kang et al., 2005; Means et al., 1999; Schlesinger, 1993). For example, a scavenger receptor called the macrophage receptor with collagenous structure (MARCO) recognizes Trehalose-6,6-dimycolate (Bowdish et al., 2009). Interestingly, it has been shown that this scavenger receptor is required also in zebrafish larvae for efficient phagocytosis and pro-inflammatory response after intravenous *M. marinum* infection and thus controls the replication of mycobacteria (Benard et al., 2014). In addition, complement receptors are required for efficient phagocytosis (BoseDasgupta and Pieters, 2018; Ferguson et al., 2004; Hirsch et al., 1994). The recognition is then followed by phagocytosis and phagosome maturation as well as the immune response and several cellular processes (reviewed in Stamm et al., 2015). When the bacteria are in the phagosomes, bacterial DNA is leaked into the cytosol and recognized by DNA sensors inducing IFN beta production which contributes to *M. tuberculosis* pathogenesis (Manzanillo et al., 2012). Infected alveolar macrophages secrete antimicrobial peptides, IL1α/β, tumor necrosis factor (TNF),

IL12p40 and IL6 (Dorhoi and Kaufmann, 2015; Mayer-Barber and Barber, 2015; Xu et al., 2015; O'Garra et al., 2013).

TNF is secreted by various immune cells, such as macrophages, neutrophils, dendritic cells and T cells (Mayer-Barber and Barber, 2015; O'Garra et al., 2013; Flynn and Chan, 2001). TNF activates macrophages to produce nitric oxide, which has a significant antimicrobial effect against *M. tuberculosis*, and induces the production of chemokines (Sharma et al., 2004; Roach et al., 2002; Flynn and Chan, 2001). As shown in mice treated with anti-TNF antibodies or lacking the TNF receptor or *Tnf* gene, TNF is essential in the immune defense against *M. tuberculosis* and especially for granuloma formation (Bean et al., 1999; Flynn et al., 1995).

Neutrophils (Eum et al., 2010) and dendritic cells are also infected with *M. tuberculosis* (Wolf et al., 2007). Once recruited and stimulated by *M. tuberculosis*, neutrophils secrete antimicrobial peptides, chemokines and proinflammatory cytokines (O'Garra et al., 2013; Riedel and Kaufmann, 1997). Neutrophils also facilitate the naïve antigen-specific CD4+ T cell activation by delivering *M. tuberculosis* bacilli to dendritic cells (Blomgran and Ernst, 2011), which migrate to the lymph nodes and present antigens to naïve T cells (Khader et al., 2006; Vermaelen et al., 2001). The role of neutrophils is contradictory since protection against *M. tuberculosis* is improved after neutrophils have been eliminated from susceptible mouse strains with an originally high number of neutrophils (Keller et al., 2006; Eruslanov et al., 2005).

The innate immune response may be able to clear *M. tuberculosis* infection. However, *M. tuberculosis* has developed advanced evasion strategies, such as an ability to escape pattern recognition receptors, to avoid clearance (reviewed in Zhai et al., 2019; Goldberg et al., 2014). When clearance by the innate immune response fails, the adaptive immune response is initiated by innate immune cells.

2.2.2 Adaptive immune response to *M. tuberculosis*

The hypersusceptibility of HIV patients to tuberculosis can be associated with a decreased number of cluster of differentiation 4 (CD4) positive T cells (Geldmacher et al., 2010; Geldmacher et al., 2008). In addition to this, the inability of CD4+ T cell deficient mice to restrict the growth of *M. tuberculosis* (Mogues et al., 2001) indicates that adaptive immune responses, and especially CD4+ T cells, are crucial in the immune defense against tuberculosis.

Moreover, particularly the Th1 cell response is essential in the immune defense against tuberculosis. This is demonstrated by the hypersusceptibility of IFNG, IL12 and TBX21 (T-box 21) deficient mice after *M. tuberculosis* exposure (Sullivan et al., 2005; Cooper et al., 1997; Cooper et al., 1993), as well as by the fact that individuals born with defects on the IL12/IFNG axis are hypersusceptible to usually less virulent mycobacteria (Mayer-Barber and Barber, 2015; van de Vosse et al., 2013; Filipe-Santos et al., 2006). By secreting IFNG, Th1 cells activate macrophages to produce cytokines and microbicidal factors, such as nitric oxide synthase iNOS, to control bacterial growth (Travar et al., 2016; O'Garra, et al., 2013).

Although understood to a smaller extent, CD8+ T cells also have a role in the immune defense against tuberculosis (reviewed in Lin et al., 2015). Also poorly understood is the role of B cells in the immune defense against tuberculosis. The role of B cells in tuberculosis remains contradictory probably due to the variation between the used *M. tuberculosis* strains and the genetic background of studied hosts, as well as the different suggested roles of B cells at various stages of the tuberculosis disease spectrum (Dyatlov et al., 2019; O'Garra et al., 2013). A role for B cells in the defense against tuberculosis is suggested in the presence of activated B cells in the granulomas of non-human primates (Phuah et al., 2012), as well as B cell aggregates in the lungs of tuberculosis patients (Ulrichs et al., 2004). B cells and the antibodies they produce assumedly control host defenses or immunomodulation, or both, in the lungs of *M. tuberculosis* infected individuals (reviewed in Achkar et al., 2015; Maglione and Chan, 2009). Nevertheless, during *M. tuberculosis* infection, B cells interact with other type of immune cells (reviewed in Dyatlov et al., 2019).

Defense against tuberculosis is a collaboration of innate and adaptive immune responses. This usually does not lead to the elimination of *M. tuberculosis* bacilli, but to the containment of them inside granulomas. Thus, more information on the immune defense against tuberculosis is needed in order to find successful treatments for this disease.

2.2.3 Latent tuberculosis infection

In the latent state of tuberculosis infection, a part of the *M. tuberculosis* bacilli are in a dormant state but at least part of them are able to replicate (Batyrshina and Schwartz, 2019; Dutta and Karakousis, 2014). Dormancy has been described *in vitro* as a series of events in which *M. tuberculosis* shuts down metabolic functions, stops replicating and gains phenotypical tolerance to isoniazid (Wayne and Hayes, 1996).

The genetic factors of both the bacteria and the host affect the length of latency. In *M. tuberculosis*, dormancy survival regulator transcription factor affects approximately 50 genes, which regulate dormancy (Park et al., 2003). The central core of a granuloma is hypoxic and the expression of these genes is actually induced in such conditions (Galagan et al., 2013; Voskuil et al., 2003). In addition, these genes are induced when external growth factors inhibit the growth of *M. tuberculosis* (Karakousis et al., 2004). However, other genes are also important for the dormancy and survival of *M. tuberculosis* in the host (reviewed in Peddireddy et al., 2017). For example, *M. tuberculosis* encodes 11 regulatory proteins for the two-component signal transduction system which regulates numerous genes and thus is able to create conditions that favor mycobacterial dormancy inside the host for long time periods (Cole et al., 1998; Peddireddy et al., 2017). *M. tuberculosis* is also able to promote calcification of granulomas which results in an environment favorable for dormancy (Peddireddy et al., 2017). In addition, many metabolic genes affect the virulence, survival and dormancy of *M. tuberculosis*. Fatty acids are the primary carbon source for *M. tuberculosis* (Cole et al., 1998; Bloch and Segal, 1956). In addition, when residing in macrophages, *M. tuberculosis* harvests amino acids from the host and uses them, especially glutamine, as nitrogen sources (Borah et al., 2019). It has been shown *in vitro* that sulfur metabolism is upregulated when mycobacteria are adapting to the dormancy (Hampshire et al., 2004) and that sulfur metabolic pathways are also important for mycobacterial virulence (Senaratne et al., 2006). Transporting phosphates is also crucial for establishing infection in mouse lungs and for the replication of the bacteria inside macrophages (Rengarajan et al., 2005). *M. tuberculosis* bacteria also require metals such as iron and excess of iron promotes progression of tuberculosis (Weiss and Schaible, 2015; Gangaidzo et al., 2001; Lounis et al., 2001). *M. tuberculosis* gets iron for example by producing exochelins to release iron from iron-binding proteins of the host or by utilizing mycobactins to acquire iron from iron pools inside macrophages (Weiss and Schaible, 2015; Luo et al., 2005; Olakanmi et al., 2002; Gobin and Horwitz, 1996; Gobin et al., 1995).

The effect of host genetics on the development of latent tuberculosis has been seen in genome-wide association and linkage studies but also in numerous *in vitro* and *in vivo* studies. The greater risk of HIV positive individuals for reactivation is not only due to decreased CD4+ T cell number, but also due to malfunctions in T cell proliferation, cytolytic T cell responses, intracellular killing mechanisms and the production of cytokines after mycobacterial antigen challenge (reviewed in Ahmed et al., 2016; Bruchfeld et al., 2015; Dutta and Karakousis, 2014). Moreover, a doubled risk for tuberculosis has been seen in HIV positive individuals already prior to a

decrease in CD4+ T cell levels (Sonnenberg et al., 2005) which, as stated by Dutta and Karakousis (2014), indicates that it is not the only reason why HIV increases the risk of tuberculosis.

In addition to CD4+ T cells, the roles of CD8+ T cells and B cells have also been investigated in the context of maintaining latent tuberculosis even though their role remains less clear (reviewed in Dyatlov et al., 2019; Dutta and Karakousis, 2014). The genetic mechanisms maintaining latency both in the bacteria and the host are important to understand since this information could help to prevent or predict reactivation.

2.2.4 Granulomas

A granuloma is a hallmark structure of tuberculosis, which consists of both innate and adaptive immune cells and contains *M. tuberculosis* bacilli (Figure 2). Human granulomas are heterogenic in their structure (Cadena et al.; 2017). The inner layers of the granuloma consist of infected macrophages, stimulated macrophages differentiated into multinucleated giant cells, foamy macrophages full of lipid droplets and epithelioid cells, neutrophils, natural killer (NK) cells and dendritic cells (Martinot, 2018; Cadena et al., 2017; Ramakrisnan 2012; Russell et al., 2009). Typically for human tuberculous granulomas (Tsai et al., 2006) and also shown in guinea pig, non-human primate, rabbit (Via et al., 2008) and zebrafish (Myllymäki et al., 2018) models, as a result of cell death, there is a necrotic, caseous, hypoxic area at the center of the granuloma. The inner layers of the granuloma are surrounded by CD4+ and CD8+ T cells, B cells and fibroblasts; the first being the most dominant component of the outer layer (Cadena et al., 2017; O'Garra et al., 2013: Ramakrishnan, 2012). Fibroblasts secrete a fibrotic collagen capsule that surrounds the outermost layer of the granuloma (Warsinske et al., 2017).

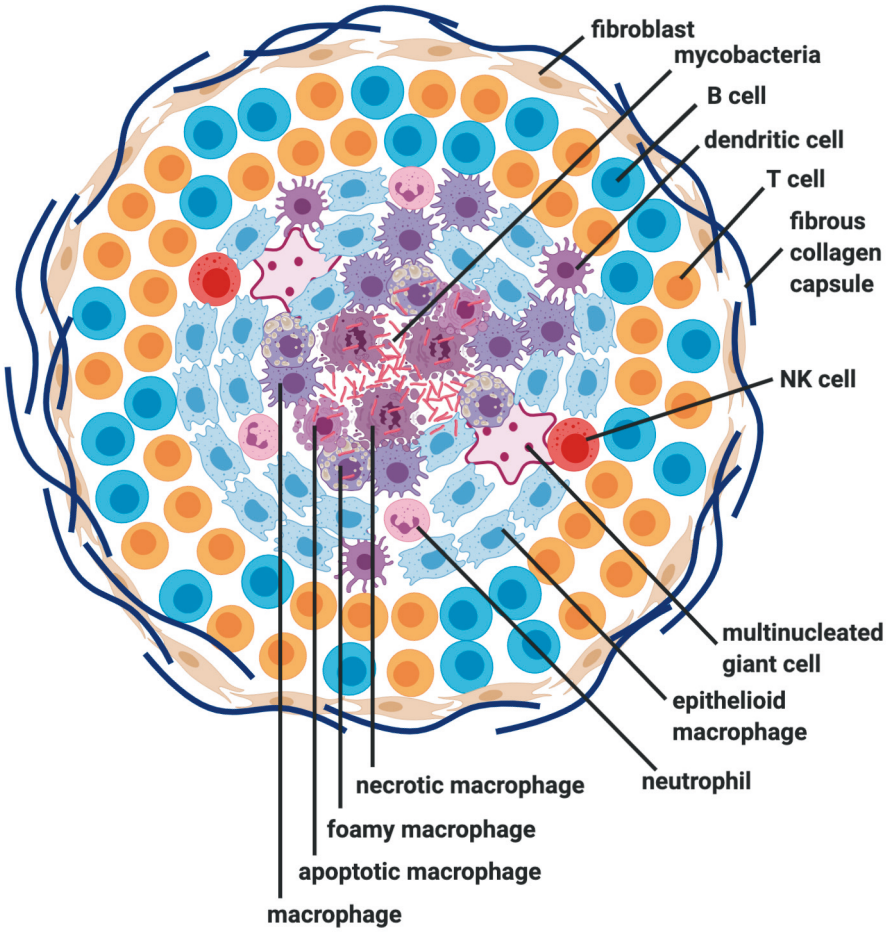

Figure 2. Structure of granuloma. The necrotic center of granuloma is surrounded by epithelioid macrophages. The outer layers of granuloma consist of lymphocytes and fibrous capsule secreted by fibroblasts. The figure was created with BioRender.com.

Macrophages inside granulomas aim to preserve the granuloma structure through a microbicidal immune response meant to prevent the infection from spreading to the extracellular space (Ndlovy and Marakalala, 2016; Pagán and Ramakrishnan, 2014). However, relatively recent studies have also shown that the bacteria themselves benefit from the granuloma and, in fact, *M. tuberculosis* manipulates the host responses to accelerate granuloma formation (Pagán and Ramakrishnan, 2014; Davis and Ramakrishnan, 2009; Volkman et al., 2004). As mentioned in sections 2.2.6 "Manipulation of the host responses by *M. tuberculosis*" and 2.4.2.4 "New

insights into tuberculosis from the zebrafish model" granuloma acts as a safe environment for the bacteria and facilitates their dissemination (Davis and Ramakrishnan, 2009; Cosma et al., 2008; Cosma et al., 2004). As stated by Ramakrishnan (2012), gaining a full understanding of granuloma formation and structure will provide more tools for developing new tuberculosis treatments.

2.2.5 Primary active and reactivated tuberculosis

Host factors affect to the likelihood of developing primary active tuberculosis after exposure to *M. tuberculosis*, since young children, individuals suffering from malnutrition or a chronic illness, individuals receiving immunosuppressive medication and HIV positive individuals have the highest risk (Chandrasekaran et al., 2017; Nachiappan et al., 2017; Rangaka et al., 2015; Sia and Wieland, 2011).The symptoms of primary pulmonary tuberculosis include mild fever and are minor in general, whereas the general clinical signs of reactivated pulmonary tuberculosis are fever, night sweats, weight loss, cough and fatigue (Loddenkemper et al., 2015; Sia and Wieland, 2011). Even though pulmonary tuberculosis is the most common, tuberculosis can also spread to other tissues of the body (Loddenkemper et al., 2015; Sia and Wieland, 2011).

Many factors that can cause reactivation have been recognized, but in some cases the factors that result in active tuberculosis infection remain a mystery (Pai et al., 2016). HIV is a predisposing factor for reactivation, but the association between HIV and the tuberculosis contagion is actually negative mainly due to the earlier diagnosis and death of HIV positive patients (Corbett et al., 2006). In addition, there is a theory that the antigen-specific activation of CD4+ T cells that occurs in humans during tuberculosis infection would actually be beneficial for the bacteria (Comas et al., 2010).

From the host point of view, predisposing factors for reactivation of tuberculosis are TNF neutralizing antibodies (Pai et al., 2016). TNF is important for maintaining the latency and preventing reactivation as it has been shown that TNF deficiency as well as neutralization in mice results in the reactivation of latent or persistent *M. tuberculosis* infection with lethal consequences (Botha and Ryffel, 2003; Mohan et al., 2001). Correspondingly, individuals carrying latent tuberculosis infection and receiving anti-TNF therapy to treat rheumatoid arthritis or Crohn's disease have a risk of developing active tuberculosis soon after the initiation of treatment (O'Garra et al., 2013; Keane et al., 2001). In addition, primary immune deficiencies on the

IL12-IFNG axis predispose individuals to active tuberculosis (reviewed in Boisson-Dupuis, 2020; Bustamante, 2020; Bustamante et al., 2014).

The unpredictability of reactivation presents one of the greatest challenges to the diagnosis, prevention and treatment of tuberculosis. Thus, the characterization of the mechanisms and reasons behind reactivation would help in the battle against tuberculosis.

2.2.6 Manipulation of the host responses by *M. tuberculosis*

One explanation for the great success of *M. tuberculosis* as a disease-causing agent is its ability to harness host mechanisms to its own benefit and to survive inside macrophages (Figure 3).

Autophagy is one mechanism by which the host kills intracellular bacteria (Gutierrez et al., 2004). *M. tuberculosis* has been suggested to evade autophagy in different ways (reviewed in Khan and Jagannath, 2017; Cambier et al., 2014; Goldberg et al., 2014). It has been shown to create itself an environment inside the macrophage in which to survive by preventing the fusion of phagosomes and lysosomes and acidification of phagosomes (Pahari et al., 2018; Khan and Jagannath, 2017; O'Garra et al., 2013; Gutierrez et al., 2004, Malik et al., 2001; Sturgill-Koszyck et al., 1994; Armstrong and Hart, 1971). Related to the initial recognition and phagocytosis of *M. tuberculosis* described in the section 2.2.1 "Innate immune response to *M. tuberculosis*", mannose receptor recognizes mannosylated lipoarabinomannan (ManLAM) on the mycobacterial surface which limits phagosome-lysosome fusion (Kang et al., 2005; Fratti et al., 2003). It has also been shown that *M. tuberculosis* is able to escape from phagosomes and phagolysosomes to the cytosol in myeloid cells, replicating there and causing cell death (Jamwal et al., 2016; van der Wel et al., 2007), and that *M. marinum* is able to escape from phagosomes to cytoplasm in macrophages and to spread to other cells (Stamm et al., 2003).

Cell death of infected cells is another process that *M. tuberculosis* bacilli can manipulate for their own good. They can prevent apoptosis and thus are able to replicate inside alveolar macrophages (Keane et al., 2000). Whether infected alveolar macrophages die through apoptosis or necrosis is of importance for the progress of the infection. Apoptosis results in controlled bacterial replication since the plasma membrane of the cell stays intact, whereas necrotic cell death results in the dissemination of the bacilli (Chen et al., 2006). However, the phagocytosis of

apoptotic macrophages in granulomas by noninfected macrophages facilitates the proliferation of mycobacteria (Davis and Ramakrishnan, 2009).

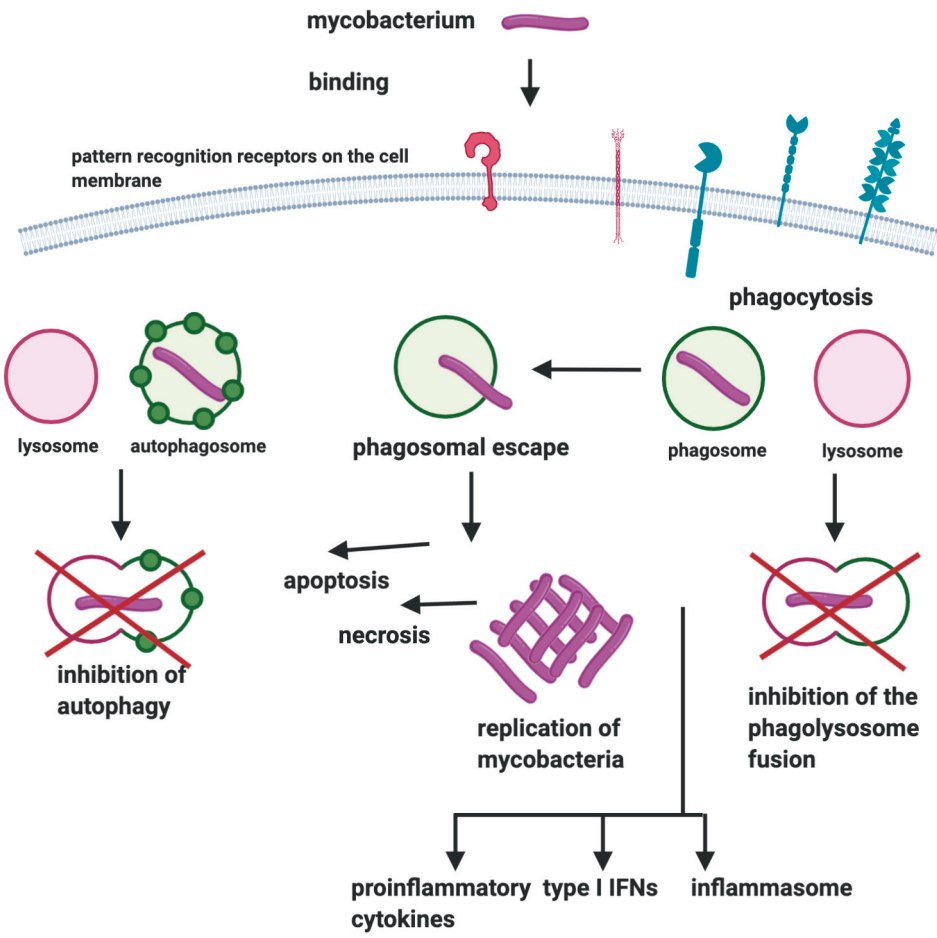

Figure 3. Simplified illustration of the events following the entry of *Mycobacterium tuberculosis* bacilli to macrophage. Mycobacteria are recognized by pattern recognition receptors on the surface of macrophages. Through intracellar signaling cascades this leads to the production of proinflammatory cytokines and type I interferons and inflammasome activation. However, mycobacterium is also able to escape from phagosomes, prevent autophagy and phagolysosome fusion and affect the cell death. The figure was created with BioRender.com.

There is evidence that the granuloma itself is beneficial not only to the host but also to mycobacteria, since it provides a shelter for the bacteria (Rhoades et al., 2003).

In consensus with this, *M. tuberculosis* has ways to promote granuloma formation. Mycobacteria are able to induce the production of matrix metalloproteinase-9 resulting in tissue remodeling and enhanced recruitment of macrophages (Volkman et al., 2010; Bansal et al., 2009; Taylor et al., 2006). In addition, *M. tuberculosis* lipids are able to induce the production of chemokines and pro-inflammatory cytokines from mononuclear cells, which also promotes granuloma formation (Korb et al., 2016).

In addition, *M. tuberculosis* is able to evade and delay adaptive immune responses for example by affecting dendritic cell maturation, inhibiting antigen presentation and disrupting the migration of Th1 cells from lymph nodes to lungs (reviewed in Zhai et al., 2019; Ernst, 2018; Korb et al., 2016; Goldberg et al., 2014). *M. tuberculosis* is also able to manipulate the course of infection by other means, for example by affecting lipid metabolism of the host (reviewed in Korb et al., 2016). By knowing the mechanisms behind this manipulation, there opens up the possibility for prevention.

2.3 Challenges in the treatment of tuberculosis

Despite extensive research, existing treatment and prevention strategies against tuberculosis are inadequate. Currently, according to recommendations by The American Thoracic Society, Centers for Disease Control and Prevention, Infectious Diseases Society of America and World Health Organization, active tuberculosis is treated with an antibiotic cocktail: isoniazid, rifampicin, pyrazinamide and ethambutol daily for the first two months, and after that with isoniazid and rifampicin for four months (Nahid et al., 2016; WHO, Guidelines for treatment of tuberculosis, 2010). In 2017, tuberculosis was treated successfully in 85% of cases (WHO, Global tuberculosis report, 2019).

An inadequate or incomplete treatment increases the risk for development of drug resistant *M. tuberculosis* strains (Sharma and Moran, 2006). According to the latest data collected in 2016, only 56% of multidrug-resistant and rifampicin-resistant and 39% of extensively drug-resistant tuberculosis cases could be cured (WHO, Global tuberculosis report, 2019). Of drug-resistant strains, isoniazid-resistant are the most common (Furin et al., 2019), while the number of rifampicin monoresistant cases is constantly increasing (Furin et al., 2019; Coovadia et al., 2013). World Health Organization (WHO) has recommended treating this and multidrug-resistant forms of tuberculosis with a drug combination including bedaquiline (WHO, Rapid

Communication, 2018), which unfortunately has a world-wide accessibility problem (Cox et al., 2018). Several other new antibiotics are also under development and in clinical testing, some of them are also included in WHO treatment recommendations (reviewed in Furin et al., 2019; Tiberi et al., 2018). In addition to antibiotic resistance, the severity of the disease should be considered when choosing a treatment regimen (Furin et al., 2019). Among children this has already been considered. Individuals with a less severe form of multidrug-resistant tuberculosis are treated for 9-12 months, whereas those with drug-susceptible extrapulmonary disease are treated for 12 months (Furin et al., 2019; Harausz et al., 2017).

There is an existing vaccine against tuberculosis, Bacillus Calmette-Guérin (BCG). It is an attenuated *Mycobacterium bovis* strain (Andersen and Doherty, 2005). It does not protect adults effectively from transmission of tuberculosis infection, pulmonary tuberculosis or the reactivation of the latent state (Tang et al., 2016), but is effective among children against severe and disseminated forms of tuberculosis (Furin et al., 2019; Mangtani et al., 2014). However, in a small number of vaccinated infants, it causes disseminated BCG disease that can be fatal (Hesseling et al., 2007; Jounanguy et al., 1996). According to current beliefs, the BCG vaccine does not induce long term immunization (Sterne et al., 1998) even though the aerosol or intranasally delivered forms have shown to be more immunogenic (Garcia-Contreras et al., 2008; Giri et al., 2006; Chen et al., 2004). Due to the above-mentioned reasons and the relatively low incidence of tuberculosis in our country, the vaccine has been removed from the general vaccine scheme in Finland (Zwerling et al., 2011).

All in all, many challenges still remain in the field of tuberculosis treatment and prevention strategies. Thus basic research to understand the genetic mechanisms underlying the immune defense against tuberculosis and new approaches, like developing DNA vaccines in zebrafish (Oksanen et al., 2013; Myllymäki et al., 2017; Myllymäki et al., 2018), are needed.

2.4 Zebrafish as a model organism

Zebrafish (*Danio rerio*) is a small teleost fish, which has made its way from its native environment in India, Pakistan and Bhutan through to home aquariums and research facilities (Spence et al., 2008; van der Sar et al., 2004a). The reason for the popularity of zebrafish is that it is a vertebrate and thus physiologically closer to humans than invertebrates, but with the advantages of invertebrate model organisms (Lieschke and Currie, 2007). Due to its small size, zebrafish can be easily maintained and in

high numbers, also cost-effectively (Meeker and Trede, 2008; Lieschke and Currie, 2007). Zebrafish have high fecundity, *ex-utero* development and its larvae are transparent during the first few days of their lives (Meeker and Trede, 2008; Lieschke and Currie, 2007; van der Sar, 2004a). These features have made the zebrafish embryo/larva an especially popular research model for developmental studies and genetic screens, since visualizing of different phenotypes is feasible (Lieschke and Currie, 2007). In addition, the zebrafish genome has been sequenced revealing that 71.4% of human genes have a zebrafish ortholog (Howe et al., 2014). There is a wide variety of tools available to manipulate zebrafish genetically (Parant and Yeh, 2016; Lawson and Wolfe, 2011). In order to track specific functions *in vivo*, transgenic zebrafish lines have been created by marking specific cells with a fluorescent reporter (Lieschke and Currie, 2007; Udvadia and Linney, 2003). For example, the *mpo:gfp* line in which the neutrophils express green fluorescent protein (*GFP*) and the *pu.1:EGFP* line in which the myeloid cell precursors express enhanced green fluorescent protein (*EGFP*), have been produced for studying inflammation and acute myeloid leukemia, respectively (Renshaw et al., 2006; Hsu 2004).

The limited selection of some tools, such as antibodies and cell lines, is one disadvantage of zebrafish as a model organism (Tobin et al., 2012a; Meeker and Trede, 2008; Lieschke and Currie, 2007). Secondly, from an immunological point of view, human pathogens are usually adapted to the human body temperature, 37 °C, whereas ectothermic zebrafish are maintained at 28 °C (Lieschke and Currie, 2007; Van der sar et al., 2004a). As a non-mammalian model organism, zebrafish are not anatomically and physiologically as close to humans as mammalian model organisms (Lieschke and Currie, 2007). For example, from a tuberculosis research point of view, zebrafish do not have lungs. A further challenge for zebrafish research is an additional whole-genome duplication event as compared to other vertebrates - the teleost-specific genomic duplication, which occurred during the course of evolution (Glasauer and Neuhauss, 2014; Howe et al., 2014; Dehal and Boore, 2005; Meyer and Schartl, 1999). Due to this, there are several copies of a large portion of zebrafish genes and 53% of human genes with at least one zebrafish ortholog actually have more than one corresponding gene in the zebrafish genome (Howe et al., 2014). This must be considered when choosing targets for gene knockdowns and knockouts. Moreover, annotation of the zebrafish genome is constantly being updated and predictions for zebrafish orthologs of human genes may change.

The good selection of genetic tools and successful genetic screens to study vertebrate development made zebrafish a popular research model in developmental biology (Lieschke and Currie, 2007). Since the zebrafish is neurologically the most

underdeveloped model organism with both innate and adaptive immune responses, it has also gained popularity as an immunological research model. Zebrafish infection models have been developed for a wide variety of pathogens such as *Edwardsiella tarda* (Pressley et al., 2005), *Salmonella typhimurinum* (van der Sar et al., 2003), *Streptococcus agalactiae* (Patterson et al., 2012), *Streptococcus pneumoniae* (Saralahti et al., 2014; Rounioja et al., 2012), *Mycobacterium leprae* (Madigan et al., 2017) and *Mycobacterium marinum* (Prouty et al., 2003; Davis et al., 2002).

2.4.1 The zebrafish immune system

2.4.1.1 The zebrafish innate immune system

Zebrafish have an immune system with counterparts for the main cellular and humoral components of the human immune system. Zebrafish larvae lack a functional adaptive immune system (Lam et al., 2004), which allows for the separate study of innate mechanisms. Adult zebrafish have both innate and adaptive immunity (Meeker and Trede, 2008), which in turn allows the study of both innate and adaptive immunity simultaneously. This is important when studying mycobacterial infection, for example.

Zebrafish myeloid cells have been identified and characterized. Zebrafish have neutrophils and macrophages (Le Guyader et al., 2008; Lieschke et al., 2001; Herbomel et al., 1999), mast cells (Dobson et al., 2008) and eosinophils (Balla et al., 2010). There is also evidence of NK cells since NK-like cells have been identified from single-cell transcriptome analysis and putative novel immune-type receptors (NITR) have been suggested as equivalents for classical natural killer (NK) receptors in humans (Carmona et al., 2017; Yoder et al., 2007; Wei et al., 2007; Yoder et al., 2001). Dendritic cells have also been identified in zebrafish (Lin et al., 2009; Lugo-Villarino et al., 2010).

Mature myeloid cells of the zebrafish have similar functions and expression patterns as corresponding mammalian cells (Meeker and Trede, 2008). In zebrafish, macrophages are the main phagocytosing cells (Lieschke and Trede, 2009; Carradice and Lieschke, 2008). Moreover, zebrafish innate immune cells produce microbicidal compounds such as reactive oxygen species and nitric oxide (Lieschke and Trede, 2009; Hermann et al., 2004; van der Sar et al., 2004a; Saeij et al., 2000), the latter being especially interesting from a tuberculosis research point of view. Zebrafish also have a complement system with classical, alternative and mannose-lectin activation

pathways, even though the functions of many proteins have not yet been characterized (Zhang and Cui, 2014; Holland and Lambris, 2002). For the recognition of pathogen-associated molecular patterns, zebrafish have pattern recognition receptors similar to those in humans, such as Toll-like receptors (Jault et al., 2004; Meijer et al., 2004), peptidoglycan recognition proteins (Chang et al., 2007; Li et al., 2007) and NOD-like receptors (Hu et al., 2017; Howe et al., 2016). Thus the key immunological mechanisms are present in zebrafish (Lieschke and Trede, 2009). To conclude, the high conservation of the innate immune system between zebrafish and humans makes zebrafish a valid model for the study of the innate immune response against various pathogens.

2.4.1.2 The zebrafish adaptive immune system

The adaptive immune system of the zebrafish is not fully developed until four to six weeks post fertilization (Lam et al., 2004). Zebrafish have both T (Yoon et al., 2015; Langenau et al., 2004) and B lymphocytes (Page et al., 2013; Danilova and Steiner, 2002). The different types of T lymphocytes have been recognized: Th1, Th2, Th17 and regulatory T cells (Kasheta et al., 2017; Dee et al., 2016; Holt et al., 2011; Mitra et al., 2010). Zebrafish T cells express marker genes homologous to human genes. Such are *lymphocyte-specific protein tyrosine kinase* (*lck*), *ikaros*, *recombination activating gene 1 (rag1)* and *rag2* for T cells, *cd4-1* especially for T helper cells, *tbx21* for Th1, *gata3* and *signal transducer and actvator of transcription 6* (*stat6*) for Th2 cells and *forkhead box P3a* (*foxp3a)* for regulatory T cells (Yoon et al., 2015; Mitra et al, 2010; Schorpp et al., 2006; Langenau et al., 2004; Lam et al., 2004, Willett et al., 1997). In addition, Foxp3a has been shown to be important in maintaining immune tolerance in zebrafish (Sugimoto et al., 2017). Zebrafish T cell receptors also have a conserved structure (Lieschke and Trede, 2009; Danilova et al., 2004). Rag dependent V(D)J recombination occurs in zebrafish T cells (Meeker and Trede, 2008; Wienholds et al., 2002) and T cell receptor (TCR) α, β, γ and δ loci have been found and studied (Covacu et al., 2016; Seelye et al., 2016; Meeker et al., 2010; Yazawa et al., 2008; Schorpp et al., 2006; Haire et al., 2000). $\gamma\delta$ T cells have an important role in the immune defense against *M. tuberculosis* infection (reviewed in Zhao et al., 2018; Chen, 2016). Zebrafish $\gamma\delta$ T cells act, for example, as antigen presenting cells demonstrating their evolutionary conserved role (Wan et al., 2017; Schorpp et al., 2006). Macrophages, dendritic cells and B cells act as antigen presenting cells in zebrafish (Lewis et al., 2014). Zebrafish have three classes of major

histocompatibility complex (MHC) molecules (Michalová et al., 2000; Sültmann et al., 2000; Bingulac-Popovic et al., 1997).

As for zebrafish B cells, they have some significant differences to their human counterparts. Zebrafish B cells undergo Rag dependent V(D)J recombination (Weinstein et al., 2009; Meeker and Trede, 2008: Haire et al., 2000; Willett et al., 1997). However, zebrafish have only three immunoglobulin classes IgD, IgM and IgZ/T (Zimmerman et al., 2011), which is a significant difference compared to humans and moreover, there is no class switching (Barreto et al., 2005; Magor et al., 1999) and somatic hypermutation is inefficient (Marianes and Zimmerman, 2011). Genes used as markers for zebrafish B cells are for example *immunoglobulin heavy constant mu* (*ighm*, previously *IgM*) (Hu et al., 2010) and *paired box 5* (*pax5*) (Wittamer et al., 2011).

Compared to humans, early hematopoiesis occurs in intermediate cell mass in zebrafish and since zebrafish do not have bone marrow, adult hematopoiesis occurs in kidney marrow (Meeker and Trede, 2008; Murayama et al., 2006; Al-Adhami and Kunz, 1977). Zebrafish also do not have lymph nodes and thus antigen presentation is thought to occur in spleen and intestine (Renshaw and Trede, 2012; Lugo-Villarino et al., 2010). Nevertheless, despite some differences, the zebrafish adaptive immune system has the same basic components as in humans. Therefore, several zebrafish adaptive immunity models such as models for autoimmunity, immunodeficiency and leukemia have been developed (Sugimoto et al., 2017; Iwanami, 2014; Teittinen et al., 2012; Meeker and Trede, 2008).

2.4.2 *M. marinum* infection in zebrafish as a model for tuberculosis

2.4.2.1 *M. marinum* compared to *M. tuberculosis*

M. marinum, a natural pathogen of fish and amphibians and *M. tuberculosis*, the disease-causing agent in human tuberculosis, are close relatives with 3000 protein orthologs and an average amino acid identity of 85% (Stinear et al., 2008; Tobin and Ramakrishnan, 2008). *M. tuberculosis* has by estimation 3974 coding sequences and *M. marinum* 5424, with the same important virulence determinants (Stinear et al., 2008; Tobin and Ramakrishnan, 2008; Cosma et al., 2006; Gao et al., 2004). Both bacteria infect macrophages and survive in them (El-Etr et al., 2001; Barker et al., 1997).

Both *M. marinum* and *M. tuberculosis* use exogenous fatty acids for their growth (Wilburn et al., 2018; Stinear et al., 2008). The gene orthology of *M. marinum* with *M. tuberculosis* suggests production of adenosine triphosphate by oxidative phosphorylation during aerobic growth (Stinear et al., 2008). However, the larger number of *M. marinum* genes contains factors enabling it to survive extracellularly and in different environments (Stamm and Brown, 2004; Clark and Shepard, 1963), whereas *M. tuberculosis* is specialized to live intracellularly in mammalian hosts (Cambier et al., 2014; Becq et al., 2007). Also *M. marinum* is able to infect humans resulting in the infections in skin, soft tissues or, more rarely, in other locations such as bones and joints (Petrini, 2006).

From a researcher's point of view, *M. marinum* has practical and safety advantages compared to *M. tuberculosis*. As a biosafety level class 2 pathogen *M. marinum* sets fewer demands for a research facility than class 3 *M. tuberculosis* (Tükenmez et al., 2019). Moreover, in laboratory conditions, the generation time of *M. marinum* is only four to six hours (Clark and Shepard, 1963), compared to approximately 24 hours for *M. tuberculosis* (Cole et al., 1998), which makes performing experiments with *M. marinum* less time-consuming than with *M. tuberculosis*. The fact that *M. marinum* shares the key virulence determinants and several other features with *M. tuberculosis* and is a natural pathogen of fish, has made this bacterium an attractive tool for tuberculosis research.

2.4.2.2 The progression of *M. marinum* infection in zebrafish

M. marinum causes a systemic infection in zebrafish that has led to problems for example in research facilities (Watral and Kent, 2007; Kent et al., 2004). In the first publication using this infection as a research model for tuberculosis, Lalita Ramakrishnan's research group showed that *M. marinum* infects macrophages, the outcome of the infection is dose-dependent and that macrophage aggregates are formed in zebrafish larvae after *M. marinum* infection (Davis et al., 2002). They also showed that these aggregates had the features of tuberculous granulomas and that granuloma-specific *Mycobacterium* genes were activated in these structures.

In fact, mainly macrophages, not neutrophils, are responsible for the phagocytosis of *M. marinum* bacilli in early infection of zebrafish larvae, with it suggested that macrophages also control the growth of bacteria (Clay et al., 2007). Related to this, Clay and colleagues (2007) also showed that in the first phases of infection, macrophages have a role in the dissemination of mycobacteria deeper into host tissues. Nevertheless, in newly-forming granulomas, neutrophils are attracted

to dying infected macrophages, phagocytosing them with some neutrophils able to use oxidative mechanisms to kill the *M. marinum* bacilli they have phagocytosed with macrophages (Yang et al., 2012). Similarly to human tuberculosis, Tnf signaling also plays an important role in *M. marinum* infection in zebrafish. Clay and colleagues (2008) showed that the absence of this signaling route leads to the increased mortality of a host. This was preceded by enhanced proliferation of intracellular bacteria as well as enhanced formation of granulomas, which resulted in the necrotic death of infected macrophages and granuloma breakdown (Clay et al., 2008). However, it has been shown that a hyperinflammatory phenotype due to a deficiency in *protein tyrosine phosphatase, non-receptro type 6* (*ptpn6*) expression led to impaired control of *M. marinum* proliferation in zebrafish larvae (Kanwal et al., 2013). Also related to the innate immune defense against zebrafish *M. marinum* infection in zebrafish larvae, Myeloid differentiation primary response 88 (MyD88) has been shown to restrict granuloma formation and mycobacterial replication and affects the induction of important innate immune genes, such as *il1b*, *tnfa* and *matrix metalloproteinase* (*mmp9*) during infection (van der Vaart et al., 2013). Myd88 is a central adaptor molecule in TLR signaling (van der Sar et al., 2006; Akira and Takeda, 2004). TLR signaling in turn initiates the production of reactive nitrogen species, which is a defense mechanism against mycobacteria, which mycobacteria nevertheless are able to attenuate (Elks et al., 2014; Flynn and Chan, 2001).

Adult zebrafish has been used as a research model much less than zebrafish larvae. However, in adult zebrafish, the progression of *M. marinum* infection has also been shown to be dose-dependent since an infection with small bacterial inoculate results in chronic infection, whereas high inoculate causes an active progressive disease (Swaim et al., 2006; Prouty et al., 2003). In addition, these studies showed that infection results in the formation of granulomatous structures.

The progression of *M. marinum* infection in zebrafish has the same main features as the progression of *M. tuberculosis* infection in humans. Moreover, the zebrafish model has brought new insights to the progression of these infections.

2.4.2.3 Zebrafish in comparison with other animal models for tuberculosis

Several research models to study tuberculosis have been developed. A widely used model has been the *M. tuberculosis* infection in the mouse and mouse studies have indeed provided a lot of information on the pathogenesis of tuberculosis (Kramnik and Beamer, 2016). However, research models that would better mimic the features of human tuberculosis are still needed. The main features together with advantages

and disadvantages of different vertebrate animal models for tuberculosis are presented in Table 1.

Table 1. Comparison of different vertebrate models for studying tuberculosis.

	mouse	non-human primate	guinea pig	rabbit	cattle	zebrafish
host + natural pathogen	-	+	-	-	+	+
spontaneous latency	-	+	-	+	?	+
reactivation	+	+	-	+	?	+
granuloma/granuloma-like structure	+	+	+	+	+	+
hypoxic granulomas	-	+	+	+	+	+
necrotic granulomas	-	+	+	+	+	+
small size	+	-	-	-	-	+
low cost	+	-	-	-	-	+
ethically good	-	-	-	-	+	+
mammal	+	+	+	+	+	-
lungs	+	+	+	+	+	-

There are also several other animal models, such as zebrafish, guinea pig, cattle, rabbit and non-human primate models, like macaque (reviewed in Myllymäki et al., 2015). *M. tuberculosis* is not a natural mouse pathogen (Kramnik and Beamer, 2016), but it is a natural pathogen of non-human primates (Lin et al., 2009; Lerche et al., 2008). *M. tuberculosis* infection in the guinea pig is also a suitable tuberculosis model since guinea pigs are highly susceptible to this pathogen and develop disease after a low dose aerosol exposure with similar symptoms and pathophysiological features to human tuberculosis (Padilla-Carlin et al., 2008). Other good models are *M. bovis* infection in cattle and *M. marinum* infection in zebrafish, as these mycobacteria are natural pathogens for these hosts (Tobin and Ramakrishnan, 2008; Cassidy, 2006).

Spontaneous latency does not occur in the mouse but caused by a preceding BCG vaccination to enhance the immune response of the host or preventing the development of active infection by treating the host with antibiotics after infection (Nuermberger et al., 2004; McCune et al., 1956). There is also a reactivation model in mouse using the TNF-neutralizing antibody (Dutta et al., 2014). Spontaneous latency does occur in rabbit and non-human primate models (Subbian et al., 2012; Capuano et al., 2003). Reactivation can also be modeled in non-human primate models by administrating TNF neutralizing agent (Lin et al., 2010), in rabbits by injecting triamcinolone (Subbian et al., 2012) and in the zebrafish model for example by dexamethasone feeding (Myllymäki et al., 2018).

Lesions resembling granulomas and containing macrophages and lymphocytes are formed in mouse but the structure of these lesions is not spherical like in human

granulomas (Orme et al., 2014; Tsai et al., 2006; Rhoades et al., 1997). Moreover, they are not hypoxic inside like in humans, non-human primates, guinea pigs, rabbits, cattle or zebrafish (Myllymäki et al., 2018; Via et al., 2008; Tsai et al., 2006). Macrophages inside the granulomas also do not undergo necrosis and consequently granulomas do not contain the caseous necrotic tissue (Via et al., 2008; Rhoades et al., 1997), such is the case in nonhuman primates, cattle, guinea pig, rabbit and zebrafish (Myllymäki et al., 2018; Subbian et al., 2011; Lin et al., 2009; Via et al., 2008; Cassidy, 2006; Swaim et al., 2006). Zebrafish granulomas have epithelioid or foamy macrophages surrounding the necrotic center but fewer neutrophils and lymphocytes than in human granulomas (see Figure 2) (Cheng et al., 2020; van Leeuwen et al., 2014; Swaim et al., 2006; van der Sar et al., 2004b).

Despite many tuberculosis mammalian models mimicking the spectrum of human tuberculosis well, there are drawbacks. Many of these model animals are big in size and thus not so easy to handle, are expensive and raise ethical concerns (Myllymäki et al., 2015). Although the zebrafish is a non-mammalian model organism with its deficiencies, as a model organism it overcomes many of the problems of mammalian models. There are also other less developed animals used as models in tuberculosis research, such as the amoeba, *Dictyostelium discoideum*, and fruit fly, *Drosophila melanogaster*, but as a vertebrate with both innate and adaptive immunity, zebrafish is closer to humans than these (Myllymäki et al., 2015; Dionne et al., 2006; Solomon et al., 2003).

2.4.2.4 New insights into tuberculosis from the zebrafish model

Granuloma formation has traditionally been thought to be the result of both innate and adaptive immune cell function (Ramakrishnan, 2012; Russell et al., 2009). However, Davis and colleagues (2002) showed that granuloma-like macrophage aggregates are formed also in zebrafish larvae, that is, without the presence of adaptive immunity. These aggregates were identified as granulomas because macrophages undergo typical morphological changes in mature adult granulomas (Davis et al., 2002; Adams, 1976). In addition, such bacterial genes, which are shown to specifically activate in mature adult frog granulomas, are activated in these macrophage aggregates, (Chan et al., 2002; Ramakrishnan et al., 2000).

The central dogma concerning granulomas has been that granuloma formation is an immune mechanism to protect the host from mycobacteria (Pagán and Ramakrishnan, 2014). However, this view has been challenged by the zebrafish larval model. Volkman and colleagues (2004) showed that when zebrafish larvae are

infected with *M. marinum* deficient in the RD1 virulence determinant, granuloma formation is not efficient. This was associated with an inability for macrophages infected with RD1 deficient bacteria to produce a signal to promote macrophage aggregation. Moreover, they showed that *M. marinum*-induced macrophage aggregation was associated with the dissemination of bacteria to other cells and increased bacterial burden (Volkman et al., 2004). More precisely, it has been shown that new macrophages arrive at a granuloma, phagocytose the dying macrophages and some then exit the granuloma and initiate new granulomas (Davis and Ramakrishnan, 2009).

The importance of TNF in the immune defense against tuberculosis is well recognized. However, studies in humans have also suggested that an excess of TNF is associated with the pathogenesis of tuberculosis (Agarwal et al., 2009). Indeed, the traditional view on the role of TNF during mycobacterial infection has been elaborated on in studies using zebrafish larvae. It has been shown that excessive inflammation caused by an excess of leukotriene B_4 (LTB_4) results in increased susceptibility to *M. marinum* (Tobin et al., 2012b). Moreover, Roca and Ramakrishnan (2013) showed that excess Tnf induces production of reactive oxygen species, which kills mycobacteria and infected macrophages but also leads to the necrosis of macrophages. This in turn results in the release of bacteria into the extracellular space (Roca and Ramakrishnan, 2013).

Research in zebrafish larvae has also brought new information regarding the development of antibiotic tolerance *in vivo*. Traditionally it has been thought that latency and the nonreplicating state of *M. tuberculosis* leads to the appearance of antibiotic tolerant mycobacteria (Berg and Ramakrishnan, 2012). Nevertheless, it has been shown that during *M. marinum* infection in zebrafish larvae, multidrug-tolerant mycobacteria appear inside macrophages already a few days after infection, replicating also during treatment, and are spread by traveling inside macrophages which leave granulomas (Adams et al., 2011).

These findings further prove that *M. marinum* infection in zebrafish is a valid model for tuberculosis. The results in this model have not only reiterated the main features of mycobacterial infection but also brought new information.

2.5 Whole-genome level transcriptome studies

Various research models have been used to study the host immune response to mycobacteria (Table 2). Several transcriptome analyses have been made in human

peripheral blood cell samples to study changes in the expression profile upon *M. tuberculosis* infection. Human peripheral blood is easy to obtain in the required quantities and it contains several types of immune cells: neutrophils, basophils, eosinophils, T cells and B cells (Blankley et al., 2014). These studies indicate that Fc gamma receptor 1, Janus kinase (JAK)-STAT, IFN and TLR signaling are more induced in active tuberculosis compared to the latent disease (Maertzdorf et al., 2011). In addition, IFN inducible genes are dominant in the expression profile of active tuberculosis compared to healthy controls, other diseases and to individuals under treatment (Berry et al., 2010).

Several transcriptome studies have also been performed in the mouse tuberculosis model. Many of the studies compare susceptible mouse strains to resistant strains. In general, these studies revealed that upregulation of genes related to inflammation associated with a high susceptibility to *M. tuberculosis* infection, whereas the upregulation of genes involved in cell signaling, regulation of the immune response and the activation of protective mechanisms after infection associated with better resistance (Shepelkova et al., 2013; Orlova et al., 2006; Keller et al., 2004).

Several transcriptome analyses have been made in the zebrafish *M. marinum* infection model. Four of these studies analyzed the expression profile of adult zebrafish during infection. Meijer (2005), Van der Sar (2009) and Ojanen and colleagues (2019) utilized microarrays, whereas Hegedüs and colleagues (2009) used deep sequencing. In the larval model, transcriptome analyses have been done with microarrays (van der Vaart et al., 2012; van der Sar et al., 2009) and RNA sequencing (Rougeot et al., 2019; Kenyon et al., 2017; Benard et al., 2016; Rougeot et al., 2014) techniques.

Meijer and colleagues (2005) analyzed the transcriptional response of adult zebrafish at the late stage of infection to two *M. marinum* strains, which both cause chronic infection. One strain, M strain, has been isolated from humans and the other one, the less virulent E11, from sea bass, with genomic diversity demonstrated between the two strains (Das et al., 2018; Swaim et al., 2006; Meijer et al., 2005; Van der Sar et al., 2004b). Meijer and colleagues (2005) used three different microarray setups and ended up with a reference set of 159 genes, which were differentially expressed after infection with both of the used bacterial strains. Thus the reference set reflects transcriptional responses to chronic infection despite some variation in experimental set-up. The genes of this reference set were divided into categories according to their function. Many of these categories, for example metabolism and other general cellular processes, included both up- and downregulated genes (Meijer

et al., 2005). Coagulation factors and genes involved in complement activation as well as in acute phase, stress and defense responses were especially upregulated, whereas genes associated with antigen presentation, immune response and muscle were downregulated (Meijer et al., 2005).

Hegedüs and colleagues (2009) compared the deep sequencing and microarray methods and came to the conclusion that they both identified the same functional groups of regulated genes. However, they state that digital gene expression analysis provides aspects that traditional microarray analysis cannot. Such are a good method for confirming predicted gene models and recognition of switching between different transcript isoforms by mycobacterial infection (Hegedüs et al., 2009).

van der Sar and colleagues (2009) compared transcriptional changes in adult zebrafish after an infection with two different bacterial strains; acute disease causing Mma20 and chronic disease causing E11. First, they detected that infection with Mma20 bacteria leads to terminal symptoms already at 6 days post infection (dpi) whereas with E11 this takes 6-8 weeks post infection (wpi). They showed the expression profile was more similar between the two different strains at the later time-point than between the early and late time-points after the infection with E11 strain. The genes upregulated in the late stages of both infections encode immunity-related transcription factors and chemokine receptors and cytokines, in addition to TLR signaling related proteins. They also compared the expression profiles of larvae and adult zebrafish infected with the E11 strain. A large number of transcription factors were differentially expressed in both larvae and adults. (van der Sar et al., 2009.)

"Biotagged" nuclei isolation and flow cytometry-based enrichment of fluorescent labeled immune cells in transgenic lines have also been utilized for RNA sequencing studies in zebrafish. Kenyon and colleagues (2017) did nuclear transcriptome analysis from neutrophils of zebrafish larvae at 3 days post *M. marinum* infection using a transgenic line and a nuclei isolation method. Their analysis revealed upregulation of several inflammasome related genes. The activation of the inflammasome is part of the inflammatory response during *M. tuberculosis* infection (reviewed in Wawrocki and Druszczynska, 2017). Rougeot and colleagues (2019) sorted fluorescent macrophages from zebrafish larvae of a transgenic line with flow cytometry and analyzed the transcriptomic response in macrophages after *M. marinum* infection.

Table 2. Main results from selected transcriptome studies in human, mouse and zebrafish.

Model	Studies	Sample	Main results
human	• Maertzdorf et al., 2011 • Berry et al., 2010	peripheral blood, active tuberculosis	**upregulated** • Fc gamma receptor 1 signaling • TLR signaling • IFN I and II signaling • myeloid cell genes
mouse	• Moreira-Teixeira et al., 2020 • Shepelkova et al., 2013; • Orlova et al., 2006; • Keller et al., 2004	• peripheral blood • lung • lung macrophages • bone marrow derived macrophages	**upregulated** in susceptible strains • IFN I signaling • neutrophil activation and recruitment • inflammation in resistant strains • B, NK and T cell responses • cell signaling • regulation of the immune response • protective mechanisms
zebrafish	• Meijer et al., 2005 • van der Sar et al., 2009	adult	**upregulated** in the early stage chronic infection • small GTPase • histone genes in the late stage of chonic infection • coagulation factors • extracellular matrix proteins • complement activation • acute phase response • stress response • defense response in the early stage of acute infection • MHC class I • matrix metalloproteases • transcription factors • cytokines
	• Kenyon et al., 2017 • Rougeot et al., 2019	larvae • neutrophils • macrophages	**upregulated** • inflammasome genes • proinflammatory M1 genes **downregulated** • anti-inflammatory M2 genes

As described above, the previously performed transcriptome analyses have shed light on the progression of mycobacterial infection and identified genes whose expression may affect whether the resulting infection is chronic or acute, as well as providing potential novel therapeutic targets and biomarker genes for diagnostics. Since *M. tuberculosis* infection in mice differs from that of humans, the transcriptional studies in mouse are not the best for providing information on the progression of latent tuberculosis (Nuermberger et al., 2004; McCune et al., 1956). On the other hand, transcriptional analyses on patient samples are often restricted to a certain population (Blankley et al., 2014). Zebrafish *M. marinum* infection mimics the main characteristics of tuberculosis. However, most transcriptome analyses in zebrafish during *M. marinum* infection do not emulate tuberculosis in humans the best, since they pertain to zebrafish larvae which have no functional adaptive immunity (Lam et al., 2004). Moreover, among analyses done in adult zebrafish, there is no study concentrating on the expression profile of immune cells during latent mycobacterial infection. Techniques for transcriptome analyses have developed during recent years. Since costs have also lowered, these methods have become more feasible and popular instead of small-scale gene expression analyses such as quantitative polymerase chain reaction (PCR). Moreover, genome-wide transcriptome analyses can be used as a starting point for reverse genetics studies.

2.6 Genetic approaches for studying tuberculosis

2.6.1 Association studies and genome-wide linkage studies

Whether a gene associates with disease susceptibility can be studied in genome-wide association or linkage studies (GWAS or GWLS), or in candidate gene studies (Yim and Selvaraj, 2010). GWAS can be used to identify single nucleotide polymorphisms, which associate with tuberculosis susceptibility or resistance (Möller et al., 2010). In GWAS, thousands of different polymorphisms are analyzed, resulting in a large amount of data with several variations studied for each gene. Thus, the same gene can be associated with both susceptibility and resistance of a given disease. Moreover, the found polymorphism is not necessarily the one causing the susceptibility or resistance to the disease, but may be another allele that is in linkage disequilibrium with it (reviewed in Ardlie et al., 2002). When considering tuberculosis, association study results may be very dependent on the population

under study, the age of subjects and the bacterial lineage (Dallmann-Sauer et al., 2018; Mahasirimongkol et al., 2012). GWLS searches for chromosomal regions that include putative susceptibility genes in large affected families assuming nonrandom segregation of the chromosomal regions with disease (Möller et al., 2010). When linkage between the region and disease is identified, the region is restricted by genetic and physical gene mapping so that the gene of interest can be indentified either by choosing a candidate gene or performing positional cloning (Abel and Dessein, 1997).

Many polymorphisms that have been associated with tuberculosis in GWAS or GWLS or in candidate gene studies are linked to genes with well-known immunological functions. For example, the importance of *IFNG* in the defense against tuberculosis has been demonstrated by other types of studies (Boisson-Dupuis, 2020; Bustamante et al., 2014; Cooper et al., 1993) and support for this can be found in association studies. *IFNG* has been associated with susceptibility to tuberculosis in several populations, however, in other populations the same polymorphism had no association (e.g. Moran et al., 2007; Rossouw et al., 2003; Lio et al., 2002). Moreover, one study suggests that a certain *IFNG* polymorphism modulates how a patient responds to tuberculosis treatment and thus provides information that helps public health decisions (Shibasaki et al., 2009). Some TNF polymorphisms have also been associated with susceptibility to tuberculosis (e.g. Azad et al., 2012) and some to protection (e.g. Correa et al., 2005; Scola et al., 2003). Of note and supporting the controversial results from association studies, a dual role for TNF during mycobacterial infection has been shown in the zebrafish model, illustrating the complexity of interplay between bacteria and host (Roca and Ramakrishnan, 2013).

To conclude, despite variation in the GWAS, GWLS and candidate gene studies, many results have been confirmed in several studies. Furthermore, many of the results have been verified in disease models. Thus, genetic studies can be successfully used to identify genes with important roles in the pathophysiology of a selected disease. Valid disease models are then required to understand the significance of these genetic variations at a mechanistic level.

2.6.2 Forward genetics

Due to its small size, easy maintenance and high fecundity, zebrafish is a feasible tool for forward genetic screens (Meeker and Trede, 2008; Lieschke and Currie, 2007).

When performing a genetic screen, random mutations are first produced in the genome (Lawson and Wolfe, 2011). Mutated individuals are used as founders of the screen to produce lines with unknown mutations (Lawson and Wolfe, 2011; Patton and Zon, 2001). These lines are used to screen for specific phenotypes, for example increased susceptibility to tuberculosis (Lawson and Wolfe, 2011).

Various methods can be used for mutagenesis. These include chemical and irradiation-based methods, retroviral insertional methods and transposon mediated insertional mutagenesis (Lawson and Wolfe, 2011; Parant and Yeh, 2016). The most common problem with mutagenesis methods, especially with chemical and irradiation-based methods, is the generation of several mutations per genome, which makes it hard to define which mutation is behind a particular phenotype (Lawson and Wolfe, 2011). Identification of one mutation requires several rounds of outcrossing. Another problem related to this is the phenotype may not be the result of the found mutation but another one co-segregated with it. However, finding the phenotype causing mutations has become easier since the whole zebrafish genome has been sequenced (Howe et al., 2013). Moreover, next-generation sequencing (NGS) techniques have been developed so that mapping unknown mutations is more feasible and less expensive (Henke et al., 2013).

Even though the zebrafish is an ethical model organism to screen for host factors and allows large scale studies, it is not the only model that fills these criteria. Screens for host genes affecting the outcome of tuberculosis have been made in macrophages. *Drosophila melanogaster,* for example, is well-suited to screen macrophage-related phenotypes (Rämet et al., 2002), and a genome-wide RNA interference screen identified several evolutionarily conserved molecules required for mycobacterial infection (Philips et al., 2005). Furthermore, Kumar and colleagues (2010) performed a genome-wide small interfering RNA (siRNA) screen and identified a set of 275 genes that affect the survival of *M. tuberculosis* inside human macrophages. Interestingly, all these genes were associated with each other (Kumar et al., 2010). Another similar siRNA screen was made in murine macrophages against all known kinases and phosphatases (Jayaswal et al., 2010). *in vitro* and *in vivo* studies in mice revealed that this screen identified some potential targets for anti-tuberculosis drug development. Another approach is to screen not for host but bacterial factors affecting the characteristics of the bacteria, for example antibiotic tolerance or growth in the host (Baker and Abramovitch, 2018; MacGurn and Cox, 2007; Cox et al., 1999). Bioinformatics methods are also useful when further studying the results from screens, since they can be used to find interactions between identified genes (Chandra et al., 2011). To conclude, some characteristics of

tuberculosis can be unraveled by screening in cell models *in vitro* but these studies do not provide adaptive immune response data during infection. All in all, these models and mathematical modeling are feasible tools and allow large scale studies, but do not replace the information gained from a living model organism with both innate and adaptive arms of immunity infected with a natural pathogen. For this purpose the adult zebrafish is a feasible tool.

2.6.2.1 Mutagenesis by chemical treatment or irradiation

The first approach to produce heritable mutagenic lesions in zebrafish was to use γ-irradiation, which leads to chromosomal breaks and thus embryonic mutant phenotypes (Chakrabarti et al., 1983). Besides point mutations, irradiation methods can lead to large deletions, translocations or other gross chromosomal aberrations, which affect multiple genes, leading to uncertainty in determining which gene caused the observed mutant phenotype (Lawson and Wolfe, 2011; Patton and Zon, 2001; Walker and Streisinger, 1983)

N-ethyl-N-nitrosurea (ENU) has been successfully used especially for screening genes important during the development of zebrafish (Driever et al., 1996; Haffter et al., 1996). It is an effective mutagen, which produces mainly point mutations (Patton and Zon, 2001; Solnica-Krezel et al., 1994). ENU mutagenesis is used, for example, in the zebrafish mutation project conducted at the Sanger Institute (Kettleborough et al., 2013). The aim of the project is to generate a mutant line for each zebrafish gene with mutations identified with the help of NGS. Another chemical tested for mutagenesis is ethyl methanesulphonate, but it has proved to be less efficient than ENU (Solnica-Krezel et al., 1994). Mutations causative for a phenotype can also be identified by positional or candidate cloning (e.g. Just et al., 2016; Zhang et al., 1998; Brand et al., 1996; Talbot et al., 1995). Rescue experiments are required to conclusively demonstrate that the candidate mutation causes the identified phenotype (Lawson and Wolfe, 2011).

Producing haploid or gynogenetic diploid zebrafish larvae are methods for skipping one generation in forward genetic screens and identifying phenotypes caused by recessive mutations (Patton and Zon, 2001). When producing haploid zebrafish, the sperm from the male is treated with ultraviolet (UV) irradiation, which destroys the male DNA but not the ability of the sperm to fertilize female eggs (Kroeger et al., 2014). When eggs are fertilized with the sperm, the resulting progeny is 50% WT and 50% mutants (Kroeger et al., 2014; Patton and Zon, 2001). Zebrafish larvae are able to survive haploid for several days, allowing time for experiments

(Kroeger et al., 2014). Gynogenetic diploid embryos are able to develop into adults and are produced by fertilizing female eggs with UV treated sperm and manipulating the cell cycle of the eggs for example by heat shock or early pressure treatment (Baars et al., 2016; Heier et al., 2015; Walker et al., 2009; Trede et al., 2008; Patton and Zon, 2001).

Ramakrishnan's group has conducted ENU mutagenesis in zebrafish followed by gynogenetic diploid screen to identify host factors having a role in immune defenses against *M. marinum* infection in zebrafish larvae. These results demonstrate the feasibility of the zebrafish model for screening susceptibility factors of tuberculosis. Based on their findings, they have described a role for *leukotriene A4 hydrolase* (*lta4h*) (Tobin et al., 2012b; Tobin et al., 2010) and *cathepsin L.1* (*ctsl.1*) (Berg et al., 2016) during *M. marinum* infection in zebrafish. *lta4h* catalyzes the last reaction in the synthesis of a chemoattractant and proinflammatory eicosanoid, leukotriene B_4 (LTB_4) (reviewed in Haeggström, 2004). Tobin et al. (2010) suggested that as a result of *lta4h* deficiency, anti-inflammatory lipoxin is produced instead of LTB_4 and the resulting anti-inflammatory state leads to a dampening of *tnfa* production, which in turn results in enhanced proliferation of *M. marinum*. Altogether, their data suggests that Ltah4 is important in balancing pro- and anti-inflammatory states during *M. marinum* infection. Validating the zebrafish larvae as a tuberculosis model, Tobin and colleagues (2010) also showed that in humans, heterozygosity for *LTA4H* polymorphisms affecting LTB_4 production result in protection against tuberculosis and another mycobacterial disease, multibacillary leprosy.

The second mutation causing hypersusceptibility in the screen by Ramakrishnan's group was located in a gene called *small nuclear RNA activating complex, polypeptide 1b* (*snapc1b*) (Berg et al., 2016). The mutation resulted in decreased expression of *cathepsins B* and *L.1*, which in turn led to increased mycobacterial growth. They also showed with the help of morpholinos that the phenotype was mostly caused by reduced *ctsl.1* expression (Berg et al., 2016). Ctsl.1 as well as its human orthologs, CTSL and CTSV, are lysosomal cysteine proteases (Turk et al., 2000; Turk et al., 2012; Santamaria et al., 1998). Whereas CTSL is expressed ubiquitously, expression of CTSV is limited to testis, thymus and macrophages (Turk et al., 2012; Brömme et al., 1999; Santamaria et al., 1998; Yasuda et al., 2004). Lysosomal cathepsins also have a role in antigen presentation (Turk et al., 2002). Berg and colleagues (2016) showed that lysosomal storage of undigested cell debris led to very large lysosomes inside macrophages, which in turn resulted in the inability of macrophages to migrate to *M. marinum*. These macrophages could also not engulf *M. marinum* or infected macrophages in granulomas (Berg et al., 2016). Eventually, this led to an increase in

mycobacterial growth since infected macrophages did not undergo apoptosis but necrosis releasing *M. marinum*. In addition, they showed an accumulation of non-biological particles, beads, in lysosomes led to inhibition of macrophage migration. This situation also has a similarity to human tuberculosis, again verifying zebrafish as a tool to screen tuberculosis susceptibility factors. Research showed that tobacco smoke particles accumulated in alveolar macrophages leading to impaired macrophage migration and presumably to tobacco smokers' increased susceptibility to tuberculosis. (Berg et al., 2016.)

2.6.2.2 Insertional mutagenesis

The difficulty in identifying mutation sites when using ENU mutagenesis inspired development of new methods. The first insertional mutagenesis method was retroviral mutagenesis (Gaiano et al., 1996b). This method is based on the observation that high titer mouse retroviruses can be used to cause germline mutations in zebrafish (Gaiano et al., 1996a, Gaiano et al., 1996b). Retrovirus is injected into 1,000-2,000-cell stage zebrafish embryos and a retroviral insertion tag allows identification of the insertion site with inverse PCR (Amsterdam et al., 1999). Wang and colleagues (2007) showed that retroviral insertions are most likely on the upstream side of the gene and that the majority of insertions are in intron 1. They also showed that 80% of these insertions resulted in more than a 70% decrease in the expression of a gene (Wang et al., 2007). This means that this method more often causes knockdown rather than knockout phenotypes (Parant and Yeh, 2016; Wang et al., 2007). The disadvantage of the retroviral methods compared to ENU mutagenesis is that the mutation rate is much lower, resulting in a need for more F2 families (Parant and Yeh, 2016; Amsterdam et al., 1999). However, this can be improved by prescreening the fish produced by insertional mutagenesis in the F1 generation by choosing individuals with a high number of inserts per genome (Amsterdam et al., 1999).

A transposon-based mutagenesis has advantages compared to retroviral mutagenesis because it does not require for instance viral titers in the cell culture (Parant and Yeh, 2016). DNA transposons are genetic elements able to move within the genome through transposition, which is a mutagenic process since it includes the insertion of DNA to a new locus (Kawakami et al., 2017). Transposons can have a variety of effects on gene expression (reviewed in Feschotte, 2008). There are several types of transposons which can be used, for example gene-breaking *Sleeping Beauty* (Davidson et al., 2003) and *Tol2* transposon systems (Kawakami et al., 2000). *Sleeping*

Beauty transposon-based screen has demonstrated for example the role of the histone 2a family member z in larval development (Sivasubbu et al., 2006), and *Tol2* mediated mutagenesis has been successfully used in zebrafish to identify genes affecting for example β cell and hepatocyte development (Zhong et al., 2019), embryonic development (Gao et al., 2011), nicotine response (Petzold et al., 2009) and T lymphocyte development (Seiler et al., 2005). The *Tol2* transposon has a higher mutagenesis efficiency compared to *Sleeping beauty* and other mutagenesis methods (Kawakami et al., 2004). However, consideration in choosing each component of a vector construct is required for the optimal mutagenesis efficiency (Sivasubbu et al., 2007).

When injected into zebrafish embryos at the 1-cell stage together with *Tol2* transposase mRNA, a gene-breaking transposon, pGBT-RP2 inserts into the zebrafish genome, potentially disrupting normal gene expression and causing random mutations into the germline as it includes a protein trap cassette with a transcriptional stop and 3' exon trap cassettes (Clark et al., 2011). The insertion of RP2 into a reading frame of a gene results in at least 97% knockdown of normal transcript levels but gene-breaking transposons are also able to mutate genes when inserted into intronic areas since normal splicing is affected there resulting in the reduction of gene expression (Clark et al., 2011; Sivasubbu et al., 2007).

RP2 contains a GFP tag allowing the identification of the mutation carrying embryos based on ubiquitous *GFP* expression and a red fluorescent protein (*RFP*) tag whose expression reflects the expression pattern of the mutated gene if RP2 is integrated in the reading frame (Clark et al., 2011). These are advantages compared to ENU mutagenesis since mutation-carrying fish can be identified even though they would not carry an easily detectable phenotype. Like retroviral insertions, the insertion sites of transposons can be rather easily identified with inverse-PCR (Kawakami et al., 2017; Clark et al., 2011). Another advantage compared to ENU mutagenesis is that the insertion of a foreign DNA fragment usually causes a more severe alteration in the gene than point mutations resulting in stronger phenotypes (Kawakami et al., 2017). Noteworthy, RP2 is the first system outside the mouse model that creates systematic conditional mutant alleles, since the effect can be reversed either by using *Cre* recombinase or temporarily with splice blocking morpholinos (Clark et al., 2011).

The wide variety of different methods to produce untargeted mutations in the zebrafish genome provides a good starting point for large-scale genetic screens. In general, the methods have improved throughout the years in safety and practicality.

Nevertheless, each method has its own advantages and disadvantages and the method should be chosen according to demands of the study.

2.6.3 Reverse genetics

When a reverse genetics approach is taken, a gene of interest is mutated with some of the methods available for targeted mutagenesis (Lawson and Wolfe, 2011). For zebrafish, there are several methods available for silencing a gene at the larval stage and also for generating stable mutant lines (reviewed in Parant and Yeh, 2016; Lawson and Wolfe, 2011).

Morpholino oligonucleotide knockdown is a technique in which either translation or splicing of mRNA is inhibited with a custom made oligo which has morpholine backbone (Draper et al., 2001; Summerton and Weller, 1997; Partridge et al., 1996). The successful delivery of morpholinos and their antisense activity was first demonstrated in HeLa cells (Partridge et al., 1996). In whole organisms, morpholinos were first used in the mouse (Qin et al., 2000), rat (Arora et al., 2000) and *Xenopus* (Lawson and Wolfe, 2011; Heasman et al., 2000), but was then applied to zebrafish (Nasevicius and Ekker, 2000). Morpholinos are injected into the yolk sac of early stage zebrafish embryos with the effect lasting only a few days depending on the characteristics of the target mRNA (Heasman, 2002; Nasevicius and Ekker, 2000). Moreover, knockdown may be disrupted by maternal contribution (Lawson, 2016; Borovina and Ciruna, 2013). The efficiency of splice blocking morpholinos can be controlled by analyzing the target mRNA with reverse transcriptase PCR (Draper et al., 2001). Controlling for translation blocking morpholinos is done by either immunostaining or western blotting, but the poor availability of zebrafish antibodies required for both presents a problem (Heasman, 2002). A few years ago, morpholinos were heavily criticized because of off-target effects (Lawson, 2016; Kok et al., 2015). However, problematic genetic compensation occurs in fish mutants but not when using morpholino knockdown (Tian et al., 2017; Rossi et al., 2015). Moreover, gene silencing with morpholinos is easy to conduct because the injection technique is simple, allowing large sample sizes.

To overcome the limitations of morpholinos, other methods to generate targeted mutations have been developed such as Targeting Induced Local Lesions IN Genomes (TILLING), Zinc-Finger Nucleases (ZFN) and Transcription Activator-like Effector Nucleases (TALENs) (Parant and Yeh, 2016; Lawson and Wolfe, 2011). When TILLING is applied to zebrafish, chemically mutagenized males are

used to produce a F1 generation from which mutations are identified with the help of various methods (Parant and Yeh, 2016; Lawson and Wolfe, 2011; Wienholds et al., 2003; Wienholds et al., 2002). Nowadays this is usually done with next-generation sequencing like in the Sanger Institute Zebrafish Mutation Project (Kettleborough et al., 2013).

The Clustered Regularly Interspaced Short Palindromic Repeats (CRISPR)/ CRISPR-associated (Cas) system has gained popularity in different model organisms as a method to produce mutants (Parant and Yeh, 2016; Wiedenheft et al., 2012). Target-specific single-guide RNA (sgRNA) forms together with Cas9, a complex which binds to foreign DNA and causes a double stranded break (Jinek et al., 2013; Jinek et al., 2012). After this a DNA repair pathway is activated (Ran et al., 2013). The non-homologous end joining (NHEJ) mechanism causes random insertion or deletion (indel) at the cut site, possibly resulting in a frameshift mutation and stop codon (Ran et al., 2013; Perez et al., 2008). Alternatively, a repair template can be used which may result in homology-directed repair (HDR) and small modifications, like single nucleotide changes, in the genome (Ran et al., 2013; Chen et al., 2011). To use this method in zebrafish, sgRNA and Cas9-encoding RNA or Cas9 protein are injected into the cell of 1-cell-stage embryos (Hwang et al., 2013; Gagnon et al., 2014). Off-target mutations are also a concern with this method but the number can be decreased with careful guide design (Parant and Yeh, 2016; Fu et al., 2013). Another problem is the possibility the mutated gene is compensated by another, resulting in absence of the desired phenotype (Tian et al., 2017; Lawson, 2016; Rossi et al., 2015). Furthermore, some genes are difficult to target due to a restricting chromatin structure (Uusi-Mäkelä et al., 2018). Combining both knockdown and knockout, for example morpholino and CRISPR/Cas9, allows more certain results.

2.7 Interleukin 10

Interleukin 10 (IL10) is an anti-inflammatory cytokine (reviewed in Neumann et al., 2019; Ouyang and O'Garra, 2019; Wei et al., 2019; Moore et al., 2001). First observed in mouse cell studies, IL10 is secreted by Th2 cells and inhibits Th1 cells from secreting cytokines, which explains its original name, cytokine synthesis inhibitory factor (CSIF) (Moore et al., 1990; Fiorentino et al., 1989). However, other types of T cells also produce IL10: type 1 regulatory T cells (Groux et al., 1997), Th1 cells (Anderson et al., 2007; Jankovic et al., 2007), Th17 cells (Aschenbrenner et al., 2018) and CD8+ T cells (Richards et al., 2000; Kohyama et al., 1998). Other immune cells

producing IL10 are monocytes (Lenart et al., 2017), macrophages (Fiorentino et al., 1991), dendritic cells (Dillon et al., 2006), B cells (reviewed in Shen and Fillatreau, 2015), mast cells (Masuda et al., 2002), eosinophils (Huang et al., 2014) and NK cells (Lee et al., 2009). Even non-immune cells, including keratinocytes (da Silva et al., 2018), epithelial cells (Rabiei et al., 2019) and tumor cells (Sato et al., 1996) secrete IL10. IL10 is essential for preventing autoinflammation for example in the mouse gut, since IL10 deficient mice develop enterocolitis over time (Gomes-Santos et al., 2012).

IL10 activates several signaling cascades affecting many cells (Verma et al., 2016). Induction of JAK/SAT signaling by IL10 has been shown in human T cells and monocytes (Finbloom and Winestock, 1995). The role of the JAK/STAT cascade in inhibiting proinflammatory responses was demonstrated by a study where IL10 treated JAK1 or STAT3 deficient murine macrophages were unable to inhibit lipopolysaccharide induced TNF production (Riley et al., 1999). IL10 also activates the p38 mitogen-activated protein kinase (MAPK) pathway, which has been shown to result in the induction of anti-inflammatory heme oxygenase-1 production from murine macrophages (Lee and Chau, 2002).

The association of several IL10 polymorphisms with tuberculosis has been investigated in several studies (Yu et al., 2019; Redford et al., 2011; Zhang et al., 2011). The outcome of the studies seems to be dependent on the polymorphism under study and the ethnic background of the study subjects, thus results vary from susceptibility to protection or to no effect (Yu et al., 2019; Asgharzadeh et al., 2016; Redford et al., 2011; Zhang et al., 2011; Pacheco at al., 2008; Shin et al., 2005; Delgado et al., 2002; Bellamy et al., 1998). There are however, also other studies on the role of IL10 during mycobacterial infection. Differential expression of IL10 and its receptor alpha/CD210 has been detected in mice lungs at several time-points following aerosol infection with *M. tuberculosis* (Gonzalez-Juarrero et al., 2009). Enhanced secretion of IL10 from bone marrow derived macrophages after *M. tuberculosis* infection has been associated with resistant mouse strains (Keller et al., 2004). In contrast to this, it has been shown that following intravenous *M. tuberculosis* infection, T cells from susceptible mice produced more IL10, whereas cells from resistant mouse strains produced more IFNG (Lyadova et al., 2000). In addition to the different cell type analyzed, this difference may be due to the different infection routes and different mouse strains used. Different mouse and bacterial strains and laboratory conditions for example may affect mouse gut flora and are considered to contribute to the sometimes contradictory results gained from IL10 mouse studies (Abdalla et al., 2016; Redford et al., 2011). There are also many mouse studies about

the effect of IL10 deficiency on Th1 cell response and IFNG production during *M. tuberculosis* infection (Cyktor et al., 2013; Redford et al., 2010; Beamer et al., 2008). These studies indicate that a lack of functional IL10 signaling leads to an enhanced Th1 cell mediated response.

Il10 has been identified in zebrafish and its expression in various tissues and its conserved structure across species has been shown (Piazzon et al., 2016; Zhang et al., 2005). Moreover, the Il10 receptor 1 has been found and studied in zebrafish and goldfish and the results suggest conservation throughout evolution (Grayfer and Belosevic, 2012). Since the role of IL10 during *M. tuberculosis* infection is not unambiguous, the role of this protein is worth studying also in the *M. marinum* zebrafish infection model.

3 AIMS OF THE STUDY

The complexity of the disease caused by *M. tuberculosis* and constantly emerging new drug resistant strains guarantee that the battle against tuberculosis is far from over. By estimation, 22% of the world's population carries latent tuberculosis infection, and the existing vaccine does not prevent its transmittion or development into active disease (WHO, Global Tuberculosis Report, 2019; Tang et al., 2016). There are also no diagnostic means available to reliably predict reactivation (Furin et al., 2019; Rangaka et al., 2012). In order to develop new treatments, the genes having a role in defense mechanisms against mycobacterial infection should be better characterized. The effect of the host's genetic background on the outcome of tuberculosis is recognized in numerous genome-wide association and candidate gene studies, but also in *in vitro* and *in vivo* studies using patient samples or animal models. Characterization of the effect of different genetic variations requires *in vivo* studies since defense against tuberculosis is an interplay of several cell types. An ideal animal model for tuberculosis research has been lacking. It should mimic the whole disease spectrum, including spontaneous latency, and also allow for large-scale experiments and also take into account ethical aspects. In this thesis, *M. marinum* infection in zebrafish was considered as a model meeting these terms.

The specific aims of this study were:

1) To use histological methods and transcriptional analysis to study the progression of *M. marinum* infection in adult zebrafish.
2) To use the developed model to study the role of *il10* in *M. marinum* infection in zebrafish.
3) To perform a forward genetic screen to identify host genes involved in the immune defense against *M. marinum* in adult zebrafish.

4 MATERIALS AND METHODS

4.1 Zebrafish maintenance I-III

In this study 3-15 month-old zebrafish from two wild type (WT) lines, the AB and the TL (*Tüpfel long fin, gja*$^{t1/t1}$, *lof*$^{tl2/tl2}$) (from Tampere Zebrafish Core Facility), and two mutant lines, the *il10*^{e46} (both homozygous and WT fish) (from Wellcome Trust Sanger Institute, Hinxton, Cambridgeshire, UK; Kettleborough et al., 2013) and the *rag1*^{hu1999} (homozygous fish) (from ZIRC, Zebrafish International Resource Center, University of Oregon, Eugene, Oregon, USA) were used. The fish were maintained based on standard protocols (Nüsslein-Volhard and Dahm, 2002). Briefly, zebrafish embryos were kept on Petri dishes in embryonic medium (5 mM NaCL, 0.17 mM KCl, 0.33 mM $CaCl_2$, 0.33 mM $MgSO_4$, 10% methylene blue) at 28.5 °C. They were fed SDS100 (Special Diet Services, Witham, Essex, UK) or GEMMA Micro 75 (Skretting, Stavanger, Norway) dry food starting at 5 days post fertilization (dpf). At 6 dpf, they were transferred to tanks in a flow-through system (Aquatic Habitats, Apopka, Florida, USA). The unchallenged adult zebrafish were maintained in this system at 28 °C with a light/dark cycle of 14/10 hours and fed SDS 400 (Special Diet Services) and in-house grown *Artemia nauplia* both once a day or alternatively once a day with GEMMA Micro 500 (Skretting). Infected fish were maintained similarly in a flow-through system (Aquatic Habitats or Aqua Schwarz GmbH, Göttingen Germany) and fed twice a day with SDS 400 or once a day with GEMMA Micro 500.

4.2 Ethics statement I-III

All experiments, breeding and maintaining of zebrafish during this study have been approved by the Animal Experiment Board in Finland (permits: LSLH-2007-7254/Ym-23, ESAVI/10079/04.10.06/2015, ESLH-2008-07610/Ym-23, ESAVI-2010-08379/Ym-23, ESAVI-2106/04.10.03/2011, ESAVI/4234/04.10.03/2012, ESAVI/6403/04.10.03/2012, ESAVI/8125/04.10.07/2013, ESAVI/10823/04.10.07/2016, ESAVI/6407/04.10.03/2012,

ESAVI/733/04.10.07/2013, ESAVI/8108/04.10.07/2015, ESAVI/10366/04.10.07/2016, ESAVI/2464/04.10.07/2017, ESAVI/2776/2019 and ESAVI/10539/2019). In addition, this work was performed according to the Finnish Act of the Protection of Animals Used for Scientific or Educational Purposes (497/2013) and the EU Directive on the Protection of Animals used for Scientific Purposes (2010/63/EU). The well-being of unchallenged and infected zebrafish was followed daily throughout this study and fish meeting the humane endpoint criteria determined in the animal experiment permits were euthanized with an overdose of 3-aminobenzoic acid ethyl ester, tricaine (Sigma-Aldrich, St. Louis, Missouri, USA) (pH = 7.0).

4.3 Experimental *M. marinum* infections I, II, III

4.3.1 Bacterial culture I, II, III

M. marinum strain ATCC 927 was cultured as previously done (Swaim et al., 2006) with two exceptions: culturing was done at 29 °C and in the liquid culture 0.2% Tween 80 (Sigma-Aldrich) was used. *M. marinum* was cultured on 7H10 agar plates (Becton, Dickinson and Company (BD), Franklin Lakes, New Jersey, USA). For experiments, approximately after one week of culturing, bacteria were transferred to liquid 7H9 medium (BD) and cultured for three to four days. After that approximately 1 ml of *M. marinum* suspension was added to 9 ml of fresh medium and the dilution cultured for two days to reach an optical density (OD) at 600 nm of 0.495-0.680.

For performing infections, *M. marinum* was resuspended in 0.2 M KCl or phosphate buffered saline (PBS) and diluted to the desired concentration. In addition, the dilution included 0.3 mg/ml phenol red (Sigma-Aldrich) for visualization, and when performing yolk sac infections also 2% polyvinylpyrrolidone-40 (Sigma-Aldrich) was included for maintaining the suspension of bacteria. The final infection dose was confirmed by plating the injected suspension on 7H10 agar.

4.3.2 Experimental infection in zebrafish embryos II, III

In the second original communication II, zebrafish embryos were infected at 0-6 hours post fertilization (hpf) by injecting 1 nl of diluted *M. marinum* suspension into yolk sac using aluminosilicate capillary needles (Sutter Instruments Co., Novato, California, USA), a micromanipulator (Narishige International, London, UK) and a PV830 Pneumatic PicoPump microinjector (World Precision Instruments, Sarasota, Florida, USA). In the third original communication, III, at 1 day post fertilization (dpf), zebrafish embryos were dechorionated, anesthetized with 0.02% tricaine and infected by injecting 2 nl of diluted *M. marinum* suspension into the caudal vein with borosilicate capillary needles (Sutter Instruments Co.) using a micromanipulator and a microinjector.

When injected into the yolk sac, zebrafish embryos were kept in embryonic medium at 28.5 °C on Petri dishes until 1 day post infection (dpi) and then placed on 24-well plates, one embryo per well. Embryos were dechorionated at 2 dpi and their survival was checked once a day until 7 dpi. When injected into the caudal vein, the embryos were treated similarly but dechorionation was done before infections. At the end of the experiment the remaining larvae were euthanized with an overdose of tricaine and survival was analyzed by drawing Kaplan-Meier survival curves.

4.3.3 Experimental infection in adult zebrafish I, II, III

Adult zebrafish were anesthetized with 0.02% tricaine and infected by injecting 5 µl of diluted *M. marinum* suspension into the abdominal cavity with a 30 gauge Omnican 100 insulin needle (Braun, Melsungen, Germany).

During the follow-up period, adult zebrafish were kept in a stand-alone flow-through system (Aquatic Habitats or Aqua Schwarz). Their well-being was checked once or twice a day and they were euthanized with an overdose of tricaine when humane end-point criteria defined in the animal experiment permits were met. At the end of the experiment the remaining fish were euthanized. Kaplan-Meier survival curves were drawn to analyze survival of the fish.

4.4 Experimental *S. pneumoniae* infections III

S. pneumoniae WT strain TIGR4 (T4), of serotype 4 and sequence type 205 (Aaberge et al., 1995), was cultured and inoculated into zebrafish as previously done (Rounioja

et al., 2012). Briefly, T4 was grown at 37 °C and 5% CO_2 overnight on 5% lamb blood agar plates (Tammer-Tutkan maljat Oy, Tampere, Finland). After this, T4 was transferred to 5 ml of Todd Hewitt broth (BD) and grown from an OD_{620} of 0.1 to an OD_{620} of 0.4. At 2 dpf, zebrafish embryos were anesthetized with 0.02% tricaine and infected by injecting 2 nl of bacteria suspended in 0.2 M KCl including 1% 70 kDa Rhodamine Dextran (Invitrogen™, Thermo Fisher Scientific, Waltham, Massachusetts, USA) into the blood circulation valley with a borosilicate capillary using a micromanipulator and microinjector.

During a five-day follow-up the survival of embryos/larvae was checked once a day. At the end of the experiment, the remaining fish were euthanized with an overdose of tricaine and Kaplan-Meier survival curves were drawn to analyze survival of the fish. The final infection dose was confirmed by plating the injected suspension on 5% lamb blood agar.

4.5 Nucleic acid extraction II, III

For nucleic acid extractions from internal organs, adult zebrafish were euthanized with an overdose of tricaine and organs from the abdominal cavity were collected separately or as a block on dry ice and transferred to -80 °C for storage. Before extraction the reagent chosen based on the extraction protocol was added to samples. After this, samples were homogenized with the PowerLyzer24 (Mobio, Carlsbad, California, USA) at a speed of 3,200 for 40 seconds three times with 30 second pauses in between.

4.5.1 Total RNA extraction III

Total RNA from adult zebrafish kidney for the RNA sequencing and qPCR was extracted with the RNeasy Mini Kit (Qiagen, Hilden, Germany). After homogenization, the manufacturer's protocol was followed. The RapidOut DNA Removal Kit (Thermo Scientific, Thermo Fisher Scientific) was used to remove the remaining genomic DNA from samples. The NanoDrop™ 2000 Spectrophotometer (Thermo Scientific, Thermo Fisher Scientific) was used to check purity of the samples and the Qubit™ RNA BR Assay Kit (Invitrogen™, Thermo Fisher Scientific) to measure concentrations. The Fragment Analyzer (Advanced Analytical Technologies, Ankeny, Iowa, USA), the Standard Sensitivity RNA Analysis Kit

(Advance Analytical Technologies) and the PROSize® 2.0 Data Analysis Software (Advanced Analytical Technologies) were used to choose samples with an RNA integrity number (RIN) ≥ 7.8 for RNA sequencing.

4.5.2 RNA-DNA coextraction II, III

RNA and DNA were extracted using TRI Reagent® (Molecular Research Center, Cincinnati, Ohio, USA). After homogenization, tissue samples were sonicated in a water bath sonicator (m08, Finnsonic, Lahti, Finland) for nine minutes. From this point on, the manufacturer's protocol was followed. The RapidOut DNA Removal Kit was used to remove the remaining genomic DNA from the RNA samples. NanoDrop™ 2000 Spectrophotometer (Thermo Scientific, Thermo Fisher Scientific) was used to check the purity of samples and measure concentrations.

4.6 Genotyping II, III

For genotyping, genomic DNA of zebrafish was extracted from a tail fin cut. For cutting tail fins, zebrafish were anesthetized with 0.02% tricaine. The cut tail fins were incubated overnight in 100 µl of lysis buffer (10 mM Tris (pH 8.2), 10 mM ethylenediaminetetraacetic acid (EDTA), 200 mM NaCl, 0.5% sodium dodecyl sulfate (SDS) and 200 µg/µl Proteinase K (Thermo Scientific, Thermo Fisher Scientific)). After this, DNA was extracted from the resulting homogenous lysate following a standard ethanol precipitation protocol.

The genotypes of *il10*$^{e46/e46}$ and *rag*$^{hu1999/hu1999}$ were determined with Sanger sequencing. For this, the mutation site was amplified by PCR from genomic DNA. The sequences of the used primers are given in Table 3.

Table 3. Primers used to amplify mutation sites for sequencing.

Gene	ZFIN ID	Sequence 5'-3'	Reference	Used in
il10	ZDB-GENE-051111-1	F: GCTCTGCTCACGCTTCTTCT R: AACGGAGCTCCCTCAGTCTT	F: Kizil et al. 2012	II
rag1	ZDB-GENE-990415-234	F: CAGCCATGATGAAAATCTCG R: TCAGTCGCATTGCCAATATC		III

4.7 Quantification of *M. marinum* II, III

The *M. marinum* burden (colony forming units, CFU) was determined from DNA extracted from abdominal organ blocks (+/- kidney) with qPCR using *M. marinum* specific primers designed for 16S-23S ITS sequence (forward: 5'-caccacgagaaacactccaa-3', reverse: 5'-acatcccgaaaccaacagag-3') and the Sensifast™ SYBR® No-ROX (Bioline, London, UK) kit, following the manufacturer's protocol. The CFX96 qPCR machine (Bio-Rad, Hercules, California, USA) and CFX Manager software v1.6 or v3.1 (Bio-Rad) were used to perform the analysis. Non-template controls were used to exclude contamination and unchallenged zebrafish were used as a negative control. The specificity of qPCR products was confirmed by a melt curve analysis and 1.5% TAE agarose gel electrophoresis from random samples.

4.8 Quantification of gene expression II, III

4.8.1 qPCR II, III

cDNA synthesis was performed with the SensiFAST™ cDNA synthesis kit (BioLine). Following the manufacturer's protocol, PowerUp™ SYBR® master mix (Applied Biosystems™, Thermo Fisher Scientific) was then used to perform qPCR to quantify the relative gene expression levels of target genes. The sequences of the used primers are given in Table 4. The expression levels relative to the expression of *eukaryotic translation elongation factor 1 alpha 1, like 1* (*eef1a1l1*) was calculated with the $2^{-\Delta Ct}$ method (Tang et al., 2007). The CFX96 qPCR machine (Bio-Rad) and CFX Manager software v1.6 or v3.1 (Bio-Rad) were used to perform the analysis. Genomic DNA and other contamination were excluded by including no reverse transcriptase controls from random RNA samples and non-template controls in qPCR runs. The specificity of qPCR products was confirmed by a melt curve analysis and 1.5% TAE agarose gel electrophoresis from random samples. In the expression analysis a Ct value of 40 was given to samples with no PCR product or a product with an incorrect melt curve.

Table 4. Primers used for gene expression analysis by qPCR.

Gene	ZFIN ID	Sequence 5'-3'	Reference	Used in
eef1a1l1	ZDB-GENE-990415-52	F: CTGGAGGCCAGCTCAAACAT R: ATCAAGAAGAGTAGTACCGCTAGCATTAC	Tang et al., 2007	II, III
il10	ZDB-GENE-051111-1	F: GCTCTGCTCACGCTTCTTCT R: AACGGAGCTCCCTCAGTCTT	F: Kizil et al., 2012	II
tnfa	ZDB-GENE-050317-1	F: GGGCAATCAACAAGATGGAAG R: GCAGCTGATGTGCAAAGACAC		II
tnfb	ZDB-GENE-050601-2	F: GCATGTGATGAAGCCAAACG R: GATTGTCCTGAAGGGTCACC		II
Il1b	ZDB-GENE-040702-2	F: TGGACTTCGCAGCACAAAATG R: GTTCACTTCACGCTCTTGGATG	Pressley et al., 2005	II
cd4-1	ZDB-GENE-100922-280	F: TAAAGCACAAGAAAGCCATG R: TACTCTGCGGGTTCCTGTTG		II
cd8a	ZDB-GENE-060210-2	F: GGAGTACCAGATCCAGTAACACAC R: AACCTCCGACCAGAGATGTG		II
IgM (ighm)	ZDB-GENE-030925-46	F: AGATCCAATACAAAGATACTATGC R: TGGTGAAATGGAATTGTGG	Yoon et al., 2015	II
tbx21	ZDB-GENE-080104-3	F: GGCCTACCAGAATGCAGACA R: GGTGCGTACAGCGTGTCATA	Hammarén et al., 2014	II
gata3	ZDB-GENE-990415-82	F: GGATGGCACCGGTCACTATT R: CAGCAGACAGCCTCCGTTT	Hammarén et al., 2014	II
foxp3a	ZDB-GENE-061116-2	F: CAAAAGCAGAGTGCCAGTGG R: CGCATAAGCAC CGATTCTGC	Hammarén et al., 2014	II
ifng1	ZDB-GENE-040629-1	F: CTTTCCAGGCAAGAGTGCAGA R: TCAGCTCAAACAAAGCCTTTCG	Vojtech et al., 2009	II
il4	ZDB-GENE-100204-1	F: CCAGAGTGTGAATGGGATCC R: TTTCCAGTCCCGGTATATGC		II
fabp6	ZDB-GENE-040625-49	F: CTGCAAACTGATCGGTATCC R: GCTCTCTTTGCCTACGATGA		III
scd	ZDB-GENE-031106-3	F: ATGGCCTTCCAGAATGACAT R: CTAGTTTGCGTCCTCTCTCG		III
unc119b	ZDB-GENE-050201-2	F: CATCCCCATCAATAACTTCC R: CTCACGAATGAGATCCTCAG		III
si:ch211-236p5.3	ZDB-GENE-081028-31	F: GGACAAGCTCAACATGGATA R: CTGCTTCATTGTCACAAGTG		III

4.8.2 mRNA sequencing III

The cDNA library for mRNA sequencing was prepared and RNA sequencing itself was performed at Novogene, Hong Kong. The 150 bp paired-end sequencing of the 250-300 bp DNA library was performed on the Illumina platform reaching a sequencing depth of > 20 million reads/sample.

FastQC (Andrews, 2010) was used for quality checking reads and STAR with default parameters (Dobin et al., 2013) used to align reads against the GRCz10 reference genome. Feature Counts (Liao et al., 2014) using Ensembl GRCz10.91 (Hubbard et al., 2002) as the reference gene set was used to quantify gene expression. R-package DeSeq2 was used to normalize raw expressions and to find differentially expressed genes (Love et al., 2014). In further analysis, genes with ≥ 3-fold change

between groups as determined by DeSeq2 and ≥ 3-fold difference in group medians were considered differentially expressed. Furthermore, only genes having at least two samples with ≥ 20 normalized reads in the same group were considered.

The GO Enrichment Analysis (GO Ontology Database released 1st of January and Panther Overrepresentation Test released 13th of November, 2018) were used to perform further analysis (The Gene Ontology Consortium, 2019; Mi et al., 2017; Ashburner et al., 2000). Since this tool did not recognize all genes, upregulated genes were also classified based on data available in the Ensembl genome browser (Zerbino et al., 2018) versions 91 and 95, Reactome (Fabregat et al., 2018), the Zebrafish Information Network ZFIN (Howe et al., 2013), InterPro (Mitchell et al., 2019), the PROSITE database (Sigrist et al., 2013), Pfam 32.0 (El-Gebali et al., 2019), NCBI gene database (Gene, 2004), the NCBI BioSystems database (Geer et al., 2010) and literature and downregulated genes based on the Gene Ontology process data available in Ensembl, ZFIN and NCBI gene databases. The preferred name, if given in the NCBI gene database, was used as the gene name if the gene concerned lacked an official name/description.

4.9 Immunosuppression for induction of reactivation I

In order to cause immunosuppression and reactivate latent *M. marinum* infection in adult zebrafish, we placed adult zebrafish at a density of 5 fish/80 ml of water in glass flasks and treated fish with 25 Gray (Gy) of γ-irradiation using Gammacell® 1000 irradiator (Best™ Theratronics Ltd, Ottawa, Ontario, Canada). Uninfected zebrafish were similarly treated to use as controls.

4.10 A forward genetic screen for identifying genes affecting *M. marinum* infection in adult zebrafish III

The gene-breaking Tol2 transposon-based mutagenesis method was used to produce mutant zebrafish carrying random mutations for forward genetic screen. Plasmids used, pGBT-RP2-1 (addgene #31828) and pT3TS-Tol2 (addgene #31831) were a generous gift from Professor Stephen C. Ekker's laboratory (Mayo Clinic, Rochester, Minnesota, USA) (Clark et al., 2011). After both plasmids were transformed into *E. coli* One Shot TOP10 cells (Invitrogen™, Thermo Fisher Scientific), the QIAGEN Plasmid Plus Maxi Kit (Qiagen) was used to extract plasmid DNA. The success of

transformation was checked by sequencing. The pT3TS-Tol2 plasmid was digested with FastDigest BamHI (Thermo Scientific, Thermo Fisher Scientific). The resulting linearized plasmid was used as a template for *in vitro* transcription when *tol2* mRNA was produced with the mMessage mMachine Transcription Kit following the manufacturer's protocol (Invitrogen™, Thermo Fisher Scientific).

For mutagenesis, WT AB zebrafish embryos were microinjected into the cell at the 1-cell stage with 12.5 pg of both the pGBT-RP2-1 plasmid and *tol2* mRNA in 1xPBS containing 0.6% phenol red (Sigma-Aldrich). Embryos carrying transposons, that is, successfully injected embryos, were selected based on the mosaic expression of *GFP* using either a Lumar V.12 fluorescence stereomicroscope (Carl Zeiss MicroImaging GMBH, Göttingen, Germany) or Nikon AZ100 Fluorescence Macroscope (Nikon, Minato, Tokyo, Japan). These embryos were the founder fish in the genetic screen and designated as F0.

In order to produce zebrafish mutant lines, the F0 generation was crossed according to the breeding scheme presented in Figure 4. First, F0 fish were crossed to WT TL which produced the F1 generation in which each F1 individual is in theory heterozygous for different mutations. F1 fish were designated with a running number, which is also the name of the resulting mutant zebrafish lines. F1 zebrafish were then outcrossed to TL, which resulted in the F2 generation consisting of fish heterozygous for the mutations from the F1 generation. When the F2 generation was incrossed, the result was a F3 generation having 25% homozygous, 50% heterozygous and 25% WT fish with regards to mutations. The F3 generation was incrossed until a F5 generation to produce mutant fish for the screen. Some lines were outcrossed again to TL in order to ensure the line. For *M. marinum* infection experiments in larvae, an F7 generation was produced from one line. In each generation, the transposon (mutation) carrying embryos were chosen based on *GFP* expression. To screen for mutant lines with altered susceptibility to *M. marinum* infection, adult zebrafish were infected with a low-dose of *M. marinum* as described in chapter 4.3.3 "Experimental infection in adult zebrafish".

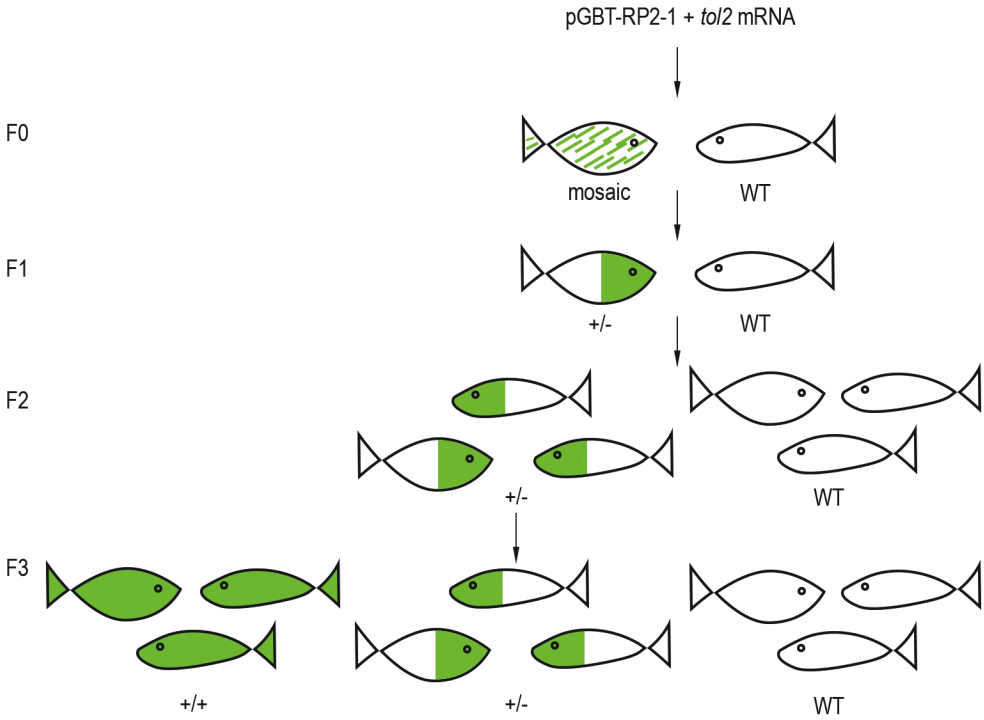

Figure 4. Schematic presentation of crossing zebrafish for the forward genetic screen. WT = wild type, +/- heterozygous, +/+ homozygous.

4.11 Histological analysis I, II

For histological analysis, adult zebrafish were euthanized with an overdose of tricaine and torsos were excised and incubated for 5-11 days in 10% phosphate buffered formalin (pH 7.0) at room temperature (RT) for fixing. Following this, decalcification was performed by incubating samples in 20% EDTA-citrate (pH 7.2) for seven days at RT after which samples were incubated in rising ethanol series, transferred to xylene and embedded in paraffin. The samples were longitudinally cut and 5 μm sections were placed on slides, leaving 200 μm in between saved sections. Ziehl-Neelsen and Mallory's trichrome stainings were carried out according to standard protocols. In the original communication I, stained sections were analyzed with 200x magnification using BX51 microscope (Olympus, Shinjuku, Tokyo, Japan). In the second original communication II, slides were scanned into a digitized

form at a resolution of 0.4 μm/pixel using an Objective Imaging Surveyor virtual slide scanner (Objective Imaging, Cambridge, United Kingdom) and 20x Plan Apochromatic microscope objective, converted to JPEG2000 format as described previously (Tuominen and Isola, 2009) and analyzed similarly to Myllymäki and colleagues (2018).

4.12 Flow cytometry II

Flow cytometry analysis from adult zebrafish kidney blood cells was carried out as previously described (Ojanen et al., 2015; Langenau et al., 2004). Briefly, adult zebrafish were euthanized with an overdose of tricaine, their kidneys collected, suspended in 1xPBS supplemented with 0.5% fetal bovine serum (Gibco/Thermo Fisher Scientific) and filtered through 35 μm cell strainer caps (Corning/Thermo Fisher Scientific). After this, runs were performed with a FACSCanto II (BD) instrument. Data analysis was carried out based on Langenau and colleagues (2004) using FlowJo program, version 7.5 (Tree Star Inc, Ashland, Oregon, USA) to determine relative amounts of lymphocytes, blood cell precursors and myeloid cells in samples. The remaining kidney blood cell samples were washed with 1xPBS and stored for RNA extractions in TRI Reagent® at -20 °C and other abdominal organs of fish were stored for DNA extractions at -80 °C to determine gene expression and *M. marinum* quantity, respectively.

4.13 Imaging of zebrafish intestine II

A Nikon SMZ745T microscope and DS-Vi1 camera (Nikon) were used to photograph the intestine of *il10*$^{e46/e46}$ mutants and WT zebrafish. NIS-Elements D 4.2 software (Nikon) was used to measure the scale bar.

4.14 Whole genome sequencing II

For whole genome sequencing, DNA from abdominal organs of 10 adult zebrafish were pooled together for one sample. RNA removal, DNA library preparation and 150 bp paired-end sequencing on the Illumina platform were performed at the

Institute for Molecular Medicine Finland FIMM Technology Centre, Helsinki, Finland, reaching a sequencing depth of > 110 gigabases/sample.

Cutadapt-1.11 (Martin, 2011) in paired mode and an in-house algorithm were used to trim adapters and low-quality bases at read ends, respectively, from paired-end reads. Bowtie-2.3.0 (Langmead and Salzberg, 2012) was then used to align reads against the GRCz11 zebrafish genome and samblaster0.1.24 (Faust and Hall, 2014) to remove optical and PCR duplicates. An in-house pipeline and ANNOVAR (Wang et al., 2010) were used to identify mutations from samples and to annotate mutations and their effects at the protein level, respectively. The final list of frameshift and stop-gain mutations was checked with Integrative Genomics Viewer (IGV) (Robinson et al., 2011) to discard false positives.

4.15 Statistical analysis I, II, III

Prism program, version 5.02 (GraphPad Software Inc, San Diego, California, USA) was used to analyze statistical significance of survival, flow cytometry and qPCR results. For survival data a log-rank (Mantel-Cox) test, flow cytometry data a non-parametric two-tailed Mann-Whitney and for qPCR data a one- or two-tailed Mann-Whitney (two groups) or Kruskal-Wallis test with Dunn's multiple comparison post-test (three groups) were used. *P* values for each mutation found in the whole genome sequencing (II) were determined between the two sample groups with Fisher's exact test. For statistical analysis of the gene ontology enrichment analyses (III), Fisher's exact test was used with Bonferroni correction. In all analyses, $P < 0.05$ was considered significant.

5 SUMMARY OF THE RESULTS

5.1 Adult zebrafish model for tuberculosis I, II, III

5.1.1 Granuloma formation during *M. marinum* infection in adult zebrafish I, II, III

In publication I, we studied the progression of systemic *M. marinum* infection in adult zebrafish. This thesis concentrates on the histological analysis of this infection. In publication I, adult zebrafish were infected by injecting a low-dose (34 ± 15 CFU) or a high-dose (2029 ± 709 CFU) of *M. marinum* into the abdominal cavity. The histopathological features of the infection were studied in longitudinal sections mainly with Ziehl-Neelsen staining at the time-points 2, 4, 8 and 20 wpi.

In this analysis, gonads, pancreas, liver, spleen, gut and kidney, in addition to mesentery and muscle were examined for granulomas and free bacteria. Of note, the severity of the disease was dependent on infection dose. A low-dose infection resulted in a stable number of granulomas and infected organs from 4 wpi onwards whereas in high-dose infection bacteria were more widely spread already at 2 wpi and the number of granulomas kept rising until the last analyzed time-point, 20 wpi (Figures 1C-D in I). This demonstrates that a low-dose infection spontaneously leads to a latent state of *M. marinum* infection in most zebrafish individuals whereas a high-dose leads to progressive disease.

Histological analysis showed that granulomas formed during the course of infection regardless of the initial dose (Figures 1D and 2 in I). At the first analyzed time-point, 2 wpi, there were areas with free bacteria (Figure 2C in I). In addition, there were areas representing early granulomas (Figure 2A in I), lacking the surrounding fibrous capsule, as analyzed with Mallory's trichrome staining (Figure 2B in I). As the infection proceeded, clearer granulomas with bacterial aggregates were seen (Figures 2D and F in I). Formation of granulomas was further verified with Mallory's trichrome staining, which showed the fibrous capsule surrounding the granuloma (Figures 2E in I). By the last time-point analyzed, 20 wpi, the majority of

mature granulomas were clearly separated from the surrounding tissue, surrounded by a fibrous or cellular layer, or both.

In original communication III, we performed a whole-genome level transcriptome analysis at 14 days post a low-dose (5-9 CFU) *M. marinum* infection from RNA extracted from the kidney. The kidney is the main hematopoietic organ of adult zebrafish (Willett et al., 1999; Willett et al., 1997) and was chosen in most of the analyses with the assumption that it would best reflect the gene expression of blood cell-related immunological genes. We indentified 96 upregulated and 105 downregulated genes (Figure 5). The transcriptome data reflects known responses to mycobacterial challenge. *M. marinum* bacilli are mainly engulfed by macrophages, which then induce a local proinflammatory response, secreting for example *TNF* and a set of various chemokines resulting in the recruitment of mononuclear cells and eventually leading to granuloma formation (Russell, 2007; Algood et al., 2004). In this analysis, one putative *microfibril-associated glycoprotein 4-like,* (*MFAP4*) variant was upregulated ≥ 3-fold compared to unchallenged zebrafish (Figure 6A). *mfap4* is known to be expressed in macrophages in mycobacterial granulomas (Walton et al., 2015). The expression level of *tnfa* as well as another inflammatory cytokine *il1b* was highest in fish with the highest *M. marinum* measured burden (Figure 6B). In addition, several chemokines and putative chemokines as well as two other genes, *CABZ01001434.1* and *relaxin family peptide receptor 1* (*rfxp1*) (Figueiredo et al., 2006), which or whose orthologs have a postulated or reported role in chemotaxis or cell migration, were upregulated (Figure 6C).

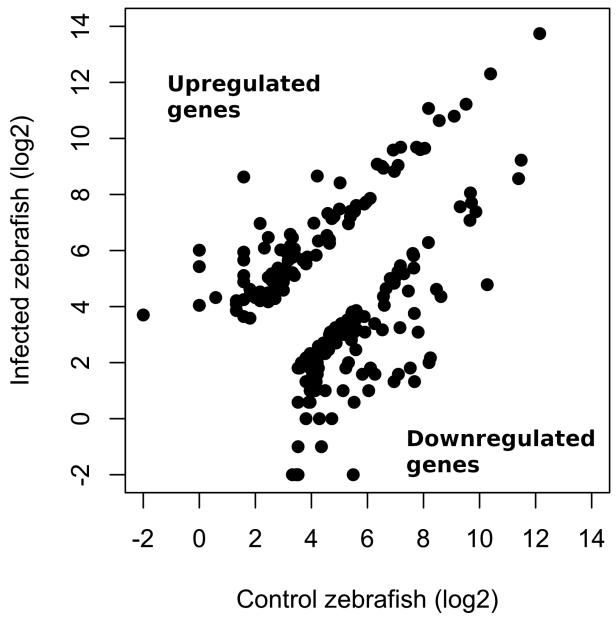

Figure 5. Upregulated and downregulated genes identified in the transcriptome analysis presented as a scatter plot. The fish were infected with a low dose (5-9 colony forming units, CFU) of *M. marinum* and the kidney samples were collected at 14 days post infection (dpi). Unchallenged zebrafish were used as a control group. The illustration presents the median of normalized reads (log2) in the infected fish group versus the median of normalized reads (log2) in the control fish group. If the median of normalized reads equals to 0, for this illustration the log2 value is set to -2. The figure was created with R (R Core team, 2016).

Related to the granuloma formation, we measured expression levels of proinflammatory cytokines *tnfa*, its paralog *tnfb* and *il1b* with qPCR during *M. marinum* infection (II). At 1 and 6 dpi there was no increase in expression of these genes in abdominal organs, but a significant decrease in *tnfa* expression compared to the mock (PBS) injected fish (Figures 4B-4D in II). This suggests that the inflammatory response is not yet induced at the early time-point of a low-dose infection. We also measured expression of these genes in kidneys of unchallenged fish and fish at 4 and 8 wpi (II) and saw an increase in the expression of all of these genes in the kidney compared to unchallenged fish (Figure 6D).

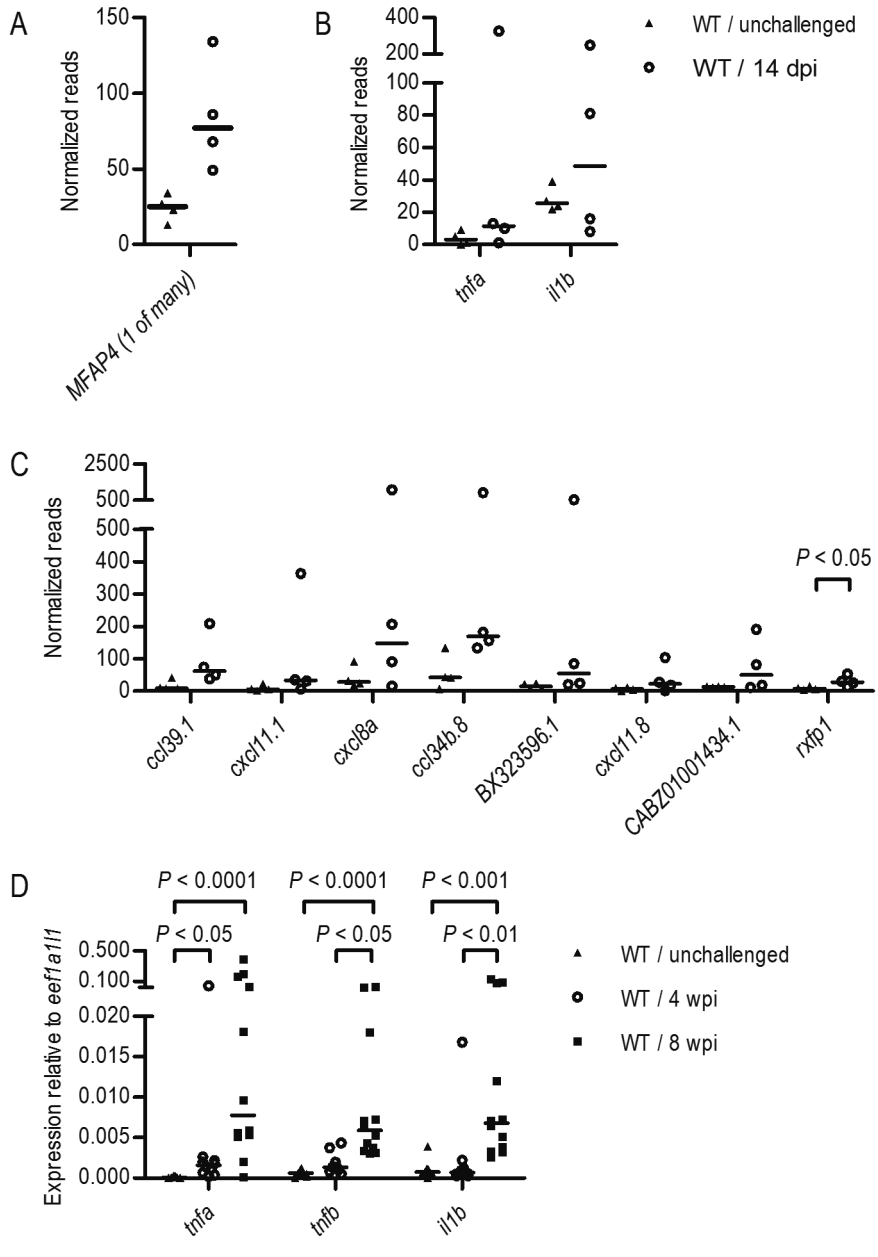

Figure 6. *M. marinum* infection in adult zebrafish induces expression of genes related to granuloma formation. A-C) Normalized read counts of the macrophage related gene, *MFAP4*, proinflammatory cytokines *tnfa* and *il1b* and genes related to chemotaxis and cell migration, were measured with RNA sequencing from kidneys of unchallenged wild type

(WT) and WT zebrafish at 14 days post a low-dose (5-9 colony forming units, CFU) *M. marinum* infection (*n* = 4 in both groups). Genes in panels A) and C) were induced ≥ 3-fold upon *M. marinum* infection. D) The expression of proinflammatory cytokines *tnfa*, *tnfb* and *il1b* were measured with qPCR from kidney cells of unchallenged WT (*n* = 10) and WT zebrafish at 4 and 8 weeks post low-dose (2-9 CFU) *M. marinum* infection (*n* = 10-12). Expression levels were normalized to expression of *eef1a1l1*. In panels A)-D) data are presented as a scatter dot plot and median. Note the different scales on *y*-axes and divided *y*-axis in panels B), C) and D). dpi = days post infection; wpi = weeks post infection. *MFAP = microfibril-associated glycoprotein 4-like*; *ccl39.1 = chemokine (C-C motif) ligand 39, duplicate 1*; *cxcl11.1 = chemokine (C-XC motif) ligand 11, duplicate 1*; *cxcl8a =chemokine (C-X-C motif) ligand 8a*; *ccl34b.8 = chemokine (C-C motif) ligand 34b, duplicate 8*; *cxcl11.8 = chemokine (C-X-C motif) ligand 11, duplicate 8*; *rxfp1 = relaxin family peptide receptor 1*.

5.1.2 The role of the innate immune response in the defense against *M. marinum* infection III

In our whole-genome level transcriptome analysis, most immune system related genes induced ≥ 3-fold at 14 days post a low-dose *M. marinum* infection are associated with the innate immune response (Figure 7; Tables 1-2 in III). This is expected because the adaptive immune response is not yet fully active at that point (reviewed in Liu et al., 2017; Robinson et al., 2015; Cooper, 2009; van Crevel et al., 2002). Even some upregulated genes primarily associated with the adaptive immune response, also have a role in innate immunity, for example *immunoglobulin heavy variable* (*ighv*) *5-5*, *immunoglobulin heavy variable* (*ighv*) *4-1* and *immunoglobulin heavy variable* (*ighv*) *13-2* (Table 2 in III).

To gain information about the amount of different innate immune cell types during *M. marinum* infection, we studied expression levels of known innate immune cell marker genes from our transcriptome data (Supplementary Figure 2A in III). There were no ≥ 3-fold differences though there was a 2.4-fold increase in the expression of *myeloid-specific peroxidase* (*mpx*) and a 1.5-fold increase in *lysozyme* (*lyz*) expression at 14 dpi compared to unchallenged fish. These immune responsive genes have been used as neutrophil markers (Wittamer et al., 2011; Renshaw et al., 2006). However, expression of the third analyzed neutrophil marker, *colony stimulating factor 3 receptor (granulocyte)* (*csf3r*) was not increased. In addition, several other genes associated with the immune response in neutrophils were upregulated upon infection (Figure 7; Tables 1-2 in III). *Lysozyme g-like 2* (*lygl2*) has a postulated role in lysozyme activity and five other upregulated genes have a postulated role in neutrophil

degranulation. These results indicate expression of immune responsive genes in neutrophils has enhanced rather than the absolute number of neutrophils.

There were several other genes related to the innate immune response upregulated in our data set (Figure 7; Table 2 in III). *forkhead box Q1a* (*foxq1a*) has been reported to be expressed in zebrafish macrophages following bacterial challenge (Earley et al., 2018), whereas dendritic cells were represented by two upregulated genes, purinergic receptor *P2Y G-protein coupled, 11* (*p2ry11*) (Berchtold et al., 1999) and putative cytochrome *P450, family 21, subfamily A, polypeptide 2* (*cyp21a2*) (Poliani et al., 2010), and mast cells by potential *mast cell protease 1A* (*si:dkey-21e2.15*). Moreover, a set of genes having a role in immune cell signaling and regulation were upregulated in our data as well as the antimicrobial peptides *hepcidin antimicrobial peptide* (*hamp*) and *liver-expressed antimicrobial peptide 2* (*leap2*), together with an acute phase protein *serum amyloid A* (*saa*) (Figure 7; Table 2 in III).

As part of the innate immune response, a group of inflammasome-related genes were upregulated in our data (Figure 7; Table 2 in III). *si:ch211-233m11.1* and *si:ch211-236p5.3* encode putative inflammasome components, a NOD-like receptor, NACHT, LRR and PYD domains-containing protein 12 (Hu et al., 2017; Vladimer et al., 2012) and predicted NACHT, LRR and PYD domains-containing protein 3-like protein, respectively. *V-fos FBJ murine osteosarcoma viral oncogene homolog Ab (fosab)* codes for a transcription factor, which is as other Fos family members, a part of the activator protein (AP-1) protein complex (reviewed in Chinenov and Kerppola, 2001; van Dam and Castellazzi, 2001) and thus has a role in inflammasome activation (Malik and Kanneganti, 2017). Since inflammasomes have a role in the production of active IL1B (reviewed in Church et al., 2008), also *early growth response 3* (*egr3*) encoding a positive regulator of *il1b*, (Kenyon et al., 2017) associates with inflammasomes.

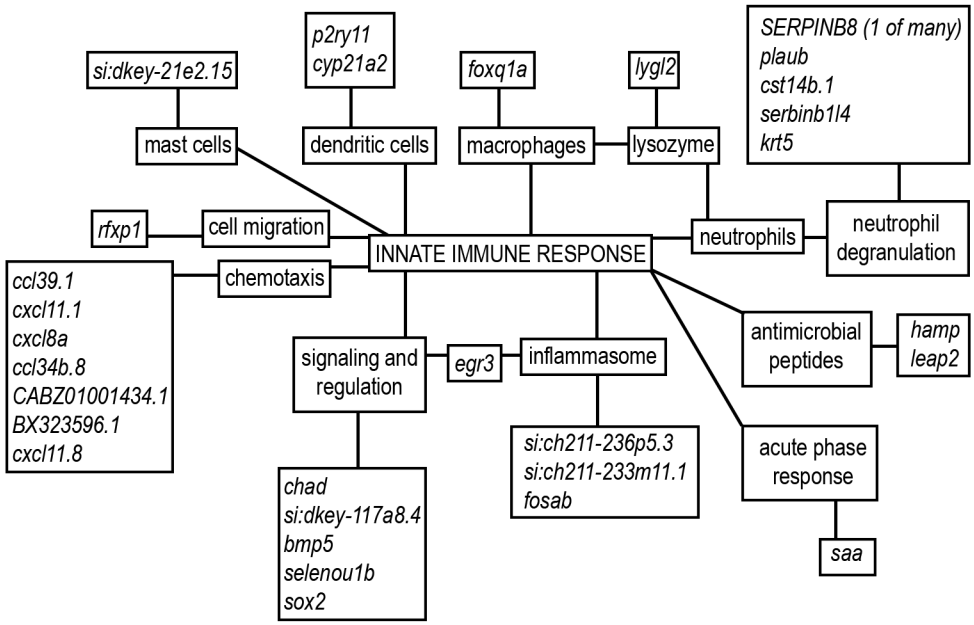

Figure 7. Schematic presentation of the protein coding genes associated with the innate immune response induced ≥ 3-fold upon *M. marinum* infection in wild type zebrafish. Whole genome level transcriptome analysis was performed on kidneys from unchallenged wild type (WT) and WT zebrafish (n = 4 in both groups) at 14 days post a low-dose (5-9 colony forming units, CFU) infection. Genes were classified as described in chapter 4.8.2.

In addition to the upregulation of gene expression upon infection, downregulation may also be important. In our data, four genes related to immune defense were downregulated ≥ 3-fold (Figure 1B and Supplementary Table 3 in III). All of these, *pentraxin 3, long b* (*ptx3b*), *mannan-binding lectin serine peptidase 1* (*masp1*), *ectonucleotide pyrophosphatase/phophodiestererase 1* (*enpp1*) and *platelet-derived growth factor receptor, beta polypeptide* (*pdgfrb*) (Lim et al., 2017) are associated with innate immune responses.

5.1.3 The role of the adaptive immune response in the defense against *M. marinum* infection II, III

In order to study the adaptive immune response, we studied expression of adaptive cell markers at different time-points during *M. marinum* infection. We compared

expression of a Th cell marker *cd4-1*, Tc cell marker *cd8a* and B cell marker *IgM* (*ighm*) in abdominal organs of infected fish with mock (PBS) injected controls with qPCR and saw no differences at 1 or 6 dpi (Supplementary Figure S4 in II). This is in line with the fact that the adaptive immune system is not yet activated during the first week following mycobacterial challenge (Cooper, 2009; Chackerian et al., 2002; van Crevel et al., 2002). We also studied the expression of common adaptive immune cell markers in kidney 14 days post a low-dose *M. marinum* infection from our transcriptome analysis data, but there were no clear differences in their expression between infected and unchallenged fish (Supplementary Figure 2B in III).

Nevertheless, our transcriptome analysis at 14 dpi reveals upregulation of a set of genes with reported or predicted roles in the adaptive immune response (Figure 8A; Tables 1-2 in III). Many of these genes are associated with T or B cell activation. This is in consensus with the fact that at this time-point the adaptive immune response is being activated. Predicted *ighv 5-5*, *ighv 4-1* and *ighv 13-2* are potential positive regulators of B cell activation whereas the human ortholog of *unc-119 homolog b (C. elegans)* (*unc119b*) has a role in T cell activation (Stephen et al., 2018; Gorska et al., 2004). The human ortholog of *egr1* has a role in the positive regulation of T and B cell activation (reviewed in Gómez-Martin et al., 2010). Interestingly, besides the innate immunity related role of *egr3*, its human ortholog *EGR3* codes for a negative regulator of T cell activation (Safford et al., 2005). In addition, predicted *ras-related C3 botulinum toxin substrate 1-like* has a postulated role in T and B cell receptor signaling (*RAC1)* and predicted *BX649608* codes for a member of Claudin 1 -protein family, which has reported expression in human T and B lymphocytes (Mandel et al., 2012).

In addition to the above-mentioned genes, *transmembrane protein 176l.3b* (*tmem176l.3b*), which has suggested adaptive immunity related roles (Zuccolo et al., 2010), was also upregulated. There were also suggestions of antibody production, since four of the upregulated genes, *CU896602.3*, *si:dkey-234i14.12*, *zgc:153659* and *immunoglobulin light 3 variable 1* (*igl3v1*) are predicted to have a role in immunoglobulin production.

To analyze later time-points, we measured expression of adaptive immune cell markers with qPCR (II). *cd4-1*, *cd8a* and *IgM* were significantly induced in kidney cells at four- and/or eight weeks post *M. marinum* infection compared to unchallenged fish (Figure 8B). This emphasizes the importance of the adaptive immune response in the later stages of infection. In addition, the Th1 hallmark cytokine *ifng1*, was significantly upregulated at 4 and 8 wpi compared to unchallenged fish (Figure 8C).

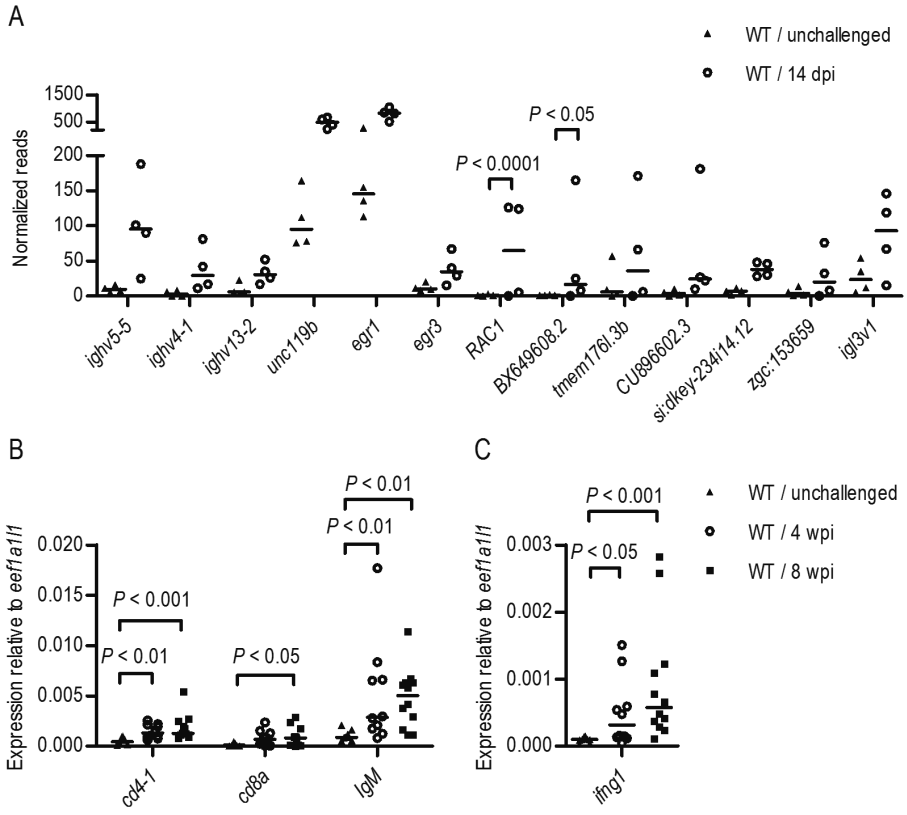

Figure 8. *M. marinum* infection in adult zebrafish induces expression of genes related to the adaptive immune response. A) The normalized read counts of adaptive immune response related genes induced ≥ 3-fold upon *M. marinum* infection when measured with RNA sequencing from kidneys of unchallenged wild type (WT) and WT zebrafish at 14 days post a low-dose (5-9 colony forming units, CFU) infection (n = 4 in both groups). B)-C) Expression of adaptive immune cell markers *cd4-1*, *cd8a*, *IgM* and Th1 cytokine *ifng1* were measured with qPCR from kidneys of unchallenged WT (n = 9-10) and WT zebrafish at 4 and 8 weeks post a low-dose (2-9 CFU) *M. marinum* infection (n = 10-12). Expression levels were normalized to expression of *eef1a1l1*. In panels A)-C) data are presented as a scatter dot plot and median. Note the different scales on *y*-axes. dpi = days post infection; wpi = weeks post infection. *ighv5-5 = immunoglobulin heavy variable 5-5*; *ighv4-1 = immunoglobulin heavy variable 4-1*; *ighv13-2 = immunoglobulin heavy variable 13-2*; *unc119b = unc-119 homolog b (C. elegans)*; *egr1 = early growth response 1*; *egr3 = early growth response 3*; *RAC1 = ras-related C3 botulinum toxin substrate 1-like*; *tmem176l.3b = transmembrane protein 176l.3b*; *igl3v1 = immunoglobulin light variable 1*.

5.1.4 Histological changes in granulomas during reactivation of latent infection by gamma irradiation I, II, III

In publication I, we showed that latent mycobacterial infection in zebrafish can be reactivated by γ-irradiation. To study histological changes in fish during reactivation, we analyzed fish with Ziehl-Neelsen staining after γ-irradiation. The analysis revealed large areas of free bacteria without clear granuloma structures (Figure 5C-D in I) while controls with latent infection had clear granuloma structures surrounded by a fibrous and/or cellular cuff (Figure 2D-F in I). In the second original communication, there were less fibrotic granulomas than nascent granulomas or areas with free bacteria at both 4 and 9 weeks post a low-dose infection in WT zebrafish (Figure 9A; Figure 3D in II). In addition, survival kinetics suggested progressive infection (Figure 3B in II) with *M. marinum* burden increasing between 4- and 8/9- week post infection (median of 65,000 vs 645,000 CFU) (Figure 3C in II). However, there were less free bacteria compared to reactivated samples in the first original communication. Therefore in this case, the outcome of low-dose infection seems to be chronic progressive infection, which is controlled by the host in granulomas.

Transcriptome analysis at 14 dpi also provides insights in the maintenance of latent or slowly progressive infection since some differentially expressed genes are associated with survival and the spread of mycobacteria. *M. tuberculosis* manipulates lipid metabolism of the host in order to facilitate its own survival (reviewed in Stutz et al., 2018; Barisch and Soldati, 2017). Altogether nine genes associated with lipid binding and metabolism were upregulated ≥ 3-fold upon *M. marinum* infection at 14 dpi (Figure 9B; Figure 1A and Table 3 in III). Among the upregulated genes was *neutral cholesterol ester hydrolase 1a* (*nceh1a*). The human ortholog, *NCEH1*, codes for an enzyme that is critical for the hydrolysis of cholesterol ester and thus the removal of cholesterol from foamy macrophages, which are abundant in granulomas (Igarashi et al., 2010; Russell et al., 2009). The upregulated lipid associated genes also have possible immunological roles related to the survival and spreading of bacteria. For example, vitamin A and retinoic acid have been shown to enhance autophagy of intracellular bacteria (Coleman et al., 2018), and *retinol binding protein 7b, cellular* (*rbp7b*) and *cellular retinoic acid binding protein* (*crabp1b*) were among upregulated genes. Another of the upregulated genes was *arachidonate 5-lipoxygenase b, tandem duplicate 2* (*alox5b.2*). Virulent *M. tuberculosis* activates the *Alox5* pathway to inhibit apoptosis and promote necrosis in mouse macrophages (Divangahi et al., 2010; Divangahi et al., 2009), facilitating spread of the bacteria (Roca and Ramakrishnan, 2013; Chen et al., 2006).

Reflecting the role of host lipid metabolism during mycobacterial infection, ten genes associated with lipid metabolism and transport were downregulated in our data (Figure 1B and Supplementary Table 3 in III). Moreover, the majority of significantly enriched processes among downregulated genes were associated with lipid metabolism and transport (Supplementary Table 2 in III).

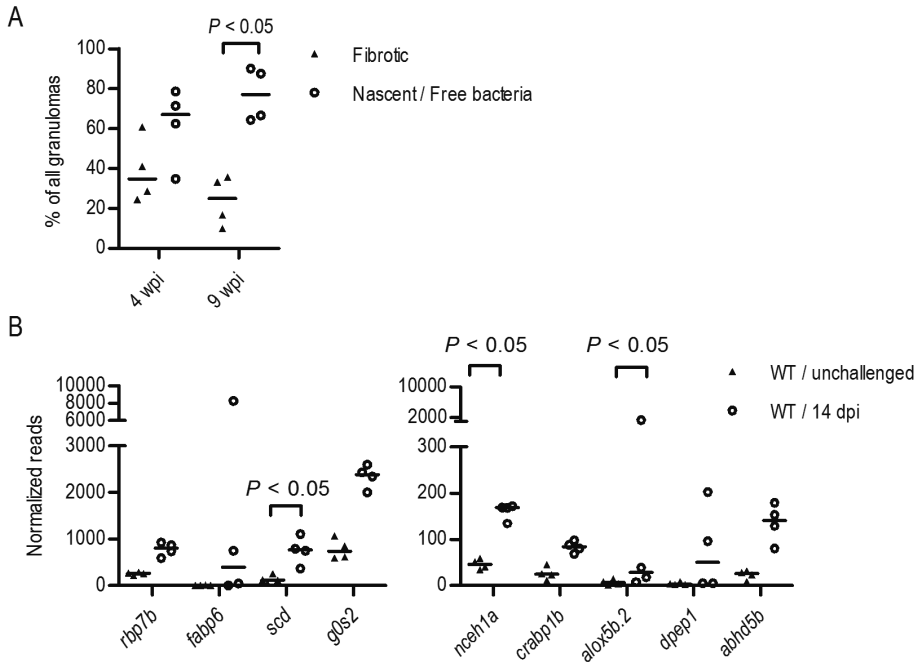

Figure 9. *M. marinum* infection in adult zebrafish induces expression of genes associated with lipid binding and metabolism, which are potentially related to bacterial survival in granulomas. A) The number of fibrotic and nascent granulomas/areas of free bacteria were counted from Ziehl-Neelsen stained sections of wild type (WT) zebrafish at 4 and 9 weeks post a low-dose (2-9 CFU, colony forming units) *M.marinum* infection (n = 4 in each group). B) The normalized read counts of genes associated with lipid binding and metabolism induced ≥ 3-fold upon *M. marinum* infection when measured with RNA sequencing from kidneys of unchallenged WT and WT zebrafish at 14 days post a low-dose (5-9 colony forming units, CFU) infection (n = 4 in both groups). In panels A)-B) data are presented as a scatter dot plot and median. Note the different scales on y-axes and divided y-axes in panel B). wpi = weeks post infection. *rbp7b = retinol binding protein 7b, cellular*; *fabp6 = fatty acid binding protein 6, ileal (gastropin)*; *scd = stearoyl-CoA desaturase (delta-9-desaturase)*; *g0s2 = G0/G1 switch 2*; *nceh1a = neutral cholesterol ester hydrolase 1a*; *crabp1b = cellular retinoic acid binding protein 1b*; *alox5b.2 = arachidonate 5-lipoxygenase b, tandem duplicate*; *dpep1 = dipeptidase 1*; *adhd5b = abhydrolase domain containing 5b.*

5.2 The role of Il10 in zebrafish *M. marinum* infection II, III

5.2.1 Unchallenged *il10*$^{e46/e46}$ zebrafish mutants express a normal phenotype II

In order to study the role of Il10 in the immune defense against a low-dose *M. marinum* infection in zebrafish, we used the *e46* mutant zebrafish line. We obtained the line from the Wellcome Trust Sanger Institute (Kettleborough et al., 2013). This line carries a nonsense mutation in *il10*, which results in a premature stop codon and truncated protein (Figure 1A in II). To study whether the effect of the mutation is seen at a transcriptional level, we measured expression of *il10* in various tissues (Figures 1B, 6A and Supplementary Figure S2A in II). Since there was no significant difference in *il10* expression between *il10*$^{e46/e46}$ mutant fish and WT controls, the mutation did not induce compensation on the transcriptional level or nonsense mediated decay-based degradation of the mutant transcripts (Nickless et al., 2017).

IL10 is an anti-inflammatory cytokine (Fiorentino et al., 1989; Fiorentino et al., 1991) and IL10 deficient mice develop age-related enterocolitis (Gomes-Santos et al., 2012). Thus, we studied if the *il10*$^{e46/e46}$ zebrafish have an inflammatory phenotype in the unchallenged state. First, when maintaining fish, we observed that the *il10*$^{e46/e46}$ mutant zebrafish were phenotypically normal and also bred normally. For further analysis, we collected spleen, liver, kidney and intestine separately as well as all abdominal organs of *il10*$^{e46/e46}$ mutants. *il10*$^{e46/e46}$ fish did not express an inflammatory phenotype but expression of *il1b*, *tnfa* and *tnfb* were at the same level as WT control fish in all analyzed tissues (Figure 8 and Supplementary Figures S1 and S2A in II). Moreover, intestines of the *il10*$^{e46/e46}$ mutants at the age of one year had a normal visual appearance (Supplementary Figure S2B in II).

Of the other analyzed genes including adaptive immune cell markers and transcription factors, unchallenged *il10*$^{e46/e46}$ fish had elevated expression of the B cell marker *IgM* in kidney cells (Figure 6 in II) and decreased expression of *IgM* in liver as well as the Th1 transcription factor *tbx21* in the intestine. This probably indicates differential expression of these genes in various tissues. All in all, analysis showed expression of *il10* is very low in analyzed tissues in an unchallenged state in zebrafish (Figures 1B and 6A and Supplementary Figure S2A in II).

5.2.2 *il10*$^{e46/e46}$ mutants show improved survival and decreased bacterial burden when challenged with a low-dose *M. marinum* infection II

In order to study the role of Il10 in zebrafish *M. marinum* infection, we utilized the research model developed in original communication I. We measured if the expression of *il10* is induced during low-dose infection. Our qPCR analysis showed that compared to mock (PBS) injected zebrafish, *il10* was upregulated in abdominal organ blocks of *il10*$^{e46/e46}$ mutant fish infected with 2-9 CFU at 6 dpi (P = 0.009, Figure 4 in II). In addition, we saw upregulation of *il10* in kidney in both WT controls and *il10*$^{e46/e46}$ mutant fish at 8 wpi when compared to unchallenged fish (Figure 10). These results suggest that *il10* has a role in the immune defense against *M. marinum* infection in adult zebrafish.

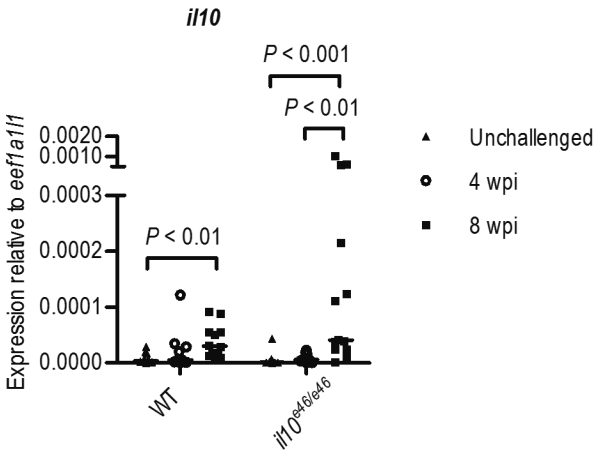

Figure 10. Expression of *il10* is induced upon *M. marinum* infection in adult zebrafish. The expression of *il10* was measured with qPCR from kidneys of unchallenged *il10*$^{e46/e46}$ (n = 10) and wild type (WT) zebrafish (n = 10) and *il10*$^{e46/e46}$ (n = 10-14) and WT (n = 10-12) zebrafish at 4 and 8 weeks post a low-dose (2-9 CFU, colony forming units) infection. Expression levels were normalized to expression of *eef1a1l1*. Data are presented as a scatter dot plot and median. Note the divided y-axis. wpi = weeks post infection.

We challenged *il10*$^{e46/e46}$ mutants and WT controls with a 2-156 CFU of *M. marinum* and followed their survival. The data was collected from four experiments lasting from 16 to 20 weeks and indicated that *il10*$^{e46/e46}$ fish have improved survival against a low-dose *M. marinum* infection (Figure 3B in II). Until 8 wpi, survival kinetics of both groups were similar, resulting in approximately 20% mortality at this

point of the infection. Thereafter, however, deaths occurred more frequently in the WT group resulting in an endpoint survival of 44% compared to 63% in the *il10*$^{e46/e46}$ group (P = 0.037). We also injected 3-29 CFU of *M. marinum* into the yolk sac of zebrafish embryos, which do not have a functional adaptive immune system (Lam et al., 2004), on the day of fertilization. In this setting, survival of mutants did not significantly differ from WT fish during the 7-day follow-up, as endpoint survival was approximately 30% in both groups (Figure 3A in II). These data suggest Il10 does not affect the innate immune response against *M. marinum* but rather the adaptive immune response.

After discovering the difference in survival rate of *il10*$^{e46/e46}$ we studied whether improved resistance or tolerance was underlying this difference. It has been shown that IL10 deficiency in mice leads to formation of mature granulomas with fibrotic capsules (Cyktor et al., 2013). Based on results of original communication I, we hypothesized the improved survival of *il10*$^{e46/e46}$ could associate with more restricted infection with fewer, structurally more organized granulomas. Nevertheless, in our small-scale histological analysis at 4 and 9 weeks post a low-dose (2-9 CFU) infection (Figure 3D and Supplementary Figure S3 in II), the total number of granulomas or infected organs did not significantly differ between *il10*$^{e46/e46}$ mutants and WT control fish. There was also no significant difference in the number of multicentric granulomas nor in the number of nascent granulomas and areas of free bacteria between Il10 deficient and WT fish. Based on Ziehl-Neelsen staining, the number of fibrotic granulomas was also equal in the two study groups.

Another approach in investigating the decreased susceptibility of *il10*$^{e46/e46}$ mutants, we measured the relative amount of different blood cell populations in kidney with flow cytometry at 4 and 8 weeks post a low-dose (1-18 CFU) *M. marinum* infection (Figure 5 in II). Interestingly, the analysis revealed an increase in the relative amount of myeloid cells (P = 0.014) in *il10*$^{e46/e46}$ compared to WT control fish. There was no increase in the relative amount of lymphocytes.

In order to measure the bacterial burden with a qPCR-based method, we collected abdominal organ blocks of *il10*$^{e46/e46}$ and WT zebrafish infected with 1-18 CFU of *M. marinum* from three different experiments at 1 dpi, 6 dpi, 4 wpi and 8/9 wpi. In consensus with survival, the difference between mutants and WT was not observed until 8/9 wpi when the elevated bacterial copy number median was 645,000 in the WT group compared to 86,000 in the *il10*$^{e46/e46}$ group (P = 0.039) (Figure 3C in II). From these results we concluded that the *il10*$^{e46/e46}$ zebrafish have a higher resistance rather than tolerance during low-dose *M. marinum* infection.

5.2.3 Improved survival associates with enhanced *ifng1* expression in *il10*$^{e46/e46}$ mutants in a low-dose *M. marinum* infection II, III

In order to further characterize the differences in WT zebrafish underlying improved survival of the *il10*$^{e46/e46}$ mutants during *M. marinum* infection, we measured expression of the most common cytokines and immune cell markers at different time-points after low-dose infection. For this, we used two types of samples: the abdominal organ block and kidney cells.

As an anti-inflammatory cytokine, *IL10* is known for dampening the production of proinflammatory cytokines (reviewed in Peñaloza et al., 2016; Couper et al., 2008). To address this, we measured expression of the *il1b* and *TNF* orthologs *tnfa* and *tnfb* (Figures 4 and 8 in II) post a low-dose, 1-18 CFU *M. marinum* infection. Interestingly, we saw decreased expression of *tnfb* in kidney cells at 8 wpi ($P = 0.048$) and of *il1b* in kidney cells at 8 wpi and the organ block at 9 wpi ($P = 0.029$ and $P = 0.043$, respectively) in *il10*$^{e46/e46}$ mutants compared to WT controls (Figure 8 in II). This may reflect the slower progress of infection. This assumption is supported by previous results from our group associating increased expression of proinflammatory cytokines with a high *M. marinum* burden in zebrafish, that is, with more progressed infection (Myllymäki et al., 2018).

Next, we measured the expression of *cd4-1*, *cd8a* and *IgM* (Figure 6 in II). We observed a significantly elevated expression of *cd4-1* in kidney cells of *il10*$^{e46/e46}$ fish compared to WT controls at 8 wpi ($P = 0.017$), and decreased expression of *cd8a* in organ blocks of mutants at 4 wpi ($P = 0.032$). Even though *cd4-1* expression may originate from several types of immune cells, elevated expression of *cd4-1* may suggest an enhanced Th cell response. Based on these results and the known immunoregulatory role of IL10 (Paul et al., 2012), we measured the relative expression of Th1 cell transcription factor *tbx21*, Th2 cell transcription factor *gata3* and regulatory T cell marker *foxp3a* and the hallmark Th1 and Th2 cytokines *ifng1* and *il4*, respectively (Figure 7 in II). Interestingly, at 8 wpi *tbx21* had elevated expression in kidney cells of *il10*$^{e46/e46}$ mutants ($P = 0.042$) whereas expression of *gata3* was decreased compared to WT ($P = 0.033$). Expression of *ifng1* was also significantly increased in *il10*$^{e46/e46}$ kidney cells compared to WT ($P = 0.025$). However, expression of *il4* was upregulated in the abdominal organ blocks of mutant fish ($P = 0.023$) at 9 wpi, possibly reflecting the different effect of Il10 deficiency on Th gene expression in various tissues. Our results showing the differential expression of Th1 cell response related genes between *il10*$^{e46/e46}$ mutant zebrafish and WT controls is not seen until 8 wpi are supported by the transcriptome analysis of

original communication III. At the time-point when the adaptive immune response starts to activate, at 14 dpi, our transcriptome analysis showed a clear upregulation of *ifng1* only in one fish, which had a higher *M. marinum* burden compared to others (Figure 11). This also reflects previously reported variation among individuals in resisting infection (Hammarén et al., 2014), which is probably due to the heterogeneity of WT zebrafish. The expression levels of *tbx21* and *cd4-1* were also low (Supplementary Figure 2B in III). This highlights the significance of Th1 cell response increases as *M. marinum* infection in zebrafish proceeds. All in all, elevated *cd4-1*, *tbx21* and *ifng1* expression together with reduced *gata3* expression in *il10*$^{e46/e46}$ mutant zebrafish at 8 wpi suggest that *il10* mutation causes a shift towards a Th1 cell type response at least at the transcriptional level, which appears favorable in the control of *M. marinum* infection in adult zebrafish.

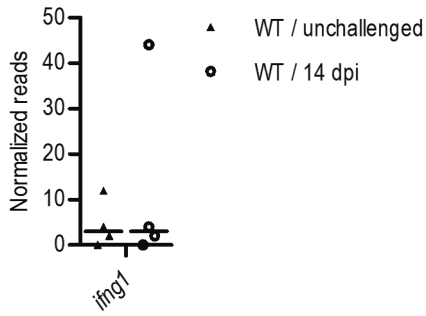

Figure 11. Expression of Th1 cytokine *ifng1* in adult zebrafish kidney at 14 days post *M. marinum* infection. The figure presents normalized read counts of *ifng1* measured with RNA sequencing from kidneys of unchallenged WT and WT zebrafish at 14 days post a low-dose (5-9 colony forming units, CFU) *M. marinum* infection (n = 4 in both groups). Data are presented as a scatter dot plot and median. dpi = days post infection.

Since the *il10*^{e46} mutant line is produced with ENU mutagenesis (Kettleborough et al., 2013) it carries also other mutations besides *e46*. To take this into account, we outcrossed *il10*$^{e46/e46}$ mutants to WT AB and incrossed the heterozygous progeny. After this we infected ungenotyped progeny with a low-dose, 8-17 CFU, of *M. marinum* and performed a gene expression analysis from kidneys at 8 wpi (Figure 9 in II). This time there was no significant difference in expression of *cd4-1*, *tbx21* or *gata3* between *il10*$^{e46/e46}$ mutants and WT controls whereas the expression of *ifng1*

was again elevated in homozygous mutants ($P = 0.044$) confirming the shift towards a Th1 cell type response in *il10*$^{e46/e46}$ mutants.

5.3 A forward genetic screen identified ten hypersusceptible zebrafish lines to *M. marinum* infection and one resistant line III

In order to identify predisposing genetic host factors to *M. marinum* infection in adult zebrafish, we performed a forward genetic screen using a gene-breaking Tol2 transposon-based mutagenesis (Figure 12) (Clark et al., 2011) and screened in total 127 mutant zebrafish lines carrying a set of random mutations for altered susceptibility to *M. marinum* infection (III). In order to perform the screen, we injected 1-72 CFU of *M. marinum* into the abdominal cavity of 3-15 month-old zebrafish and followed their survival for 12-14 weeks. If the line showed impaired or improved survival at least three times, it was considered as having altered susceptibility. *rag1*$^{hu1999/hu1999}$ mutants, which have no functional adaptive immunity (Wienholds et al., 2002), were occasionally included as positive controls. In the screen, in total we identified ten zebrafish mutant lines, which were more susceptible and one line, which was less susceptible to *M. marinum* infection compared to WT. The most susceptible line, mutant463, was chosen for further analysis. At the 14 wpi endpoint it showed 8% survival compared to 74% survival of WT control fish ($P < 0.0001$), and 83% survival of mutant189 ($P < 0.0001$) and 68% survival of mutant229 ($P < 0.0001$) (Figure 2A in III). When injected with PBS, mutant463 fish showed 100% survival (Supplementary Figure 3A in III). Of note, when 1 dpf embryos were infected into the caudal vein with 32-198 CFU of *M. marinum* no difference in survival was observed in mutant463 compared to controls (Supplementary Figure 3C in III). However, infection with 220-328 CFU of *S. pneumoniae* (T4 strain) into the blood circulation valley of 2 dpf embryos resulted in mildly impaired survival of mutant463 fish compared to WT (Supplementary Figure 3B in III).

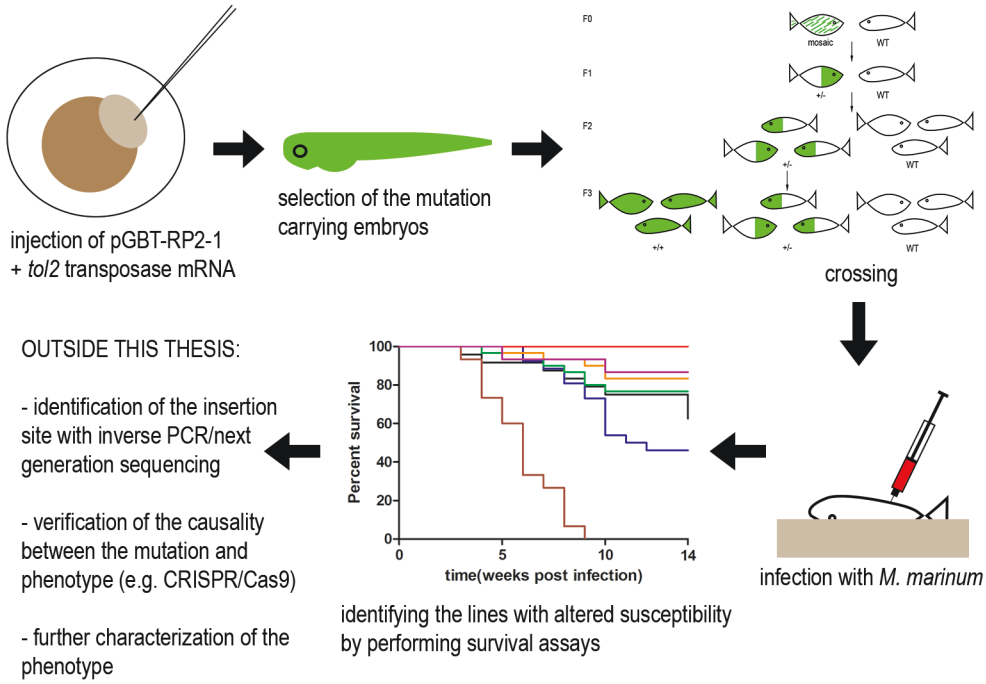

Figure 12. Schematic presentation of work-flow of the forward genetic screen performed in this thesis. pGBT-RP2-1 transposon was injected into one-cell stage wild type (WT) embryos. Successfully injected embryos were selected based on *green fluorescent protein (GFP)* expression and crossed further to produce zebrafish lines carrying unknown mutations. The lines were infected with a low-dose of *M. marinum* and lines with altered susceptibility were selected based on survival for further studies. Outside this thesis work, mutation sites in the selected lines will be identified with PCR based methods and phenotypes verified with targeted mutants. After verification, phenotypes will be further characterized. CRISPR/Cas9 = Clustered Regularly Interspaced Short Palindromic Repeats/ CRISPR-associated.

In order to further study whether the increased susceptibility of mutant463 zebrafish is due to impaired resistance or tolerance, we measured bacterial burden with a qPCR-based method from the abdominal organ blocks (excluding kidney) post a low-dose (5-9 CFU) *M. marinum* infection (Figure 2B in III). For analysis, we chose 7 dpi and 14 dpi as time-points since they give information about the situation preceding the drastic increase in mortality of the mutants. At 7 dpi, the bacterial burden was not significantly higher in mutant463 compared to WT control fish (estimated copy number median 206 vs. 440 CFU, respectively) while at 14 dpi mutant463 indeed carried a heavier bacterial burden (copy number median 23,076 CFU vs. 701 CFU, $P = 0.042$, respectively). To conclude, this result indicates that

the hypersusceptibility of mutant463 zebrafish is due to poor resistance rather than poor tolerance.

5.3.1 A whole-genome level transcriptome analysis reveals candidate genes underlying susceptibility of a mutant zebrafish line III

In order to find genes underlying the susceptibility of the mutant463 zebrafish line to *M. marinum* infection, we performed a whole-genome level transcriptome analysis in which we compared mutants to WT fish. The analysis revealed a set of 27 genes with ≥ 3 -fold decrease in expression compared to WT at 14 days post a low-dose (5-9 CFU) *M. marinum* infection (Figure 13; Table 4 in III). When genes were divided into categories based on available databases and the literature, seven had a role in immune response, four in metabolism, 14 had other roles and no reported or predicted role was found for two genes.

First, we hypothesized that mutant463 might have a deficiency in some immune cell population. Thus we studied expression of common innate and adaptive immune cell markers and transcription factors from transcriptome data (Supplementary Figure 2 in III). None of these markers had ≥ 3 -fold reduction in their expression in mutant463 fish compared to WT. Nevertheless, there was a 2.3 -fold reduction in the eosinophil marker *gata2a*.

Out of seven immunological genes with decreased expression in mutant463 fish compared to WT, four has a predicted or reported role clearly associated with the innate immune defense (Figure 13). In order to verify our RNA sequencing results and achieve more solid information on expression of the selected genes, we carried out a qPCR analysis with a larger sample size and at two additional time-points. Of the selected genes, *si:ch211-236p.5.3*, postulated *NACHT, LRR and PYD domains-containing protein 3-like* potentially has an inflammasome-related role. Expression in mutant463 was significantly decreased compared to WT at 14 and 28 dpi (1848.4-fold reduction, $P < 0.0001$ and 493.7-fold reduction, $P = 0.0002$, respectively) (Figure 3C in III) in qPCR analysis. In fact, this gene was expressed above the detection limit only in one fish. Two genes have postulated roles in eliminating bacteria, *plasminogen activator, urokinase b* (*plaub*) in neutrophil degranulation and *leap2*. The fourth gene poorly expressed in mutant463 and having a possible role in innate immunity is *si:dkey-21e2.15*, suggested to be *mast cell protease 1A*.

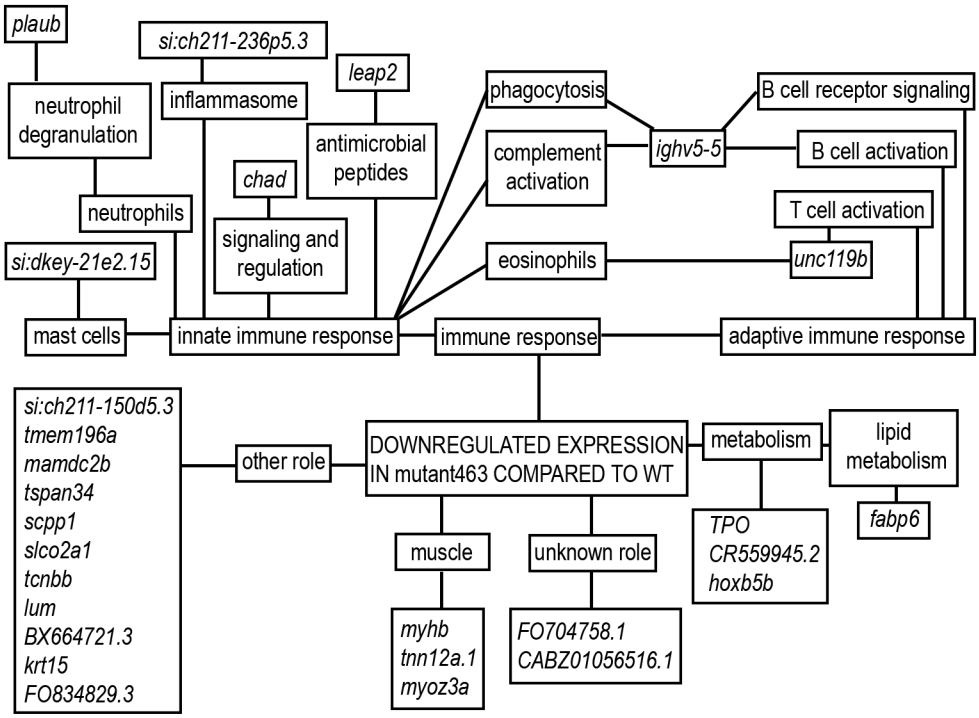

Figure 13. Schematic presentation of the protein coding genes downregulated ≥ 3-fold in mutant463 compared to wild type zebrafish during *M. marinum* infection. Whole-genome level transcriptome analysis was performed from adult zebrafish kidneys (n = 4 in both groups) at 14 days post a low-dose (5-9 CFU, colony forming units) infection. Genes were classified as described in chapter 4.8.2.

Two of the genes with immunological roles, *ighv5-5* and *unc119b*, are strongly associated with the adaptive immune response (Figure 13). However, *ighv5-5* has postulated roles also in phagocytosis and in the activation of the classical pathway of the complement system, with *UNC119* in humans also shown to have a role in the survival of eosinophils (Cen et al., 2003). This is especially interesting from our point of view since both the expression of *unc119b* and eosinophil marker *gata2a* were decreased in our analysis (Table 4 and Supplementary Figure 2A in III). However, *UNC119* has been actively studied in the context of T cell activation (Stephen et al., 2018; Gorska et al., 2004). Our qPCR analysis showed decreased expression in mutants at each of the analyzed time-points: 11.4-fold reduction at 7 dpi (P = 0.019), 8.4-fold reduction at 14 dpi (P = 0.003) and 76.0-fold reduction at 28 dpi (P = 0.0002) (Figure 3D in III).

The seventh immune-system related gene with decreased expression in mutant463, *chondroadherin* (*chad*), has postulated roles in the cytokine-mediated signaling pathway and negative regulation of the JAK-STAT signaling cascade (Figure 13). Of note, mutant463 have higher expression of proinflammatory cytokines *tnfa* (26.7 -fold) and *il1b* (11.5 -fold) (Figure 14), which, as suggested in the original communication II and previous results from our group by Myllymäki and colleagues (2018), is associated with higher bacterial burden and more progressed infection.

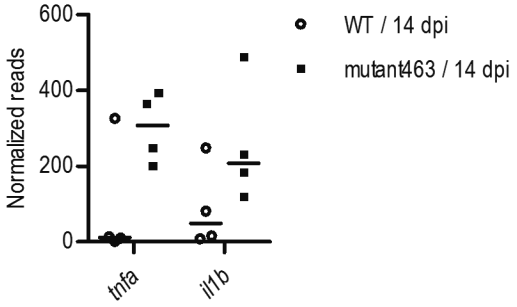

Figure 14. The expression of proinflammatory cytokines *tnfa* and *il1b* is increased upon *M. marinum* infection in mutant463 compared to wild type zebrafish. The figure presents normalized read counts of *tnfa* and *il1b* measured with RNA sequencing from kidneys of wild type (WT) and mutant463 adult zebrafish (n = 4 in both groups) at 14 days post a low-dose (5-9 colony forming units, CFU) *M. marinum* infection. Data are presented as a scatter dot plot and median. wpi = weeks post infection.

Among metabolic gene that had decreased expression in mutant463 compared to WT control fish was the most upregulated gene in the transcriptome data, *fatty acid binding protein 6, ileal (gastropin)* (*fabp6*). When measured with qPCR, *fabp6* was induced 14.9-fold at 7 dpi (P = 0.007) and 25.1-fold at 14 dpi in WT fish and reduced 6.1-fold in mutant463 fish at 28 dpi compared to WT (Figure 3A in III).

6 DISCUSSION

6.1 Zebrafish as a model organism to study tuberculosis I, II, III

M. tuberculosis has co-existed with humans throughout the ages. A reason for the persistence of *M. tuberculosis* is its ability to utilize host physiology, hide from immune defenses and attack when the host is at its weakest. A comprehensive study of host-pathogen interactions is only possible in living organisms and therefore animal models are required. A challenge for animal models is to cover the whole disease spectrum of tuberculosis. Moreover, there are also other aspects to consider, like the ethicality of the model and its feasibility (see Table 1 "Comparison of different vertebrate animal models for studying tuberculosis" in section 2.4.2.3 "Zebrafish in comparison with other animal models for tuberculosis"). In this thesis, we have used a *M. marinum* infection in zebrafish as a research model for tuberculosis and as a solution to meet these challenges.

M. marinum infection in zebrafish embryos has proved itself as a good research model for tuberculosis by mimicking the main features of the disease and more importantly, by providing new insights into the progression of tuberculosis. Even though zebrafish embryos and larvae do not have a functional adaptive immune response, the combination of *M. marinum* as a natural pathogen and the transparency of zebrafish embryos and larvae with many alternative infection routes provide an invaluable tool for studying host-pathogen interactions during mycobacterial infection (Davis et al., 2002; Benard et al., 2012). Using the information available from this starting point, we especially wanted to include the aspect of the adaptive immune response in the zebrafish model and to utilize the less frequently used adult zebrafish as a tuberculosis model.

As zebrafish do not have lungs, the infection route of *M. marinum* bacilli is different to human tuberculosis. In natural conditions, zebrafish presumably consume the dead infected individuals. In fact, it seems that zebrafish are mainly infected with mycobacteria via the gastrointestinal tract from which the bacteria are then disseminated to other organs (Harriff et al., 2007). In this thesis we used intraperitonial injection for practical reasons. That way we could better control the number of bacteria delivered to the fish than by feeding the bacteria to the fish.

Injection of *M. marinum* results in zebrafish larvae in different kind of systemic or local infections depending on the injection site (Meijer, 2016) and in adults in a systemic disease (I) whereas when *M. tuberculosis* is transmitted through the airways to the lungs of the new host, pulmonary tuberculosis is the most common result (Loddenkemper et al., 2015). However, also pulmonary tuberculosis can then spread from lungs to other tissues via bloodstream or lymphatic system (Loddenkemper et al., 2015).

The course of *M. marinum* in zebrafish embryo/larval model has been widely studied (reviewed in Meijer, 2016). When the intravenous infection of zebrafish embryos is used, macrophages phagocytose bacteria in the bloodstream from where the infected macrophages migrate to other tissues and form granulomas (Davis et al., 2002). In adult zebrafish, *M. marinum* has been detected in leukocytes, probably macrophages, in the intestine after infection via oral route and from there bacteria spread to the spleen and liver (Løvmo et al., 2017). Since mouse peritoneal macrophages are infected with *M. tuberculosis* after intraperitoneal infection (e.g. Wang et al., 2017), we assume that *M. marinum* infects peritoneal macrophages after intraperitoneal infection in zebrafish. Moreover, we have seen the granuloma formation in the intraperitoneal organs, which supports this assumption. Different macrophage populations have differences in the gene expression profile (Gautier et al., 2012; Lavin et al., 2014). When lung and peritoneal macrophages were compared in mouse, for example transcripts with predicted functions in lipid metabolism and leukocyte extravasation were enriched in lung macrophages and transcripts predicted to have role in eicosanoid signaling, IL12 signaling and production, acute phase response and complement system in peritoneal macrophages (Gautier et al., 2012). Noteworthy, out of pattern recognition receptor genes, *Tlr2*, is more expressed in lung than in peritoneal macrophages and C type lectin, *Clec4d*, more expressed in peritoneal macrophages (Gautier et al., 2012). Lavin and colleagues (2014) showed in mouse that *carbonic anhydrase 4* is population-specific gene for lung macrophages and *Transforming growth factor, beta 2*, for peritoneal macrophages.

The formation of the hallmark structure of tuberculosis, the granuloma, initiates as one of the first events after the infection when *M. tuberculosis* bacilli encounter alveolar macrophages and are engulfed by them (O'Garra et al., 2013). The infected macrophages start to produce a set of various cytokines and chemokines and to attract other cells to the infection site, resulting in the formation of a granuloma (Russell, 2007). In this thesis we showed the upregulation of a set of chemokines as well as other cell migration associated genes, and in the case of the highest bacterial load, the production of proinflammatory cytokines (III). It has been shown in the

cynomolgus macaque (*Macaca fascicularis*) that *CXCL9*, *CXCL10* and *CXCL11*(Fuller et al., 2003), and in mice that *Cxcl10* (Rhoades et al., 1995), which are *CXCR3* binding chemokines, are extensively induced upon *M. tuberculosis* infection. In line with this, two genes induced in our studies in adult zebrafish kidney at 14 dpi, *BX323596.1* and *cxcl11.8* (III) are orthologs for human, macaque and mouse *CXCL9*.

The role of Cxcr3-Cxcl11 signaling in facilitating the recruitment of macrophages and thus in the dissemination of *M. marinum* and formation of granulomas has been shown in zebrafish larvae (Torraca et al., 2015). Moreover, it was recently shown in an RNA sequencing analysis from the macrophages of *M. marinum* infected zebrafish larvae that *cxcl11.1* is the most strongly expressed of proinflammatory M1 macrophage-associated genes (Rougeot et al., 2019). The upregulation of this gene is also seen in our data (III). It has been shown that *M. tuberculosis* is able to promote differentiation of proinflammatory M1 macrophages but also, when beneficial for itself, differentiation to anti-inflammatory M2 macrophages (Refai et al., 2018). To conclude, even though the inflammatory response is an important defense mechanism, our results in combination with others' reflect the possible benefit to the pathogen. Another way for mycobacteria to facilitate its survival is to promote necrosis of the infected macrophages instead of apoptosis. This can be associated with our data through the induction of *alox5b.2*. It has been shown that *Alox5* deficient mouse macrophages infected with virulent *M. tuberculosis* undergo apoptosis rather than necrosis (Divangahi et al., 2009) and that *Alox5* deficient mice are more resistant to chronic *M. tuberculosis* infection (Bafica et al., 2005). It has also been shown that *ALOX5* polymorphisms in humans affect tuberculosis susceptibility (Herb et al., 2008).

In this thesis, we showed the granuloma is formed in adult zebrafish in both low dose infection mimicking latent disease and in high-dose infection mimicking primary active disease (I). We recognized different types of granulomas during the course of *M. marinum* infection from Ziehl-Neelsen stainings: free bacteria in predicting the formation of granuloma, loosely structured nascent granulomas, mature granulomas with fibrous and cellular capsule, and necrotic granulomas with caseous tissue, intensively stained and thus containing a high density of bacteria (Figure 15; I, II, Myllymäki et al., 2018). Moreover, we were able to verify the presence of a fibrous capsule with Mallory's trichrome staining (I). These findings are in consensus with what is known about the structure of human granulomas. Of note, Swaim and colleagues (2006) failed to show the formation of the fibrotic capsule, which may be due their use of a different bacterial strain than us.

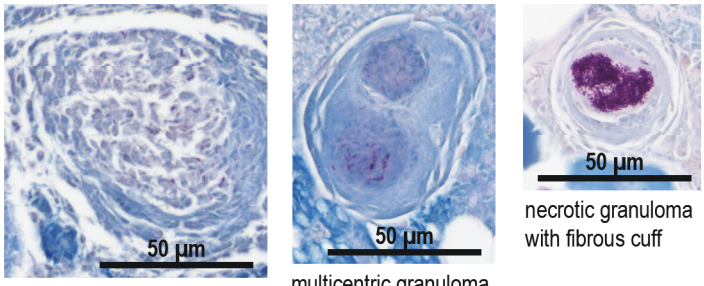

nascent granuloma/
free bacteria

multicentric granuloma
with fibrous cuff

necrotic granuloma
with fibrous cuff

Figure 15. Examples of different types of granulomas formed during *M. marinum* infection in adult zebrafish. Granulomas were identified from Ziehl-Neelsen stained tissue sections collected from adult zebrafish 4 or 9 weeks post a low-dose (2-9 CFU) *M. marinum* infection. Multicentric and necrotic granulomas presented here are also fibrotic.

Associated with granuloma formation, at 14 days post a low-dose infection in adult zebrafish, lipid metabolism-related genes stood out, both among the upregulated and downregulated genes (III). It has been shown that *M. tuberculosis* has ways to facilitate differentiation of macrophages into foamy macrophages with large lipid droplets and thus providing itself a source of nutrients inside the granuloma (Vermeulen et al., 2017; Peyron et al., 2008). Moreover, *Mycobacterium avium* infected bone marrow-derived mouse macrophages treated with very-low-density lipoprotein have been suggested to work as a model for studying the metabolism of mycobacteria in foamy macrophages and to provide information on mycobacterial latency and reactivation (Caire-Brändli et al., 2014).

As for the killing of the bacteria and the arrival of neutrophils to the infection site, we saw an upregulation of antimicrobial peptides *hamp* and *leap2* in our data as well as a set of genes with a postulated role in neutrophil degranulation and *lygl2* with postulated lysozyme activity (III). The lytic activity of *lysozyme g* upon infection has actually been shown in an Indian carp species, rohu (Mohapatra et al., 2018). Two of the induced genes are associated with vitamin A, which has been shown to have antimicrobial activity against *M. tuberculosis* (Wheelwright et al., 2014). Moreover, the role of vitamin A deficiency as a susceptibility factor for tuberculosis has been recognized (Aibana et al., 2017; Ramachandran et al., 2004).

Zebrafish is considered as a good model to study adaptive immune response. Compared to mammals, zebrafish have lower number of T cells which facitilitates to study TCR repertoire (Covacu et al., 2016). The innate immune response against

mycobacteria is often inadequate in preventing disease. This is also seen in the zebrafish model, since possible clearance of the *M. marinum* infection mostly happens only after the onset of the adaptive immune response, at approximately 2 wpi (Hammarén et al., 2014). In this thesis, we analyzed the survival of fish and bacterial burden during the course of zebrafish *M. marinum* infection (II). On the one hand, the bacterial burden in *il10*$^{e46/e46}$ fish remained the same between 4 and 8/9 wpi whereas at the beginning of the infection it increased. On the other hand, based on survival, fish were in latent or a slowly progressing chronic infection. In other words, the infection was under control. This suggests onset of the adaptive immune response is important for controlling the infection. This is further demonstrated by the inability of *rag1* mutants to control infection (I, III).

When considering the value of *M. marinum* infection in adult zebrafish as a research model for tuberculosis, the most important findings of this thesis is the spontaneous latency that occurs in zebrafish and the reactivation that can be caused by immunosuppression. As described in section 2.4.2.3 "Zebrafish in comparison with other animal models for tuberculosis", there are also other such models. However, zebrafish have both practical and ethical properties, which favor this model. Spontaneous latency in zebrafish was seen in this thesis as a stable granuloma count and in a lack of bacterial spreading from 4 wpi onwards, and in the other results from the original communication I as stable *M. marinum* burden after 4 wpi and low mortality during the infection in general (I). Latency is reached after a low-dose infection and can be reactivated by immunosuppression caused by exposing latently infected zebrafish twice to γ-irradiation (I). In this thesis, reactivation was seen at the tissue level as areas covered with free bacteria and large necrotic areas. When relative amounts of blood cell populations in the kidney were measured with flow cytometry, a decrease in the lymphocyte population was detected (I).

Suggestions of the initation of adaptive immunity was also seen in this thesis through the upregulation of many genes with predicted and reported adaptive immune related roles at 14 dpi (III). It has been shown in mice that *M. tuberculosis* activates the 5-lipoxygenase pathway and thus inhibits dendritic cells from cross-presenting antigens and delaying initiation of T cell immunity (Divangahi et al., 2010). This suggests the upregulation of *aloxb.2* observed by us, could well be associated with a delayed T cell response. Another gene upregulated in our data, *tmem176l.3b* can also be associated with antigen presenting cells prior to their maturation. Expression of *Tmem176A* and *Tmem176B* has been shown in especially immature antigen presenting cells in rats (Condamine et al., 2010; Louvet et al., 2005). The results of this thesis show that in a low-dose infection the number of

granulomas and affected organs rises until 4 wpi, that is, until after the onset of adaptive immune response. This result together with the other results from the original communication I suggest the adaptive immune response has a role in reaching and maintaining latency.

Emphasizing the heterogenicity of the zebrafish population, in addition to induced reactivation (I, Myllymäki et al., 2018), spontaneous reactivation occurs in some adult zebrafish, allowing the study of genetic mechanisms underlying it (Hammarén et al., 2014). All in all, in this thesis we have demonstrated that *M. marinum* infection in adult zebrafish mimics the different phases of tuberculosis, as in addition to latent infection, primary active tuberculosis can be modeled with a high-dose infection.

6.2 The role of IL10 in tuberculosis II, III

The of role IL10 during tuberculosis infection has been widely studied in human cell models and in mice. According to the literature, both the protective and negative effect of *il10* is possible since both improved (Beamer et al., 2008) and impaired survival (Higgins et al., 2009) of mice lacking functional IL10 signaling after *M. tuberculosis* challenge has been reported. It seems the anti-inflammatory effect of IL10 causes complex effects. On one hand, it dampens the protective proinflammatory immune response, especially the Th1 cell response, but on the other hand, the lack of its anti-inflammatory effect may eventually lead to a fatal inflammatory condition. Due to the reported controversial roles of IL10 during mycobacterial infection, we studied its role in the immune defense against *M. marinum* infection in adult zebrafish (II). Since the low-dose *M. marininum* infection in adult zebrafish reflects the different stages of tuberculosis disease spectrum, we chose to use it for our studies.

As an anti-inflammatory cytokine IL10 is well-known for its role in maintaining homeostasis particularly in the mouse model. Accordingly, IL10 deficient mice suffer chronic enterocolitis (Gomes-Santos et al., 2012; Kühn et al., 1993). However, our analysis of unchallenged *il10*$^{e46/e46}$ fish revealed no signs of inflammation either based on gene expression measured in intestine, kidney, liver, spleen or abdominal organ block, or the physical appearance of fish (II). It has been shown that deficiency of *foxp3a* leads to an inflammatory phenotype in adult zebrafish (Sugimoto et al., 2017). FOXP3 controls the development and function of regulatory T cells (Fontenot et al., 2003; Hori et al., 2003), which are required for preventing autoimmunity (reviewed in Scheinecker et al., 2019; Sakaguchi, 2000). Sugimoto and colleagues

(2017) however, did not observe such a drastic phenotype as expected based on mice experiments and suggested this was due to attenuated effector cell responses of aquatic vertebrates that may underlie the scarless regeneration ability that zebrafish also possess. The lack of inflammation despite the mutation in *il10* may make zebrafish a more feasible model compared to mice in studying the role of Il10 during infection, since Il10 deficiency itself does not apparently cause impairment to the fish.

The expression of *il10* was upregulated during low-dose *M. marinum* infection in adult zebrafish (II) at 6 dpi suggesting it has a role during infection. Induction of *il10* is in consensus with literature showing upregulation of *IL10* in active tuberculosis patients, after lipopolysaccharide stimulation in mice and in mice infected aerogenically with *M. tuberculosis* (Beamer et al., 2008; Verbon et al., 1999; Barsig et al., 1995). Some mice studies have concluded that IL10 deficiency does not improve resistance of mice against *M. tuberculosis* even though it leads to an enhanced Th1 response (Higgins et al., 2009; Jung et al., 2003; North, 1998). In our hands however, and also supporting the result that Il10 deficiency itself does not cause mortality in zebrafish, *il10*$^{e46/e46}$ showed improved survival during *M. marinum* infection and decreased bacterial burden compared to WT fish (II). The effect was detectable at 8/9 wpi and not before at 1 dpi, 6 dpi or 4 wpi, suggesting that Il10 inhibits protective adaptive immune responses. This is in fact in line with mice studies since IL10 deficient mice show decreased bacterial burden only after 60 days post aerosol infection (Cyktor et al., 2013; Redford et al., 2010).

It is generally known that IL10 dampens production of Th1 cytokines (Fiorentino et al., 1989; Fiorentino et al., 1991). Thus it was expected that *il10*$^{e46/e46}$ mutant zebrafish would show increased expression of Th1 transcription factor *tbx21* and Th1 cytokine *ifng1* as well as decreased expression of Th2 transcription factor *gata3* in kidney samples at 8 wpi compared to WT controls (II). This is supported by several studies both in *M. tuberculosis* infected mice and in patients with active tuberculosis showing IL10 dampens Th1 cell mediated defense responses. It has been shown that *M. tuberculosis* -induced IFNG production is higher in healthy tuberculin reactors compared to HIV positive tuberculosis patients, and IL10 neutralizing antibody treatment of peripheral blood mononuclear cells collected from HIV negative and HIV positive tuberculosis patients enhances IFNG production (Gong et al., 1996; Zhang et al., 1994). Thus, it was suggested that IL10 dampens the Th1 response and contributes to a more severe form of tuberculosis in HIV patients (Zhang et al., 1994). In addition, *IL6/IL10* co-expression has been

associated with decreased expression of Th1 cytokines in tuberculosis patients (Harling et al., 2019).

Also supporting our results (II), several mouse studies have shown deficient IL10 signaling leads not only to enhanced IFNG and Th1 response but also to decreased bacterial burden and improved survival (Cyktor et al., 2013; Redford et al., 2010; Beamer et al., 2008). TBX21 deficient mice have also been shown to be more susceptible to *M. tuberculosis* infection and have increased bacterial burden in lung, liver and spleen, and elevated IL10 production from CD4+ T cells (Sullivan et al., 2005). It has recently been shown in mice that influenza A virus, which increases the risk of death in tuberculosis patients, increases bacterial load and impairs survival and CD4+ T cell responses (Ring et al., 2019). This was accompanied by rapidly increased production of IL10 and, moreover, the bacterial burden could be decreased by blocking IL10 signaling (Ring et al., 2019). Recently, the inhibitory effect of IL10 on Th1 polarization was further characterized by showing that mannose-capped lipoarabinomannan of *M. tuberculosis* induces IL10 production from specific regulatory B cells and inhibits polarization to Th1 cells (Yuan et al., 2019). On the other hand, it has been reported that the main cellular source of IL10 causing susceptibility to *M. tuberculosis* in mice are activated effector T cells expressing TBX21 and CD44 (Moreira-Teixeira et al., 2017). This points to Th1 cells since a CD44 deficiency in mice promotes Th2 polarization of CD4 T cells by upregulating GATA3 while inhibiting Th1 polarization by downregulating TBX21 expression at a transcriptional level (Guan et al., 2009). Moreover, it is known that *M. tuberculosis* is able to induce IL10 production (Wang et al., 2018) and the gene downregulating the expression of *Il10* during *M. tuberculosis* infection in mice, *basic helix-loop-helix family member e40* (*Bhlbhe40*) has been identified (Huynh et al., 2018). Recently, IL10 deficiency has been linked to better protection of BCG vaccination against tuberculosis in the mouse model since it leads to enhanced Th1 and cytotoxic T cell responses compared to WT (Xu et al., 2019). These results support the harmful role of IL10 during tuberculosis infection.

Recently, expression of immunosuppressive *Foxp3* and *Il10* has been shown in the necrotic center of encapsulated granulomas, which are formed in C3HeB/FeJ mice (Carow et al., 2019). According to several studies, IL10 has a role in formation of the hallmark structure of tuberculosis, granuloma. Our small-scale histological analysis revealed no difference in location of granulomas, their number nor their morphology in adult zebrafish (II). This might be due to the fact that WT zebrafish spontaneously form mature granulomas, whereas well-structured granulomas are not formed in most tuberculosis mouse models (Orme et al., 2014; Tsai et al., 2006;

Rhoades et al., 1997). Actually, in the tuberculosis susceptible mouse strain CBA/J, the absence of functional IL10 signaling during the first month after infection led to the formation of more mature and fibrotic granulomas compared to WT (Cyktor et al., 2013). Another study demonstrating a lack of IL10 eventually led to a harmfully intense immune response, showed granulomas of IL10 knockout mice on a tuberculosis-resistant C57BL/6J background are larger and contain more epithelioid macrophages, foamy cells, lymphocytes and neutrophils compared to WT granulomas (Higgins et al., 2009). Nevertheless, it has been shown in the *Mycobacterium bovis* Calmette-Guérin bacillus infection model that IL10 deficient mice eliminated bacteria faster than WT controls (Jacobs et al., 2000). This was suggested to be due to a higher number and larger size of granulomas with, for example, more antigen presenting cells and T cells, and higher TNF expression in macrophages facilitating the clearance of bacteria (Jacobs et al., 2000). On the other hand, there is a lot of evidence that granuloma is a beneficial structure not only to the host but also for mycobacteria. It has been shown that mycobacteria are able to stimulate IL10 production by activating extracellular signal-regulated kinase (ERK) signaling in infected host macrophages (Richardson et al., 2015) and IL10 can facilitate bacterial persistence and proliferation in granulomas by inhibiting phagosome maturation in *M. tuberculosis* infected macrophages (O'Leary et al., 2011). It has also been suggested that IL10 together with TNF inhibits apoptosis of infected macrophages in granulomas to the benefit of tuberculous mycobacteria (Mustafa et al., 2007).

Our transcriptome data provide another interesting aspect on results from experiments with *il10*$^{e46/e46}$ mutants (II, III). Among upregulated genes at 14 days post a low dose infection was *alox5b.2* (III). This is in consensus with the suggestion that *M. tuberculosis* facilitates its own survival by activating the *Alox5* pathway (Divangahi et al., 2010). It has been shown that *Alox5* deficient mice have increased expression of *Ifng* at 41 days post *M. tuberculosis* infection (Bafica et al., 2005). This was also associated with improved survival and decreased bacterial burden. Therefore, this further supports the role of a Th1 cell response during mycobacterial infection and our result that an improved *ifng* response in particular, would facilitate survival of adult zebrafish during *M. marinum* infection.

6.3 Genetic screen to identify host factors affecting *M. marinum* susceptibility in zebrafish I, II, III

Performing a large forward genetic screen is very laborious and time-consuming and thus exerts a lot of pressure on the choice of research model and method used. The research model selection is a choice between practicality and resemblance to the real situation. For example, when screening susceptibility factors for tuberculosis, it is possible to use human cells (e.g. Kumar et al., 2010). However, cell culture does not provide information that an *in vivo* model does. Non-human primates are physiologically close to humans and their *M. tuberculosis* infection has very similar features to human tuberculosis (Lin et al., 2010; Capuano et al., 2003) but they are very expensive and require large spaces. In addition, ethical aspects must be considered. On the other hand, *M. tuberculosis* model in mice is a widely used model but does not spontaneously follow the course of tuberculosis in humans since *M. tuberculosis* is not a natural mouse pathogen (Kramnik and Beamer, 2016; Myllymäki et al., 2015). Although not a mammal, zebrafish is a vertebrate model organism with an immune system including both innate and adaptive arms. Zebrafish larvae are more practical to use for screening than adults but rely on only innate immune defenses. Since the adaptive immune response, especially the T cell response, is indisputably crucial in the defense against tuberculosis, we wanted to perform a forward genetic screen to identify susceptibility factors for mycobacterial infection using adult zebrafish, thus considering both the innate and adaptive arms of the immune defense (III).

Regarding the choice of mutagenesis method, the downside of ENU mutagenesis was demonstrated in the second original publication of this thesis, when we used a mutant line created using ENU exposure (II). Since ENU produces a large number of mutations per genome, the line we used, *il10*^{e46}, presumably contained also several other mutated alleles besides *e46*. Thus we performed whole genome sequencing and compared the coding regions of *il10*$^{e46/e46}$ and their WT siblings. This revealed co-segregation of nonsense or frameshift mutations with *e46* mutation is unlikely since no other mutations on chromosome 11 were found (II). Another way to control the effect of unspecific mutations is to use WT sibling controls (II). For our forward genetic screen, we ended up using transposon-based mutagenesis, since it produces less mutations per genome compared to ENU and the mutation site can be identified with PCR based methods by locating the insert (III; Clark et al., 2011).

As described in section 2.6.2.1 "Mutagenesis by chemical treatment or irradiation" Lalita Ramakrishnan's group has performed an ENU based mutagenesis

screen to identify susceptibility factors for *M. marinum* infection in zebrafish larvae. They have identified a *M. marinum* susceptible mutant line carrying a mutation in the *lta4h* gene (Tobin et al., 2010). Our transcriptome data from adult WT zebrafish kidney also suggests the role of leukotrienes in *M. marinum* infection (III). As *lta4h*, upregulated *alox5b.2* potentially participates in LTB_4 synthesis (Bafica et al., 2005) and also another upregulated gene, lipid metabolism-related *dipeptidase 1* (*dpep1*) has a postulated role in leukotriene synthesis (III).

High-dose *M. marinum* infection in zebrafish mimics acute tuberculosis (I). However, we were interested in studying the whole tuberculosis spectrum and chose low-dose infection in adult zebrafish for our screen (III). The primary output of our screen was the survival of fish. In addition to hypersusceptibility, we were also interested to see whether some lines would be less susceptible to infection, which could imply to the clearance of the infection such as predicted by epidemiological studies in humans (Cobat et al., 2009). In their screen Ramakrishnan's group found three kinds of phenotypes (Tobin et al., 2010). The largest group was hypersusceptible lines characterized by increased bacterial burden. Two other groups were hyperresistant lines with decreased bacterial burden and lines with insufficient granuloma formation. In our screen, we identified ten mutant lines with impaired and one line with improved survival during low-dose *M. marinum* infection (III).

Of the ten hypersusceptible lines, mutant463 had the most drastic phenotype in survival often resulting in 100% mortality in a few weeks (III). The survival kinetics of mutant463 zebrafish compared to WT suggests the infection does not reach the latent or chronic progressive state as seen in WT fish in the first and second original publications (I, II, III). In larvae, *M. marinum* infection caused no abnormal phenotype in survival compared to WT and only a minor decrease in survival occurred with *S. penumoniae* infection (III). This suggests mutant463 do not have significant defects in the innate immune response but rather in the adaptive arm of the immune system. Furthermore, the elevated number of *M. marinum* CFU in mutants indicated impaired resistance against mycobacterial infection (III).

Whole-genome level transcriptome analysis comparing mutant463 to WT at 14 dpi revealed decreased expression of 27 genes in mutant463 fish (III). Although determining which of these are behind the impaired resistance of the mutants against *M. marinum* infection would require generation of targeted mutants for each gene, some of these genes stand out as interesting candidates. Some have arisen from other transcriptome or other studies on mycobacterial infection responses using human samples, mice or fish. It has been shown from the serum samples of active pulmonary tuberculosis patients that the amount of Liver expressed antimicrobial

peptide, LEAP2, is increased two-fold compared to non-tuberculosis samples (de Groote et al., 2017). It has been shown in two teleost species, mud loach (*Misgurnus mizolepis*) (Lee and Nam, 2017) and ayu (*Plecoglossus altivelis*) (Li et al., 2015) that expression levels of *LEAP2A* and *LEAP2B* were significantly elevated in kidney upon *Edwardsiella tarda* and *LEAP2* upon *Vibrio anguillarum* infection, respectively. This, together with our data, shows expression of *leap2*, despite its name, is not solely restricted to liver.

fabp6 expression has previously been detected in several zebrafish organs, including kidney (Alves-Costa et al., 2008). Bile acids have a role in inflammation in liver and kidney (reviewed in Herman-Edelstein et al., 2018; Li et al., 2017;) and thus as a bile acid binding protein (Capaldi et al., 2009), Fabp6 potentially also has a role in the immune response. Another interesting point is that *fabp6* also has a postulated role in lipid binding and metabolism. In the first original communication we showed that in moribund fish with reactivated infection, granuloma structure has disappeared from large areas. Since lipid metabolism has been shown to have a role in granulomas and the survival of mycobacteria inside granulomas (reviewed in Russell et al., 2009), downregulation of lipid metabolism associated genes could have a role in the predicted inability of mutant463 fish to reach latency. Moreover, downregulation of another gene encoding a fatty acid binding protein family member, *Fabp7*, has been shown in infected macrophages of tuberculosis susceptible mice (Keller et al., 2004).

Since inflammasome activation is part of an efficient inflammatory response against intracellular pathogens (reviewed in Mitchell and Isberg, 2017), including *M. tuberculosis* (reviewed in Wawrocki and Druszczynska, 2017), it was interesting that in our analysis several inflammasome-associated genes were upregulated in WT fish (III). In addition, inflammasome components have conserved between zebrafish and mammals (reviewed in Forn-Cuní et al. 2019). The upregulation of a group of such genes, including *fosab*, was also found in neutrophils of *M. marinum* infected zebrafish larvae in the transcriptome analysis performed by Kenyon and colleagues (2017). One potentially inflammasome related gene, *si:ch211-236p5.3* had practically no expression in mutant463 fish in qPCR analysis (III). According to the InterPro database, this gene contains a leucine-rich repeat and NACHT nucleoside triphosphatase and NACHT associated domains present in inflammasome proteins (Mitchell et al., 2019). This finding suggests that mutant463 could have a defect in inflammasome function.

Nevertheless, when considering the assumption that the defect in mutant463 zebrafish would be in the adaptive arm of immunity and the fact that T cells are

crucial in the immune defense against mycobacterial disease, a gene called *unc119b* stands out from our data as a potential candidate causing impaired survival of mutant463 (III). The human ortholog of this gene, Unc-119 lipid binding chaperone (*UNC119*) has a role in T cell activation as it is an activator of LCK/FYN (Stephen et al., 2018; Gorska et al., 2009; Gorska et al., 2004). Mutation in *UNC119* has been shown to cause T cell lymphopenia (Gorska and Alam, 2012) and therefore it would be rational that it causes a drastically increased susceptibility to mycobacterial infection. Moreover, survival kinetics of mutant463 also support this. The mortality of fish increases at the time of onset of the adaptive immune response and T cell activation. This occurs similarly with *rag1*$^{hu1999/hu1999}$ mutants, which have no functional T or B cells (Wienholds et al., 2002). All in all, our results together with the literature demonstrate zebrafish as a feasible model organism to screen for tuberculosis susceptibility factors.

7 SUMMARY AND CONCLUSIONS

Tuberculosis, caused by *M. tuberculosis*, still remains one of the leading causes of death in the world. The exact disease mechanisms and details related to the different stages of the disease warrant further studies and novel approaches. One way to gain more information on tuberculosis is to study the effect of host genetics on the outcome of infection. This can be done with two different approaches both used in this thesis: forward and reverse genetics. For this, valid animal models are required. Zebrafish is a small vertebrate, which is easy to maintain and thus allows for large scale genetic studies. Moreover, *M. marinum* infection in zebrafish is a promising model for tuberculosis.

In this thesis work we studied the progression of *M. marinum* infection in adult zebrafish with histological methods. We showed that after *M. marinum* infection in adult zebrafish, granulomas are formed, similar to those in human tuberculosis patients. We were able to visualize granulomas with Ziehl-Neelsen staining and show the fibrous capsule around mature granulomas with Mallory's trichrome staining. We showed that following a low-dose infection, the number of granulomas per fish stabilized from four weeks post infection onwards, whereas after high-dose infection the number of granulomas kept increasing. Thus, latent tuberculosis can be modeled with a low-dose *M. marinum* infection and primary active tuberculosis with a high-dose infection. In addition, our analysis showed after experimental reactivation of latent infection the number of clear granuloma structures decreases. The histological model we developed also provides a tool for analyzing susceptible phenotypes resulted as a consequence of a mutation. Susceptibility may be due to the inability of mutants to reach latency or the increased tendency to spontaneously reactivate. By examining the structure of granulomas at different infection time-points with histological methods, these hypotheses can be tested.

We also studied the response to *M. marinum* infection in adult zebrafish by performing a whole-genome level transcriptome analysis in kidney cells at 14 days post low-dose infection. To our knowledge, this was the first transcriptome analysis done on kidney of *M. marinum* infected adult zebrafish. The analysis revealed the induction of immune response related processes with an emphasis on innate immunity. More precisely, our analysis showed upregulation of several genes

involved in cell migration, reflecting for example granuloma formation, which, according to our results, also occurs in kidney, as well as several adaptive immune response -related genes giving indications of the onset of the adaptive immune response. Moreover, our analysis showed differential expression of many genes involved in lipid metabolism, which can be associated with the known ability of mycobacteria to manipulate and utilize the host metabolism for its own purposes.

We took a reverse genetics approach to study the role of *il10* in *M. marinum* infection in zebrafish. In our studies, adult *il10*$^{e46/e46}$ mutant zebrafish showed improved survival following the mycobacterial challenge and decreased bacterial burden at 8/9 post low-dose infection. This was associated with increased expression of Th1 cytokine *ifng1*. This is in line with studies in other tuberculosis models and the known function of IL10. This further suggests that the tuberculosis model developed in this thesis can be utilized in tuberculosis research.

The third aim of this thesis was to perform a forward genetic screen to identify host factors involved in the immune defense against a low-dose *M. marinum* infection in adult zebrafish. In our screen, we identified ten zebrafish lines hypersusceptible to *M. marinum* infection and one less susceptible line compared to WT zebrafish. In a whole-genome level transcriptome analysis performed on kidney cells of the most susceptible line, mutant463, at 14 days post low-dose *M. marium* infection, we saw impaired expression of several genes compared to WT fish. Some of these genes are associated with the immune response. Two of the most poorly expressed genes with a suggested immunological role were *si:ch211-236p5.3* potentially coding for an inflammasome component and *unc119b*, which has a possible role in T cell activation. However, further studies are warranted to identify the genes behind the susceptibility of this line. Furthermore, by identifying mutated genes from other mutant lines with altered susceptibility, more genes having a role in the zebrafish mycobacterial infection can be found.

Since our results are in line with results from other research models, they present the zebrafish as a valid tuberculosis model. Furthermore, this thesis provides candidate genes, which may have a role during *M. marinum* infection in adult zebrafish. When further studied, these results may bring information useful to the development of new treatments against tuberculosis.

8 REFERENCES

Aaberge IS, Eng J, Lermark G, Lovik M. Virulence of *Streptococcus pneumoniae* in mice: a standardized method for preparation and frozen storage of the experimental bacterial inoculum. Microb Pathog. 1995. 18; 141-152.

Abel L, Dessein AJ. The impact of host genetics on susceptibility to human infectious diseases. Curr Opin Immunol. 1997. 9; 509-516.

Abdalla AE, Lambert N, Duan X, Xie J. Interleukin-10 family and tuberculosis: An old story renewed. Int J Biol Sci. 2016. 12; 710-717.

Achkar JM., Chan J, Casadevall A. B cells and antibodies in the defense against *Mycobacterium tuberculosis* infection. Immunol Rev. 2015. 264; 167-181.

Adams DO. The granulomatous inflammatory response. A review. Am J Pathol. 1976. 84; 164-192.

Adams KN, Takaki K, Connolly LE, Wiedenhoft H, Winglee K, Humbert O, Edelstein PH, Cosma CL, Ramakrishnan L. Drug tolerance in replicating mycobacteria mediated by a macrophage-induced efflux mechanism. Cell. 2011. 145; 39-53.

Ahmed A, Rakshit S, Vyakarnam A. HIV-TB co-infection: mechanisms that drive reactivation of *Mycobacterium tuberculosis* in HIV infection. Oral Dis. 2016. 22; 53-60.

Aibana O, Franke MF, Huang CC, Galea JT, Calderon R, Zhang Z, Becerra MC, Smith ER, Ronnenberg AG, Contreras C, Yataco R, Lecca L, Murray MB. Impact of vitamin A and carotenoids on the risk of tuberculosis progression. Clin Infect Dis. 2017. 65; 900-909.

Agarwal N, Lamichhane G, Gupta R, Nolan S, Bishai WR. Cyclic AMP intoxication of macrophages by a *Mycobacterium tuberculosis* adenylate cyclase. Nature. 2009. 460; 98-102.

Akira S, Takeda K. Toll-like receptor signalling. Nat Rev Immunol. 2004. 4; 499-511.

Al-Adhami MA, Kunz YW. Ontogenesis of haematopoietic sites in *Brachydanio rerio* (Hamilton-Buchanan) (*Teleostei*). Develop growth and differ. 1977. 19; 171.

Algood HM, Lin PL, Yankura D, Jones A, Chan J, Flynn JL. TNF influences chemokine expression of macrophages *in vitro* and that of CD11b+ cells *in vivo* during *Mycobacterium tuberculosis* infection. J Immunol. 2004. 172; 6846-6857.

Alves-Costa FA, Denovan-Wright EM, Thisse C, Thisse B, Wright JM. Spatio-temporal distribution of fatty acid-binding protein 6, (*fabp6*) gene transcripts in the developing and adult zebrafish (*Danio rerio*). FEBS J. 2008. 275; 3325-3334.

Amsterdam A, Burgess S, Golling G, Chen W, Sun Z, Townsend K, Farrington S, Haldi M, Hopkins N. A large-scale insertional mutagenesis screen in zebrafish. Genes Dev. 1999. 13; 2713-2724.

Andersen P, Doherty TM. The success and failure of BCG - implications for a novel tuberculosis vaccine. Nat Rev Microbiol. 2005. 3; 656-662.

Anderson CF, Oukka M, Kuchroo VJ, Sacks D. CD4(+)CD25(-)Foxp3(-) Th1 cells are the source of IL-10-mediated immune suppression in chronic cutaneous leishmaniasis. J Exp Med. 2007. 204; 285-297.

Andrews, S. FastQC: A quality control tool for high throughput sequence data. 2010. Available online at: http://www.bioinformatics.babraham.ac.uk/projects/fastqc/.

Ardlie KG, Kruglyak L, Seielstad M. Patterns of linkage disequilibrium in the human genome. Nat Rev Genet. 2002. 3; 299-309.

Armstrong JA, Hart PD. Response of cultured macrophages to *Mycobacterium tuberculosis*, with observations on fusion of lysosomes with phagosomes. J Exp Med. 1971. 134; 713-740.

Arora V, Knapp DC, Smith BL, Statdfield ML, Stein DA, Reddy MT, Weller DD, Iversen PL. c-Myc antisense limits rat liver regeneration and indicates role for c-Myc in regulating cytochrome P-450 3A activity. J Pharmacol Exp Ther. 2000. 292; 921-928.

Aschenbrenner D, Foglierini M, Jarrossay D, Hu D, Weiner HL, Kuchroo VK, Lanzavecchia A, Notarbartolo S, Sallusto F. An immunoregulatory and tissue-residency program modulated by c-MAF in human T_H17 cells. Nat Immunol. 2018. 19; 1126-1136.

Asgharzadeh M, Ghorghanlu S, Rashedi J, Mahdavi Poor B, Khaki-Khatibi F, Moaddab SR, Samadi-Kafil H, Pourostadi M. Association of promoter polymorphisms of interleukin-10 and interferon-gamma genes with tuberculosis in Azeri population of Iran. Iran J Allergy Asthma Immunol. 2016. 15; 167-173.

Ashburner M, Ball CA, Blake JA, Botstein D, Butler H, Cherry JM, Davis AP, Dolinski K, Dwight SS, Eppig JT, Harris MA, Hill DP, Issel-Tarver L, Kasarskis A, Lewis S, Matese JC, Richardson JE, Ringwald M, Rubin GM, Sherlock G. Gene ontology: tool for the unification of biology. The Gene Ontology Consortium. Nat Genet. 2000. 25; 25-29.

Azad AK, Sadee W, Schlesinger LS. Innate immune gene polymorphisms in tuberculosis. Infect Immun. 2012. 80; 3343-3359.

Baars DL, Takle KA, Heier J, Pelegri F. Ploidy manipulation of zebrafish embryos with heat shock 2 treatment. J Vis Exp. 2016. 118; e54492.

Bafica A, Scanga CA, Serhan C, Machado F, White S, Sher A, Aliberti J. Host control of *Mycobacterium tuberculosis* is regulated by 5-lipoxygenase-dependent lipoxin production. J Clin Invest. 2005. 115; 1601-1606.

Baker JJ, Abramovitch RB. Genetic and metabolic regulation of *Mycobacterium tuberculosis* acid growth arrest. Sci Rep. 2018. 8; 4168.

Balla KM, Lugo-Villarino G, Spitsbergen JM, Stachura DL, Hu Y, Bañuelos K, Romo-Fewell O, Aroian RV, Traver D. Eosinophils in the zebrafish: prospective isolation, characterization, and eosinophilia induction by helminth determinants. Blood. 2010. 116; 3944-3954.

Bansal K, Kapoor N, Narayana Y, PUzo G, Gilleron M, Balaji KN. PIM2 induced COX-2 and MMP-9 expression in macrophages requires PIK and Notch1 signaling. PLoS One. 2009. 4; e4911.

Barisch C, Soldati T. Breaking Fat! How mycobacteria and other intracellular pathogens manipulate host lipid droplets. Biochimie. 2017. 141; 54-61.

Barker LP, George KM, Falkow S, Small PL. Differential trafficking of live and dead *Mycobacterium marinum* organisms in macrophages. Infect Immun. 1997. 65; 1497-1504.

Barreto VM, Pan-Hammarstrom Q, Zhao Y, Hammarstrom L, Misulovin Z, Nussenzweig MC. AID from bony fish catalyzes class switch recombination. J exp Med. 2005. 202; 733-738.

Barry CE 3rd, Boshoff HI, Dartois V, Dick T, Ehrt S, Flynn J, Schnappinger D, Wilkinson RJ, Young D. The spectrum of latent tuberculosis: rethinking the biology and intervention strategies. Nat Rev Microbiol. 2009. 7; 845-855.

Barsig J, Küsters S, Vogt K, Volk HD, Tiegs G, Wendel A. Lipopolysaccharide-induced interleukin-10 in mice: role of endogenous tumor necrosis factor-alpha. Eur J Immunol. 1995. 25; 2888-2893.

Batyrshina YR, Schwartz YS. Modeling of *Mycobacterium tuberculosis* dormancy in bacterial cultures. Tuberculosis (Edinb). 2019. 117; 7-17.

Beamer GL, Flaherty DK, Assogba BD, Stromberg P, Gonzalez-Juarrero M, de Waal Malefyt R, Vesosky B, Turner J. Interleukin-10 promotes *Mycobacterium tuberculosis* disease progression in CBA/J mice. J Immunol. 2008. 181; 5545-5550.

Bean AG, Roach DR, Briscoe H, France MP, Korner H, Sedgwick JD, Britton WJ. Structural deficiencies in granuloma formation in TNF gene-targeted mice underlie the heightened susceptibility to aerosol *Mycobacterium tuberculosis* infection, which is not compensated for by lymphotoxin. J Immunol. 1999. 162; 3504-3511.

Becq J, Gutierrez MC, Rosas-Magallanes V, Rauzier J, Gicquel B, Neyrolles O, Deschavanne P. Contribution of horizontally acquired genomic islands to the evolution of the tubercle bacilli. Mol Biol Evol. 2007. 24; 1861-1871.

Bellamy R, Ruwende C, Corrah T, McAdam KP, Whittle HC, Hill AV. Assessment of the interleukin 1 gene cluster and other candidate gene polymorphisms in host susceptibility to tuberculosis. Tuber Lung Dis. 1998. 79; 83-89.

Benard EL, Roobol SJ, Spaink HP, Meijer AH. Phagocytosis of mycobacteria by zebrafish macrophages is dependent on the scavenger receptor Marco, a key control factor of pro-inflammatory signalling. Dev Comp Immunol. 2014. 47; 223-233.

Benard EL, Rougeot J, Racz PI, Spaink HP, Meijer AH. Transcriptomic approaches in the zebrafish model for tuberculosis-insights into host- and pathogen-specific determinants of the innate immune response. Adv Genet. 2016. 95; 217-251.

Benard EL, van der Sar AM, Ellett F, Lieschke GJ, Spaink HP, Meijer AH. Infection of zebrafish embryos with intracellular bacterial pathogens. J Vis Exp. 2012. 61; e3781.

Berchtold S, Ogilvie AL, Bogdan C, Mühl-Zürbes P, Ogilvie A, Schuler G, Steinkasserer A. Human monocyte derived dendritic cells express functional P2X and P2Y receptors as well as ecto-nucleotidases. FEBS Lett. 1999. 458; 424-428.

Berg RD, Ramakrishnan L. Insights into tuberculosis from the zebrafish model. Trends Mol Med. 2012. 18; 689-690.

Berg RD, Levitte S, O'Sullivan MP, O'Leary SM, Cambier CJ, Cameron J, Takaki KK, Moens CB, Tobin DM, Keane J, Ramakrishnan L. Lysosomal disorders drive susceptibility to tuberculosis by compromising macrophage migration. Cell. 2016. 165; 139-152.

Berry MP, Graham CM, McNab FW, Xu Z, Bloch SA, Oni T, Wilkinson KA, Banchereau R, Skinner J, Wilkinson RJ, Quinn C, Blankenship D, Dhawan R, Cush JJ, Mejias A, Ramilo O, Kon OM, Pascual V, Banchereau J, Chaussabel D, O'Garra A. An interferon-inducible neutrophil-driven blood transcriptional signature in human tuberculosis. Nature. 2010. 466; 973-977.

Bingulac-Popovic J, Figueroa F, Sato A, Talbot WS, Johnson SL, Gates M, Postlethwait JH, Klein J. Mapping of Mhc class I and class II regions to different linkage groups in the zebrafish, *Danio rerio*. Immunogenetics. 1997. 46; 129-134.

Blankley S, Berry MP, Graham CM, Bloom CI, Lipman M, O'Garra A. The application of transcriptional blood signatures to enhance our understanding of the host response to infection: the example of tuberculosis. Philos Trans R Soc Lond B Biol Sci. 2014. 369; 20130427.

Bloch H, Segal W. Biochemical differentiation of *Mycobacterium tuberculosis* grown *in vivo* and *in vitro*. J Bacteriol. 1956. 72; 132-141.

Blomgran R, Ernst JD. Lung neutrophils facilitate activation of naïve antigen-specific CD4+ T cells during *Mycobacterium tuberculosis* infection. J Immunol. 2011. 186; 7110-7119.

Boisson-Dupuis S. The monogenic basis of human tuberculosis. Hum Genet. 2020. 10.1007/s00439-020-02126-6.

Borah K, Beyß M, Theorell A, Wu H, Basu P, Mendum TA, Nöh K, Beste DJV, McFadden J. Intracellular *Mycobacterium tuberculosis* exploits multiple host nitrogen sources during growth in human macrophages. Cell Rep. 2019. 29; 3580-3591.

Borovina A, Ciruna B. IFT88 plays a cilia- and PCP-independent role in controlling oriented cell divisions during vertebrate embryonic development. Cell Rep. 2013. 5; 37-43.

BoseDasgupta S, Pieters J. Macrophage-microbe interaction: lessons learned from the pathogen *Mycobacterium tuberculosis*. Semin Immunopathol. 2018. 40; 577-591.

Botha T, Ryffel B. Reactivation of latent tuberculosis infection in TNF-deficient mice. J Immunol. 2003. 171; 3110-3118.

Bowdish DM, Sakamoto K, Kim MJ, Kroos M, Mukhopadhyay S, Leifer CA, Tryggvason K, Gordon S, Russell DG. MARCO, TLR2 and CD14 are required for macrophage cytokine responses to mycobacterial trehalose dimycolate and *Mycobacterium tuberculosis*. PLoS Pathog. 2009. 5; e1000474.

Brand M, Heisenberg CP, Jiang YJ, Beuchle D, Lun K, Furutani-Seiki M, Granato M, Haffter P, Hammerschmidt M, Kane DA, Kelsh RN, Mullins MC, Odenthal J, van Eeden FJ, Nüsslein-Volhard C. Mutations in zebrafish genes affecting the formation of the boundary between midbrain and hindbrain. Development. 1996. 123; 179-190.

Bruchfeld J, Correia-Neves M, Källenius G. Tuberculosis and HIV coninfection. Cold Spring Harb Perspect Med. 2015. 5; a017871.

Brömme D, Li Z, Barnes M, Mehler E. Human cathepsin V functional expression, tissue distribution, electrostatic surface potential, enzymatic characterization, and chromosomal localization. Biochemistry. 1999. 38; 2377-2385.

Bustamante J. Mendelian susceptibility to mycobacterial disease: recent discoveries. Hum Genet. 2020. 10.1007/s00439-020-02120-y.

Bustamante J, Boisson-Dupuis S, Abel L, Casanova JL. Mendelian susceptibility to mycobacterial disease: genetic, immunological and clinical features of inborn errors of IFN-γ immunity. Semin Immunol. 2014; 26: 454-470.

Cadena AM, Fortune SM, Flynn JL. Heterogeneity in tuberculosis. Nat Rev Immunol. 2017. 17; 691-702.

Caire-Brändli I, Papadopoulos A, Malaga W, Marais D, Canaan S, Thilo L, de Chastellier C. Reversible lipid accumulation and associated division arrest of *Mycobacterium avium* in lipoprotein-induced foamy macrophages may resemble key events during latency and reactivation of tuberculosis. Infect Immun. 2014. 82; 476-490.

Cambier CJ, Falkow S, Ramakrishnan L. Host evasion and exploitation schemes of *Mycobacterium tuberculosis*. Cell. 2014. 159; 1497-1509.

Capaldi S, Saccomani G, Fessas D, Signorelli M, Perduca M, Monaco HL. The X-ray structure of zebrafish (*Danio rerio*) ileal bile acid-binding protein reveals the presence of binding sites on the surface of the protein molecule. J Mol Biol. 2009. 385; 99-116.

Capuano SV 3rd, Croix DA, Pawar S, Zinovik A, Myers A, Lin PL, Bissel S, Fuhrman C, Klein E, Flynn JL. Experimental *Mycobacterium tuberculosis* infection of cynomolgus macaques closely resembles the various manifestations of human *M. tuberculosis* infection. Infect Immun. 2003. 71; 5831-5844.

Carmona SJ, Teichmann SA, Ferreira L, Macaulay IC, Stubbington MJ, Cvejic A, Gfeller D. Single-cell transcriptome analysis of fish immune cells provides insight into the evolution of vertebrate immune cell types. Genome Res. 2017. 27; 451-461.

Carow B, Hauling T, Qian X, Kramnik I, Nilsson M, Rottenberg ME. Spatial and temporal localization of immune transcripts defines hallmarks and diversity in the tuberculosis granuloma. Nat Commun. 2019. 10; 1823.

Carradice D, Lieschke GJ. Zebrafish in hematology: sushi or science? Blood. 2008. 111; 3331-3342.

Cassidy JP. The pathogenesis and pathology of bovine tuberculosis with insights from studies of tuberculosis in humans and laboratory animal models. Vet Microbiol. 2006. 112; 151-161.

Cattamanchi A, Smith R, Steingart KR, Metcalfe JZ, Date A, Coleman C, Marston BJ, Huang L, Hopewell PC, Pai M. Interferon-gamma release assays for the diagnosis of latent tuberculosis infection in HIV-infected individuals: a systematic review and meta-analysis. J Acquir Immune Defic Syndr. 2011. 56: 230-238.

Cen O, Gorska MM, Stafford SJ, Sur S, Alam R. Identification of UNC119 as a novel activator of SRC-type tyrosine kinases. J Biol Chem. 2003. 278; 8837-8845.

Chackerian AA, Alt JM, Perera TV, Dascher CC, Behar SM. Dissemination of *Mycobacterium tuberculosis* is influenced by host factors and precedes the initiation of T-cell immunity. Infect Immun. 2002. 70; 4501-4509.

Chakrabarti S, Streisinger G, Singer F, Walker C. Frequency of gamma-ray induced specific locus and recessive lethal mutations in mature germ cells of the zebrafish, *Brachydanio rerio*. Genetics. 1983. 103; 109-123.

Chan K, Knaak T, Satkamp L, Humbert O, Falkow S, Ramakrishnan L. Complex pattern of *Mycobacterium marinum* gene expression during long-term granulomatous infection. Proc Natl Acad Sci USA. 2002. 99; 3920-3925.

Chandra N, Kumar D, Rao K. Systems biology of tuberculosis. Tuberculosis (Edinb). 2011. 91; 487-496.

Chandrasekaran P, Saravanan N, Bethunaickan R, Tripathy S. Malnutrition: Modulator of immune responses in tuberculosis. Front Immunol. 2017. 8; 1316.

Chang MX, Nie P, Wei LL. Short and long peptidoglycan recognition proteins (PGRPs) in zebrafish, with findings of multiple PGRP homologs in teleost fish. Mol Immunol. 2007. 44; 3005-3023.

Chen F, Pruett-Miller SM, Huang Y, Gjoka M, Duda K, Taunton J, Collingwood TN, Frodin M, Davis GD. High frequency genome editing using ssDNA oligonucleotides with zinc finger nucleases. Nat Methods. 2011. 8; 753-755.

Chen L, Wang J, Zganiacz A, Xing Z. Single intranasal mucosal *Mycobacterium bovis* BCG vaccination confers improved protection compared to subcutaneous vaccination against pulmonary tuberculosis. Infect Immun. 2004. 72; 238-246.

Chen M, Gan H, Remold HG. A mechanism of virulence: virulent *Mycobacterium tuberculosis* strain H37Rv, but not attenuated H37Ra, causes significant mitochondrial inner membrane disruption in macrophages leading to necrosis. J Immunol. 2006. 176; 3707-3716.

Chen ZW. Protective immune responses of major Vγ2Vδ2 T-cell subset in *M. tuberculosis* infection. Curr Opin Immunol. 2016. 42; 105-112.

Cheng T, Kam JY, Johansen MD, Oehlers SH. High content analysis of granuloma histology and neutrophilic inflammation in adult zebrafish infected with *Mycobacterium marinum*. Micron. 2020. 129; 102782.

Chinenov Y, Kerppola TK. Close encounters of many kinds: Fos-Jun interactions that mediate transcription regulatory specificity. Oncogene. 2001. 20; 2438-2452.

Church LD, Cook GP, McDermott MF. Primer: inflammasomes and interleukin 1beta in inflammatory disorders. Nat Clin Pract Rheumatol. 2008. 4; 34-42.

Clark HF, Shepard CC. Effect of environmental temperatures on infection with *Mycobacterium marinum* (Balnei) of mice and a number of poikilothermic species. J Bacteriol. 1963. 86; 1057-1069.

Clark KJ, Balciunas D, Pogoda HM, Ding Y, Westcot SE, Bedell VM, Greenwood TM, Urban MD, SKuster KJ, Petzold AM, Ni J, Nielsen AL, Patowary A, Scaria V, Sivasubbu S, Xu X, Hammerschmidt M, Ekker SC. *In vivo* protein trapping produces a functional expression codex of the vertebrate proteome. Nat Methods. 2011. 8; 506-515.

Clay H, Volkman HE, Ramakrishnan L. Tumor necrosis factor signaling mediates resistance to mycobacteria by inhibiting bacterial growth and macrophage death. Immunity. 2008. 29; 283-294.

Clay H, Davis JM, Beery D, Huttenlocher A, Lyons SE, Ramakrishnan L. Dichotomous role of the macrophage in early *Mycobacterium marinum* infection of the zebrafish. Cell Host Microbe. 2007. 2; 29-39.

Cobat A, Gallant CJ, Simkin L, Black GF, Stanley K, Hughes J, Doherty TM, Hanekom WA, Eley B, Jaïs JP, Boland -Auge A, van Helden P, Casanova JL, Abel L, Hoal EG, Schurr E, Alcaïs A. Two loci control tuberculin skin test reactivity in an area hyperendemic for tuberculosis. J Exp Med. 2009. 206; 2583-2591.

Cole ST, Brosch R, Parkhill J, Garnier T, Churcher C, Harris D, Gordon SV, Eiglmeier K, Gas S, Barry CE 3rd, Tekaia F, Badcock K, Basham D, Brown D, Chillingworth T, Connor R, Davies R, Devlin K, Feltwell T, Gentles S, Hamlin N, Holroyd S, Hornsby T, Jagels K, Krogh A, McLean J, Moule S, Murphy L, Oliver K, Osborne J, Quail MA, Rajandream MA, Rogers J, Rutter S, Seeger K, Skelton J, Squares R, Squares S, Sulston JE, Taylor K, Whitehead S, Barrell BG. Deciphering the biology of *Mycobacterium tuberculosis* from the complete genome sequence. Nature. 1998. 393; 537-544.

Coleman MM, Basdeo SA, Coleman AM, Cheallaigh CN, Peral de Castro C, McLaughlin AM, Dunne PJ, Harris J, Keane J. All-*trans* retinoic acid augments autophagy during intracellular bacterial infection. Am J Respir Cell Mol Biol. 2018. 59; 548-556.

Comas I, Chakravartti J, Small PM, Galagan J, Niemann S, Kremer K, Ernst JD, Gagneux S. Human T cell epitopes of *Mycobacterium tuberculosis* are evolutionarily hyperconserved. Nat Genet. 2010. 42; 498-503.

Condamine T, Le Texier L, Howie D, Lavault A, Hill M, Halary F, Cobbold S, Waldmann H, Cuturi MC, Chiffoleau E. Tmem176B and Tmem176A are associated with the immature state of dendritic cells. J Leukoc Biol. 2010. 88; 507-515.

Connolly LE, Edelstein PH, Ramakrishnan L. Why is long-term therapy required to cure tuberculosis? PLoS Med. 2007. 4; e120.

Cooper AM. Cell-mediated immune responses in tuberculosis. Annu Rev Immunol. 2009. 27; 393-422.

Cooper AM, Magram J, Ferrante J, Orme IM. Interleukin (IL-12) is crucial to the development of protective immunity in mice intravenously infected with *Mycobacterium tuberculosis*. J Exp Med. 1997. 186; 39-45.

Cooper AM, Dalton DK, Stewart TA, Griffin JP, Russell DG, Orme IM. Disseminated tuberculosis in interferon gamma gene-disrupted mice. J Exp Med. 1993. 178; 2243-2247.

Coovadia YM, Mahomed S, Pillay M, Werner L, Mlisana K. Rifampicin mono-resistance in *Mycobacterium tuberculosis* in KwaZulu-Natal, South Africa: a significant phenomenon in a high prevalence TB-HIV region. PLoS One. 2013. 8; e77712.

Corbett, EL., Marston B., Churchyard GJ, De Cock KM. Tuberculosis in sub-Saharan Africa: opportunities, challenges, and change in the era of antiretroviral treatment. Lancet. 2006. 367; 926-937.

Corleis B, Dorhoi A. Early dynamics of innate immunity during pulmonary tuberculosis. Immunol Lett. 2020. 221; 56-60.

Correa PA, Gomez LM, Cadena J, Anaya JM. Autoimmunity and tuberculosis. Opposite association with TNF polymorphism. J Rheumatol. 2005. 32; 219-224.

Cosma CL, Humbert O, Ramakrishnan L. Superinfecting mycobacteria home to established tuberculous granulomas. Nat Immunol. 2004. 5; 828-835.

Cosma CL, Humbert O, Sherman DR, Ramakrishnan L. Trafficking of superinfecting *Mycobacterium* organisms into established granulomas occurs in mammals and is independent of the Erp and ESX-1 mycobacterial virulence loci. J Infect Dis. 2008. 198; 1851-1855.

Cosma CL, Klein K, Kim R, Beery D, Ramakrishnan L. *Mycobacterium marinum* Erp is a virulence determinant required for cell wall integrity and intracellular survival. Infect Immun. 2006. 74; 3125-3133.

Couper KN, Blount DG, Riley EM. IL-10: the master regulator of immunity to infection. J Immunol. 2008. 180; 5771-5777.

Covacu R, Philip H, Jaronen M, Almeida J, Kenison JE, Darko S, Chao CC, Yaari G, Louzoun Y, Carmel L, Douek DC, Efroni S, Quintana FJ. System-wide analysis of the T cell response. Cell Rep. 2016. 14; 2733-2744.

Cox JS, Chen B, McNeil M, Jacobs WR Jr. Complex lipid determines tissue-specific replication of *Mycobacterium tuberculosis* in mice. Nature. 1999. 402; 79-83.

Cox V, Brigden G, Crespo RH, Lessem E, Lynch S, Rich ML, Waning B, Furin J. Global programmatic use of bedaquiline and delamanid for the treatment of multidrug-resistant tuberculosis. Int J Tuberc Lung Dis. 2018. 22; 407-412.

Cyktor JC, Carruthers B, Kominsky RA, Beamer GL, Stromberg P, Turner J. IL-10 inhibits mature fibrotic granuloma formation during *Mycobacterium tuberculosis* infection. J Immunol. 2013. 190; 2778-2790.

Daley CL, Small PM, Schecter GF, Schoolnik GK, McAdam RA, Jacobs WR Jr, Hopewell PC. An outbreak of tuberculosis with accelerated progression among persons infected with the human immunodeficiency virus. An analysis using restriction-fragment-length polymorphisms. N Engl J Med. 1992. 326; 231-235.

Dallmann-Sauer M, Correa-Macedo W, Schurr E. Human genetics of mycobacterial disease. Mamm Genome. 2018. 29; 523-538.

Danilova N, Hohman VS, Sacher F, Ota T, Willett CE, Steiner LA. T cells and the thymus in developing zebrafish. Dev Comp Immunol. 2004. 28; 755-767.

Danilova N, Steiner LA. B cells develop in the zebrafish pancreas. Proc Natl Acad Sci USA. 2002. 99; 13711-13716.

Das S, Pettersson BMF, Behra PRK, Mallick A, Cheramie M, Ramesh M, Shirreff L, DuCote T, Dasgupta S, Ennis DG, Kirsebom LA. Extensive genomic diversity among *Mycobacterium marinum* strains revealed by whole genome sequencing. Sci Rep. 2018. 8; 12040.

da Silva ACG, Chilchia AR, de Ávila RI, Valadares MC. Mechanistic-based non-animal assessment of eye toxicity: Inflammatory profile of human keratinocytes cells after exposure to eye damage/irritant agents. Chem Biol Interact. 2018. 292; 1-8.

Davidson AE, Balciunas D, Mohn D, Shaffer J, Hermanson S, Sivasubbu S, Cliff MP, Hackett PB, Ekker SC. Efficient gene delivery and gene expression in zebrafish using the Sleeping Beauty transposon. Dev Biol. 2003. 263; 191-202.

Davis JM, Clay H, Lewis JL, Ghori N, Herbomel P, Ramakrishnan L. Real-time visualization of mycobacterium-macrophage interactions leading to initiation of granuloma formation in zebrafish embryos. Immunity. 2002. 17; 693-702.

Davis JM, Ramakrishnan. The role of the granuloma in expansion and dissemination of early tuberculous infection. Cell. 2009. 136; 37-49.

Dee CT, Nagaraju RT, Athanasiadis EI, Gray C, Fernandez Del Ama L, Johnston SA, Secombes CJ, Cvejic A, Hurlstone AF. CD4-transgenic zebrafish reveal tissue-resident Th2- and regulatory T cell-like populations and diverse mononuclear phagocytes. J Immunol. 2016. 197; 3520-3530.

De Groote MA, Sterling DG, Hraha T, Russell TM, Green LS, Wall K, Kraemer S, Ostroff R, Janjic N, Ochsner UA. Discovery and validation of a six-marker serum protein signature for the diagnosis of active pulmonary tuberculosis. J Clin Microbiol. 2017. 55; 3057-3071.

Dehal P, Boore JL. Two rounds of whole genome duplication in the ancestral vertebrate. PLos Biol. 2005. 3; e314.

Delgado JC, Baena A, Thim S, Goldfeld AE. Ethnic-specific genetic associations with pulmonary tuberculosis. J Infect Dis. 2002. 186; 1463-1468.

Denis M. Killing of *Mycobacterium tuberculosis* within human monocytes: activation by cytokines and calcitriol. Clin Exp Immunol. 1991. 84; 200-206.

Dillon S, Agrawal S, Banerjee K, Letterio J, Denning TL, Oswald-Richter K, Kasprowicz DJ, Kellar K, Pare J, van Dyke T, Ziegler S, Unutmaz D, Pulendran B. Yeast zymosan, a stimulus for TLR2 and dectin-1, induces regulatory antigen-presenting cells and immunological tolerance. J Clin Invest. 2006. 116; 916-928.

Dionne MS, Pham LN, Shirasu-Hiza M, Schneider DS. Akt and FOXO dysregulation contribute to infection-induced wasting in *Drosophila*. Curr Biol. 2006. 16; 1977-1985.

Divangahi M, Desjardins D, Nunes-Alves C, Remold HG, Behar SM. Eicosanoid pathways regulate adaptive immunity to *Mycobacterium tuberculosis*. Nat Immunol. 2010. 11; 751-758.

Divangahi M, Chen M, Gan H, Desjardins D, Hickman TT, Lee DM, Fortune S, Behar SM, Remold HG. *Mycobacterium tuberculosis* evades macrophage defenses by inhibiting plasma membrane repair. Nat Immunol. 2009. 10; 899-906.

Divangahi M, Mostowy S, Coulombe F, Kozak R, Guillot L, Veyrier F, Kobayashi KS, Flavell RA, Gros P, Behr MA. NOD2-deficient mice have impaired resistance to *Mycobacterium tuberculosis* infection through defective innate and adaptive immunity. J Immunol. 2008. 181; 7157-7165.

Dobin A, Davis CA, Schlesinger F, Drenkow J, Zaleski C, Jha S, Batut P, Chaisson M, Gingeras TR. STAR: ultrafast universal RNA-seq aligner. Bioinformatics. 2013. 29; 15-21.

Dobson JT, Seibert J, Teh EM, Da'as S, Fraser RB, Paw BH, Lin TJ, Berman JN. Carboxypeptidase A5 identifies a novel mast cell lineage in the zebrafish providing new insight into mast cell fate determination. Blood. 2008. 112; 2969-2972.

Dorhoi A, Kaufmann SH. Versatile myeloid cell subsets contribute to tuberculosis-associated inflammation. Eur J Immunol. 2015. 45; 2191-2202.

Draper BW, Morcos PA, Kimmel CB. Inhibition of zebrafish *fgf8* pre-mRNA splicing with morpholino oligos: a quantifiable method for gene knockdown. Genesis. 2001. 30; 154-156.

Driever W, Solnica-Krezel L, Schier AF, Neuhauss SC, Malicki J, Stemple DL, Stainier DY, Zwartkruis F, Abdelilah S, Rangini Z, Belak J, Boggs C. A genetic screen for mutations affecting embryogenesis in zebrafish. Development. 1996. 123; 37-46.

Dutta NK, Karakousis PC. Latent tuberculosis infection: myths, models, and molecular mechanisms. Microbiol Mol Biol Rev. 2014. 78; 343-371.

Dutta NK, Illei PB, Jain SK, Karakousis PC. Characterization of a novel necrotic granuloma model of latent tuberculosis infection and reactivation in mice. Am J Pathol. 2014. 184; 2045-2055.

Dyatlov AV, Apt AS, Linge IA. B lymphocytes in anti-mycobacterial immune responses: Pathogenesis or protection? Tuberculosis (Edinb). 2019. 114; 1-8.

Earley AM, Dixon CT, Shiau CE. Genetic analysis of zebrafish homologs of human *FOXQ1*, *foxq1a* and *foxq1b*, in innate immune cell development and bacterial host response. PLoS One. 2018. 13; e0194207.

El-Etr SH, Yan L, Cirillo JD. Fish monocytes as a model for mycobacterial host-pathogen interactions. Infect Immun. 2001. 69; 7310-7317.

El-Gebali S, Mistry J, Bateman A, Eddy SR, Luciani A, Potter SC, Qureshi M, Richardson LJ, Salazar GA, Smart A, Sonnhammer ELL, Hirsh L, Paladin L, Piovesan D, Tosatto SCE, Finn RD. The Pfam protein families database in 2019. Nucleic Acids Res. 2019. 47; D427-D432.

Elks PM, van der Vaart, van Hensbergen V, Schutz E, Redd MJ, Murayama E, Spaink HP, Meijer AH. Mycobacteria counteract a TLR-mediated nitrosative defense mechanism in a zebrafish infection model. PLoS One. 2014. 9; e100928.

Ernst JD. Mechanisms of *M. tuberculosis* immune evasion as challenges of TB vaccine design. Cell Host Microbe. 2018. 24; 34-42.

Eruslanov EB, Lyadova IV, Kondratieva TK, Majorov KB, Scheglov IV, Orlova MO, Apt AS. Neutrophil responses to *Mycobacterium tuberculosis* infection in genetically susceptible and resistant mice. Infect Immun. 2005. 73; 1744-1753.

Eum SY, Kong JH, Hong MS, Lee YJ, Kim JH Hwang SH, Cho SN, Via LE, Barry CE 3rd. Neutrophils are the predominant infected phagocytic cells in the airways of patients with active pulmonary TB. Chest. 2010. 137; 122-128.

Fabregat A, Jupe S, Matthews L, Sidiropoulos K, Gillespie M, Garapati P, Haw R, Jassal B, Korninger F, May B, Milacic M, Roca CD, Rothfels K, Sevilla C, Shamovsky V, Shorser S, Varusai T, Viteri G, Weiser J, Wu G, Stein L, Hermjakob H, D'Eustachio P. The Reactome Pathway Knowledgebase. Nucleic Acids Res. 2018. 46; D649-D655.

Farhat M, Greenaway C, Pai M, Menzies D. False-positive tuberculin skin tests; what is the absolute effect of BCG and non-tuberculous mycobacteria? Int J Tuberc Lung Dis. 2006. 10; 1192-1204.

Faust GG, Hall IM. SAMBLASTER: fast duplicate marking and structural variant read extraction. Bioinformatics. 2014. 30; 2503-2505.

Fennelly KP, Jones-López EC, Ayakaka I, Kim S, Menyha H, Kirenga B, Muchwa C, Joloba M, Dryden-Peterson S, Reilly N, Okwera A, Elliott AM, Smith PG, Mugerwa RD, Eisenach KD, Ellner JJ. Variability of infectious aerosols produced during coughing by patients with pulmonary tuberculosis. Am J Respir Crit Care Med. 2012. 186; 450-457.

Ferguson JS, Weis JJ, Martin JL, Schlesinger LS. Complement protein C3 binding to *Mycobacterium tuberculosis* is initiated by the classical pathway in human bronchoalveolar lavage fluid. Infect Immun. 2004. 72; 2564-2573.

Feschotte C. Transposable elements and the evolution of regulatory networks. Nat Rev Genet. 2008. 9; 397-405.

Figueiredo KA, Mui AL, Nelson CC, Cox ME. Relaxin stimulates leukocyte adhesion and migration through a relaxin receptor LGR7-dependent mechanism. J Biol Chem. 2006. 281; 3030-3039.

Filipe-Santos O, Bustamante J, Chapgier A, Vogt G, de Beaucoudrey L, Feinberg J, Jouanguy E, Boisson-Dupuis S, Fieschi C, Picard C, Casanova JL. Inborn errors of IL-12/23- and IFN-gamma-mediated immunity: molecular, cellular, and clinical features. Semin Immunol. 2006. 18; 347-361.

Finbloom DS, Winestock KD. IL-10 induces the tyrosine phosphorylation of Tyk2 and Jak1 and the differential assembly of STAT1 alpha and STAT3 complexes in human T cells and monocytes. J Immunol. 1995. 155; 1079-1090.

Fiorentino DF, Bond MW, Mosmann TR. Two types of mouse helper cell. IV. Th2 clones secrete a factor that inhibits cytokine production by Th1 clones. J Exp Med. 1989. 170; 2081-2095.

Fiorentino DF, Zlotnik A, Mosmann TR, Howard M, O'Garra A. IL-10 inhibits cytokine production by activated macrophages. J Immunol. 1991. 147; 3815-3822.

Flynn JL, Chan J. Immunology of tuberculosis. Annu Rev Immunol. 2001. 19; 93-129.

Flynn JL, Goldstein MM, Chan J, Triebold KJ, Pfeffer K, Lowenstein CJ, Schreiber R, Mak TW, Bloom BR. Tumor necrosis factor-alpha is required in the protective immune response against *Mycobacterium tuberculosis* in mice. Immunity. 1995. 2; 561-572.

Fontenot JD, Gavin MA, Rudensky AY. Foxp3 programs the development and function of CD4+CD25+ regulatory T cells. Nat Immunol. 2003. 4; 330-336.

Forn-Cuní G, Meijer AH, Varela M. Zebrafish in inflammasome research. Cells. 2019. 8; E901.

Fratti RA, Chua J, Vergne I, Deretic V. *Mycobacterium tuberculosis* glycosylated phosphatidylinositol causes phagosome maturation arrest. Proc Natl Acad Sci USA. 2003. 100; 5437-5442.

Fu Y, Foden JA, Khayter C, Maeder ML, Reyon D, Joung JK, Sander JD. High-frequency off-target mutagenesis induced by CRISPR-Cas nucleases in human cells. Nat Biotechnol. 2013. 31; 822-826.

Fuller CL, Flynn JL, Reinhart TA. *In situ* study of abundant expression of proinflammatory chemokines and cytokines in pulmonary granulomas that develop in cynomolgus macaques experimentally infected with *Mycobacterium tuberculosis*. Infect Immun. 2003. 71; 7023-7034.

Furin J, Cox H, Pai M. Tuberculosis. Lancet. 2019. 393; 1642-1656.

Gagnon JA, Valen E, Thyme SB, Huang P, Akhmetova L, Pauli A, Montague TG, Zimmerman S, Richter C, Schier AF. Efficient mutagenesis by Cas9 protein mediated oligonucleotide insertion and large-scale assessment of single-guide RNAs. PLoS One. 2014. 9; e98186.

Gaiano N, Allende M, Amsterdam A, Kawakami K, Hopkins N. Highly efficient germ-line transmission of proviral insertions in zebrafish. Proc Natl Acad Sci USA. 1996a. 93; 7777-7782.

Gaiano N, Amsterdam A, Kawakami K, Allende M, Becker T, Hopkins N. Insertional mutagenesis and rapid cloning of essential genes in zebrafish. Nature. 1996b. 383; 829-832.

Galagan JE, Minch K, Peterson M, Lyubetskaya A, Azizi E, Sweet L, Gomes A, Rustad T, Dolganov G, Glotova I, Abeel T, Mahwinney C, Kennedy AD, Allard R, Brabant W, Krueger A, Jaini S, Honda B, Yu WH, Hickey MJ, Zucker J, Garay C, Weiner B, Sisk P, Stolte C, Winkler JK, van de Peer Y, Iazzetti P, Camacho D, Dreyfuss J, Liu Y, Dorhoi A, Mollenkopf HJ, Drogaris P, Lamontagne J, Zhou Y, Piquenot J, Park ST, Raman S, Kaufmann SH, Mohney RP, Chelsky D, Moody DB, Sherman DR, Schoolnik GK. The *Mycobacterium tuberculosis* regulatory network and hypoxia. Nature. 2013. 499; 178-183.

Gangaidzo IT, Moyo VM, Mvundura E, Aggrey G, Murphee NL, Khumalo H, Saungweme T, Kasvosve I, Gomo ZA, Roualt T, Boelaert JR, Gordeuk VR. Association of pulmonary tuberculosis with increased dietary iron. J Infect Dis. 2001. 184; 936-939.

Gao LY, Guo S, McLaughlin B, Morisaki H, Engel JN, Brown EJ. A mycobacterial virulence gene cluster extending RD1 is required for cytolysis, bacterial spreading and ESAT-6 secretion. Mol Microbiol. 2004. 53; 1677-1693.

Gao W, Xu L, Guan R, Liu X, Han Y, Wu Q, Xiao Y, Qi F, Zhu Z, Lin S, Zhang B. Wdr18 is required for Kupffer's vesicle formation and regulation of body asymmetry in zebrafish. PLoS One. 2011. 6; e23386.

Garcia-Contreras L, Wong YL, Muttil P, Padilla D, Sadoff J, Derousse J, Germishuizen WA, Goonesekera S, Elbert K, Bloom BR, Miller R, Fourie PB, Hickey A, Edwards D. Immunization by a bacterial aerosol. Proc Natl Acad Sci USA. 2008. 105; 4656-4660.

Gautier EL, Shay T, Miller J, Greter M, Jakubzick C, Ivanov S, Helft J, Chow A, Elpek KG, Gordonov S, Mazloom AR, Ma'ayan A, Chua WJ, Hansen TH, Turley SJ, Merad M, Randolph GJ; Immunological Genome Consortium. Gene-expression profiles and transcriptional regulatory pathways that underlie the identity and diversity of mouse tissue macrophages. Nat Immunol. 2012. 13; 1118-1128.

Geer LY, Marchler-Bauer A, Geer RC, Han L, He J, He S, Liu C, Shi W, Bryant SH. The NCBI BioSystems database. Nucleic Acids Res. 2010. 38; D492-D496.

Geldmacher C, Schuetz, A, Ngwenyama N, Casazza JP, Sanga E, Saathoff E, Boehme C, Geis S, Maboko L, Singh M, Minja F, Meyerhans A, Koup RA, Hoelscher M. Early depletion of *Mycobacterium tuberculosis*-specific T helper 1 cell responses after HIV-1 infection. J Infect Dis. 2008. 198; 1590-1598.

Geldmacher C, Ngwenyama N, Schuetz A, Petrovas C, Reither K, Heeregrave EJ, Casazza JP, Ambrozak DR, Louder M, Ampofo W, Pollakis G, Hill B, Sanga E, Saathoff E, Maboko L, Roederer M, Paxton WA, Hoelscher M, Koup RA. Preferential infection and depletion of *Mycobacterium tuberculosis*-specific CD4 T cells after HIV-1 infection. J Exp Med. 2010. 207; 2869-2881.

Gene, 2004. Bethesda (MD): National Library of Medicine (US), National Center for Biotechnology Information. 2019. https://www.ncbi.nlm.nih.gov/gene/ (accessed 14 April 2019).

Giri PK, Verma I, Khuller GK. Protective efficacy of intranasal vaccination with *Mycobacterium bovis* BCG against airway *Mycobacterium tuberculosis* challenge in mice. J Infect. 2006. 53; 350-356.

Glasauer SM, Neuhauss SC. Whole-genome duplication in teleost fishes and its evolutionary consequences. Mol Genet Genomics. 2014. 289; 1045-1060.

Gobin J, Horwitz MA. Exochelins of *Mycobacterium tuberculosis* remove iron from human iron-binding proteins and donate iron to mycobactins in the *M. tuberculosis* cell wall. J Exp Med. 1996. 183; 1527-1532.

Gobin J, Moore CH, Reeve JR Jr, Wong DK, Gibson BW, Horwitz MA. Iron acquisition by *Mycobacterium tuberculosis*: isolation and characterization of a family of iron-binding exochelins. Proc Natl Acad Sci USA. 1995. 92; 5189-5193.

Goldberg MF, Saini NK, Porcelli SA. Evasion of innate and adaptive immunity by *Mycobacterium tuberculosis*. Microbiol Spectr. 2014. 2; MGM2-0005-2013.

Gomes-Santos AC, Moreira TG, Castro-Junior AB, Horta BC, Lemos L, Cruz DN, Guimarães MA, Cara DC, McCafferty DM, Faria AM. New insights into the immunological changes in IL-10-deficient mice during the course of spontaneous inflammation in the gut mucosa. Clin Dev Immunol. 2012. 2012; 560817.

Gomes MC, Mostowy S. The case for modeling human infection in zebrafish. Trends Microbiol. 2020. 28; 10-18.

Gómez-Martin D, Diaz-Zamudio M, Galindo-Campos M, Alcocer-Varela J. Early growth response transcription factors and the modulation of immune response: implications towards autoimmunity. Autoimmun Rev. 2010. 9; 454-458.

Gong JH, Zhang M, Modlin RL, Linsley PS, Iyer D, Lin Y, Barnes PF. Interleukin-10 downregulates *Mycobacterium tuberculosis*-induced Th1 responses and CTLA-4 expression. Infect Immun. 1996. 64; 913-918.

Gonzalez-Juarrero M, Kingry LC, Ordway DJ, Henao-Tamayo M, Harton M, Basaraba RJ, Hanneman WH, Orme IM, Slayden RA. Immune response to *Mycobacterium tuberculosis* and identification of molecular markers of disease. Am J Respir Cell Mol Biol. 2009. 40; 398-409.

Gorska MM, Alam R. A mutation in the human Uncoordinated 119 gene impairs TCR signaling and is associated with CD4 lymphopenia. Blood. 2012. 119; 1399-1406.

Gorska MM, Liang Q, Karim Z, Alam R. Uncoordinated 119 protein controls trafficking of Lck via the Rab11 endosome and is critical for immunological synapse formation. J Immunol. 2009. 183; 1675-1684.

Gorska MM, Stafford SJ, Cen O, Sur S, Alam R. Unc119, a novel activator of LCK/Fyn, is essential for T cell activation. J Exp Med. 2004. 199; 369-379.

Grayfer L, Belosevic M. Identification and molecular characterization of the interleukin-10 receptor 1 of the zebrafish (*Danio rerio*) and the goldfish (*Carassius auratus* L.). Dev Comp Immunol. 2012. 36; 408-417.

Groux H, O'Garra A, Bigler M, Rouleau M, Antonenko S, de Vries JE, Roncarolo MG. A CD4+ T-cell subset inhibits antigen-specific T-cell responses and prevents colitis. Nature. 1997. 389; 737-742.

Guan H, Nagarkatti PS, Nagarkatti M. Role of CD44 in the differentiation of Th1 and Th2 cells: CD44-deficiency enhances the development of Th2 effectors in response to sheep RBC and chicken ovalbumin. J Immunol. 2009. 183: 172-180.

Guilliams M, Lambrecht BN, Hammad H. Division of labor between lung dendritic cells and macrophages in the defense against pulmonary infections. Mucosal Immunol. 2013. 6; 464-473.

Gutierrez MG, Master SS, Singh SB, Taylor GA, Colombo MI, Deretic V. Autophagy is a defense mechanism inhibiting BCG and *Mycobacterium tuberculosis* survival in infected macrophages. Cell. 2004. 119; 753-766.

Haeggström JZ. Leukotriene A4 hydrolase/aminopeptidase, the gatekeeper of chemotactic leukotriene B4 biosynthesis. J Biol Chem. 2004. 279: 50639-50642.

Haffter P, Granato M, Brand M, Mullins MC, Hammerschmidt M, Kane DA, Odenthal J, van Eeden FJ, Jiang YJ, Heisenberg CP, Kelsh RN, Furutani-Seiki M, Vogelsang E, Beuchle D, Schach U, Fabian C, Nüsslein-Volhard C. The identification of genes with unique and essential functions in the development of the zebrafish, *Danio rerio*. Development. 1996. 123: 1-36.

Haire RN, Rast JP, Litman RT, Litman GW. Characterization of three isotypes of immunoglobulin light chains and T-cell antigen receptor alpha in zebrafish. Immunogenetics. 2000. 51; 915-923.

Hammarén MM, Oksanen KE, Nisula HM, Luukinen BV, Pesu M, Rämet M, Parikka M. Adequate Th2-type response associates with restricted bacterial growth in latent mycobacterial infection of zebrafish. PLoS Pathog. 2014. 10; e1004190.

Hampshire T, Soneji S, Bacon J, James BW, Hinds J, Laing K, Stabler RA, Marsh PD, Butcher PD. Stationary phase gene expression of *Mycobacterium tuberculosis* following a progressive nutrient depletino: a model for persistent organisms? Tuberculosis (Edinb). 2004. 84; 228-238.

Harausz EP, Garcia-Prats AJ, Seddon JA, Schaaf HS, Hesseling AC, Achar J, Bernheimer J, Cruz AT, D'Ambrosio L, Detjen A, Graham SM, Hughes J, Jonckheere S, Marais BJ, Migliori GB, McKenna L, Skrahina A, Tadolini M, Wilson P, Furin J. New and repurposed drugs for pediatric multidrug-resistant tuberculosis. Practice-based recommendations. Am J Respir Crit Care Med. 2017. 195; 1300-1310.

Harling K, Adankwah E, Güler A, Afum-Adjei Awuah A, Adu-Amoah L, Mayatepek E, Owusu-Dabo E, Nausch N, Jacobsen M. Constitutive STAT3 phosphorylation and IL-6/IL-10 co-expression are associated with impaired T-cell function in tuberculosis patients. Cell Mol Immunol. 2019. 16; 275-287.

Harriff MJ, Bermudez LE, Kent ML. Experimental exposure of zebrafish, *Danio rerio* (Hamilton), to *Mycobacterium marinum* and *Mycobacterium peregrinum* reveals the gastrointestinal tract as the primary route of infection: a potential model of environmental mycobacterial infection. J Fish Dis. 2007. 30: 587-600.

Heasman J. Morpholino oligos: making sense of antisense? Dev Biol. 2002. 243; 209-214.

Heasman J, Kofron M, Wylie C. Beta-catenin signaling activity dissected in the early *Xenopus* embryo: a novel antisense approach. Dev Biol. 2000. 222; 124-134.

Hegedüs Z, Zakrzewska A, Ágoston VC, Ordas A, Rácz P, Mink M, Spaink HP, Meijer AH. Deep sequencing of the zebrafish transcriptome response to mycobacterium infection. Mol Immunol. 2009. 46; 2918-2930.

Heier J, Takle KA, Hasley AO, Pelegri F. Ploidy manipulation and induction of alternate cleavage patterns through inhibition of centrosome duplication in the early zebrafish embryo. Dev Dyn. 2015. 244; 1300-1312.

Henke K, Bowen ME, Harris MP. Perspectives for identification of mutations in the zebrafish: making use of next-generation sequencing technologies for forward genetic approaches. Methods. 2013. 62; 185-196.

Herb F, Thye T, Niemann S, Browne EN, Chinbuah MA, Gyapong J, Osei I, Owusu-Dabo E, Werz O, Rüsch-Gerdes S, Horstmann RD, Meyer CG. *ALOX5* variants associated with susceptibility to human pulmonary tuberculosis. Hum Mol Genet. 2008. 17; 1052-1060.

Herbomel P, Thisse B, Thisse C. Ontogeny and behaviour of early macrophages in the zebrafish embryo. Development. 1999. 126; 3735-3745.

Herman-Edelstein M, Weinstein T, Levi M. Bile acid receptors and the kidney. Curr Opin Nephrol Hypertens. 2018. 27; 56-62.

Hermann AC, Millard PJ, Blake SL, Kim CH. Development of a respiratory burst assay using zebrafish kidneys and embryos. J Immunol Methods. 2004. 292; 119-129.

Hesseling AC, Marais BJ, Gie RP, Schaaf HS, Fine PE, Godfrey-Faussett P, Beyers N. The risk of disseminated Bacille Calmette-Guerin (BCG) disease in HIV-infected children. Vaccine. 2007. 25; 14-18.

Higgins DM, Sanchez-Campillo J, Rosas-Taraco AG, Lee EJ, Orme IM, Gonzalez-Juarrero M. Lack of IL-10 alters inflammatory and immune responses during pulmonary *Mycobacterium tuberculosis* infection. Tuberculosis (Edinb). 2009. 89; 149-157.

Hirsch CS, Ellner JJ, Russell DG, Rich EA. Complement receptor-mediated uptake and tumor necrosis factor-alpha-mediated growth inhibition of *Mycobacterium tuberculosis* by human alveolar macrophages. J Immunol. 1994. 152; 743-753.

Holland MC, Lambris JD. The complement system in teleosts. Fish Shellfish Immunol. 2002. 12; 339-420.

Holt A, Mitra S, van der Sar AM, Alnabulsi A, Secombes CJ, Bird S. Discovery of zebrafish (*Danio rerio)* interleukin-23 alpha (IL-23α) chain, a subunit important for the formation of IL-23, a cytokine involved in the development of Th17 cells and inflammation. Mol Immunol. 2011. 48; 981-991.

Hori S, Nomura T, Sakaguchi S. Control of regulatory T cell development by the transcription factor Foxp3. Science. 2003. 299; 1057-1061.

Howe DG, Bradford YM, Conlin T, Eagle AE, Fashena D, Frazer K, Knight J, Mani P, Martin R, Moxon SA, Paddock H, Pich C, Ramachandran S, Ruef BJ, Ruzicka L, Schaper K, Shao X, Singer A, Sprunger B, van Slyke CE, Westerfield M. ZFIN, the Zebrafish Model Organism Database: increased support for mutants and transgenics. Nucleic Acids Res. 2013. 41; D854-D860.

Howe K, Schiffer PH, Zielinski J, Wiehe T, Laird GK, Marioni JC, Soylemez O, Kondrashov F, Leptin M. Structure and evolutionary history of a large family of NLR proteins in the zebrafish. Open Biol. 2016. 6; 160009.

Howe K, Clark MD, Torroja CF, Torrance J, Berthelot C, Muffato M, Collins JE, Humphray S, McLaren K, Matthews L, McLaren S, Sealy I, Caccamo M, Churcher C, Scott C, Barrett JC, Koch R, Rauch GJ, White S, Chow W, Kilian B, Quintais LT, Guerra-Assunção JA, Zhou Y, Gu Y, Yen J, Vogel JH, Eyre T, Redmond S, Banerjee R, Chi J, Fu B, Langley E, Maguire SF, Laird GK, Lloyd D, Kenyon E, Donaldson S, Sehra H, Almeida-King J, Loveland J, Trevanion S, Jones M, Quail M, Willey D, Hunt A, Burton J, Sims S, McLay K, Plumb B, Davis J, Clee C, Oliver K, Clark R, Riddle C, Elliot D, Threadgold G, Harden G, Ware D, Begum S, Mortimore B, Kerry G, Heath P, Phillimore B, Tracey A, Corby N, Dunn M, Johnson C, Wood J, Clark S, Pelan S, Griffiths G, Smith M, Glithero R, Howden P, Barker N, Lloyd C, Stevens C, Harley J, Holt K, Panagiotidis G, Lovell J, Beasley H, Henderson C, Gordon D, Auger K, Wright D, Collins J, Raisen C, Dyer L, Leung K, Robertson L, Ambridge K, Leongamornlert D, McGuire S, Gilderthorp R, Griffiths C, Manthravadi D, Nichol S, Barker G, Whitehead S, Kay M, Brown J, Murnane C, Gray E, Humphries M, Sycamore N, Barker D, Saunders D, Wallis J, Babbage A, Hammond S, Mashreghi-Mohammadi M, Barr L, Martin S, Wray P, Ellington A, Matthews N, Ellwood M, Woodmansey R, Clark G, Cooper J, Tromans A, Grafham D, Skuce C, Pandian R, Andrews R, Harrison E, Kimberley A, Garnett J, Fosker N, Hall R, Garner P, Kelly

D, Bird C, Palmer S, Gehring I, Berger A, Dooley CM, Ersan-Ürün Z, Eser C, Geiger H, Geisler M, Karotki L, Kirn A, Konantz J, Konantz M, Oberländer M, Rudolph-Geiger S, Teucke M, Lanz C, Raddatz G, Osoegawa K, Zhu B, Rapp A, Widaa S, Langford C, Yang F, Schuster Sc, Carter NP, Harrow J, Ning Z, Herrero J, Searle SM, Enright A, Geisler R, Plasterk RH, Lee C, Westerfield M, de Jong PJ, Zon LI,Postlethwait JH, Nüsslein-Volhard C, Hubbard TJ, Roest Crollius H, Rogers J, Stemple DL. The zebrafish reference genome sequence and its relationship to the human genome. Nature. 2013. 496; 498-503.

Hsu K, Traver D, Kutok JL, Hagen A, Liu TX, Paw BH, Rhodes J, Berman JN, Zon LI, Kanki JP, Look AT. The pu.1 promoter drives myeloid gene expression in zebrafish. Blood. 2004. 104; 1291-1297.

Hu YL, Xiang LX, Shao JZ. Identification and characterization of a novel immunoglobulin Z isotype in zebrafish: implications for a distinct B cell receptor in lower vertebrates. Mol Immunol. 2010. 47; 738-746.

Hu YW, Wu XM, Ren SS, Cao L, Nie P, Chang MX. NOD1 deficiency impairs CD44a/Lck as well as PI3K/Akt pathway. Sci Rep. 2017. 7; 2979.

Huang L, Gebreselassie NG, Gagliardo LF, Ruyechan MC, Lee NA, Lee JJ, Appleton JA. Eosinophil-derived IL-10 supports chronic nematode infection. J Immunol. 2014. 193; 4178-4187.

Hubbard T, Barker D, Birney E, Cameron G, Chen Y, Clark L, Cox T, Cuff J, Curwen V, Down T, Durbin R, Eyras E, Gilbert J, Hammond M, Huminiecki L, Kasprzyk A, Lehvaslaiho H, Lijnzaad P, Melsopp C, Mongin E, Pettett R, Pocock M, Potter S, Rust A, Schmidt E, Searle S, Slater G, Smith J, Spooner W, Stabenau A, Stalker J, Stupka E, Ureta-Vidal A, Vastrik I, Clamp M. The Ensembl genome database project. Nucleic Acids Res. 2002. 30; 38-41.

Huynh JP, Lin CC, Kimmey JM, Jarjour NN, Schwarzkopf EA, Bradstreet TR, Shchukina I, Shpynov O, Weaver CT, Taneja R, Artyomov MN, Edelson BT, Stallings CL. Bhlhe40 is an essential repressor of IL-10 during *Mycobacterium tuberculosis* infection. J Exp Med. 2018. 215; 1823-1838.

Hwang WY, Fu Y, Reyon D, Maeder ML, Tsai SQ, Sander JD, Peterson RT, Yeh JR, Joung JK. Efficient genome editing in zebrafish using a CRISPR-Cas system. Nat Biotechnol. 2013. 31; 227-229.

Igarashi M, Osuga J, Uozaki H, Sekiya M, Nagashima S, Takahashi M, Takase S, Takanashi M, Li Y, Ohta K, Kumagai M, Nishi M, Hosokawa M, Fledelius C, Jacobsen P, yagyu H, Fukayama M, Nagai R, Kadowaki T, Ohashi K, Ishibashi S. The critical role of neutral cholesterol ester hydrolase 1 in cholesterol removal from human macrophages. Circ Res. 2010. 107; 1387-1395.

Iwanami N. Zebrafish as a model for understanding the evolution of the vertebrate immune system and human primary immunodeficiency. Exp Hematol. 2014. 42; 697-706.

Jacobs M, Brown N, Allie N, Gulert R, Ryffel B. Increased resistance to mycobacterial infection in the absence of interleukin-10. Immunology. 2000. 100; 494-501.

Jamwal SV, Mehrotra P, Singh A, Siddiqui Z, Basu A, Rao KV. Mycobacterial escape from macrophage phagosomes to the cytoplasm represents an alternate adaptation mechanism. Sci Rep. 2016. 6; 23089.

Jankovic D, Kullberg MC, Feng CG, Goldszmid RS, Collazo CM, Wilson M, Wynn TA, Kamanaka M, Flavell RA, Sher A. Conventional T-bet(+)Foxp3(-) Th1 cells are the major source of host-protective regulatory IL-10 during intracellular protozoan infection. J Exp Med. 2007. 204; 273-283.

Jault C, Pichon L, Chluba J. Toll-like receptor gene family and TIR-domain adapters in *Danio rerio*. Mol Immunol. 2004. 40; 759-771.

Jayaswal S, Kamal MA, Dua R, Gupta S, Majumdar T, Das G, Kumar D, Rao KV. Identification of host-dependent survival factors for intracellular *Mycobacterium tuberculosis* through an siRNA screen. PLoS Pathog. 2010. 6; e1000839.

Jinek M, Chylinski K, Fonfara I, Hauer M, Doudna JA, Charpentier E. A programmable dual-RNA-guided DNA endonuclease in adaptive bacterial immunity. Science. 2012. 337; 816-821.

Jinek M, East A, Cheng A, Lin S, Ma E, Doudna J. RNA-programmed genome editing in human cells. Elife. 2013. 2; e00471.

Jones-López EC, Namugga O, Mumbowa F, Ssebidandi M, Mbabazi O, Moine S, Mboowa G, Fox MP, Reilly N, Ayakaka I, Kim S, Okwera A, Joloba M, Fennelly KP. Cough aerosols of *Mycobacterium tuberculosis* predict new infection; a household contact study. Am J Respir Crit Care Med. 2013. 187; 1007-1015.

Jouanguy E, Altare F, Lamhamedi S, Revy P, Emile JF, Newport M, Levin M, Blanche S, Seboun E, Fischer A, Casanova JL. Interferon-gamma-receptor deficiency in an infant with fatal bacille Calmette-Guérin infection. N Engl J Med. 1996. 335; 1956-1961.

Jung YJ, Ryan L, LaCourse R, North RJ. Increased interleukin-10 expression is not responsible for failure of T helper 1 immunity to resolve airborne *Mycobacterium tuberculosis* infection in mice. Immunology. 2003. 109; 295-299.

Just S, Raphel L, Berger IM, Bühler A, Keßler M, Rottbauer W. Tbx20 is an essential regulator of embryonic heart growth in zebrafish. PLoS One. 2016. 11; e0167306.

Kaipilyawar V, Salgame P. Infection resisters: targets of new research for uncovering natural protective immunity against *Mycobacterium tuberculosis*. F1000Res. 2019. 8; F1000 Faculty Rev-1698.

Kang PB, Azad AK, Torrelles JB, Kaufman TM, Beharka A, Tibesar E, DesJardin Le, Schlesinger LS. The human macrophage mannose receptor directs *Mycobacterium tuberculosis* lipoarabinomannan-mediated phagosome biogenesis. J Exp Med. 2005. 202; 987-999.

Kanwal Z, Zakrzewska A, den Hertog J, Spaink HP, Schaaf MJ, Meijer AH. Deficiency in hematopoietic phosphatase ptpn6/Shp1 hyperactivates the innate immune system and impairs control of bacterial infections in zebrafish embryos. J Immunol. 2013. 190; 1631-1645.

Karakousis PC, Yoshimatsu T, Lamichhane G, Woolwine SC, Nuermberger EL, Grosset J, Bishai WR. Dormancy phenotype displayed by extracellular *Mycobacterium tuberculosis* within artificial granulomas in mice. J Exp Med. 2004. 200; 647-657.

Kasheta M, Painter CA, Moore FE, Lobbardi R, Bryll A, Freiman E, Stachura D, Rogers AB, Houvras Y, Langenau DM, Ceol CJ. Identification and characterization of T reg-like cells in zebrafish. J Exp Med. 2017. 214; 3519-3530.

Kawakami K, Largaespada DA, Ivics Z. Transposons as tools for functional genomics in vertebrate models. Trends Genet. 2017. 33; 784-801.

Kawakami K, Shima A, Kawakami N. Identification of a functional transposase of the Tol2 element, an Ac-like element from the Japanese medaka fish, and its transposition in the zebrafish germ lineage. Proc Natl Acad Sci USA. 2000. 97; 11403-11408.

Kawakami K, Takeda H, Kawakami N, Kobayashi M, Matsuda N, Mishina M. A transposon-mediated gene trap approach identifies developmentally regulated genes in zebrafish. Dev Cell. 2004. 7; 133-144.

Keane J, Remold HG, Kornfeld H. Virulent *Mycobacterium tuberculosis* strains evade apoptosis of infected alveolar macrophages. J Immunol. 2000. 164; 2016-2020.

Keane J, Gershon S, Wise RP, Mirabile-Levens E, Kasznica J, Schwieterman WD, Siegel JN, Braun MM. Tubeculosis associated with infliximab, a tumor necrosis factor alpha-neutralizing agent. N Engl J Med. 2001. 345; 1098-1104.

Keller C, Lauber J, Blumenthal A, Buer J, Ehlers S. Resistance and susceptibility to tuberculosis analysed at the transcriptome level: lessons from mouse macrophages. Tuberculosis (Edinb). 2004. 84; 144-158.

Keller C, Hoffmann R, Lang R, Brandau S, Hermann C, Ehlers S. Genetically determined susceptibility to tuberculosis in mice causally involves accelerated and enhanced recruitment of granulocytes. Infect Immun. 2006. 74; 4295-4309.

Kent ML, Whipps CM, Matthews JL, Florio D, Watral V, Bishop-Stewart JK, Poort M, Bermudez L. Mycobacteriosis in zebrafish (*Danio rerio*) research facilities. Comp Biochem Physiol C Toxicol Pharmacol. 2004. 138; 383-390.

Kenyon A, Gavriouchkina D, Zorman J, Napolitani G, Cerundolo V, Sauka-Spengler T. Active nuclear transcriptome analysis reveals inflammasome-dependent mechanism for early neutrophil response to *Mycobacterium marinum*. Sci Rep. 2017. 7; 6505.

Kettleborough RN, Busch-Nentwich EM, Harvey SA, Dooley CM, de Bruijn E, van Eeden F, Sealy I, White RJ, Herd C, Nijman IJ, Fényes F, Mehroke S, Scahill C, Gibbons R, Wali N, Carruthers S, Hall A, Yen J, Cuppen E, Stemple DL. A systematic genome-wide analysis of zebrafish protein-coding gene function. Nature. 2013. 496; 494-497.

Khader SA, Partida-Sanchez S, Bell G, Jelley-Gibbs DM, Swain S, Pearl JE, Ghilardi N, Desauvage FJ, Lund FE, Cooper AM. Interleukin 12p40 is required for dendritic cell migration and T cell priming after *Mycobacterium tuberculosis* infection. J Exp Med. 2006. 203; 1805-1815.

Khan A, Jagannath C. Analysis of host-pathogen modulators of autophagy during *Mycobacterium tuberculosis* infection and therapeutic repercussions. Int Rev Immunol. 2017. 36; 271-286.

Kizil C, Dudczig S, Kyritsis N, Machate A, Blaesche J, Kroehne V, Brand M. The chemokine receptor *cxcr5* regulates the regenerative neurogenesis response in the adult zebrafish brain. Neural Dev. 2012. 7; 27.

Kleinnijenhuis J, Oosting M, Joosten LA, Netea MG, van Crevel R. Innate immune recognition of *Mycobacterium tuberculosis*. Clin Dev Immunol. 2011. 2011; 405310.

Kohyama M, Kakehi M, Totsuka M, Hachimura S, Hisatsune T, Kaminogawa S. Selective induction of CD8+ T cell functions by single substituted analogs of an antigenic peptide: distinct signals for IL-10 production. FEBS Lett. 1998. 423; 138-142.

Kok FO, Shin M, Ni CW, Gupta A,, Grosse AS, van Impel A, Kirchmaier BC, Peterson-Maduro J, Kourkoulis G, Male I, DeSantis DF, Sheppard-Tindell S, Ebarasi L, Betsholtz C, Schulte-Merker S, Wolfe SA, Lawson ND. Reverse genetic screening reveals poor correlation between morpholino-induced and mutant phenotypes in zebrafish. Dev Cell. 2015. 32; 97-108.

Korb VC, Chuturgoon AA, Moodley D. *Mycobacterium tuberculosis*: Manipulator of protective immunity. Int J Mol Sci. 2016. 17; 131.

Kramnik I, Beamer G. Mouse models of human TB pathology: roles in the analysis of necrosis and the development of host-directed therapies. Semin Immunopathol. 2016. 38; 221-237.

Kroeger PT Jr, Poureetezadi SJ, McKee R, Jou J, Miceli R, Wingert RA. Production of haploid zebrafish embryos by *in vitro* fertilization. J Vis Exp. 2014. 89; e51708.

Kühn R, Löhler J, Rennick D, Rajewsky K Müller W. Interleukin-10-deficient mice develop chronic enterocolitis. Cell. 1993. 75; 263-274.

Kumar D, Nath L, Kamal MA, Varshney A, Jain A, Singh S, Rao KV. Genome-wide analysis of the host intracellular network that regulates survival of *Mycobacterium tuberculosis*. Cell. 2010. 140; 731-743.

Lam SH, Chua HL, Gong Z, Lam TJ, Sin YM. Development and maturation of the immune system in zebrafish, *Danio rerio*: a gene expression profiling, in situ hybridization and immunological study. Dev Comp Immunol. 2004. 28; 9-28.

Langenau DM, Ferrando AA, Traver D, Kutok JL, Hezel JP, Kanki JP, Zon Li, Look AT, Trede NS. *In vivo* tracking of T cell development, ablation, and engraftment in transgenic zebrafish. Proc Natl Acad Sci USA. 2004. 101; 7369-7374.

Langmead B, Salzberg SL. Fast gapped-read alignment with Bowtie 2. Nat Methods. 2012. 9; 357-359.

Lavin Y, Winter D, Blecher-Gonen R, David E, Keren-Shaul H, Merad M, Jung S, Amit I. Tissue-resident macrophage enhancer landscapes are shaped by the local microenvironment. Cell. 2014. 159; 1312-1326.

Lawson ND. Reverse genetics in zebrafish: Mutants, morphants, and moving forward. Trends Cell Biol. 2016. 26; 77-79.

Lawson ND, Wolfe SA. Forward and reverse genetic approaches for the analysis of vertebrate development in the zebrafish. Dev Cell. 2011. 21; 48-64.

Lee SH, Kim KS, Fodil-Cornu N, Vidal SM, Biron CA. Activating receptors promote NK cell expansion for maintenance, IL-10 production, CD8 T cell regulation during viral infection. J Exp Med. 2009. 206; 2235-2251.

Lee SY, Nam YK. Gene structure and expression characteristics of liver-expressed antimicrobial peptide-2 isoforms in mud loach (*Misgurnus mizolepis*, Cypriniformes). Fisheries and Aquatic Sciences. 2017. 20; 31.

Lee TS, Chau LY. Heme oxygenase-1 mediates the anti-inflammatory effect of interleukin-10 in mice. Nat Med. 2002. 8; 240-246.

Leemans JC, Juffermans NP, Florquin S, van Rooijen N, Vervoordeldonk MJ, Verbon A, van Deventer SJ, van der Poll T. Depletion of alveolar macrophages exerts protective effects in pulmonary tuberculosis in mice. J Immunol. 2001. 166; 4604-4611.

Leemans JC, Thepen T, Weijer S, Florquin S, van Rooijen N, van de Winkel JG, van der Poll T. Macrophages play a dual role during pulmonary tuberculosis in mice. J Infect Dis. 2005. 191; 65-74.

Le Guyader D, Redd MJ, Colucci-Guyon E, Murayama E, Kissa K, Briolat V, Mordelet E, Zapata A, Shinomiya H, Herbomel P. Origins and unconventional behavior of neutrophils in developing zebrafish. Blood. 2008. 111; 132-141.

Lenart M, Rutkowska-Zapala M, Baj-Krzyworzeka M, Szatanek R, Węglarczyk K, Smallie T, Ziegler-Heitbrock L, Zembala M, Siedlar M. Hyaluronan carried by tumor-derived microvesicles induces IL-10 production in classical ($CD14^{++}CD16^{-}$) monocytes via PI3K/Akt/mTOR-dependent signalling pathway. Immunobiology. 2017. 222; 1-10.

Lerche NW, Yee JL, Capuano SV, Flynn JL. New approaches to tuberculosis surveillance in nonhuman primates. ILAR J. 2008. 49; 170-178.

Lewis KL, Del Cid N, Traver D. Perspectives on antigen presenting cells in zebrafish. Dev Comp Immunol. 2014. 46; 63-73.

Li HX, Lu XJ, Li CH, Chen J. Molecular characterization of the liver-expressed antimicrobial peptide 2 (LEAP-2) in a teleost fish, *Plecoglossus altivelis*: antimicrobial activity and molecular mechanism. Mol Immunol. 2015. 65; 406-415.

Li M, Cai SY, Boyer JL. Mechanisms of bile acid mediated inflammation in the liver. Mol Aspects Med. 2017. 56; 45-53.
Li X, Wang S, Qi J, Echtenkamp SF, Chatterjee R, Wang M, Boons GJ, Dziarski R, Gupta D. Zebrafish peptidoglycan recognition proteins are bactericidal amidases essential for defense against bacterial infections. Immunity. 2007. 27; 518-529.
Liao Y, Smyth GK, Shi W. featureCounts: an efficient general purpose program for assigning sequence reads to genomic features. Bioinformatics. 2014. 30; 923-30.
Lieschke GJ, Currie PD. Animal models of human disease: zebrafish swim into view. Nat Rev Genet. 2007. 8; 353-367.
Lieschke GJ, Trede NS. Fish immunology. Curr Biol. 2009. 19; R678-R682.
Lieschke GJ, Oates AC, Crowhurst MO, Ward AC, Layton JE. Morphologic and functional characterization of granulocytes and macrophages in embryonic and adult zebrafish. Blood. 2001. 98; 3087-3096.
Lim SE, Esain V, Kwan W, Theodore LN, Cortes M, Frost IM, Liu SY, North TE. HIF1α-induced PDGFRβ signaling promotes developmental HSC production via IL-6 activation. Exp Hematol. 2017. 46; 83-95.
Lin AF, Xiang LX, Wang QL, Dong WR, Gong YF, Shao JZ. The DC-SIGN of zebrafish: insights into the existence of a CD209 homologue in a lower vertebrate and its involvement in adaptive immunity. J Immunol. 2009. 183; 7398-7410.
Lin HH, Ezzati M, Murray M. Tobacco smoke, indoor air pollution and tuberculosis: a systematic review and meta-analysis. PLoS Med. 2007. 4; e20.
Lin PL, Flynn JL. CD8 T cells and *Mycobacterium tuberculosis* infection. Semin Immunopathol. 2015. 37; 239-249.
Lin PL, Rodgers M, Smith L, Bigbee M, Myers A, Bigbee C, Chiosea I, Capuano SV, Fuhrman C, Klein E. Flynn JL. Quantitative comparison of active and latent tuberculosis in the cynomolgus macaque model. Infect Immun. 2009. 77; 4631-4642.
Lin PL, Myers A, Smith L, Bigbee C, Bigbee M, Fuhrman C, Grieser H, Chiosea I, Voitenek NN, Capuano SV, Klein E, Flynn JL. Tumor necrosis factor neutralization results in disseminated disease in acute and latent *Mycobacterium tuberculosis* infection with normal granuloma structure in a cynomolgus macaque model. Arthritis Rheum. 2010. 62; 340-350.
Lio D, Marino V, Serauto A, Gioia V, Scola L, Crivello A, Forte GI, Colonna-Romano G, Candore G, Caruso C. Genotype frequencies of the +874T--> A single nucleotide polymorphism in the first intron of the interferon-gamma gene in a sample of Sicilian patients affected by tuberculosis. Eur J Immunogenet. 2002. 29; 371-374.
Liu CH, Liu H, Ge B. Innate immunity in tuberculosis: host defense vs pathogen evasion. Cell Mol Immunol. 2017. 14; 963-975.
Loddenkemper R, Lipman M, Zumla A. Clinical aspects of adult tuberculosis. Cold Spring Harb Perspect Med. 2015. 6; a017848.
Lönnroth K, Williams BG, Stadlin S, Jaramillo E, Dye C. Alcohol use as a risk factor for tuberculosis – a systematic review. BMC Public Health. 2008. 8; 289.
Lounis N, Truffot-Pernot C, Grosset J, Gordeuk VR, Boelaert JR. Iron and *Mycobacterium tuberculosis infection*. J Clin Virol. 2001. 20; 123-126.
Louvet C, Chiffoleau E, Heslan M, Tesson L, Heslan JM, Brion R, Bériou G, Guillonneau C, Khalife J, Anegon I, Cuturi MC. Identification of a new member of the CD20/FcepsilonRIbeta family overexpressed in tolerated allografts. Am J Transplant. 2005. 5; 2143-2153.

Love MI, Huber W, Anders S. Moderated estimation of fold change and dispersion for RNA-seq data with DESeq2. Genome Biol. 2014. 15; 550.

Løvmo SD, Speth MT, Repnik U, Koppang EO, Griffiths GW, Hildahl JP. Translocation of nanoparticles and *Mycobacterium marinum* across the intestinal epithelium in zebrafish and the role of the mucosal immune system. Dev Comp Immunol. 2017. 67; 508-518.

Lugo-Villarino G, Balla KM, Stachura DL, Bañuelos K, Werneck MB, Traver D. Identification of dendritic antigen-presenting cells in the zebrafish. Proc Natl Acad Sci USA. 2010. 107; 15850-15855.

Luo M, Fadeev EA, Groves JT. Mycobactin-mediated iron acquisition within macrophages. Nat Chem Biol. 2005. 1; 149-153.

Lyadova IV, Eruslanov EB, Khaidukov SV, Yeremeev VV, Majorov KB, Pichugin AV, Nikonenko Bv, Kondratieva TK, Apt AS. Comparative analysis of T lymphocytes recovered from the lungs of mice genetically susceptible, resistant, and hyperresistant to *Mycobacterium tuberculosis*-triggered disease. J Immunol. 2000. 165; 5921-5931.

MacGurn JA, Cox JS. A genetic screen for *Mycobacterium tuberculosis* mutants defective for phagosome maturation arrest identifies components of the ESX-1 secretion system. Infect Immun. 2007. 75; 2668-2678.

Madigan CA, Cameron J, Ramakrishnan L. A zebrafish model of *Mycobacterium leprae* granulomatous infection. J Infect Dis. 2017. 216; 776-779.

Maertzdorf J, Ota M, Repsilber D, Mollenkopf HJ, Weiner J, Hill PC, Kaufmann SH. Functional correlations of pathogenesis-driven gene expression signatures in tuberculosis. PLoS One. 2011. 6; e26938.

Maglione PJ, Chan J. How B cells shape the immune response against *Mycobacterium tuberculosis*. Eur J Immunol. 2009. 39; 676-686.

Magor BG, Ross DA, Pilström L, Warr GW. Transcriptional enhancers and the evolution of the IgH locus. Immunol Today. 1999. 20; 13-17.

Mahasirimongkol S, Yanai H, Mushiroda T, Promphittayarat W, Wattanapokayakit S, Phromjai J, Yuliwulandari R, Wichukchinda N, Yowang A, Yamada N, Kantipong P, Takahashi A, Kubo M, Sawanpanyalert P, Kamatani N, Nakamura Y, Tokunaga K. Genome-wide association studies of tuberculosis in Asians identify distinct at-risk locus for young tuberculosis. J Hum Genet. 2012. 57; 363-367.

Malik A, Kanneganti TD. Inflammasome activation and assembly at a glance. J Cell Sci. 2017. 130: 3955-3963.

Malik ZA, Iyer SS, Kusner DJ. *Mycobacterium tuberculosis* phagosomes exhibit altered calmodulin-dependent signal transduction: contribution to inhibition of phagosome-lysosome fusion and intracellular survival in human macrophages. J Immunol. 2001. 166; 3392-3401.

Mandel I, Paperna T, Glass-Marmor L, Volkowich A, Badarny S, Schwartz I, Vardi P, Koren I, Miller A. Tight junction proteins expression and modulation in immune cells and multiple sclerosis. J Cell Mol Med. 2012. 16; 765-775.

Mangtani P, Abubakar I, Ariti C, Beynon R, Pimpin L, Fine PE, Rodrigues LC, Smith PG, Lipman M, Whiting PF, Sterne JA. Protection by BCG vaccine against tuberculosis: a systematic review of randomized controlled trials. Clin Infect Dis. 2014. 58; 470-480.

Manzanillo PS, Shiloh MU, Portnoy DA, Cox JS. *Mycobacterium tuberculosis* activates the DNA-dependent cytosolic surveillance pathway within macrophages. Cell Host Microbe. 2012. 11; 469-480.

Marianes AE, Zimmerman AM. Targets of somatic hypermutation within immunoglobulin light chain genes in zebrafish. Immunology. 2011. 132; 240-255.
Martin M. Cutadapt removes adapter sequences from high-throughput sequencing reads. EMBnet.journal. 2011. 17; 12.
Martinot AJ. Microbial offense vs host defense: Who controls the TB granuloma? Vet Pathol. 2018. 55; 14-26.
Masuda A, Yoshikai Y, Aiba K, Matsuguchi T. Th2 cytokine production from mast cells is directly induced by lipopolysaccharide and distinctly regulated by c-Jun N-terminal kinase and p38 pathways. J Immunol. 2002. 169; 3801-3810.
Mayer-Barber KD, Barber DL. Innate and adaptive cellular immune responses to *Mycobacterium tuberculosis* infection. Cold Spring Harb Perspect Med. 2015. 5; a018424.
McCune RM Jr, McDermott W, Tompsett R. The fate of *Mycobacterium tuberculosis* in mouse tissues as determined by the microbial enumeration technique. II. The conversion of tuberculous infection to the latent state by the administration of pyrazinamide and a companion drug. J Exp Med. 1956. 104; 763-802.
Means TK, Wang S, Lien E, Yoshimura A, Golenbock DT, Fenton MJ. Human toll-like receptors mediate cellular activation by *Mycobacterium tuberculosis*. J Immunol. 1999. 163; 3920-3927.
Meeker ND, Trede NS. Immunology and zebrafish: spawning new models of human disease. Dev comp immunol. 2008. 32; 745-757.
Meeker ND, Smith AC, Frazer JK, Bradley DF, Rudner LA, Love C, Trede NS. Characterization of the zebrafish T cell receptor beta locus. Immunogenetics. 2010. 62; 23-29.
Meijer AH. Protection and pathology in TB: learning from the zebrafish model. Semin Immunopathol. 2016. 38; 261-273.
Meijer AH, Krens SFG, Rodriquez IAM, He S, Bitter W, Snaar-Jagalska BE, Spaink HP. Expression analysis of the Toll-like receptor and TIR domain adaptor families of zebrafish. Mol Immunol. 2004. 40; 773-783.
Meijer AH, Verbeek FJ, Salas-Vidal E, Corredor-Adámez M, Bussman J, van der Sar AM, Otto GW, Geisler R, Spaink HP. Transcriptome profiling of adult zebrafish at the late stage of chronic tuberculosis due to *Mycobacterium marinum* infection. Mol Immunol. 2005. 42; 1185-1203.
Meyer A, Schartl M. Gene and genome duplications in vertebrates: the one-to-four (-to eight in fish) rule and the evolution of novel gene functions. Curr Opin Cell Biol. 1999. 11; 699-704.
Mi H, Huang X, Muruganujan A, Tang H, Mills C, Kang D, Thomas PD. PANTHER version 11: expanded annotation data from Gene Ontology and Reactome pathways, and data analysis tool enhancements. Nucleic Acids Res. 2017. 45; D183-D189.
Michalová V, Murray BW, Sültmann H, Klein J. A contig map of the Mhc class I genomic region in the zebrafish reveals ancient synteny. J Immunol. 2000. 164; 5296-5305.
Mishra A, Akhtar S, Jagannath C, Khan A. Pattern recognition receptors and coordinated cellular pathways involved in tuberculosis immunopathogenesis: Emerging concepts and perspectives. Mol Immunol. 2017. 87; 240-248.
Mitchell AL. Attwood TK, Babbitt PC, Blum M, Bork P, Bridge A, Brown SD, Chang HY, El-Gebali S, Fraser MI, Gough J, Haft DR, Huang H, Letunic I, Lopez R, Luciani A, Madeira F, Marchler-Bauer A, Mi H, Natale DA, Necci M, Nuka G, Orengo C, Pandurangan AP, Paysan-Lafosse T, Pesseat S, Potter SC, Qureshi MA, Rawlings ND, Redaschi N, Richardson LJ, Rivoire C, Salazar GA, Sangrador-Vegas A, Sigrist

CJA, Sillitoe I, Sutton GG, Thanki N, Thomas PD, Tosatto SCE, Yong SY, Finn RD. InterPro in 2019: improving coverage, classification and access to protein sequence annotations. Nucleic Acids Res. 2019. 47. D351-D360.

Mitchell G, Isberg RR. Innate immunity to intracellular pathogens: balancing microbial elimination and inflammation. Cell Host Microbe. 2017. 22; 166-175.

Mitra S, Alnabulsi A, Secombes CJ, Bird S. Identification and characterization of the transcription factors involved in T-cell development, *t-bet*, *stat6* and *foxp3*, within the zebrafish, *Danio rerio*. FEBS J. 2010. 277; 128-147.

Mogues T, Goodrich ME, Ryan L, LaCourse R, North RJ. The relative importance of T cell subsets in immunity and immunopathology of airborne *Mycobacterium tuberculosis* infection in mice. J Exp Med. 2001. 193; 271-280.

Mohan VP, Scanga CA, Yu K, Scott HM, Tanaka KE, Tsang E, Tsai MM, Flynn JL, Chan J. Effects of tumor necrosis factor alpha on host immune response in chronic persistent tuberculosis: possible role for limiting pathology. Infect Immun. 2001. 69; 1847-1855.

Mohapatra A, Parida S, Mohanty J, Sahoo PK. Identification and functional characterization of a g-type lysozyme gene of *Labeo rohita*, an Indian major carp species. Dev Comp Immunol. 2019. 92; 87-98.

Möller M, de Wit E, Hoal EG. Past, present and future directions in human genetic susceptibility to tuberculosis. FEMS Immunol Med Microbiol. 2010. 58; 3-26.

Moran A, Ma X, Reich RA, Graviss EA. No association between the +874T/A single nucleotide polymorphism in the IFN-gamma gene and susceptibility to TB. Int J Tuberc Lung Dis. 2007. 11; 113-115.

Moreira-Teixeira L, Redford PS, Stavropoulos E, Ghilardi N, Maynard CL, Weaver CT, Freitas do Rosário AP, Wu X, Langhorne J, O'Garra A. T cell-derived IL-10 impairs host resistance to *Mycobacterium tuberculosis* infection. J Immunol. 2017. 199; 613-623.

Moreira-Teixeira L, Tabone O, Graham CM, Singhania A, Stavropoulos E, Redford PS, Chakravarty P, Priestnall SL, Suarez-Bonnet A, Herbert E, Mayer-Barber KD, Sher A, Fonseca KL, Sousa J, Cá B, Verma R, Haldar P, Saraiva M, O'Garra A. Mouse transcriptome reveals potential signatures of protection and pathogenesis in human tuberculosis. Nat Immunol. 2020. 21; 464-476.

Moore KW, de Waal Malefyt R, Coffman RL, O'Garra A. Interleukin-10 and the interleukin-10 receptor. Annu Rev Immunol. 2001. 19; 683-765.

Moore KW, Vieira P, Fiorentino DF, Trounstine ML, Khan TA, Mosmann TR. Homology of cytokine synthesis inhibitory factor (IL-10) to the Epstein-Barr virus gene BCRFI. Science. 1990. 248; 1230-1234.

Murayama E, Kissa K, Zapata A, Mordelet E, Briolat V, Lin HF, Handin RI, Herbomel P. Tracing hematopoietic precursor migration to successive hematopoietic organs during zebrafish development. Immunity. 2006. 25; 963-975.

Mustafa T, Wiker HG, Mørkve O, Sviland L. Reduced apoptosis and increased inflammatory cytokines in granulomas caused by tuberculous compared to non-tuberculous mycobacteria: role of MPT64 antigen in apoptosis and immune response. Clin Exp Immunol. 2007. 150; 105-113.

Myllymäki H, Bäuerlein CA, Rämet M. The zebrafish breathes new life into the study of tuberculosis. Front Immunol. 2016. 7; 196.

Myllymäki H, Niskanen M, Oksanen KE, Rämet M. Animal models in tuberculosis research - where is the beef? Expert Opin Drug Discov. 2015. 10; 871-883.

Myllymäki H, Niskanen M, Luukinen H, Parikka M, Rämet M. Identification of protective postexposure mycobacterial vaccine antigens using an immunosuppression-based reactivation model in the zebrafish. Dis Model Mech. 2018. 11; dmm033175.

Myllymäki H, Niskanen M, Oksanen KE, Sherwood E, Ahava M, Parikka M, Rämet M. Identification of novel antigen candidates for a tuberculosis vaccine in the adult zebrafish (*Danio rerio*). PLos One. 2017. 12; e0181942.

Nachiappan AC, Rahbar K, Shi X, Guy ES, Mortani Barbosa EJ Jr, Shroff GS, Ocazionez D, Schlesinger AE, Katz SI, Hammer MM. Pulmonary tuberculosis: role of radiology in diagnosis and management. Radiographics. 2017. 37; 52-72.

Nahid P, Dorman SE, Alipanah N, Barry PM, Brozek JL, Cattamanchi A, Chaisson LH, Chaisson RE, Daley CL, Grzemska M, Higashi JM, Ho CS, Hopewell PC, Keshavjee SA, Lienhardt C, Menzies R, Merrifield C, Narita M, O'Brien R, Peloquin CA, Raftery A, Saukkonen J, Schaaf HS, Sotgiu G, Starke JR, Migliori GB, Vernon A. Executive Summary: Official American Thoracic Society/Centers for Disease Control and prevention/Infectious Diseases Society of America Clinical practice guidelines: treatment of drug-susceptible tuberculosis. Clin Infect Dis. 2016. 63; 853-867.

Nasevicius A, Ekker SC. Effective targeted gene 'knockdown' in zebrafish. Nat Genet. 2000. 26; 216-220.

Ndlovu H, Marakalala MJ. Granulomas and inflammation: Host-directed therapies for tuberculosis. Front Immunol. 2016. 7; 434.

Neumann C, Scheffold A, Rutz S. Functions and regulation of T cell-derived interleukin-10. Semin Immunol. 2019. 44; 101344.

Nickless A, Bailis JM, You Z. Control of gene expression through the nonsense-mediated RNA decay pathway. Cell Biosci. 2017. 7; 26.

North RJ. Mice incapable of making IL-4 or IL-10 display normal resistance to infection with *Mycobacterium tuberculosis*. Clin Exp Immunol. 1998. 113; 55-58.

Nuermberger EL, Yoshimatsu T, Tyagi S, Bishai WR, Grosset JH. Paucibacillary tuberculosis in mice after prior aerosol immunization with *Mycobacterium bovis* BCG. Infect Immun. 2004. 72; 1065-1071.

Nüsslein-Volhard C, Dahm R. Zebrafish. Oxford, New York Oxford University Press. 2002.

O'Garra A, Redford PS, McNab FW, Bloom CI, Wilkinson RJ, Berry MPR. The immune response in tuberculosis. Annu Rev Immunol. 2013. 31; 475-527.

Ojanen MJ, Turpeinen H, Cordova ZM, Hammarén MM, Harjula SK, Parikka M, Rämet M, Pesu M. The proprotein convertase subtilisin/kexin furinA regulates zebrafish host response against *Mycobacterium marinum*. Infect Immun. 2015. 83; 1431-1442.

Ojanen MJT, Uusi-Mäkelä MIE, Harjula SE, Saralahti AK, Oksanen KE, Kähkönen N, Määttä JAE, Hytönen VP, Pesu M, Rämet M. Intelectin 3 is dispensable for resistance against a mycobacterial infection in zebrafish (*Danio rerio*). Sci Rep. 2019. 9; 995.

Oksanen KE, Halfpenny NJ, Sherwood E, Harjula SK, Hammarén MM, Ahava MJ, Pajula ET, Lahtinen MJ, Parikka M, Rämet M. An adult zebrafish model for preclinical tuberculosis vaccine development. Vaccine. 2013. 31; 5202-5209.

Olakanmi O, Schlesinger LS, Ahmed A, Britigan BE. Intraphagosomal *Mycobacterium tuberculosis* acquires iron from both extracellular transferrin and intracellular iron pools. Impact of *interferon-gamma* and hemochromatosis. J Biol Chem. 2002. 277; 49727-49734.

O'Leary S, O'Sullivan MP, Keane J. IL-10 blocks phagosome maturation in *Mycobacterium tuberculosis*-infected human macrophages. Am J Respir Cell Mol Biol. 2011. 45; 172-180.

Orlova MO, Majorov KB, Lyadova IV, Eruslanov EB, M'lan CE, Greenwood CM, Schurr E, Apt AS. Constitutive differences in gene expression profiles parallel genetic patterns of susceptibility to tuberculosis in mice. Infect Immun. 2006. 74; 3668-3672.
Orme IM, Basaraba RJ. The formation of the granuloma in tuberculosis infection. Semin Immunol. 2014; 26; 601-609.
Ouyang W, O'Garra A. IL-10 family cytokines IL-10 and IL-22: from basic science to clinical translation. Immunity. 2019. 50; 871-891.
Pacheco AG, Cardoso CC, Moraes MO. IFNG +874T/A, IL10 -1082G/A and TNF -308G/A polymorphisms in association with tuberculosis susceptibility: a meta-analysis study. Hum Genet. 2008. 123; 477-484.
Padilla-Carlin DJ, McMurray DN, Hickey AJ. The guinea pig as a model of infectious diseases. Comp Med. 2008. 58; 324-340.
Pai M, Behr MA, Dowdy, D, Dheda K, Divangahi M, Boehme CC, Ginsberg A, Swaminathan S, Spigelman M, Getahun H, Menzies D, Raviglione M. Tuberculosis. Nat Rev Dis Primers. 2016. 2; 16076.
Pagán AJ, Ramakrishnan L. Immunity and immunopathology in the tuberculous granuloma. Cold Spring Harb Perspect Med. 2014. 5; a018499.
Page DM, Wittamer V, Bertrand JY, Lewis KL, Pratt DN, Delgado N, Schale SE, McGue C, Jacobsen BH, Doty A, Pao Y, Yang H, Chi NC, Magor BG, Traver D. An evolutionarily conserved program of B-cell development and activation in zebrafish. Blood. 2013. 122; e1-11.
Pahari S, Kaur G, Negi S, Aqdas M, Das DK, Bashir H, Singh S, Nagare M, Khan J, Agrewala JN. Reinforcing the functionality of mononuclear phagocyte system to control tuberculosis. Front Immunol. 2018. 9; 193.
Parant JM, Yeh JR. Approaches to inactivate genes in zebrafish. Adv Exp Med Biol. 2016. 916; 61-86.
Park HD, Guinn KM, Harrell MI, Liao R, Voskuil MI, Tompa M, Schoolnik GK, Sherman DR. Rv3133c/dosR is a transcription factor that mediates the hypoxic response of *Mycobacterium tuberculosis*. Mol Microbiol. 2003. 48; 833-843.
Partridge M, Vincent A, Matthews P, Puma J, Stein D, Summerton J. A simple method for delivering morpholino antisense oligos into the cytoplasm of cells. Antisense Nucleic Acid Drug Dev. 1996. 6; 169-175.
Patterson H, Saralahti A, Parikka M, Dramsi S, Trieu-Cuot P, Poyart C, Rounioja S, Rämet M. Adult zebrafish model of bacterial meningitis in *Streptococcus agalactiae* infection. Dev Comp Immunol. 2012. 38; 447-455.
Patton EE, Zon LI. The art and design of genetic screens: zebrafish. Nat Rev Genet. 2001. 2; 956-66.
Paul G, Khare V, Gasche C. Inflamed gut mucosa: downstream of interleukin-10. Eur J Clin Invest. 2012. 42; 95-109.
Peddireddy V, Doddam SN, Ahmed N. Mycobacterial dormancy systems and host responses in tuberculosis. Front Immunol. 2017. 8; 84.
Peñaloza HF, Schultz BM, Nieto PA, Salazar GA, Suazo I, Gonzalez PA, Riedel CA, Alvarez-Lobos MM, Kalergis AM, Bueno SM. Opposing roles of IL-10 in acute bacterial infection. Cytokine Growth Factor Rev. 2016. 32; 17-30.
Perez EE, Wang J, Miller JC, Jouvenot Y, Kim KA, Liu O, Wang N, Lee G, Bartsevich VV, Lee YL, Guschin DY, Rupniewski I, Waite AJ, Carpenito C, Carroll RG, Orange JS, Urnov FD, Rebar EJ, Ando D, Gregory PD, Riley JL, Holmes MC, June Ch.

Establishment of HIV-1 resistance in CD4+ T cells by genome editing using zinc-finger nucleases. Nat Biotechnol. 2008. 26; 808-816.

Petrini B. *Mycobacterium marinum*: ubiquitous agent of waterborne granulomatous skin infections. Eur J Clin Microbiol Infect Dis. 2006. 25; 609-613.

Petzold AM, Balciunas D, Sivasubbu S, Clark KJ, Bedell VM, Westcot SE, Myers SR, Moulder GL, Thomas MJ, Ekker SC. Nicotine response genetics in the zebrafish. Proc Natl Acad Sci USA. 2009. 106; 18662-18667.

Peyron P, Vaubourgeix J, Poquet Y, Levillain F, Botanch C, Bardou F, Daffé M, Emile JF, Marchou B, Cardona PJ, de Chastellier C, Altare F. Foamy macrophages from tuberculous patients' granulomas constitute a nutrient-rich reservoir for *M. tuberculosis* persistence. PLoS Pathog. 2008. 4; e1000204.

Philips JA, Rubin EJ, Perrimon N. *Drosophila* RNAi screen reveals CD36 family member required for mycobacterial infection. Science. 2005. 309; 1251-1253.

Phuah JY, Mattila JT, Lin PL, Flynn JL. Activated B cells in the granulomas of nonhuman primates infected with *Mycobacterium tuberculosis*. Am J Pathol. 2012. 181; 508-514.

Piazzon MC, Lutfalla G, Forlenza M. IL10, a tale of an evolutionarily conserved cytokine across vertebrates. Crit Rev Immunol. 2016. 36; 99-129.

Poliani PL, Kisand K, Marrella V, Ravanini M, Notarangelo LD, Villa A, Peterson P, Facchetti F. Human peripheral lymphoid tissues contain autoimmune regulator-expressing dendritic cells. Am J Pathol. 2010. 176; 1104-1112.

Pressley ME, Phelan PE 3rd, Witten PE, Mellon MT, Kim CH. Pathogenesis and inflammatory response to *Edwardsiella tarda* infection in the zebrafish. Dev Comp Immunol. 2005. 29; 501-513.

Prouty MG, Correa NE, Barker LP, Jagadeeswaran P, Klose KE. Zebrafish-*Mycobacterium marinum* model for mycobacterial pathogenesis. FEMS Microbiol Lett. 2003. 225; 177-182.

Qin G, Taylor M, Ning YY, Iversen P, Kobzik L. *In vivo* evaluation of a morpholino antisense oligomer directed against tumor necrosis factor-alpha. Antisense Nucleic Acid Drug Dev. 2000. 10; 11-16.

Ramachandran G, Santha T, Garg R, Baskaran D, Iliayas SA, Venkatesan P, Fathima R, Narayanan PR. Vitamin A levels in sputum-positive pulmonary tuberculosis patients in comparison with household contacts and healthy 'normals'. Int J Tuberc Lung Dis. 2004. 8; 1130-1133.

Ramakrishnan L. Revisiting the role of the granuloma in tuberculosis. Nat Rev Immunol. 2012. 12; 352-366.

Ramakrishnan L, Federspiel NA, Falkow S. Granuloma-specific expression of *Mycobacterium* virulence proteins from the glycine-rich PE-PGRS family. Science. 2000. 288; 1436-1439.

Rabiei N, Ahmadi Badi S, Ettehad Marvasti F, Nejad Sattari T, Vaziri F, Siadat SD. Induction effects of *Faecalibacterium prausnitzii* and its extracellular vesicles on toll-like receptor signaling pathway gene expression and cytokine level in human intestinal epithelial cells. Cytokine. 2019. 121; 154718.

Ran FA, Hsu PD, Wright J, Agarwala V, Scott DA, Zhang F. Genome engineering using the CRISPR-Cas9 system. Nat Protoc. 2013. 8; 2281-2308.

Rangaka MX, Cavalcante SC, Marais BJ, Thim S, Martinson NA, Swaminathan S, Chaisson RE. Controlling the seedbeds of tuberculosis: diagnosis and treatment of tuberculosis infection. Lancet. 2015. 386; 2344-2353.

Rangaka MX, Wilkinson KA, Glynn JR, Ling D, Menzies D, Mwansa-Kambafwile J, Fielding K, Wilkinson RJ, Pai M. Predictive value of interferon-γ release assays for incident active tuberculosis: a systematic review and meta-analysis. Lancet Infect Dis. 2012. 12; 45-55.

Rämet M, Manfruelli P, Pearson A, Mathey-Prevot B, Ezekowitz RA. Functional genomic analysis of phagocytosis and identification of a *Drosophila* receptor for *E. coli*. Nature. 2002. 416; 644-648.

R Core Team. R: A language and environment for statistical computing. R Foundation for Statistical Computing, Vienna, Austria. Available online at: https://www.R-project.org/.

Redford PS, Murray PJ, O'Garra A. The role of IL-10 in immune regulation during *M. tuberculosis* infection. Mucosal Immunol. 2011. 4; 261-270.

Redford PS, Boonstra A, Read S, Pitt J, Graham C, Stavropoulos E, Bancroft GJ, O'Garra A. Enhanced protection to *Mycobacterium tuberculosis* infection in IL-10-deficient mice is accompanied by early and enhanced Th1 responses in the lung. Eur J Immunol. 2010. 40; 2200-2210.

Refai A, Gritli S, Barbouche MR, Essafi M. *Mycobacterium tuberculosis* virulent factor ESAT-6 drives macrophage differentiation toward the pro-inflammatory M1 phenotype and subsequently switches it to the anti-inflammatory M2 phenotype. Front Cell Infect Microbiol. 2018. 8; 327.

Rehm J, Samokhvalov AV, Neuman MG, Room R, Parry C, Lönnroth K, Patra J, Poznyak V, Popova S. The association between alcohol use, alcohol use disorders and tuberculosis (TB). A systematic review. BMC Public Health 2009. 9; 450.

Rengarajan J, Bloom BR, Rubin EJ. Genome-wide requirements for *Mycobacterium tuberculosis* adaptation and survival in macrophages. Proc Natl Acad Sci USA. 2005. 102; 8327-8332.

Renshaw SA, Loynes CA, Trushell DM, Elworthy S, Ingham PW, Whyte MK. A transgenic zebrafish model of neutrophilic inflammation. Blood. 2006. 108; 3976-3978.

Renshaw SA, Trede NS. A model 450 million years in the making: zebrafish and vertebrate immunity. Dis Model Mech. 2012. 5; 38-47.

Rhoades E, Hsu F, Torrelles JB, Turk J, Chatterjee D, Russell DG. Identification and macrophage-activating activity of glycolipids released from intracellular *Mycobacterium bovis* BCG. Mol Microbiol. 2003. 48; 875-888.

Rhoades ER, Cooper AM, Orme IM. Chemokine response in mice infected with *Mycobacterium tuberculosis*. Infect Immun. 1995. 63; 3871-3877.

Rhoades ER., Frank AA, Orme IM. Progression of chronic pulmonary tuberculosis in mice aerogenically infected with virulent *Mycobacterium tuberculosis*. Tuber Lung Dis. 1997. 78; 57-66.

Richards DF, Fernandez M, Caulfield J, Hawrylowicz CM. Glucocorticoids drive human CD8(+) T cell differentiation towards a phenotype with high IL-10 and reduced IL-4, IL-5 and il-13 production. Eur J Immunol. 2000. 30; 2344-2354.

Richardson ET, Shukla S, Sweet DR, Wearsch PA, Tsichlis PN, Boom WH, Harding CV. Toll-like receptor 2-dependent extracellular signal-regulated kinase signaling in *Mycobacterium tuberculosis*-infected macrophages drives anti-inflammatory responses and inhibits Th1 polarization of responding T cells. Infect Immun. 2015. 83; 2242-2254.

Riedel DD, Kaufmann SH. Chemokine secretion by human polymorphonuclear granulocytes after stimulation with *Mycobacterium tuberculosis* and lipoarabinomannan. Infect Immun. 1997. 65; 4620-4623.

Riley JK, Takeda K, Akira S, Schreiber RD. Interleukin-10 receptor signaling through the JAK-STAT pathway. Requirement for two distinct receptor-derived signals for anti-inflammatory action. J Biol Chem. 1999. 274; 16513-16521.

Ring S, Eggers L, Behrends J, Wutkowski A, Schwudke D, Kröger A, Hierweger AM, Hölscher C, Gabriel G, Schneider BE. Blocking IL-10 receptor signaling ameliorates *Mycobacterium tuberculosis* infection during influenza-induced exacerbation. JCI Insight. 2019. 5; 126533.

Roach DR, Bean AG, Demangel C, France MP, Briscoe H, Britton WJ. TNF regulates chemokine induction essential for cell recruitment, granuloma formation, and clearance of mycobacterial infection. J Immunol. 2002. 168; 4620-4627.

Robinson RT, Orme IM, Cooper AM. The onset of adaptive immunity in the mouse model of tuberculosis and the factors that compromise its expression. Immunol Rev. 2015. 264; 46-59.

Robinson JT, Thorvaldsdóttir H, Winckler W, Guttman M, Lander ES, Getz G, Mesirov JP. Integrative genomics viewer. Nat Biotechnol. 2011. 29; 24-26.

Roca FJ, Ramakrishnan L. TNF dually mediates resistance and susceptibility to mycobacteria via mitochondrial reactive oxygen species. Cell. 2013. 153; 521-534.

Rougeot J, Zakrzewska A, Kanwal Z, Jansen HJ, Spaink HP, Meijer AH. RNA sequencing of FACS-sorted immune cell populations from zebrafish infection models to identify cell specific responses to intracellular pathogens. Methods Mol Biol. 2014. 1197; 261-274.

Rougeot J, Torraca V, Zakrzewska A, Kanwal Z, Jansen HJ, Sommer F, Spaink HP, Meijer AH. RNAseq profiling of leukocyte populations in zebrafish larvae reveals a *cxcl11* chemokine gene as a marker of macrophage polarization during mycobacterial infection. Front Immunol. 2019. 10; 832.

Rossi A, Kontarakis Z, Gerri C, Nolte H, Hölper S, Krüger M, Stainier DY. Genetic compensation induced by deleterious mutations but not gene knockdowns. Nature. 2015. 524; 230-233.

Rossouw M, Nel HJ, Cooke GS, van Helden PD, Hoal EG. Association between tuberculosis and a polymorphic NFkappaB binding site in the interferon gamma gene. Lancet. 2003. 361; 1871-1872.

Rounioja S, Saralahti A, Rantala L, Parikka M, Henriques-Normark B, Silvennoinen O, Rämet M. Defense of zebrafish embryos against *Streptococcus pneumoniae* infection is dependent on the phagocytic activity of leukocytes. Dev Comp Immunol. 2012. 36; 342-348.

Russell DG. Who puts the tubercle in tuberculosis? Nat. Rev. Microbiol. 2007. 5; 39-47.

Russell DG, Cardona PJ, Kim MJ, Allain S, Altare F. Foamy macrophages and the progression of the human tuberculosis granuloma. Nat Immunol. 2009. 10; 943-948.

Saeij JP, Stet RJ, Groeneveld A, Verburg-van Kemenade LB, van Muiswinkel WB, Wiegertjes GF. Molecular and functional characterization of a fish inducible-type nitric oxide synthase. Immunogenetics. 2000. 51; 339-346.

Safford M, Collins S, Lutz MA, Allen A, Huang CT, Kowalski J, Blackford A, Horton MR, Drake C, Schwartz RH, Powell JD. Egr-2 and Egr-3 are negative regulators of T cell activation. Nat Immunol. 2005. 6; 472-480.

Sakaguchi S. Regulatory T cells: key controllers of immunologic self-tolerance. Cell. 2000. 101; 455-458.

Santamaria I, Velasco G, Cazorla M, Fueyo A, Campo E, López-Otin C. Cathepsin L2, a novel human cysteine proteinase produced by breast and colorectal carcinomas. Cancer Res. 1998. 58; 1624-1630.

Saralahti A, Piippo H, Parikka M, Henriques-Normark B, Rämet M, Rounioja S. Adult zebrafish model for pneumococcal pathogenesis. Dev Comp Immunol. 2014. 42; 345-353.

Sato T, McCue P, Masuoka K, Salwen S, Lattime EC, Mastrangelo MJ, Berd D. Interleukin 10 production by human melanoma. Clin Cancer Res. 1996. 2; 1383-1390.

Saunders MJ, Wingfield T, Tovar MA, Baldwin MR, Datta S, Zevallos K, Montoya R, Valencia TR, Friedland JS, Moulton LH, Gilman RH, Evans CA. A score to predict and stratify risk of tuberculosis in adult contacts of tuberculosis index cases: a prospective derivation and external validation cohort study. Lancet Infect Dis. 2017. 17; 1190-1199.

Scheinecker C, Göschl L, Bonelli M. Treg cells in health and autoimmune diseases: New insights from single cell analysis. J Autoimmun. 2019. 2019; 102376.

Schlesinger LS. Macrophage phagocytosis of virulent but not attenuated strains of *Mycobacterium tuberculosis* is mediated by mannose receptors in addition to complement receptors. J Immunol. 1993. 150; 2920-2930.

Schorpp M, Bialecki M, Diekhoff D, Walderich B, Odenthal J, Maischein HM, Zapata AG. Boehm T. Conserved functions of Ikaros in vertebrate lymphocyte development: genetic evidence for distinct larval and adult phases of T cell development and two lineages of B cells in zebrafish. J Immunol. 2006. 177; 2463-2476.

Scola L, Crivello A, Marino V, Gioia V, Serauto A, Candore G, Colonna-Romano G, Caruso C, Lio D. IL-10 and TNF-alpha polymorphisms in a sample of Sicilian patients affected by tuberculosis: implication for ageing and life span expectancy. Mech Ageing Dev. 2003. 124; 569-572.

Seelye SL, Chen PL, Deiss TC, Criscitiello MF. Genomic organization of the zebrafish (*Danio rerio*) T cell receptor alpha/delta locus and analysis of expressed products. Immunogenetics. 2016. 68; 365-379.

Seiler C, Gebhart N, Zhang Y, Shinton SA, Li YS, Ross NL, Liu X, Li Q, Bilbee AN, Varshney GK, LaFave MC, Burgess SM, Balciuniene J, Balciunas D, Hardy RR, Kappes DJ, Wiest DL, Rhodes J. Mutagenesis screen identifies *agtpbp1* and *eps15L1* as essential for T lymphocyte development in zebrafish. PLoS One. 2015. 10; e0131908.

Senaratne RH, De Silva AD, Williams SJ, Mougous JD, Reader JR, Zhang T, Chan S, Sidders B, Lee DH, Chan J, Bertozzi CR, Riley LW. 5'-Adenosinephosphosulphate reductase (CysH) protects *Mycobacterium tuberculosis* against free radicals during chronic infection phase in mice. Mol Microbiol. 2006. 59; 1744-1753.

Selwyn PA, Hartel D, Lewis VA, Schoenbaum EE, Vermund SH, Klein RS, Walker AT, Friedland GH. A prospective study of the risk of tuberculosis among intravenous drug users with human immunodeficiency virus infection. N Engl J Med. 1989. 320; 545-550.

Sharma SK, Mohan A. Multidrug-resistant tuberculosis: a menace that threatens to destabilize tuberculosis control. Chest. 2006. 130; 261-272.

Sharma S, Sharma M, Roy S, Kumar P, Bose M. *Mycobacterium tuberculosis* induces high production of nitric oxide in coordination with production of tumour necrosis factor-

alpha in patients with fresh active tuberculosis but not in MDR tuberculosis. Immunol Cell Biol. 2004. 82; 377-382.
Shen P, Fillatreau S. Suppressive functions of B cells in infectious diseases. Int Immunol. 2015. 27; 513-519.
Shepelkova G, Pommerenke C, Alberts R, Geffers R, Evstifeev V, Apt A, Schughart K, Wilk E. Analysis of the lung transcriptome in *Mycobacterium tuberculosis*-infected mice reveals major differences in immune response pathways between TB-susceptible and resistant hosts. Tuberculosis (Edinb). 2013. 93; 263-269.
Shibasaki M, Yagi T, Yatsuya H, Okamoto M, Nishikawa M, Baba H, Hashimoto N, Senda K, Kawabe T, Nakashima K, Imaizumi K, Shimokata K, Hasegawa Y. An influence of *Interferon-γ* gene polymorphisms on treatment response to tuberculosis in Japanese population. J Infect. 2009. 58; 467-469.
Shin HD, Park BL, Kim YH, Cheong HS, Lee IH, Park SK. Common interleukin 10 polymorphism associated with decreased risk of tuberculosis. Exp Mol Med. 2005. 37; 128-132.
Sia IG, Wieland ML. Current concepts in the management of tuberculosis. Mayo Clin Proc. 2011. 86; 348-361.
Sigrist CJ, de Castro E, Cerutti L, Cuche BA, Hulo N, Bridge A, Bougueleret L, Xenarios I. New and continuing developments at PROSITE. Nucleic Acids Res. 2013. 41; D344-D347.
Singer-Leshinsky S. Pulmonary tuberculosis: Improving diagnosis and management. JAAPA. 2016. 29; 20-25.
Sivasubbu S, Balciunas D, Amsterdam A, Ekker SC. Insertional mutagenesis strategies in zebrafish. Genome Biol. 2007. 8; S9.
Sivasubbu S, Balciunas D, Davidson AE, Pickart MA, Hermanson SB, Wangensteen KJ, Wolbrink DC, Ekker SC. Gene-breaking transposon mutagenesis reveals an essential role for histone H2afza in zebrafish larval development. Mech Dev. 2006. 123; 513-529.
Slama K, Chiang CY, Enarson DA, Hassmiller K, Fanning A, Gupta P, Ray C. Tobacco and tuberculosis: a qualitative systematic review and meta-analysis. Int J Tuberc Lung Dis. 2007. 11; 1049-1061.
Solnica-Krezel L, Schier AF, Driever W. Efficient recovery of ENU-induced mutations from the zebrafish germline. Genetics. 1994. 136; 1401-1420.
Solomon JM, Leung GS, Isberg RR. Intracellular replication of *Mycobacterium marinum* within *Dictyostelium discoideum*: efficient replication in the absence of host coronin. Infect Immun. 2003. 71; 3578-3586.
Sonnenberg P, Glynn JR, Fielding K, Murray J, Godfrey-Faussett P, Shearer S. How soon after infection with HIV does the risk of tuberculosis start to increase? A retrospective cohort study in South African gold miners. J Infect Dis. 2005. 191; 150-158.
Spence R, Gerlach G, Lawrence C, Smith C. The behaviour and ecology of the zebrafish, *Danio rerio*. Biol Rev Camb Philos Soc. 2008. 83; 13-34.
Stamm LM, Brown EJ. *Mycobacterium marinum*: the generalization and specialization of a pathogenic mycobacterium. Microbes Infect. 2004. 6; 1418-1428.
Stamm CE, Collins AC, Shiloh MU. Sensing of *Mycobacterium tuberculosis* and consequences to both host and bacillus. Immunol Rev. 2015. 264; 204-219.

Stamm LM, Morisaki JH, Gao LY, Jeng RL, McDonal KL, Roth R, Takeshita S, Heuser J, Welch MD, Brown EJ. *Mycobacterium marinum* escapes from phagosomes and is propelled by actin-based motility. J Exp Med. 2003. 198; 1361-1368.

Stephen LA, ElMaghloob Y, McIlwraith MJ, Yelland T, Castro Sanchez P, Roda-Navarro P, Ismail S. The ciliary machinery is repurposed for T cell immune synapse trafficking of LCK. Dev Cell. 2018. 47; 122-132.

Sterne JA, Rodrigues LC, Guedes IN. Does the efficacy of BCG decline with time since vaccination? Int J Tuberc Lung Dis. 1998. 2; 200-207.

Stinear TP, Seemann T, Harrison PF, Jenkin GA, Davies JK, Johnson PD, Abdellah Z, Arrowsmith C, Chillingworth T, Churcher C, Clarke K, Cronin A, Davis P, Goodhead I, Holroyd N, Jagels K, Lord A, Moule S, Mungall K, Norbertczak H, Quail MA, Rabbinowitsch E, Walker D, White B, Whitehead S, Small PL, Brosch R, Ramakrishnan L, Fischback MA, Parkhill J, Cole ST. Insights from the complete genome sequence of *Mycobacterium marinum* on the evolution of *Mycobacterium tuberculosis*. Genome Res. 2008. 18; 729-741.

Sturgill-Koszycki S, Schlesinger PH, Chakraborty P, Haddix PL, Collins HL, Fok AK, Allen RD, Gluck SL, Heuser J, Russell DG. Lack of acidification in *Mycobacterium* phagosomes produced by exclusion of the vesicular proton-ATPase. Science. 1994. 263; 678-681.

Stutz MD, Clark MP, Doerflinger M, Pellegrini M. *Mycobacterium tuberculosis*: Rewiring host cell signaling to promote infection. J Leukoc Biol. 2018. 103; 259-268.

Subbian S, Tsenova L, O'Brien P, Yang G, Kushner NL, Parsons S, Peixoto B, Fallows D, Kaplan G. Spontaneous latency in a rabbit model of pulmonary tuberculosis. Am J Pathol. 2012. 181; 1711-1724.

Subbian S, Tsenova L, Yang G, O'Brien P, Parsons S, Peixoto B, Taylor L, Fallows D, Kaplan G. Chronic pulmonary cavitary tuberculosis in rabbits: a failed host immune response. Open Biol. 2011. 1; 110016.

Sugimoto K, Hui SP, Sheng DZ, Nakayama M, Kikuchi K. Zebrafish FOXP3 is required for the maintenance of immune tolerance. Dev Comp Immunol. 2017. 73; 156-162.

Sullivan BM, Jobe O, Lazarevic V, Vasquez K, Bronson R, Glimcher LH, Kramnik I. Increased susceptibility of mice lacking T-bet to infection with *Mycobacterium tuberculosis* correlates with increased IL-10 and decreased IFN-gamma production. J Immunol. 2005. 175; 4593-4602.

Sültmann H, Sato A, Murray BW, Takezaki N, Geisler R, Rauch GJ, Klein J. Conservation of Mhc class III region synteny between zebrafish and human as determined by radiation hybrid mapping. J Immunol. 2000. 165; 6984-6993.

Summerton J, Weller D. Morpholino antisense oligomers: design, preparation, and properties. Antisense Nucleic Acid Drug Dev. 1997. 7; 187-195.

Swaim LE, Connolly LE, Volkman HE, Humbert O, Born DE, Ramakrishnan L. *Mycobacterium marinum* infection of adult zebrafish causes caseating granulomatous tuberculosis and is moderated by adaptive immunity. Infect Immun. 2006. 74; 6108-6117.

Talbot WS, Trevarrow B, Halpern ME, Melby AE, Farr G, Postlethwait JH, Jowett T, Kimmel CB, Kimelman D. A homeobox gene essential for zebrafish notochord development. Nature. 1995. 378; 150-157.

Tang J, Yam WC, Chen Z. *Mycobacterium tuberculosis* infection and vaccine development. Tuberculosis (Edinb). 2016. 98; 30-41.

Tang R, Dodd A, Lai D, McNabb WC, Love DR. Validation of zebrafish (*Danio rerio)* reference genes for quantitative real-time RT-PCR normalization. Acta Biochim Biophys Sin (Shanghai). 2007. 39; 384-390.

Taylor JL, Hattle JM, Dreitz SA, Troudt JM, Izzo LS, Basaraba RJ, Orme IM, Matrisian LM, Izzo AA. Role for matrix metalloproteinase 9 in granuloma formation during pulmonary *Mycobacterium tuberculosis* infection. Infect Immun. 2006. 74; 6135-6144.

Teittinen KJ, Grönroos T, Parikka M, Rämet M, Lohi O. The zebrafish as a tool in leukemia research. Leuk Res. 2012. 36; 1082-1088.

The Gene Ontology Consortium. The Gene Ontology Resource: 20 years and still GOing strong. Nucleic Acids Res. 2019. 47; D330-D338.

Tian J, Hu J, Chen M, Yin H, Miao P, Bai P, Yin J. The use of *mrp1*-deficient (*Danio rerio*) zebrafish embryos to investigate the role of Mrp1 in the toxicity of cadmium chloride and benzo[a]pyrene. Aquat Toxicol. 2017. 186; 123-133.

Tiberi S, du Plessis N, Walzl G, Vjecha MJ, Rao M, Ntoumi F, Mfinanga S, Kapata N, Mwaba P, McHugh TD, Ippolito G, Migliori GB, Maeurer MJ, Zumla A. Tuberculosis: progress and advances in development of new drugs, treatment regimens, and host-directed therapies. Lancet Infect Dis. 2018. 18; e183-e198.

Tobin DM, Ramakrishnan L. Comparative pathogenesis of *Mycobacterium marinum* and *Mycobacterium tuberculosis*. Cell Microbiol. 2008. 10; 1027-1039.

Tobin DM, May RC, Wheeler RT. Zebrafish: a see-through host and a fluorescent toolbox to probe host-pathogen interaction. PLoS Pathog. 2012a. 8; e1002349.

Tobin DM, Vary JC Jr, Ray JP, Walsh GS, Dunstan SJ, Bang ND, Hagge DA, Khadge S, King MC, Hawn TR, Moens CB, Ramakrishnan L. The *lta4h* locus modulates susceptibility to mycobacterial infection in zebrafish and humans. Cell. 2010. 140; 717-730.

Tobin DM, Roca FJ, Oh SF, McFarland R, Vickery TW, Ray JP, Ko DC, Zou Y, Bang ND, Chau TT, Vary JC, Hawn TR, Dunstan SJ, Farrar JJ, Thwaites GE, King MC, Serhan CN, Ramakrishnan L. Host genotype-specific therapies can optimize the inflammatory response to mycobacterial infections. Cell. 2012b. 148; 434-446.

Torraca V, Cui C, Boland R, Bebelman JP, van der Sar AM, Smit MJ, Siderius M, Spaink HP, Meijer AH. The CXCR3-CXCL11 signaling axis mediates macrophage recruitment and dissemination of mycobacterial infection. Dis Model Mech. 2015. 8; 253-269.

Travar M, Petkovic M, Verhaz A. Type I, II and III interferons: Regulating immunity to *Mycobacterium tuberculosis* infection. Arch Immunol Ther Exp (Warsz). 2016. 64; 19-31.

Trede NS, Ota T, Kawasaki H, Paw BH, Katz T, Demarest B, Hutchinson S, Zhou Y, Hersey C, Zapata A, Amemiya CT, Zon LI. Zebrafish mutants with disrupted early T-cell and thymus development identified in early pressure screen. Dev Dyn. 2008. 237; 2575-2584.

Tsai MC, Chakravarty S, Zhu G, Xu J, Tanaka K, Koch C, Tufariello J, Flynn J, Chan J. Characterization of the tuberculous granuloma in murine and human lungs: cellular composition and relative tissue oxygen tension. Cell Microbiol. 2006. 8; 218-232.

Tükenmez H, Edström I, Ummanni R, Fick SB, Sundin C, Elofsson M, Larsson C. *Mycobacterium tuberculosis* virulence inhibitors discovered by *Mycobacterium marinum* high-throughput screening. Sci Rep. 2019. 9; 26.

Tuominen VJ, Isola J. The application of JPEG2000 in virtual microscopy. J Digit Imaging. 2009. 22; 250-258.

Turk B, Turk D, Turk V. Lysosomal cysteine proteases: more than scavengers. Biochim Biophys Acta. 2000. 1477; 98-111.

Turk V, Turk B, Guncar G, Turk D, Kos J. Lysosomal cathepsins: structure, role in antigen processing and presentation, and cancer. Adv Enzyme Regul. 2002. 42; 285-303.
Turk V, Stoka V, Vasiljeva O, Renko M, Sun T, Turk B, Turk D. Cysteine cathepsins: from structure, function and regulation to new frontiers. Biochim Biophys Acta. 2012. 1824; 68-88.
Udvadia AJ, Linney E. Windows into development: historic, current, and future perspectives on transgenic zebrafish. Dev Biol. 2003. 256; 1-17.
Ulrichs T, Kosmiadi GA, Trusov V, Jorg S, Pradl L, Titukhina M, Mishenko V, Gushina N, Kaufmann SH. Human tuberculous granulomas induce peripheral lymphoid follicle-like structures to orchestrate local host defence in the lung. J Pathol. 2004. 204; 217-228.
Uusi-Mäkelä MIE, Barker HR, Bäuerlein CA, Häkkinen T, Nykter M, Rämet M. Chromatin accessibility is associated with CRISPR-Cas9 efficiency in the zebrafish (*Danio rerio*). PLoS One. 2018. 13; e0196238.
van Crevel R, Ottenhoff TH, van der Meer JW. Innate immunity to *Mycobacterium tuberculosis*. Clin Mirobiol Rev. 2002. 15; 294-309.
van Dam H, Castellazzi M. Distinct roles of Jun: Fos and Jun: ATF dimers in oncogenesis. Oncogene. 2001. 20; 2453-2464.
van der Sar AM, Appelmelk BJ, Vandenbroucke-Grauls CM, Bitter W. A star with stripes: zebrafish as an infection model. Trends Microbiol. 2004a. 12; 451-457.
van der Sar AM, Spaink HP, Zakrzewska A, Bitter W, Meijer AH. Specificity of the zebrafish host transcriptome response to acute and chronic mycobacterial infection and the role of innate and adaptive immune components. Mol Immunol. 2009. 46; 2317-2332.
van der Sar AM, Abdallah AM, Sparrius M, Reinders E, Vandenbroucke-Grauls CM, Bitter W. *Mycobacterium marinum* strains can be divided into two dinstinct types based on genetic diversity and virulence. Infect Immun. 2004b. 72; 6306-6312.
van der Sar AM, Musters RJ, van Eeden FJ, Appelmelk BJ, Vandenbroucke-Grauls CM, Bitter W. Zebrafish embryos as a model host for the real time analysis of *Salmonella typhimurium* infections. Cell Microbiol. 2003. 5; 601-611.
van der Sar AM, Stockhammer OW, van der Laan C, Spaink HP, Bitter W, Meijer AH. Myd88 innate immune function in a zebrafish embryo infection model. Infect Immun. 2006. 74; 2436-2441.
van der Vaart M, Spaink HP, Meijer AH. Pathogen recognition and activation of the innate immune response in zebrafish. Adv Hematol. 2012. 2012; 159807.
van der Vaart M, van Soest JJ, Spaink HP, Meijer AH. Functional analysis of a zebrafish *myd88* mutant identifies key transcriptional components of the innate immune system. Dis Model Mech. 2013. 6; 841-854.
van der Wel N, Hava D, Houben D, Fluitsma D, van Zon M, Pierson J, Brenner M, Peters PJ. *M. tuberculosis* and *M. leprae* translocate from the phagolysosome to the cytosol in myeloid cells. Cell. 2007. 129; 1287-1298.
van de Vosse E, Haverkamp MH, Ramirez-Alejo N, Martinez-Gallo M, Blancas-Galicia L, Metin A, Garty BZ, Sun-Tan Ç, Broides A, de Paus RA, Keskin Ö, Çağdaş D, Tezcan I, Lopez-Ruzafa E, Aróstegui JI, Levy J, Espinosa-Rosales FJ, Sanal Ö, Santos-Argumedo L, Casanova JL, Boisson-Dupuis S, van Dissel JT, Bustamante J. IL-12Rβ1 deficiency: mutation update and description of the IL12RB1 variation database. Hum Mutat. 2013. 34; 1329-1339.

van Leeuwen LM, van der Kuip M, Youssef SA, de Bruin A, Bitter W, van Furth AM, van der Sar AM. Modeling tuberculous meningitis in zebrafish using *Mycobacterium marinum*. Dis Model Mech. 2014. 7; 1111-1122.

Verbon A, Juffermans N, van Deventer SJ, Speelman P, van Deutekom H, van Der Poll T. Serum concentrations of cytokines in patients with active tuberculosis (TB) and after treatment. Clin Exp Immunol. 1999. 115; 110-113.

Verma R, Balakrishnan L, Sharma K, Khan AA, Advani J, Gowda H, Tripathy SP, Suar M, Pandey A, Gandotra S, Prasad TS, Shankar S. A network map of Interleukin-10 signaling pathway. J Cell Commun Signal. 2016. 10; 61-67.

Vermaelen KY, Carro-Muino I, Lambrecht BN, Pauwels RA. Specific migratory dendritic cells rapidly transport antigen from the airways to the thoracic lymph nodes. J Exp Med. 2001. 193; 51-60.

Vermeulen I, Baird M, Al-Dulayymi J, Smet M, Verschoor J, Grooten J. Mycolates of *Mycobacterium tuberculosis* modulate the flow of cholesterol for bacillary proliferation in murine macrophages. J Lipid Res. 2017. 58; 709-718.

Via LE, Lin PL, Ray SM, Carrillo J, Allen SS, Eum SY, Taylor K, Klein E, Manjunatha U, Gonzales J, Lee EG, Park SK, Raleigh JA, Cho SN, McMurray DN, Flynn JL, Barry CE 3rd. Tuberculous granulomas are hypoxic in guinea pigs, rabbits, and nonhuman primates. Infect Immun. 2008. 76; 2333-2340.

Vladimer GI, Weng D, Paquette SW, Vanaja SK, Rathinam VA, Aune MH, Conlon JE, Burbage JJ, Proulx MK, Liu Q, Reed G, Mecsas JC, Iwakura Y, Bertin J, Goguen JD, Fitzgerald KA, Lien E. The NLRP12 inflammasome recognizes *Yersinia pestis*. Immunity. 2012. 37; 96-107.

Vojtech LN, Sanders GE, Conway C, Ostland V, Hansen JD. Host immune response and acute disease in a zebrafish model of *Francisella* pathogenesis. Infect Immun. 2009. 77; 914-925.

Volkman HE, Clay H, Beery D, Chang JC, Sherman DR, Ramakrishnan L. Tuberculous granuloma formation is enhanced by a mycobacterium virulence determinant. PLoS Biol. 2004. 2; e367.

Volkman HE, Pozos TC, Zheng J, Davis JM, Rawls JF, Ramakrishnan L. Tuberculous granuloma induction via interaction of a bacterial secreted protein with host epithelium. Science. 2010. 327; 466-469.

Voskuil MI, Schnappinger D, Visconti KC, Harrell MI, Dolganov GM, Sherman DR, Schoolnik GK. Inhibition of respiration by nitric oxide induces a *Mycobacterium tuberculosis* dormancy program. J Exp Med. 2003. 198; 705-713.

Vynnycky E, Fine PE. The natural history of tuberculosis: the implications of age-dependent risks of disease and the role of reinfection. Epidemiol Infect. 1997. 119; 183-201.

Walker C, Streisinger G. Induction of mutations by gamma-rays in pregonial germ cells of zebrafish embryos. Genetics. 1983. 103; 125-136.

Walker C, Walsh GS, Moens C. Making gynogenetic diploid zebrafish by early pressure. J Vis Exp. 2009. 28; e1396.

Walton EM, Cronan MR, Beerman RW, Tobin DM. The macrophage-specific promoter *mfap4* allows live, long-term analysis of macrophage behavior during mycobacterial infection in zebrafish. PLoS One. 2015. 10; e0138949.

Walzl G, McNerney R, du Plessis N, Bates M, McHugh TD, Chegou NN, Zumla A. Tuberculosis: advances and challenges in development of new diagnostics and biomarkers. Lancet Infect Dis. 2018. 18; e199-e210.

Wan F, Hu CB, Ma JX, Gao K, Xiang LX, Shao JZ. Characterization of γδ T cells from zebrafish provides insights into their important role in adaptive humoral immunity. Front Immunol. 2017. 7; 675.

Wang D, Jao LE, Zheng N, Dolan K, Ivey J, Zonies S, Wu X, Wu K, Yang H, Meng Q, Zhu Z, Zhang B, Lin S, Burgess SM. Efficient genome-wide mutagenesis of zebrafish genes by retroviral insertions. Proc Natl Acad Sci USA. 2007. 104; 12428-12433.

Wang K, Li M, Hakonarson H. ANNOVAR: functional annotation of genetic variants from high-throughput sequencing data. Nucleic Acids Res. 2010. 38; e164.

Wang X, Wu Y, Jiao J, Huang Q. *Mycobacterium tuberculosis* infection induces IL-10 gene expression by disturbing histone deacetylase 6 and histonedeacetylase 11 equilibrium in macrophages. Tuberculosis (Edinb). 2018. 108; 118-123.

Wang X, Wang X, Zhang L, Zhang Y, Wang F, Wang C, Lu Y, Wu F, Zhang W, Wu J. The regulatory role of Mcl-1 in apoptosis of mouse peritoneal macrophage infected with *M. tuberculosis* strains that differ in virulence. Int J Clin Exp Pathol. 2017. 10; 7565-7577.

Warsinske HC, DiFazio RM, Linderman JJ, Flynn JL, Kirschner DE. Identifying mechanisms driving formation of granuloma-associated fibrosis during *Mycobacterium tuberculosis* infection. J Theor Biol. 2017. 429; 1-17.

Watral V, Kent ML. Pathogenesis of *Mycobacterium* spp. in zebrafish (*Danio rerio*) from research facilities. Comp Biochem Physiol C Toxicol Pharmacol. 2007. 145; 55-60.

Wawrocki S, Druszczynska M. Inflammasomes in *Mycobacterium tuberculosis*-driven immunity. Can J Infect Dis Med Microbiol. 2017. 2017; 2309478.

Wayne LG, Hayes LG. An *in vitro* model for sequential study of shiftdown of *Mycobacterium tuberculosis* through two stages of nonreplicating persistence. Infect Immun. 1996. 64; 2062-2069.

Wei H, Li B, Sun A, Guo F. Interleukin-10 family cytokines immunobiology and structure. Adv Exp Med Biol. 2019. 1172: 79-96.

Wei, S, Zhou JM, Chen X, Shah RN, Liu J, Orcutt TM, Traver D, Djeu JY, Litman GW, Yoder JA. The zebrafish activating immune receptor Nitr9 signals via Dap12. Immunogenetics. 2007. 59; 813-821.

Weinstein JA, Jiang N, White RA 3rd, Fisher DS, Quake SR. High-throughput sequencing of the zebrafish antibody repertoire. Science. 2009. 324; 807-810.

Weiss G, Schaible UE. Macrophage defense mechanisms against intracellular bacteria. Immunol Rev. 2015. 264; 182-203.

Wheelwright M, Kim EW, Inkeles MS, De Leon A, Pellegrini M, Krutzik SR, Liu PT. All-*trans* retinoic acid-triggered antimicrobial activity against *Mycobacterium tuberculosis* is dependent on NPC2. J Immunol. 2014. 192: 2280-2290.

Wiedenheft B, Sternberg SH, Doudna JA. RNA-guided genetic silencing systems in bacteria and archaea. Nature. 2012. 482; 331-338.

Wienholds E, Schulte-Merker S, Walderich B, Plasterk RH. Target-selected inactivation of the zebrafish rag1 gene. Science. 2002. 297; 99-102.

Wienholds E, van Eeden F, Kosters M, Mudde J, Plasterk RH, Cuppen E. Efficient target-selected mutagenesis in zebrafish. Genome Res. 2003. 13; 2700-2707.

Wilburn KM, Fieweger RA, VanderVen BC. Cholesterol and fatty acids grease the wheels of *Mycobacterium tuberculosis* pathogenesis. Pathog Dis. 2018. 76; fty021.

Willett CE, Cherry JJ, Steiner LA. Characterization and expression of the recombination activating genes (*rag1* and *rag2*) of zebrafish. Immunogenetics. 1997. 45; 394-404.

Willett CE, Cortes A, Zuasti A, Zapata AG. Early hematopoiesis and developing lymphoid organs in the zebrafish. Dev Dyn. 1999. 214; 323-336.
Willett CE, Zapata AG, Hopkins N, Steiner LA. Expression of zebrafish *rag* genes during early development identifies the thymus. Dev Biol. 1997. 182; 331-341.
Wittamer V, Bertrand JY, Gutschow PW, Traver D. Characterization of the mononuclear phagocyte system in zebrafish. Blood. 2011. 117; 7126-7135.
Wolf AJ, Linas B, Trevejo-Nuñez GJ, Kincaid E, Tamura T, Takatsu K, Ernst JD. Mycobacterium tuberculosis infects dendritic cells with high frequency and impairs their function *in vivo*. J Immunol. 2007. 179; 2509-2519.
World Health Organization. Guidelines for treatment of tuberculosis. 2010. 4th edition. htpps://www.who.int/tb/publications/2010/9789241547833/en/ (accessed 12 May 2019).
World Health Organization. Global Tuberculosis Report. 2019. https://www.who.int/tb/publications/global_report/en/ (accessed 12 April 2020).
World Health Organization. Latent tuberculosis infection: updated and consolidated guidelines for programmatic management. 2018. https://www.who.int/tb/publications/2018/latent-tuberculosis-infection/en/ (accessed 7 May 2019).
World Health Organization. Rapid communication: key changes to the treatment of multidrug- and rifampicin-resistant tuberculosis (MDR/RR-TB). 2018. http:// www.who.int/tb/publications/2018/WHO_Rapid.CommunicationMDRTB.pdf?ua =1 (accessed 12 May 2019).
Xu H, Jia Y, Li Y, Wei C, Wang W, Guo R, Jia J, Wu Y, Li Z, Wei Z, Qi X, Li Y, Gao X. IL-10 dampens the Th1 and Tc activation through modulating DC functions in BCG vaccination. Mediators Inflamm. 2019. 2019; 8616154.
Xu Y, Yang E, Huang Q, Ni W, Kong C, Liu G, Li G, Su H, Wang H. PPE57 induces activation of macrophages and drives Th1-type immune responses through TLR2. J Mol Med (Berl). 2015. 93; 645-662.
Yang CT, Cambier CJ, Davis JM, Hall CJ, Crosier PS, Ramakrishnan L. Neutrophils exert protection in the early tuberculous granuloma by oxidative killing of mycobacteria phagocytosed from infected macrophages. Cell Host Microbe. 2012. 12; 301-312.
Yasuda Y, Li Z, Greenbaum D, Bogyo M, Weber E, Brömme D. Cathepsin V, a novel and potent elastolytic activity expressed in activated macrophages. J Biol Chem. 2004. 279; 36761-36770.
Yazawa R, Cooper GA, Beetz-Sargent M, Robb A, McKinnel L, Davidson WS, Koop BF. Functional adaptive diversity of the Atlantic salmon T-cell receptor gamma locus. Mol Immunol. 2008. 45; 2150-2157.
Yim JJ, Selvaraj P. Genetic susceptibility in tuberculosis. Respirology. 2010. 15; 241-256.
Yoder JA, Orcutt TM, Traver D, Litman GW. Structural characteristics of zebrafish orthologs of adaptor molecules that associate with transmembrane immune receptors. Gene. 2007. 401; 154-164.
Yoder JA, Mueller MG, Wei S, Corliss BC, Prather DM, Willis T, Litman RT, Djeu JY, Litman GW. Immune-type receptor genes in zebrafish share genetic and functional properties with genes encoded by the mammalian leukocyte receptor cluster. Proc Natl Acad Sci USA. 2001. 98; 6771-6776.
Yoon S, Mitra S, Wyse C, Alnabulsi A, Zou J, Weerdenburg EM, van der Sar AM, Wang D, Secombes CJ, Bird S. First demonstration of antigen induced cytokine expression by

CD4-1+ lymphocytes in a poikilotherm: studies in zebrafish (*Danio rerio*). PLos One. 2015. 10; e0126378.

Yu Z, Wit W, Xiong L, Cheng Y. Associations of six common functional polymorphisms in interleukins with tuberculosis: evidence from a meta-analysis. Pathog Dis. 2019. 77; ftz053.

Young DB, Gideon HP, Wilkinson RJ. Eliminating latent tuberculosis. Trends Microbiol. 2009. 17; 183-188.

Yuan C, Qu ZL, Tang XL, Liu Q, Luo W, Huang C, Pan Q, Zhang XL. *Mycobacterium tuberculosis* mannose-capped lipoarabinomannan induces IL-10-producing B cells and hinders $CD4^{+}$Th1 immunity. iScience. 2019. 11; 13-30.

Zerbino DR, Achuthan P, Akanni W, Amode MR, Barrell D, Bhai J, Billis K, Cummins C, Gall A, Giron CG, Gil L, Gordon L, Haggerty L, Haskell E, Hourlier T, Izugo OG, Janacek SH, Juettemann T, To JK, Laird MR, Lavidas I, Liu Z, Loveland JE, Maurel T, McLaren W, Moore B, Mudge J, Murphy DN, Newman V, Nuhn M, Ogeh D, Ong CK, Parker A, Patricio M, Riat HS, Schuilenburg H, Sheppard D, Sparrow H, Taylor K, Thormann A, Vullo A, Walts B, Zadissa A, Frankish A, Hunt SE, Kostadima M, Langridge N, Martin FJ, Muffato M, Perry E, Ruffier M, Staines DM, Trevanion SJ, Aken BL, Cunningham F, Yates A, Flicek P. Ensembl 2018. Nucleic Acids Res. 2018. 46; D754-D761.

Zhai W, Wu F, Zhang Y, Fu Y, Liu Z. The immune escape mechanisms of *Mycobacterium tuberculosis*. Int J Mol Sci. 2019. 20; E340.

Zhang DC, Shao YQ, Huang YQ, Jiang SG. Cloning, characterization and expression analysis of interleukin-10 from the zebrafish (*Danio rerion*). J Biochem Mol Biol. 2005. 38; 571-576.

Zhang J, Talbot WS, Schier AF. Positional cloning identifies zebrafish *one-eyed pinhead* as a permissive EGF-related ligand required during gastrulation. Cell. 1998. 92; 241-251.

Zhang J, Chen Y, Nie XB, Wu WH, Zhang M, He XM, Lu JX. Interleukin-10 polymorphisms and tuberculosis susceptibility: a meta-analysis. Int J Tuberc Lung Dis. 2011. 15; 594-601.

Zhang M, Gong J, Iyer DV, Jones BE, Modlin RL, Barnes PF. T cell cytokine responses in persons with tuberculosis and human immunodeficiency virus infection. J Clin Invest. 1994. 94; 2435-2442.

Zhang S, Cui P. Complement system in zebrafish. Dev Comp Immunol. 2014. 46; 3-10.

Zhao Y, Lin L, Xiao Z, Li M, Wu X, Li W, Li X, Zhao Q, Wu Y, Zhang H, Yin J, Zhang L, Cho CH, Shen J. Protective role of γδ T cells in different pathogen infections and its potential clinical application. J Immunol Res. 2018. 2018; 5081634.

Zhong Y, Huang W, Du J, Wang Z, He J, Luo L. Improved *Tol2*-mediated enhancer trap identifies weakly expressed genes during liver and β cell development and regeneration in zebrafish. J Biol Chem. 2019. 294; 932-940.

Zhou J, Ling J, Song J, Wang Y, Feng B, Ping F. Interleukin 10 protects primary melanocyte by activation of Stat-3 and PI3K/Akt/NF-κB signaling pathways. Cytokine. 2016. 83; 275-281.

Zimmerman AM, Moustafa FM, Romanowski KE, Steiner LA. Zebrafish immunoglobulin IgD: unusual exon usage and quantitative expression profiles with IgM and IgZ/T heavy chain isotypes. Mol Immunol. 2011. 48; 2220-2223.

Zuccolo J, Bau J, Childs SJ, Goss GG, Sensen CW, Deans JP. Phylogenetic analysis of the MS4A and TMEM176 gene families. PLos One. 2010. 5; e9369.

Zwerling A, Behr MA, Verma A, Brewer TF, Menzies D, Pai M. The BCG World Atlas: a database of global BCG vaccination policies and practices. PLoS Med. 2011. 8; e1001012.

PUBLICATIONS

PUBLICATION I

Mycobacterium marinum **causes a latent infection that can be reactivated by gamma irradiation in adult zebrafish**

Parikka M, Hammarén MM, Harjula S-KE, Halfpenny NJA, Oksanen KE, Lahtinen MJ, Pajula ET, Iivanainen A, Pesu M, Rämet M.

PLoS Pathogens. 2012. 8(9):e1002944.
doi: 10.1371/journal.ppat.1002944.

OPEN ACCESS Freely available online

PLOS | PATHOGENS

Mycobacterium marinum Causes a Latent Infection that Can Be Reactivated by Gamma Irradiation in Adult Zebrafish

Mataleena Parikka[1☯]*, Milka M. Hammarén[1☯], Sanna-Kaisa E. Harjula[1], Nicholas J. A. Halfpenny[1], Kaisa E. Oksanen[1], Marika J. Lahtinen[1], Elina T. Pajula[1], Antti Iivanainen[2], Marko Pesu[1,3], Mika Rämet[1,4]

1 BioMediTech, University of Tampere, Tampere, Finland, **2** Department of Veterinary Biosciences, University of Helsinki, Helsinki, Finland, **3** Fimlab Laboratories, Pirkanmaa Hospital District, Tampere, Finland, **4** Department of Pediatrics, Tampere University Hospital, Tampere, Finland

Abstract

The mechanisms leading to latency and reactivation of human tuberculosis are still unclear, mainly due to the lack of standardized animal models for latent mycobacterial infection. In this longitudinal study of the progression of a mycobacterial disease in adult zebrafish, we show that an experimental intraperitoneal infection with a low dose (~35 bacteria) of *Mycobacterium marinum*, results in the development of a latent disease in most individuals. The infection is characterized by limited mortality (25%), stable bacterial loads 4 weeks following infection and constant numbers of highly organized granulomas in few target organs. The majority of bacteria are dormant during a latent mycobacterial infection in zebrafish, and can be activated by resuscitation promoting factor *ex vivo*. In 5–10% of tuberculosis cases in humans, the disease is reactivated usually as a consequence of immune suppression. In our model, we are able to show that reactivation can be efficiently induced in infected zebrafish by γ-irradiation that transiently depletes granulo/monocyte and lymphocyte pools, as determined by flow cytometry. This immunosuppression causes reactivation of the dormant mycobacterial population and a rapid outgrowth of bacteria, leading to 88% mortality in four weeks. In this study, the adult zebrafish presents itself as a unique non-mammalian vertebrate model for studying the development of latency, regulation of mycobacterial dormancy, as well as reactivation of latent or subclinical tuberculosis. The possibilities for screening for host and pathogen factors affecting the disease progression, and identifying novel therapeutic agents and vaccine targets make this established model especially attractive.

Citation: Parikka M, Hammarén MM, Harjula S-KE, Halfpenny NJA, Oksanen KE, et al. (2012) *Mycobacterium marinum* Causes a Latent Infection that Can Be Reactivated by Gamma Irradiation in Adult Zebrafish. PLoS Pathog 8(9): e1002944. doi:10.1371/journal.ppat.1002944

Editor: Marcel A. Behr, McGill University, Canada

Received July 30, 2012; **Accepted** August 18, 2012; **Published** September 27, 2012

Funding: The study was financially supported by Academy of Finland (projects 128623, 135980, M. Pesu; 121003, M. Parikka; 139225, M. Rämet), a Marie Curie International Reintegration Grant within the 7th European Community Framework Programme (M. Pesu), Emil Aaltonen Foundation (M. Pesu), Sigrid Jusélius Foundation (M. Pesu, M. Rämet), Tampere Tuberculosis Foundation (M. Pesu, M. Parikka, M. Rämet), Finnish Anti-tuberculosis Foundation (M. Parikka, K. Oksanen, M. Hammarén, the Väinö and Laina Kivi Foundation (K. Oksanen) and Competitive Research Funding of the Tampere University Hospital (M. Pesu, M.Parikka and M. Rämet). The zebrafish work was carried out at University of Tampere core facility supported by Biocenter Finland, Tampere Tuberculosis Foundation and Emil Aaltonen Foundation. The funders had no role in study design, data collection and analysis, decision to publish, or preparation of the manuscript.

Competing Interests: The authors declare that no competing interests exist.

* E-mail: mataleena.parikka@uta.fi

☯ These authors contributed equally to this work.

Introduction

Tuberculosis (TB) is caused by *Mycobacterium tuberculosis*, a highly specialized pathogen capable of evading the immune defense by various strategies. The success of the pathogen and the shortcomings of current medical interventions are reflected by the high prevalence of *M. tuberculosis* infection; one third of the world's population has been estimated to carry the pathogen and to have a latent, subclinical infection [1], which can be diagnosed using immunological sensitization to *M. tuberculosis* antigens [2]. Noteworthy, this asymptomatic infection is thought to consist of a variety of disease states that differ in bacterial phenotypes and burdens. [2,3].

According to the report of the World Health Organization (WHO), TB caused 1.7 million deaths and 9.4 million new cases in 2009, especially in developing countries. Approximately 5–10% of carriers develop an active disease during their lifetime [4], which reflects the spectrum of disease states within the population with latent TB [2,3]. This number is even higher in countries with a high prevalence of human immunodeficiency virus (HIV) [4]. The current preventive treatment against TB, the Bacille Calmette-Guérin (BCG) vaccine, protects children against the most severe forms of TB (TB meningitis or disseminated TB), but its efficacy in adults has been questioned and is thought to have limited or no protection against the disease [5,6]. A worrisome shortcoming is that BCG does not protect against the reactivation of latent, subclinical TB [7]. The prevalence of HIV seems to be one of the most important attributes to the increase in the number of active TB cases [5,8]. Tumor necrosis factor (TNF) neutralizing treatments often used in autoinflammatory diseases have also been found to increase susceptibility to TB [4,5], as do malnutrition, tobacco smoke, indoor air pollution, alcoholism, insulin dependent diabetes, renal failure, and immune suppressive treatments, such as glucocorticoids [4]. These factors may either

Author Summary

One third of the world's population has been estimated to be infected with *Mycobacterium tuberculosis*, which under the appropriate set of circumstances causes lethal lung disease. According to current understanding, mycobacteria can persist in their host without causing symptoms – a state referred to as latency or subclinical infection. However, if the immune system of the host becomes compromised, for example due to immunosuppressive medical treatments or HIV, the disease can become reactivated with detrimental consequences. The mechanisms leading to latency are not well understood. Latent tuberculosis responds poorly to antibiotics, and there is currently no effective vaccine against latent or reactivated tuberculosis. Using *Mycobacterium marinum*, a natural fish pathogen and a close relative of *M. tuberculosis*, we were able to induce a disease in adult zebrafish closely mimicking the human latent disease. We show that a dormant mycobacterial population is present in animals with a latent mycobacterial disease. Dormancy is also thought to occur in human tuberculosis. In addition, we present a method, with which the latent disease can be experimentally reactivated. Despite the evolutionary distance between man and fish, the zebrafish presents itself as a unique model for studying the mechanisms related to latency and reactivation.

cause the primary infection to progress, or an existing subclinical infection to reactivate. In general, the mechanisms for the reactivation of tuberculosis are not well established and warrant further investigation.

Various animal models have been used for studying mycobacterial infections with the ultimate aim of understanding human TB [8]. The zebrafish has lately been established as a new, genetically tractable model for studying host–mycobacterium interactions [9–11]. Zebrafish are naturally susceptible to *Mycobacterium marinum* [12–14], which is a close relative of *M. tuberculosis* [15]. *M. marinum*-induced disease in zebrafish shares the main pathological and histological features, including necrotic granulomas, with human TB [16] and is thus a highly attractive model for the human disease. Zebrafish larvae have been widely used for studying innate immune responses to *M. marinum* infection [9,11,17]. However, adaptive immune responses have also been reported to be essential for controlling human TB [18,19] and are also important for controlling *M. marinum* infection in adult zebrafish [10].

Studies on the latency, dormancy and reactivation of TB have been impeded by the lack of applicable animal models, as spontaneous latency without the help of chemotherapeutics has only been successful in the rabbit [20], and in macaque [21] models. Here, we show that a low-dose *M. marinum* infection spontaneously develops into a latent, non-progressive disease in adult zebrafish, with a static number of granulomas and a stable bacterial burden mainly consisting of dormant bacteria. The existence of a large dormant population of mycobacteria seems to be connected to the latent disease. In our model, the stable latent disease can be experimentally reactivated with γ-radiation, essentially mimicking the immune suppression-induced reactivation in human TB. This study thus presents a novel vertebrate platform suitable for large scale genetic screening, as a means of characterizing host and pathogen mechanisms underlying the transitions in TB from an acute infection to latency, and to a reactivated infection.

Results

A low-dose *M. marinum* infection leads to a latent disease with stable bacterial loads after 4 weeks

The lack of suitable and well-established animal models mimicking latent, subclinical TB in humans prompted us to investigate if such a model could be developed in zebrafish. First, we compared several methods for infecting adult zebrafish with their natural pathogen, *M. marinum*, to create a physiological infection model leading to a static phase after the primary active disease. We infected zebrafish either by injecting different bacterial doses into the abdominal cavity or by bathing, to find a suitable dose and an infection route inducing a latent infection with low mortality. The experimental groups were followed up to 32 weeks for survival. A high-dose intraperitonaeal (i.p.) infection (2,029±709 cfu) was characterized by high mortality (end-point mortality 64%), whereas most fish infected with a low dose (34±15 cfu) generally survived (end-point mortality 25%) (Figure 1A). A group of fish was also infected with 9,075 ± 2,681 cfu, but this dose lead to an extremely high mortality (80% mortality in 5 weeks)(data not shown) and the group was excluded from further characterizations. Bathing the fish in water containing 2.4×10^6 cfu/ml lead to an infection only in 50% of the individuals (determined by bacterial loads), which then developed a similar level of end-point mortality as the low-dose injected fish (data not shown). Because of the low incidence rate, bathing was not considered a suitable method for studying latent mycobacterial infection in adult zebrafish.

Latent human TB is diagnosed using tuberculin skin test (TST), interferon-γ release assays (IGRA) and characterized by a lack of clinical signs [2]. In our model, we are able to directly follow the progression of the disease by quantifying total mycobacterial burdens within the whole organism. For this purpose we developed a new, qPCR-based method specific for *M. marinum* (Supporting information, Text S1, Figure S1). In the high-dose group, an average bacterial load of 6.0×10^5 cfu/fish ($SD = 6.5\times10^5$) was measured as early as 1 week post infection (wpi). Bacterial growth during the first week after injection was close to logarithmic, suggesting that the bacteria grew in an unrestricted manner. During the 32-week follow up, the average burdens rose to 3.0×10^6 cfu/fish ($SD = 3.2\times10^6$), indicating that the high dose i.p. injection leads to a chronic progressive disease. Also in the low-dose group, the bacteria grew almost logarithmically during the first week of infection. The average bacterial load increased from the 1 weeks' 5×10^3 ($SD = 3.1\times10^3$) to 4 weeks' 5.2×10^5 cfu/fish ($SD = 1.1\times10^6$). After the four-week time point, however, the average bacterial burden ceased to grow, remaining at an unaltered level until the end of the experiment (at 32 weeks 4.4×10^5 cfu ± 4.4×10^5/fish) (Figure 1B). This result suggests that experimental infection of adult zebrafish by an i.p. injection of a small dose of *M. marinum* leads to an active primary infection, followed by a controlled state in most individuals.

Granuloma formation and spreading of the infection ceases at the onset of the stable state infection in the low-dose infection model

In order to get a more detailed and biologically relevant measure of the progression of the disease in our infection model, we carried out histological analyses at 2, 4, 8 and 20 wpi. Ziehl-Neelsen staining for mycobacteria was used for the quantification of granulomas and affected target organs. The gonads, pancreas, liver, muscle, mesentery, spleen, gut and kidney were specifically assessed for the presence of mycobacterial lesions. Early granulomatous structures characterized by cellular and bacterial

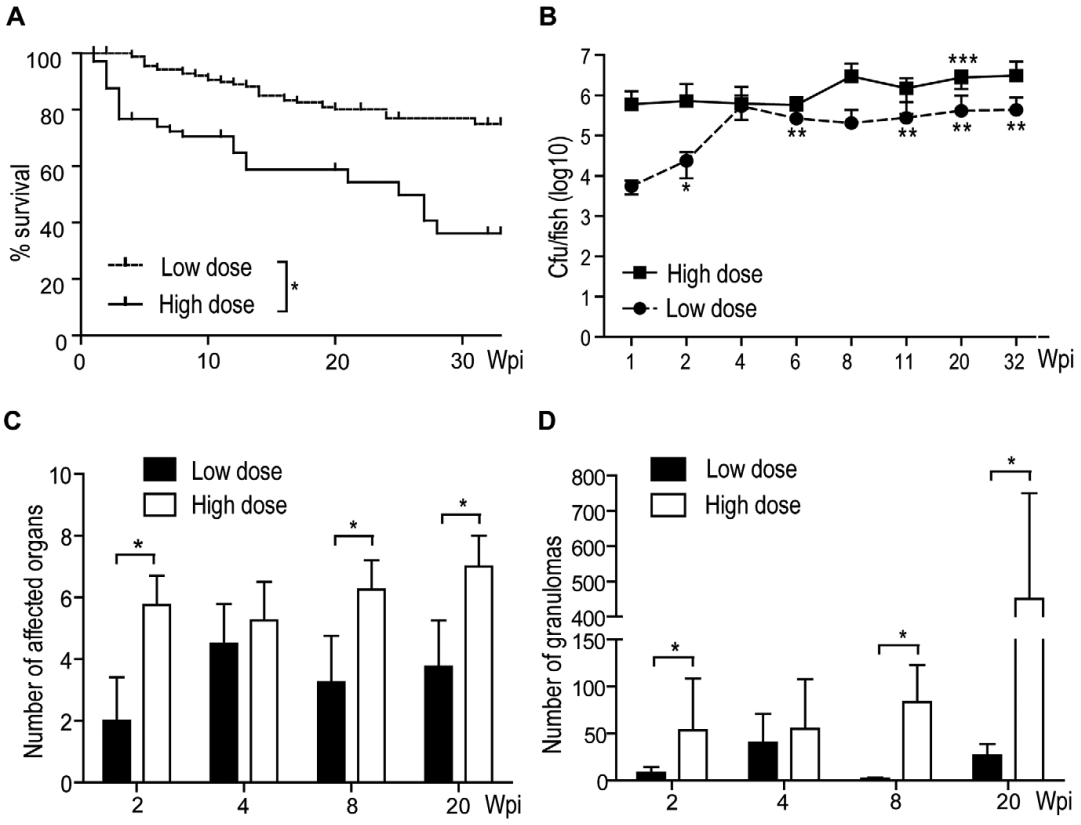

Figure 1. Zebrafish mortality, the development of bacterial load and the number of lesions have dose-dependent patterns. Adult zebrafish were i.p. infected with either a low (34±15 cfu) (n = 180) or a high dose (2029±709 cfu) (n = 104) of *M. marinum*. (A) Survival was followed for 32 weeks. * $P<0.05$ (B) The figure shows the average loads for 5 fish (except 32 wk high dose, n = 2). Low-dose statistics: * sig. diff. from 1 wk, ** sig. diff. from 1 and 2 wk. High-dose statistics: *** sig. diff. from 1, 2, 8, 11 and 20 wk. Low-dose vs. high-dose statistics: loads at time-points marked with † are sig. diff. (C) By default, 4 individuals per dose were analyzed by Ziehl-Neelsen staining (except 20 wk high dose, n = 3) per time-point The gonads, pancreas, liver, muscle, mesentery, spleen, gut and kidney were assessed and the number of organs with visible bacteria was determined. *$P<0.05$. (D) The total number of granulomas in a sample set for each individual was counted. * $P<0.05$.
doi:10.1371/journal.ppat.1002944.g001

aggregation were formed by 2 wpi in both dose groups (Figure 2A–D). The general appearance of the structures developed in the course of the infection such that at 20 weeks, most granulomas were insulated from the surrounding tissue by a fibrotic and/or cellular cuff (Figure 2E–H).

Granulomas were counted in representative sample sets for each individual (Figure 1D). Unsurprisingly, the fish infected with a low dose had significantly less granulomas at 2, 8 and 20 weeks following infection than the high-dose infected fish. The number of granulomas thus seems to be determined by the initial dose. In the high-dose infection, the number of granulomas significantly increased between 4 and 20 weeks, whereas in the low-dose infection, the number did not increase after the first 4 weeks, further supporting the relevance of our model for latent TB.

The number of affected organs was found to be determined by the initial infection dose. At 2 wpi, the low-dose infected fish had lesions in ~2 organs (most often in the pancreas and gonads), whereas fish infected with the high-dose had bacteria in ~6 organs (pancreas, kidney, gonads, liver, muscle, spleen). The number remained relatively unaltered for the duration of the experiment (Figure 1C), with the exception of a slight increasing trend in the high-dose group between 2 and 20 weeks. In the low-dose group, an increase between 2 and 4 weeks was seen (not significant), but the number of affected organs then ceased to grow, suggesting that the infection was well-controlled.

In conclusion, the histological analysis supports the idea that the high-dose infection is progressive with an increasing number of granulomas in various target organs, whereas the low-dose infection resembles a latent infection with unaltered numbers of granulomas in few target tissues.

Cytokine responses to *M. marinum* differ between low-dose and high-dose infection

To build a more detailed understanding on the different outcomes between the high and low dose infection, the early immune responses were studied by measuring cytokine expression levels in the internal organs of infected fish by reverse transcription

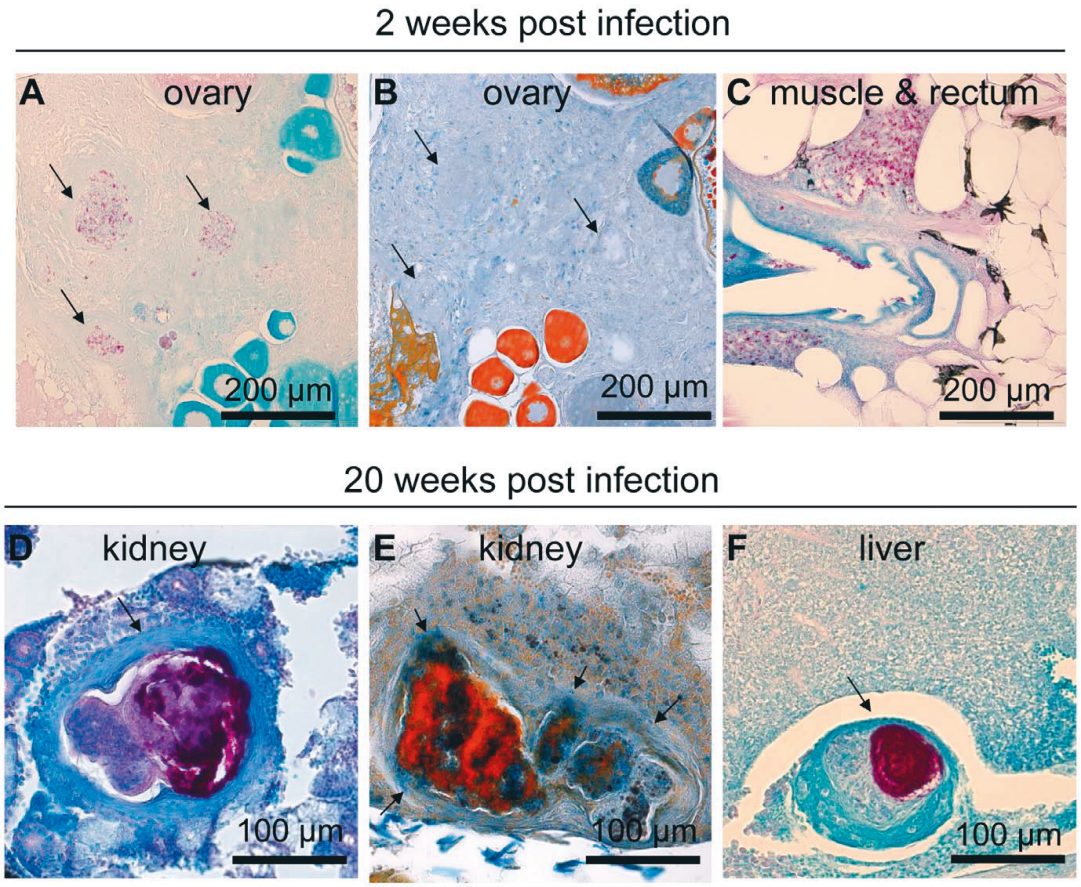

Figure 2. *M. marinum* induces the formation of granulomas that mature into well-defined structures during an infection. In fish infected with a low dose (34±15 cfu) of *M. marinum*, Ziehl-Neelsen staining at 2 wpi commonly reveals areas with free bacteria (C). Some slightly better formed and restricted areas containing bacteria, here referred to as early granulomas, are also seen (A), but as shown in (B) trichrome staining of the adjacent slide, encapsulation around the mycobacterial lesions is absent at the early stage of infection. At 20 weeks, fish that have survived have mature granulomas (D–F) many of which are multicentric surrounded by a fibrous capsule (D&E). (E) Trichrome staining shows the fibrous capsule in blue (F). The amount of bacteria inside granulomas has increased from the earliest time-points.
doi:10.1371/journal.ppat.1002944.g002

quantitative PCR (q-RT-PCR). One day after infection, the high-dose infection caused an induction of *tumor necrosis factor alpha* (*TNFα*, *ZDB-GENE-050317-1*) by 6.5-fold (SD = 6.6), *interleukin 6* (*IL-6*, *ZDB-GENE-120509-1*) by 9.6-fold (SD = 10.4) and *interleukin 12* (*IL-12*, *ZDB-GENE-060724-1*) by 2.7-fold (SD = 1.8) (Figure 3C), but no induction was seen in *interleukin 1 beta* (*IL-1β*, *ZDB-GENE-040702-2*). Among the low-dose infected fish, only *IL-6* was induced but at a lower level, 3.9-fold induction, SD = 4.8, compared to high-dose infection at 1 dpi.

As the early innate responses are known to regulate the activation of adaptive responses, it was not surprising that differences in *interferon gamma 1–2* (*IFNγ1–2*, ZDB-GENE-040629-1) and *inducible nitric oxide synthase 2b* (*Nos2b*, ZDB-GENE-080916-1) levels were seen between the high and low dose groups at later time points (2–7 wpi). *Nos2b* was consistently more highly induced with the high dose than with the low dose at 2, 4 and 7 weeks (Figure 3D). The expression was at the highest level already at 2 wpi (high-dose group 1,508-fold, SD = 2,136, low-dose group 123-fold, SD = 167), after which the level declined in both dose groups, still remaining strongly induced.

In *IFNγ1–2* expression, the high dose caused a 13.7-fold induction (SD = 16) at 2 weeks. The low dose caused a more moderate 3.0-fold induction (SD = 2.8 (Figure 3F)), which was not different from the induction in the buffer-injected group. At 4 wpi, no difference was detected in *IFNγ1–2* levels. Noteworthy, at 7 wpi, the *IFNγ1–2* expression in the high-dose group had decreased to 1.8-fold induction (SD = 1.6), whereas in the low-dose group the level had increased to 8.8-fold (SD = 11.0), compared to uninfected controls. Thus, the kinetics of *IFNγ1–2* show a decreasing trend in the high-dose group and an increasing trend in the low-dose group, but the differences at late time-points are not significant. In conclusion, these results suggest that the strong early cytokine responses with the high infection dose are associated with *Nos2b* induction at an early phase of infection

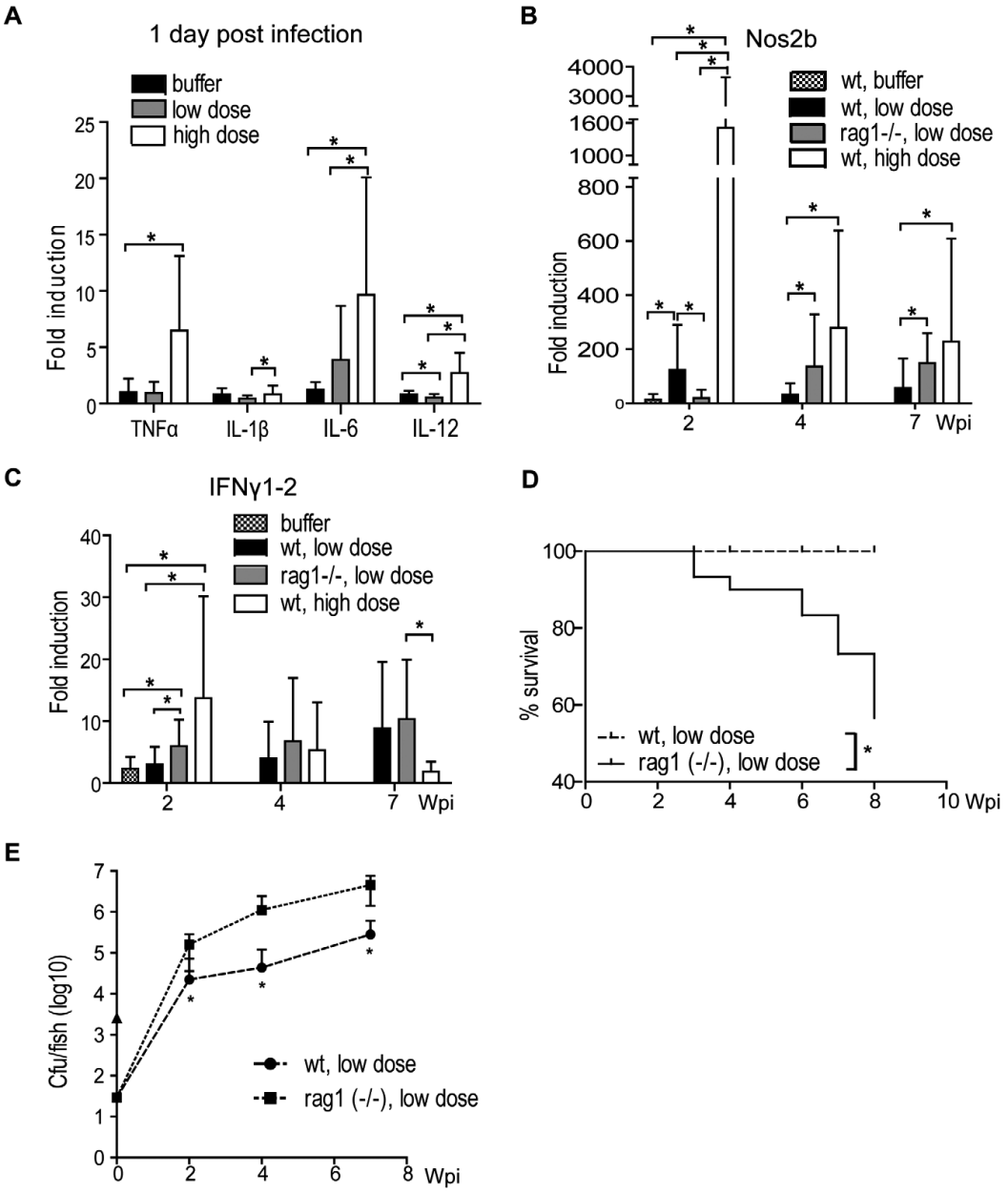

Figure 3. Bacterial dose and the presence of functional adaptive immunity define the outcome of mycobacterial infection. (A) The early cytokine response at 1 d post infection was measured from wt fish infected with a high (2029±709 cfu) or a low (34±15 cfu) dose or injected with sterile PBS buffer (n in each group 10–20). *P<0.05 (B) Wt fish were infected with a high or a low dose or sterile PBS buffer (for early time-points), and rag1 (−/−) fish were infected with a low dose Nos2b expression was measured with q-RT-PCR (n in each group was 9–20/time point). *P<0.05 (C) Fish were infected as in (B) and *IFNγ1–2* was measured with q-RT-PCR. *P<0.05. (D) Adult wt and rag1 (−/−) zebrafish were infected with a low dose (n = 30) and followed for survival. *P<0.05 (E) Adult wt and rag1 (−/−) fish were infected with a low dose. Average mycobacterial load was measured by qPCR at 2, 4, and 7 wpi (n = 10 per time point). *P<0.05.
doi:10.1371/journal.ppat.1002944.g003

(2 wpi) and to the different kinetics of *IFNγ1–2* response between the two dose groups.

Adaptive immunity is required for the restriction of bacterial growth and the induction of latency

According to the current understanding on human TB, adaptive immunity is required for efficient control of the disease [18,19]. Survival results from a previous publication suggest a role for adaptive immunity in mycobacterial infection in the zebrafish [10]. We wanted to study whether adaptive immunity is required for the establishment of latency in the zebrafish. To this end, we used a recombination activating protein 1 (*rag1*) deficient zebrafish line, which lacks functional T and B cells [22].

First, we looked at the morbidity caused by a low dose of the type strain of *M. marinum* in rag1-mutant (−/−) zebrafish. Rag1 (−/−) fish, along with wild type (wt) controls, were infected with the low dose (34±15 cfu). The fish were euthanized at the end-stage of infection and survival curves were drawn (Figure 3D). None of the wt fish showed signs of disease during the 8-week follow up, whereas 43% of the rag1 (−/−) fish reached the end-stage of disease. DNA was extracted from the end-stage rag1 (−/−) fish and the mycobacterial load was measured by qPCR. The average load was 3.89×10^7 cfu/fish (SD = 3.68×10^7), which is similar to the levels measured from terminal stage *M. marinum* infected wt fish (data not shown), indicating that the rag1 (−/−) zebrafish had suffered from an end-stage *M. marinum* infection.

Dynamic disease progression among rag1 (−/−) fish was associated with elevated mycobacterial loads compared to wt controls during the first weeks of infection. Rag1 (−/−) and wt fish were infected with the low dose for determination of bacterial burdens by qPCR. Already at 2 wpi, the loads in the rag1 (−/−) fish were significantly higher (1.61×10^5 cfu/fish, SD = 1.25×10^5) than in the wt fish (2.22×10^4 cfu/fish SD = 4.99×10^4), indicating that the adaptive immune responses are used already by 2 wpi as a means of restricting the mycobacterial infection. During the following weeks, the bacterial burdens remained significantly higher in the rag1 (−/−) mutants (3.80×10^6 cfu, SD = 3.15×10^6) compared to wt fish (2.83×10^5 cfu, SD = 3.26×10^6 at 7 wpi).

Alongside with gene-expression measurements from wt fish, *Nos2b* (Figure 3B) and *IFNγ1–2* (Figure 3C) levels were measured from low-dose infected rag1 (−/−) fish. At 2 wpi, *Nos2b* expression was significantly lower in rag1 (−/−) fish (19.6-fold, SD = 30.3) compared to the wt fish (123-fold, SD = 16), suggesting that adaptive responses affect *Nos2b* induction during the early phase of infection preceding the latency. It is generally thought that in human TB, *Nos2* is induced as a result of IFNγ production by lymphocytes, leading to macrophage activation and control of mycobacterial growth. However, in the adult zebrafish model the *Nos2b* induction at 2 wpi is not likely to be mediated by an adaptive *IFNγ1–2* induction, as the measured *IFNγ1–2* levels were significantly higher in the rag1 (−/−) mutants (6.0-fold induction, SD = 4.5) than in the wt fish (3.0-fold induction, SD = 2.8). At 4 and 7 weeks, the situation was altered so that the rag1 (−/−) mutants had significantly higher *Nos2b* expression levels (induced 136-fold, SD = 193 and 149-fold, SD = 110, respectively) than those observed in the wt (induced 31.6-fold, SD = 42.0 and 56.6-fold induction, SD = 108, respectively). These results suggest that in the adult zebrafish model, the initial macrophage activation preceding the onset of latency is mediated by adaptive responses driving Nos2b induction, but unexpectedly, not via IFNγ.

Most mycobacteria enter a dormant state during a latent infection in adult zebrafish

In human TB, the majority of bacteria are thought to enter a dormant state in response to the stress caused by the immune response and hypoxia. Dormant bacteria are viable but not culturable (VBNC) [23]. This state has been shown to be reversible by the addition of a resuscitation promoting factor (Rpf) *in vitro* [24]. The role of dormancy and resuscitation in a latent mycobacterial infection is difficult to study in humans, as the putative dormant bacteria are not accessible for visualization and cannot be cultured [23]. To investigate, whether there is a dormant bacterial population in *M. marinum* infected adult zebrafish, we tested the effect of Rpf on the number of colonies cultured from fish with a latent infection.

First, we tested if hypoxic *M. marinum* cultures can be resuscitated by an addition of *Micrococcus luteus* Rpf on antibiotic plates. Of note, the standard method of assessing the effect of Rpf on mycobacterial growth in broth culture and most probable number assay could not be used due to the fast-growing contaminating normal flora from the gut. Dilutions of active logarithmic and old hypoxic *M. marinum* broth cultures were plated with and without Rpf. As expected, Rpf significantly increased the number of colonies plated from old, hypoxic, inactive cultures (2.4-fold increase) but did not increase the number of colonies of active bacteria (Figure 4A). Altogether, these results indicate that Rpf from *M. luteus* media is active on 7H10 plates and is able to cause resuscitation of a significant proportion of dormant *M. marinum* that do not otherwise grow on culture plates. This also confirms the role of Rpf as a resuscitating enzyme for *M. marinum*, resembling its well established function for *M. tuberculosis*.

Next, adult zebrafish were infected with the low dose, and the disease was allowed to develop for twenty weeks before the fish were collected for analysis. Parallel samples were analyzed in the presence and absence of Rpf on the plate. When the diluted samples from fish with a latent infection were plated in the presence of Rpf, the number of culturable *M. marinum* increased 4-fold (32 ± 50 cfu without Rpf compared to 129 ± 134 cfu with Rpf) (Figure 4A). For early infection stage samples (1 wpi), the addition of Rpf did not have a growth promoting effect (31 ± 29 cfu without Rpf, 21 ± 22 cfu with Rpf) (Figure 4). With the high infection dose, leading to a more progressive disease, the population of resuscitable dormant bacteria were not detected at 9 wpi using Rpf (Figure 4A). Similarly, in the low-dose infected rag1 (−/−) fish, Rpf did not increase the average number of culturable mycobacteria, suggesting that adaptive immunity has a role in the efficient induction of mycobacterial dormancy. These results indicate that a distinguishable dormant mycobacterial population exists in the zebrafish with a latent infection, whereas in the active infection bacteria are predominantly in a replicative form.

To further confirm the existence of dormant mycobacterial population in the zebrafish with a latent infection, we measured the expression levels of known dormancy-associated mycobacterial genes. Based on *M. tuberculosis in vitro* dormancy microarray data [25], *HspX* (MMAR_3484), *devr* (MMAR_1516), *tgs1* (MMAR_1519) and *GltA1* (MMAR_1381) were chosen for q-RT-PCR measurements. Of these, only *GltA1*, which encodes a metabolic enzyme called citrate synthase, had generally high enough expression levels for reliable quantification from fish with a latent infection. *GltA1* expression was measured at 4 wpi from high-dose infected wt fish and low-dose infected wt and rag1 (−/−) fish. The *GltA1* expression level normalized to the number of bacteria in the low-dose infected wt fish (75.2, SD = 86.8) was significantly higher than in the high-dose wt fish (4.46, SD = 3.55), supporting the idea that in latent infection the proportion of

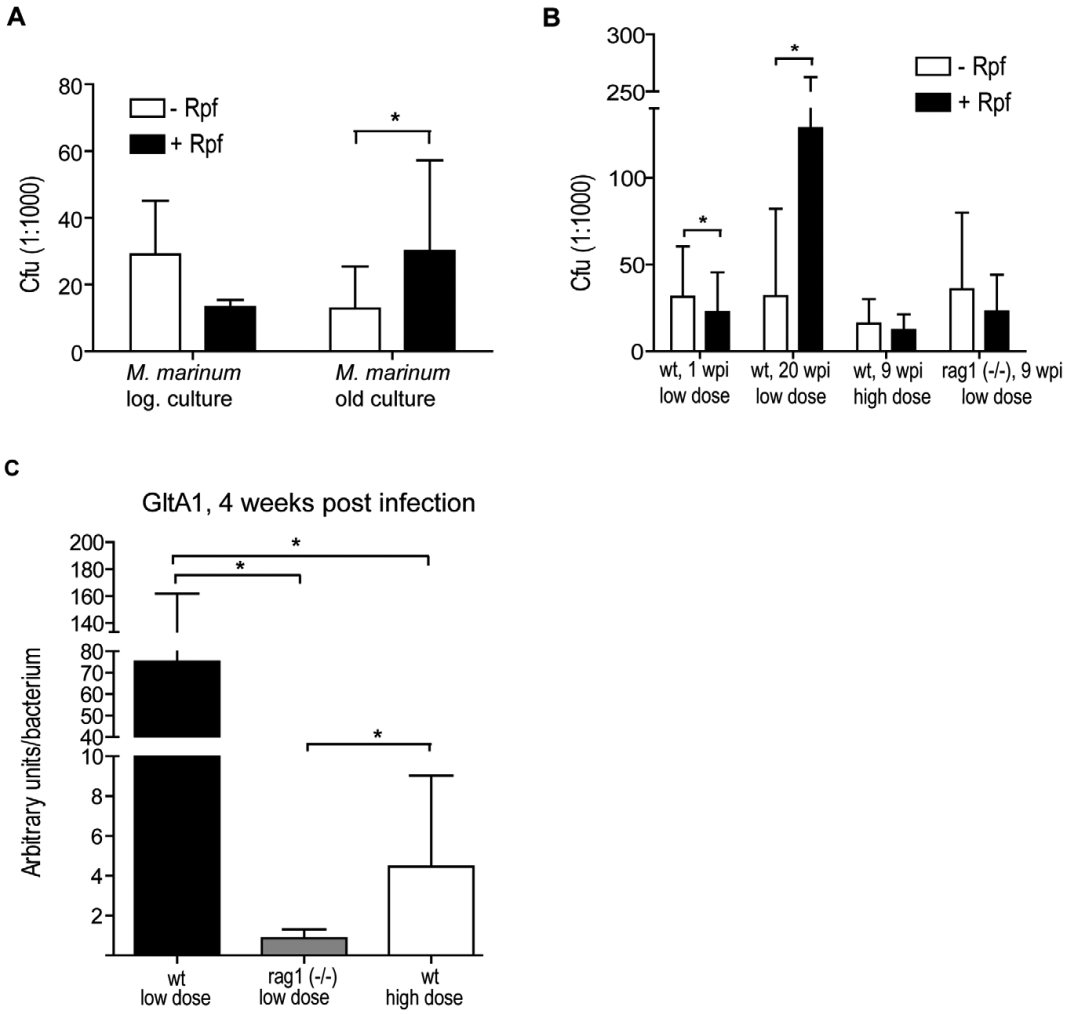

Figure 4. A major part of the mycobacteria are in a dormant state in latent infection. (A) Parallel dilutions of fresh logarithmic or old plateau phase *M. marinum* cultures were plated +/− Rpf to show the resuscitating effect of *Micrococcus luteus* Rpf on dormant *M. marinum*. (B) Parallel homogenate sample dilutions from low-dose (34±15 cfu) infected fish (wt or rag1 (−/−)) were plated at different time points +/− Rpf to detect dormant mycobacteria. (C) *GltA1* expression was measured from low-dose infected rag1 (−/−) and wt fish and high-dose infected wt fish and normalized to the total *M. marinum* load in each fish measured by qPCR. *P<0.05.
doi:10.1371/journal.ppat.1002944.g004

dormant mycobacteria is greater than in a more progressive infection. The lowest *GltA1* expression/bacterium was seen in the low-dose infected rag1 (−/−) fish (0.86, SD = 0.44). The low *GltA1* expression in rag1 (−/−) fish, together with the plating result showing no resuscitating effect by Rpf in rag1−/− fish (Figure 4B), suggests that adaptive immunity plays a role in the induction of mycobacterial dormancy *in vivo*.

The reactivation of a latent mycobacterial infection in zebrafish can be induced by γ-irradiation

Various immunosuppressive medical treatments, such as glucocorticoids [4] and radiation treatment [26], are seen as factors that increase the risk of the reactivation of latent human TB. Having established a model for latent mycobacterial infection in adult zebrafish, we next moved on to test the effect of γ-irradiation as immunosuppressive treatment to reactivate latent mycobacterial infection. Fish were infected with the low dose (34 ± 15 cfu), and five months post infection, a group of fish was irradiated with 25 Gy. Survival was followed for 1 month post irradiation, and the bacterial load was determined at 2 weeks. As a single 25 Gy dose of γ-radiation did not seem to cause sufficient reactivation of the latent mycobacterial infection in our zebrafish model system (Figure S2), two 25 Gy doses were administered to a group of fish with a latent *M. marinum* infection with one month

between the doses. Survival was followed for one month after the second irradiation. To assess the changes in the mycobacterial numbers and lesions, moribund or recently dead fish were collected and analyzed either histologically or with *M. marinum*-quantification PCR. Two 25 Gy doses of γ-radiation caused some degree of early time-point mortality in both irradiated groups. However, in the non-infected group, no deaths occurred after 16 days from the second irradiation (total mortality 40%), whereas the infected, irradiated population continued to die, reaching an end-point mortality of 88% (Figure 5A). No deaths occurred in the non-irradiated latent infection group. The immunosuppressive treatment with two 25 Gy doses of γ-irradiation lead to a significant increase in mortality among zebrafish with a latent mycobacterial infection, suggesting reactivation of the disease.

To confirm that the increased mortality after the γ-irradiation was related to the progression of the mycobacterial infection, the bacterial burdens were determined. Fish collected for qPCR 15–22 days after the second γ-radiation dose had an average bacterial load of 8.7×10^7 cfu (SD = 1.2×10^8), which was 106-fold higher compared to non-irradiated controls (average load 8.2×10^5 cfu, SD = 8.1×10^5) (Figure 5B). A histological analysis of moribund individuals revealed vast areas of free bacteria not restricted to granulomas (Figure 5C,D). Based on these results, γ-irradiation-induced reactivation of latent mycobacterial infection in adult zebrafish is a highly promising model for investigating the cellular and molecular mechanisms involved in reactivated mycobacterial infections.

Gamma irradiation-induced depletion of lymphocyte populations is associated with the reactivation of latent mycobacterial infection

To characterize the effect of γ-irradiation on blood cells, the changes in different blood cell populations were analyzed using flow cytometry (FCM). The numbers of granulo/monocytes and lymphocytes were measured from kidney homogenates. First, the immediate effects of a 25 Gy dose of γ-irradiation were studied by analyzing changes one week after the treatment (Figure 5E). The average proportion of granulocytes and monocytes was reduced by 47%, however there was a striking 80% reduction in the lymphocyte population, compared to normal levels. The efficient depletion of lymphocytes was further verified using the fish lines Tg(lck:lck-EGFP) and Tg(rag2-GFP), which express GFP in T cells, or in T and B cells, respectively. With these fish, a 67% reduction in the T cell population (lck) and a 99% reduction in the B and T cell population (rag2) were seen one week after irradiation (Figure 5E). Despite the marked leukocyte depletion, one 25 Gy dose of γ-irradiation had not been sufficient for the reactivation of a latent mycobacterial infection in zebrafish, as no significant changes were seen in mortality rates (Figure S2A) or in bacterial burdens (Figure S2B). Therefore, we next studied the recovery of leukocytes after the first irradiation, as well as the short- term effect of the second 25 Gy dose (Figure 5F). Both lymphocyte and granulocyte/monocyte populations had recovered to normal levels by five weeks after the first 25 Gy dose. The second 25 Gy dose of γ-irradiation reduced the number of lymphocytes by 53% compared to the recovery levels (Figure 5F), whereas granulocytes were not significantly affected by the second treatment. These results suggest that the effective reactivation of a latent mycobacterial infection required two 25 Gy doses of γ-irradiation because of the rapid recovery of the lymphocyte and granulocyte/monocyte populations after the first treatment. In addition, the mechanism of reactivation in this model is most likely due to the specific depletion of lymphocytes rather than a decrease in granulocytes.

Immunosuppression by γ-irradiation leads to reactivation of the dormant mycobacterial population

To assess the changes in the dormant bacterial population after the reactivation, we plated samples in the presence and absence of Rpf at 2.5 weeks after the second 25 Gy irradiation dose. In the non-irradiated fish with a latent infection, the number of colonies were 4-fold higher in the presence of Rpf than in its absence (Figure 5H), whereas after double irradiation the resuscitating effect of Rpf could no longer be seen (Figure 5G). This result supports the idea of latency-associated mycobacterial dormancy, which is reversed in reactivated disease.

Discussion

During the last couple of decades, the prevalence of active TB has substantially increased. Many of these cases are likely to be due to the reactivation of latent TB as a consequence of various immune compromising factors, such as HIV [27], diabetes [28] and glucocorticoid treatment [29]. Currently, the reactivation of latent TB is one of the greatest challenges in the field of infectious diseases, as present vaccination strategies do not protect against this phase of infection [7]. The fact that multiresistant strains of *M. tuberculosis* are arising in many parts of the world [5,30] further complicates the control of this disease. Thus, more detailed information on the mechanisms of the host–pathogen interactions in a latent mycobacterial disease and its reactivation is indispensable.

In general, the *M. marinum* infection model in zebrafish is well established. As *M. marinum* is a common pathogen of zebrafish, it can be considered a more natural model for studying host–mycobacterium interaction, than is, for example the *M. tuberculosis* mouse model. The histopathology of mycobacterial lesions in zebrafish has been shown to be more similar to human TB than is the histopathology in the mouse model (reviewed in [14]). The genetic similarities between *M. marinum* and *M. tuberculosis* are well documented [15], including the currently known genes involved in virulence and in dormancy (Dos-regulon) [31]. Thus, it is likely that the characterization of phenomena involved in latent infections and dormancy in a *M. marinum* infection, is useful for understanding human latent TB.

The concept of latent TB is problematic, and a debate over the definition as well as the nature of latent TB is on-going [32]. "Latent TB" is a broad clinical definition diagnosed with indirect immunological reactions in the tuberculin skin test (TST) or the interferon-γ release assay (IGRA) in the absence of clinical symptoms [2]. These assays do not reveal whether there are viable bacilli present in the host, but rather, whether the host has been infected with the bacterium and developed an adaptive response against it. Thus, cases diagnosed with latent TB compose a heterogeneous group with different bacterial phenotypes and loads [2,3]. In studies on latent TB patients, DNA of *M. tuberculosis* has been shown to be generally present in the lung necropsy samples of individuals with a latent infection [33,34]. These findings are in harmony with the common latency paradigm stating that in most infected individuals mycobacteria become dormant and non-replicating in the hypoxic environment of the granuloma but can be resuscitated in non-restrictive circumstances [2]. Still, the presence of mycobacterial DNA, as such, does not reveal the metabolic status (dormancy) of the bacteria. The subject warrants further investigation in applicable animal models as well as in human cohorts.

In this study we set up a novel model for latent TB using experimental *M. marinum* infection of adult zebrafish. We showed that mycobacterial dormancy is a central feature of latent TB in the zebrafish. The importance of adaptive immunity in the

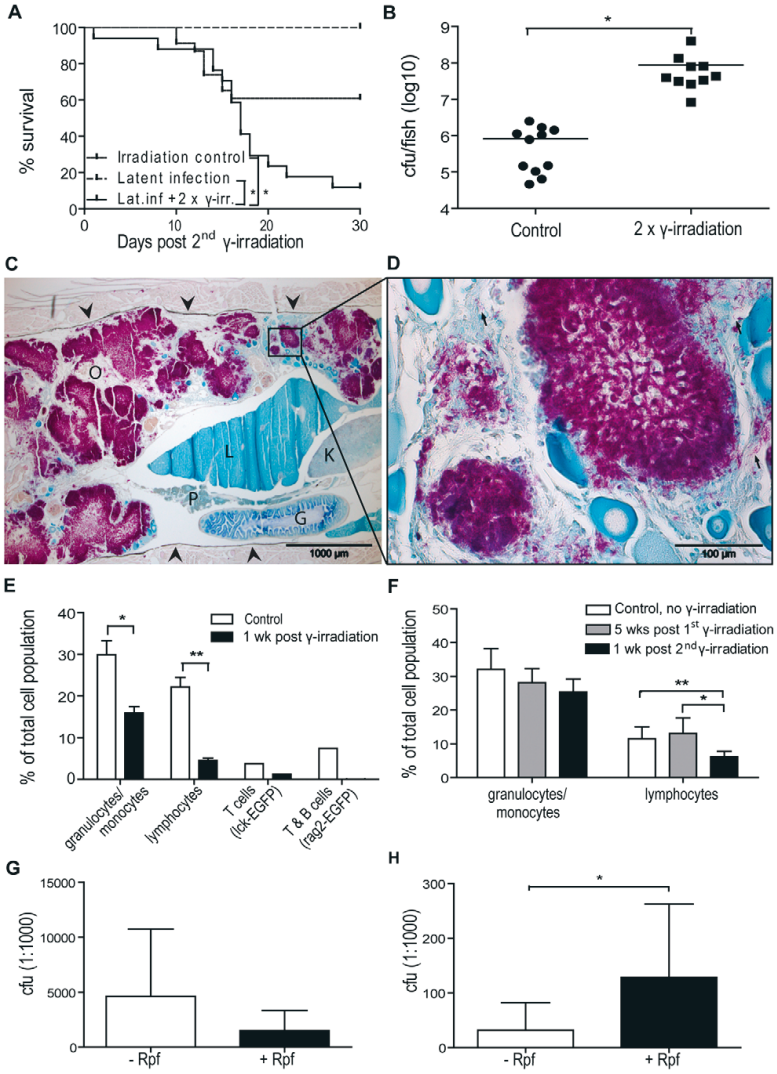

Figure 5. Gamma irradiation induces reactivation resulting in increased mortality due to uncontrolled growth of mycobacteria. (A–C) Zebrafish (n = 17) with a latent *M. marinum* infection were irradiated twice with 25 Gy with one month between the irradiations. Twice irradiated, non-infected zebrafish (n = 23) as well as zebrafish with a latent infection (n = 14) were included as controls. (A) Survival was followed for 30 days after the second dose. *P<0.05. (B) During this period, moribund or recently dead fish were collected 15–22 days after the second radiation dose. Bacterial loads were compared with those of similarly infected, non-irradiated control fish that were collected at the end-point of the experiment. *P<0.05 (C&D) A representative Ziehl-Neelsen stained sample from a reactivated fish showing large numbers of free mycobacteria (purple areas) in the zebrafish body cavity (C). The sides of the body cavity are marked with arrowheads O = ovary, P = pancreas, L = liver, G = gut, K = kidney. (D) A picture taken with a higher magnification showing individual rods (few examples pointed out with arrows). (E) Four groups of 4 adult zebrafish (1 rag2-gfp, 1 lck-gfp and 2 wild-type groups) were γ-irradiated with 25 Gy. Similar control groups were left untreated. Kidneys were collected 8 d post irradiation, pooled and analyzed by FCM. FSC-SSC -plots were gated based on cell size and granularity as described in [56] (gates shown in Figure S3) to assess the effect of irradiation on leukocyte populations. *P<0.05. For further verification of the effect of radiation on lymphocytes, a GFP gate was used for the rag2 and lck groups expressing GFP in B and T cells, or T cells, respectively. (F) Adult non-infected wt zebrafish were irradiated with 25 Gy once (grey bars) (n = 3) or twice (n = 7) (black bars) with one month between the doses. Leukocyte recovery and re-depletion were assessed by FCM. Non-irradiated fish (n = 4) were used as controls. *P<0.05 (G) Fish with a latent infection (n = 7) were irradiated twice with 25 Gy with one month between the doses and plated +/− Rpf for 18 d after the second radiation dose. (H) Fish (n = 6) with a latent infection were plated +/− Rpf.
doi:10.1371/journal.ppat.1002944.g005

establishment of a latent disease in zebrafish was shown in a number of experiments carried out with rag1 (−/−) zebrafish that lack T and B cells. In addition, we developed a pioneering adult zebrafish model, in which an immunosuppressive radiation treatment was used for reactivation of the latent disease. With this model, various aspects of the currently poorly characterized process of latency, dormancy and reactivation can be studied in a simple vertebrate system.

As a first step, we had to be able to induce a non-progressive, but persistent, infection in adult zebrafish. Based on previous work in adult zebrafish, the severity of the disease is dependent on both the dose and the strain [10,35,36]. The type strain of *M. marinum* (ATCC 927) has previously been reported to produce a moderate infection in zebrafish, but previously only high doses have been used [35]. In our hands, a low dose of this strain delivered as an injection (i.p.) was found to be the most reliable means of inducing a latent infection. In addition to injecting, bathing in water infested with different concentrations of mycobacteria was also tested. Although bathing could provide a more natural route of infection through the gills or the gut, the low incidence rate achieved by this method made it unsuitable for this study. As our scope is to study latency and reactivation and not the natural course of initial colonization, i.p. injection was considered applicable for our purposes.

The non-progressive status of the experimental infection could be verified by quantifying bacterial loads in the fish using an in-house-developed qPCR assay, and by quantifying granulomas in full-length longitudinal sections. Most fish did not show any signs of disease, and the average bacterial burdens as well as the number of granulomas and affected organs cease to grow after 4 weeks of infection remaining at a static level in the majority of individuals. This essentially demonstrates the central features of the latent disease. The disease is present in the host and has the potential to reactivate under appropriate circumstances. A centrally important feature of our model is that the non-progressive state developed naturally between the host and the mycobacteria without further intervention, and lasted for the entire duration of the 8-month study in 75% of the individuals.

The results gained with the quantitative PCR method in our model showed that the total number of mycobacteria ceased to increase after the first weeks of infection and remained stable for the entire duration of the study. Bacteria entering a non-replicating, dormant state would be a reasonable explanation for the non-progressive bacterial burdens; which is also thought to happen in human TB. To examine whether the bacteria entered a dormant state in our model system, we carried out *ex vivo* plating experiments. Comparing the efficacy of *ex vivo* growth in liquid broth and solid plate has been previously used for showing dormant *M. tuberculosis* populations in chronically infected mice [37]. We used an alternative, specific method using resuscitation promoting factor (Rpf) from *Micrococcus luteus*. Rpf has been shown to resuscitate dormant *M. luteus* but also various mycobacterial species [24]. Homologous proteins with the same function have thereafter also been found to be present in actively dividing mycobacterial cultures [38], and the functions of these muralytic enzymes has been extensively studied in mycobacterial species [39]. Mutant *M. tuberculosis* strains without functional Rpfs have been shown to be less virulent and unable to reactivate *in vivo* [40,41].

Using *M. luteus* Rpf on solid plates, we found that the majority of the bacteria in most fish with a latent infection were actually in a dormant, viable but not culturable state, and could be resuscitated by the addition of Rpf. The resuscitable population of dormant mycobacteria seen in latent wt fish was absent in rag1 (−/−) fish lacking functional adaptive immunity. Also, the expression level of the known dormancy-associated enzyme, citrate synthase (*GltA1*), in wt fish was 87-fold higher than in the rag1 (−/−) fish, indicating that effective induction of mycobacterial dormancy is mediated by adaptive immune responses. The presence of Rpf on plates did not increase the number of culturable mycobacteria in samples representing the active phases of infection; namely the primary active disease with a low dose, a progressive disease with a high dose and the reactivated infection. These results suggest that dormancy of a high proportion of the total mycobacterial population is associated with the latent disease. In this study, there was variation in all the measured parameters within the experimental grou25ps with latent infection. This variation is most likely explained by differences in disease progression between individuals within the latent groups. Similar wide disease spectrum is thought to be present also in the human latent TB [2,3]. To characterize the underlying factors leading to this typical variation in disease outcomes, it would be beneficial to follow the disease progression in individuals instead of heterogeneous groups in studies using *in vivo* models of TB.

The early cytokine responses (*TNFα, IL-6, IL-1β, IL-12*) were measured on the first day of low-dose or high-dose infection. The high dose generally evoked a stronger pro-inflammatory response, which may have contributed to the high mortality in the beginning of the infection. Conversely, the low-dose infection seemed to avoid evoking strong responses. Of the measured cytokines, only *IL-6* was induced. IL-6 has been reported to be important in restricting mycobacterial growth [42] and in efficient protection by vaccination against TB in mice [43], and as such, may have had a role in the initiation of a latent disease in the zebrafish.

The differences in the disease progression were further studied at later time-points, where *Nos2b* and *IFNγ1-2* expression levels were measured. According to current hypothesis, IFNγ induces Nos2 in macrophages activating them to more efficiently destroy intracellular mycobacteria [44–46]. In our zebrafish model, *Nos2(b)* was clearly induced with both the low and the high dose at 2–7 wpi. In the high-dose infection group, the induction at 2 weeks was as high as ~1500-fold compared to baseline levels. Despite this strong induction, most of the fish succumbed to infection, perhaps due to insufficient phagocytic capacity. At the same time, *Nos2b* was not induced in rag1−/− fish at 2 wpi, and the bacterial burdens were already significantly higher than in the wt low dose animals. Based on this, adaptive responses mediate the *Nos2b* induction and are required for the restriction of mycobacterial growth already at this stage. However, the adaptive mechanism behind this induction in the mycobacterial disease in the zebrafish remains obscure, as *IFNγ1-2* was not induced at 2 weeks in the low-dose infected wt fish. Later on, at 4 and 7 wpi, an induction of Nos2b was also seen in rag1 (−/−) fish, indicating that the innate arm of immunity alone, to some extent, can induce the production of nitric oxide as a response to the high bacterial numbers.

According to the latest hypotheses on latent TB, the grand scheme is complex with various co-existing populations of mycobacteria in different niches and metabolic states. Some of these populations have been suggested to constantly probe the environment in search of prospects for reactivation (e.g. immunodeficiency), whereas others are in a less active state, waiting for resuscitation signals from the probing population. The proportion of bacteria in each population determines the disease status. Likely, a fully functional immune system is able to keep this small active population in line. In case of immunosuppression, the active population replicates and excretes resuscitation factors, leading to

reactivation of the dormant population [23]. Our findings in the zebrafish model support this elegant hypothesis.

Latent mycobacterial infection models have previously been set up in the rabbit [20], in the mouse [47,48], in the guinea pig [49] and in the macaque [21]. Some evidence on bacterial dormancy exists in the chronic disease of vaccinated mice [37]. The rabbit and macaque models were induced with a low bacterial inoculate similarly to our zebrafish model, whereas the mouse and guinea pig models utilize chemotherapeutics. The historical Cornell's model of latency in the mouse is artificially induced by antibiotic treatment. After the antibiotics are removed, a spontaneous reactivation occurs [47]. Without antibiotic treatment, the bacterial loads continue to increase, eventually leading to the death of the mouse. Others have utilized streptomycin auxotrophic strains of *M. tuberculosis* whose growth can be arrested in the absence of streptomycin, resulting in a paucibacillary state [48,49]. However, in our zebrafish model, the infection is induced with a naturally replicating strain and generally results in a latent disease without any antibiotic treatment. Thus, it is likely that the mycobacterial infection in the zebrafish more accurately models the natural course of infection that is determined by the interplay between the pathogen and the immune response of the host. In our model, as many as 75% of the fish survived the 8-month period and managed to restrict further bacterial growth, suggesting that a latent-type disease developed. The percentage of latent-type cases was much higher in zebrafish than in the macaque model (40%) [21]. In humans, 90–95% of TB cases are subclinical [4].

Having established a potential model for latent TB, we next set up a method for reactivation *in vivo*. So far, reactivation has only been established in non-human primate models in the context of simian immunodeficiency virus (SIV) [50], in a rabbit model with dexamethasone [20] and in a murine model with aminoguanidine [51]. Even though these models are likely to replicate the human TB-HIV co-infection and glucocorticoid-induced reactivation, respectively, the zebrafish could provide a useful and ethical model for large-scale experiments on reactivation. To our knowledge, irradiation has not been previously used for inducing reactivation of latent mycobacterial infections.

First, we tested whether irradiation could be used for the reactivation of the latent disease. Surprisingly, despite irradiation killing almost all lymphocytes and half of the granulo/monocytes, a single dose (25 Gy) was found to be insufficient for a general reactivation of the mycobacterial disease during the one-month follow-up period. This could be due to the combined effect of the rapid recovery of the leukocyte population after irradiation [52] and the low growth rate of mycobacteria. In adult zebrafish, leukocyte numbers have been reported to recover to pre-irradiation levels in 2 weeks after a 20 Gy dose [52]. However, when the 25 Gy was administered to latently infected fish twice, with one month between the doses, the desired effect on the mycobacterial disease was achieved. Mortality increased significantly compared to latently infected controls and similarly irradiated healthy fish. A descriptive histological analysis of moribund individuals also revealed vast areas of free bacteria outside granulomas. The mycobacterial loads in twice irradiated fish with end-stage infection had increased by ~100-fold compared to stable state levels. The kinetics of the bacterial outgrowth in these fish is in harmony with theoretical calculations of unrestricted bacterial growth. Leukocyte numbers have been reported to reach the lowest level 6–7 days after 20 Gy of radiation [52]. At this point, the bacteria should be able to grow without limitation. In liquid culture at 29°C, the *M. marinum* used in our laboratory doubles its numbers in 24 hours and thus a 100-fold increase would require ~7 days. Indeed, in the reactivation group, a steep drop in survival after 16 days concomitant with high bacterial loads was seen. Based on these results, the zebrafish model for the reactivation of a mycobacterial disease appears highly promising.

Radiation treatments, as is well known, have various biological effects. When considering irradiation as a method for reactivating a mycobacterial infection, some of these effects need to be discussed. Firstly, the dose used in this study (25 Gy) is high and would be lethal for mammals. Zebrafish seem to be relatively resistant to the acute adverse effects caused by irradiation, as the treatment *per se* did not cause mortality. The lethal dose for adult zebrafish has been reported to be as high as 40 Gy, possibly due to the smaller genome and the lower body temperature compared to mammals [52]. For reactivation purposes, the 25 Gy dose was administered twice, which led to efficient reactivation of the mycobacterial disease, but also caused a 40% mortality *per se*, which is slightly less than the mortality caused by a single dose of 30 Gy [52]. Secondly, γ-radiation is likely to have direct effects on *M. marinum*. An aspect to be considered in the context of the reactivation model is the possibility of causing mutations in the bacterial genome, in addition to affecting the immune cell numbers of the host. *In vitro* studies have previously shown that *M. tuberculosis* is twice as radioresistant as *E. coli* [26]. Still, with doses above 1 Gy the viability of *M. tuberculosis* is adversely affected in a dose-dependent manner [26]. This has probably been the basis for the historical X-ray treatment *against* TB. Of note, also mutations advantageous to the bacteria can occur, and can be enriched in the population if a selection pressure, such as antibiotics, is applied. In our experiments, however, there was no selection pressure, but rather the pressure from the host's side was transiently relieved. Based on our FCM data, the dampened immune suppression of the host, rather than an advantageous mutation in mycobacteria, is likely to be the trigger for reactivation. Still, as a precaution, special measures should be taken to prevent the release of irradiated mycobacteria into the environment.

In conclusion, we have set up a system in which a latent mycobacterial disease can be established and assessed in adult zebrafish. The majority of the bacteria present in zebrafish enter a dormant state, with a smaller bacterial population remaining active. We were also able to induce a transition from this stable state to a progressive mode using repeated γ-irradiation mimicking immune suppressive states that cause human TB to reactivate. The reactivated infection is characterized by the absence of dormant mycobacterial population, similarly to the active primary disease preceding latency. Currently, there is no vaccine that would give proper protection against the reactivation of the latent disease. Gamma radiation induced reactivation should be an applicable model for testing new vaccine candidates, as the T cells required for protective immunity against TB are resistant to γ-radiation [53]. Thus, this proof-of-concept model for the reactivation of latent TB in a non-mammalian vertebrate shows high promise as a tool for large-scale studies on the related mechanisms.

Materials and Methods

Zebrafish lines and maintenance

For most experiments, adult (5–8 month-old) wild-type AB zebrafish were used. In addition, adult, rag1 (−/−) hu1999 mutant fish (from ZIRC) were used. For the FACS analysis, transgenic lines Tg(lck:lck-EGFP)^cz2 and Tg (rag2:GFP)^zdf8 (from ZIRC) were also used. Fish were kept in a flow-through system with a light/dark cycle of 14 h/10 h and were fed with SDS 400 food twice daily.

Ethics statement

All experiments have been accepted by the Animal Experiment Board in Finland (under the Regional State Administrative Agency for Southern Finland) and were carried out in accordance with the EU-directive 2010/63/EU on the protection of animals used for scientific purposes and with the Finnish Act on Animal Experimentation (62/2006).

Licence for the zebrafish facility: LSLH-2007-7254/Ym-23, Licence for experiments: ESLH-2008-07610/Ym-23 and 20.10.2010 ESAVI-2010-08379/Ym-23.

Experimental infection

M. marinum (ATCC 927) was cultured similarly as described in [10] with the following modifications: culture at 29°C, concentration of Tween 80 0.2%. Bacteria were first cultured on plates for 1 wk, transferred into liquid medium for 4 d, diluted once ~1:10, cultured to an OD600 of 0.495–0.680, collected by centrifugation and diluted appropriately with sterile 0.2 M KCl +0.3 mg/ml phenol red (Sigma-Aldrich). For qPCR experiments PBS without phenol red was used. The fish were briefly anesthetized in 0.02% 3-aminobenzoic acid ethyl ester (pH 7.0) (Sigma-Aldrich) and intraperitoneally (i.p.) injected with 5 µl using an Omnican 100 30 G insulin needle (Braun, Melsungen, Germany). To verify the bacterial dose, samples of bacterial dilutions were taken while infecting, diluted when needed and plated onto 7H10 plates. The low dose was 34±15 cfu and the high dose 2029±709 cfu. In survival experiments, humane end point criteria approved by a national ethical board were followed. If any of the following criteria were fulfilled, the animals were euthanized: lack of response to touch, abnormal swimming, gasping, observable swelling, observable waisting or loss of scales.

Histology

Fish were euthanized by incubation in 0.04% 3-aminobenzoic acid ethyl ester (Sigma-Aldrich) pH 7.0. Heads and tails were removed and the fish were fixed in 10% phosphate buffered formalin pH 7.0 for 5–11 days at RT. After 1 week of decalcification with 20% EDTA-citrate pH 7.2 samples were rinsed with tap water, transferred through an ethanol series with increasing concentrations, put into xylene and longitudinally embedded in paraffin. 5 µm sections were cut; every 40th section was placed on a slide. The fish were sectioned thoroughly so that the entire kidney tissue lining the spine was included. The slides were stained with Ziehl-Neelsen staining and analyzed using the 200× magnification of an Olympus BX51 microscope. For Mallory's trichrome staining standard methods were used.

qPCR

DNA extraction from mycobacteria: For determination of the bacterial load, the peritoneal cavity of the euthanized fish was emptied. The organs were put into weighed metal bead containing homogenization tubes (Mobio, California, USA) and frozen at −80°C. The mass of the organ sample was determined. The self-prepared modified enzymatic lysis buffer MELB (20 mM Tris-HCl pH 8.0, 20 mM sodium EDTA pH 8.0, 1.2% Triton X 100) was added to the samples, which were homogenized in a volume of 575 µl using the PowerLyzer24 (Mobio) at speed 3,200 for 3×20 second cycles with 30 second pauses. An appropriate proportion (sample mass <25 mg) of the homogenate was taken for DNA extraction. The samples were sonicated in an m08 water bath sonicator (Finnsonic, Lahti, Finland) for 9 min. Lysozyme (Sigma-Aldrich) was added to a final concentration of 20 mg/ml and incubated at 37°C for 2 h. After incubation, MELB was added to the samples to equalize the volume of all samples to 180 µl. From this point on the QIAGEN DNeasy Blood & Tissue Kit manufactures protocol for DNA extraction from gram-positive bacteria was used. The DNA was eluted twice with a volume of 200 µl.

RNA-DNA co-extraction from infected zebrafish: Organs were collected as above, and homogenized in tubes with ceramic beads, 3200 rpmi, 3×40 s in 1.5 ml of TRI reagent (MRC, OH, USA). RNA extraction was carried out according to the manufacturer's protocol. DNA was extracted from the same sample for determination of the mycobacterial load by adding back extraction buffer (1:1) (4 M guanidine thiocyanate (Sigma-Aldrich), 50 mM sodium citrate, 1 M Tris) on top of the lower phase after phenol-chloroform phase separation. DNA was thereafter precipitated with isopropanol, washed with ethanol twice and dissolved in sterile ddH_2O.

Primers were designed for the *M. marinum* 16S–23S ITS sequence: F: 5′-caccacgagaaacactccaa-3′ R: 5′-acatcccgaaaccaa-cagag-3′. For quantification of mycobacterial load SENSIFAST NO-ROX SYBR was used. The final reaction solution had the following composition: 1× SENSIFAST NO-ROX SYBR GreenPCR Master Mix (stock 2×), 0.4 µM MMITS1 forward primer, 0.4 µM MMITS1 reverse primer 3 µl of template. Duplicate or triplicate dilutions were made for each sample. A standard curve was made by extracting the total DNA from a known amount of bacteria (logarithmic culture) and 10-fold using serial dilutions. DNA extracted from three healthy fish were included in order to determine the background signal. The qPCR was carried out using the BIO-RAD CFX96 cycler with the following settings: 1. 3 min 95°C, 2. 5 s 95°C, 3. 10 s 65°C, 4. 5 s 72°C, 5. 39 cycles from 2. to 4. 6. Melting curve 55–95°C at 0.5 intervals.

For q-RT-PCR, primer sequences can be found in the Supporting Information (Text S2). For gene-expression measurements, Bio-Rad iScript One-Step RT-PCR Kit with SYBR Green was used according to the manufacturer's instructions. The optimal annealing temperature of each primer pair were determined using melting curve analysis and agarose gel electrophoresis. The expression of *glyceraldehyde 3-phosphate dehydrogenase* (*GAPDH*, ZDB-GENE-030115-1) was used for normalization of the host genes. The results from mycobacterial dormancy genes were normalized to the bacterial load measured from the corresponding DNA sample.

Bio-Rad CFX Manager software and GraphPad Prism 5.02 were used in the analysis. Using the standard curve, a concentration in units of bacterial genome copies was obtained for every sample. The bacterial load per fish (the visceral organs) could be calculated: (qPCR result (bact./µl of template) x qPCR sample dilution factor Y x total DNA eluate volume (µl) x homogenate dilution factor X). The limit of detection with the qPCR method was estimated to be ~10^3 cfu/fish.

Plating on antibiotic plates +/− Rpf

For production of secreted Rpf for resuscitation of dormant mycobacteria, *Micrococcus luteus* was cultured. An inoculate from a glycerol stock of *M. luteus* was revived in 10 ml of LB liquid medium at 37°C o/n in rotation (to an OD605 = 0.100). A 100 ml volume of lactate minimal medium, LMM (composition described in [54] with the exception of a lower concentration of lactate (0.5% w/v) [24] was inoculated with 4 ml of the o/n culture and was cultured aerobically in rotation (150 rpm) at 30°C for 4 days to an OD605 = 0.705. After centrifugation (10,000 g, 3 min) the supernatant was sterile filtered and aliquots were stored at −80°C. For Rpf plating an aliquot was thawed and 500 µl was absorbed

on each 7H9 antibiotic plates. On –Rpf plates, 500 µl of fresh, sterile LMM was absorbed. The concentrations of antibiotics on plates were as described in [55] and 20 µg/ml azithromycin (Sigma-Aldrich). Fish were homogenized with the same settings as for DNA extractions from mycobacteria in sterile PBS supplemented with 0.5% Tween 80 (v/v). Dilutions were plated +/− Rpf and incubated in the dark at 25°C for 15–17 days. *M. marinum* colonies were counted and the average load of culturable bacteria was determined. As controls, active logarithmic *M. marinum* broth cultures and old stationary *M. marinum* broth cultures that had been kept in closed bottles at +29°C for 5–8 months were plated +/− Rpf and cultured as described above.

Immunosuppression

Irradiation with 25 Gy was carried out with Gammacell 1000 irradiator in glass flasks with 5 fish/80 ml of water. In the reactivation experiments, low-dose infected fish were irradiated twice with one month between the doses. Non-infected controls were similarly irradiated.

Flow cytometry (FCM)

Nine days after irradiation, fish were euthanized and the kidneys were collected and placed into PBS supplemented with 1% fetal calf serum (FCS) on ice. In the first experiment (1 wk post irradiation) kidneys from each group of fish (4/group) were pooled. Fish were analyzed individually in the second one (5 weeks post 1.irradiation). Also kidneys from untreated groups of the same fish lines were similarly collected in order to determine a baseline. Kidneys were homogenized by pipetting the entire volume (1 ml) up and down 15 times. The samples were also filtered before analysis. Immune cell populations were determined using a FACSCantoII (Beckton Dickinson) and the FACSDiva software. The results were analyzed using FlowJo (Treestar Inc, Ashland, OR). Lymphocytes, blood cell precursors, erythrocytes and granulo/monocytes were identified based on the cellular granularity (SSC-A) and size (FSC), (see Figure S2) according to [56]. In addition, reporter fish lines Lck-GFP (T lymphocytes) and RAG-GFP (B and T lymphocytes) we used in some experiments to further confirm the identity of the immune cell populations. Total 30,000 events per sample were collected for analysis.

Statistical analysis

Statistical analysis was carried out using the GraphPad Prism software (5.02). For determination of statistical significance of differences in bacterial loads, number of granulomas, affected organs and leukocyte counts and gene-expression data, a non-parametric one-tailed Mann-Whitney test was used. In survival experiments, the log-rank Mantel-Cox test was used. In Rpf experiments, the plates with the same sample +/− Rpf were compared pair-wise, and a one-tailed paired t-test was used. P-values$<$0.05 were considered significant.

List of genes mentioned in the article

Zebrafish (*Danio rerio*):
Nos2b: ZDB-GENE-080916-1
IFNγ1-2: ZDB-GENE-040629-1
TNFα: ZDB-GENE-050317-1
IL-1β: ZDB-GENE-040702-2
IL-6: ZDB-GENE-120509-1
IL-12: ZDB-GENE-060724-1
GAPDH: ZDB-GENE-030115-1
M. marinum:
GltA1: MMAR_1381
HspX: MMAR_3484
DevR: MMAR_1516
GltA1: MMAR_1381
Tgs1: MMAR_1519

Supporting Information

Figure S1 qPCR and plating give similar results. Dilutions (1, 1:10, 1:1000) of mycobacterial culture (logarithmic growth phase) were added onto healthy fish organ samples. The amount of bacteria added was determined by plating dilutions of the culture (result shown as white bars). The samples were homogenized and the DNA was extracted. The bacterial concentration was determined by qPCR (result shown as black bars).
(TIF)

Figure S2 A single 25 Gy dose of gamma radiation is not sufficient for reactivation of latent tuberculosis. Latently infected adult zebrafish (n = 39) were γ-irradiated (25 Gy). Latently infected, non-irradiated zebrafish (n = 25) were used as controls. The effects of the irradiation were controlled by irradiating non-infected fish (n = 30). (A) Survival was followed for 28 days. * P$<$0.05 (B) To determine the bacterial load, 5 fish were collected 2 weeks after irradiation. Similarly infected non-irradiated controls were also collected.
(TIF)

Figure S3 Gamma irradiation depletes the lymphocyte population in adult zebrafish. 4 groups (1 Tg(rag2-GFP). 1 Tg(lck:lck-egfp) and 2 wt groups) of 4 adult zebrafish were γ-irradiated with 25 Gy or left untreated. Kidneys were collected 9 d post irradiation, pooled and analyzed by FCM. FSC-SSC –plots were gated based on [56] as follows: E = erythrocytes, G/M = granulocytes & monocytes, L = lymphocytes, P = blood cell precursors. The numbers by the gates show the percentage of cells within the gate of the total live population. For GFP-expressing lines (rag2 and lck) a GFP gate was also used. The GFP positive populations were reanalyzed on a FSC-SSC -plot. The lymphocyte population was most severely affected by irradiation, whereas the number of granulo/monocytes decreased less. An increase in the proportion of blood cell precursors was detected. A reanalysis of the GFP results verified that the GFP-expressing cells were mostly present within the lymphocyte gate.
(TIF)

Text S1 A qPCR-assay for quantifying of *M. marinum* load in adult zebrafish tissues.
(DOC)

Text S2 Sequences of the Q-RT-PCR primers used in the study.
(DOC)

Acknowledgments

We thank Leena Mäkinen, Matilda Martikainen, Annemari Uusimäki, Ilmari Tamminen, Pirjo Kerola, Hanna-Mari Seppälä, Sanna Hämäläinen and Hanna Nisula for technical assistance.

Author Contributions

Conceived and designed the experiments: M. Parikka, M.M. Hammarén, M. Rämet, A. Iivanainen. Performed the experiments: M.M. Hammarén, M. Parikka, S.-K.E. Harjula, N.J.A. Halfpenny, K.E. Oksanen, M.J. Lahtinen, E.T. Pajula. Analyzed the data: M.M. Hammarén, M. Parikka, M. Pesu. Contributed reagents/materials/analysis tools: M. Rämet, M. Parikka, M. Pesu. Wrote the paper: M.M. Hammarén, M. Parikka.

References

1. Butler D (2000) New fronts in an old war. Nature a-z Index 406: 670–672.
2. Barry CE, Boshoff HI, Dartois V, Dick T, Ehrt S, et al. (2009) The spectrum of latent tuberculosis: Rethinking the biology and intervention strategies. Nat Rev Microbiol 7: 845–855.
3. Robertson BD, Altmann D, Barry C, Bishai B, Cole S, et al. (2012) Detection and treatment of subclinical tuberculosis. Tuberculosis. E-pub ahead of print.
4. Lin PL, Flynn JAL (2010) Understanding latent tuberculosis: A moving target. J Immunol 185: 15–22.
5. Russell DG, Barry 3rd CE, Flynn JAL (2010) Tuberculosis: What we don't know can, and does, hurt us. Science 328: 852–856.
6. Behr MA, Small PM (1997) Has BCG attenuated to impotence? Nature 389: 133–134.
7. Andersen P (2007) Tuberculosis vaccines—an update. Nat Rev Microbiol 5: 484–487.
8. Flynn JAL (2006) Lessons from experimental mycobacterium tuberculosis infections. Microb Infect 8: 1179–1188.
9. Davis J, Clay H, Lewis JL, Ghori N, Herbomel P, et al. (2002) Real-time visualization of mycobacterium-macrophage interactions leading to initiation of granuloma formation in zebrafish embryos. Immunity 17: 693–702.
10. Swaim LE, Connolly LE, Volkman HE, Humbert O, Born DE, et al. (2006) Mycobacterium marinum infection of adult zebrafish causes caseating granulomatous tuberculosis and is moderated by adaptive immunity. Infect Immun 74: 6108–6117.
11. Lesley R, Ramakrishnan L (2008) Insights into early mycobacterial pathogenesis from the zebrafish. Curr Opin Microbiol 11: 277–283.
12. van der Sar AM, Appelmelk BJ, Vandenbroucke-Grauls CMJE, Bitter W (2004) A star with stripes: Zebrafish as an infection model. Trends Microbiol 12: 451–457.
13. Decostere A, Hermans K, Haesebrouck F (2004) Piscine mycobacteriosis: A literature review covering the agent and the disease it causes in fish and humans. Vet Microbiol 99: 159–166.
14. Tobin DM, Ramakrishnan L (2008) Comparative pathogenesis of mycobacterium marinum and mycobacterium tuberculosis. Cell Microbiol 10: 1027–1039.
15. Stinear TP, Seemann T, Harrison PF, Jenkin GA, Davies JK, et al. (2008) Insights from the complete genome sequence of mycobacterium marinum on the evolution of mycobacterium tuberculosis. Genome Res 18: 729.
16. Cosma CL, Humbert O, Ramakrishnan L (2004) Superinfecting mycobacteria home to established tuberculous granulomas. Nat Immunol 5: 828–835.
17. Clay H, Davis J, Beery D, Huttenlocher A, Lyons SE, et al. (2007) Dichotomous role of the macrophage in early mycobacterium marinum infection of the zebrafish. Cell Host Microbe 2: 29–39.
18. North RJ, Jung YJ (2004) Immunity to tuberculosis. Immunology 22: 599–623.
19. Cosma CL, Sherman DR, Ramakrishnan L (2003) The secret lives of the pathogenic mycobacteria. Microbiology 57: 641–676.
20. Manabe YC, Kesavan AK, Lopez-Molina J, Hatem CL, Brooks M, et al. (2008) The aerosol rabbit model of TB latency, reactivation and immune reconstitution inflammatory syndrome. Tuberculosis 88: 187–196.
21. Capuano III SV, Croix DA, Pawar S, Zinovik A, Myers A, et al. (2003) Experimental mycobacterium tuberculosis infection of cynomolgus macaques closely resembles the various manifestations of human M. tuberculosis infection. Infect Immun 71: 5831–5844.
22. Wienholds E, Schulte-Merker S, Walderich B, Plasterk RHA (2002) Target-selected inactivation of the zebrafish rag1 gene. Science 297: 99.
23. Chao MC, Rubin EJ (2010) Letting sleeping dos lie: Does dormancy play a role in tuberculosis? Annu Rev Microbiol 64: 293–311.
24. Mukamolova GV, Kaprelyants AS, Young DI, Young M, Kell DB (1998) A bacterial cytokine. Proc Natl Acad Sci U S A 95: 8916–8921.
25. Deb C, Lee CM, Dubey VS, Daniel J, Abomoelak B, et al. (2009) A novel in vitro multiple-stress dormancy model for mycobacterium tuberculosis generates a lipid-loaded, drug-tolerant, dormant pathogen. PLoS One 4: e6077.
26. Zack MB, Stottmeier K, Berg G, Kazemi H (1974) The effect of radiation on microbiologic characteristics of M tuberculosis. Chest 66: 240–243.
27. Havlir DV, Barnes PF (1999) Tuberculosis in patients with human immunodeficiency virus infection. N Engl J Med 340: 367–373.
28. Stevenson CR, Forouhi NG, Roglic G, Williams BG, Lauer JA, et al. (2007) Diabetes and tuberculosis: The impact of the diabetes epidemic on tuberculosis incidence. BMC Public Health 7: 234–241.
29. Jick SS, Lieberman ES, Rahman MU, Choi HK (2006) Glucocorticoid use, other associated factors, and the risk of tuberculosis. Arthritis Rheum 55: 19–26.
30. Alexander DC, Liu J (2006) Mycobacterial genomes. In: Chan VL, Cherman PM, Bourke B, editors. Bacterial genomes and infectious diseases. Totowa, NJ: Humana Press Inc. pp 151.
31. Lin MY, Reddy T, Arend SM, Friggen AH, Franken KLMC, et al. (2009) Cross-reactive immunity to mycobacterium tuberculosis DosR regulon-encoded antigens in individuals infected with environmental, nontuberculous mycobacteria. Infect Immun 77: 5071–5079.
32. Ehlers S (2009) Lazy, dynamic or minimally recrudescent? on the elusive nature and location of the mycobacterium responsible for latent tuberculosis. Infection 37: 87–95.
33. Hernandez-Pando R, Jeyanathan M, Mengistu G, Aguilar D, Orozco H, et al. (2000) Persistence of DNA from mycobacterium tuberculosis in superficially normal lung tissue during latent infection. The Lancet 356: 2133–2138.
34. Neyrolles O, Hernández-Pando R, Pietri-Rouxel F, Fornès P, Tailleux L, et al. (2006) Is adipose tissue a place for mycobacterium tuberculosis persistence? PLoS One 1: e43.
35. Watral V, Kent ML (2007) Pathogenesis of mycobacterium spp. in zebrafish (danio rerio) from research facilities. Comp Biochem Physiol C Toxicol Pharmacol 145: 55–60.
36. Prouty MG, Correa NE, Barker LP, Jagadeeswaran P, Klose KE (2003) Zebrafish-Mycobacterium marinum model for mycobacterial pathogenesis. FEMS Microbiol Lett 225: 177–182.
37. Dhillon J, Lowrie D, Mitchison D (2004) Mycobacterium tuberculosis from chronic murine infections that grows in liquid but not on solid medium. BMC Infect Dis 4: 51–54.
38. Mukamolova GV, Turapov OA, Young DI, Kaprelyants AS, Kell DB, et al. (2002) A family of autocrine growth factors in mycobacterium tuberculosis. Mol Microbiol 46: 623–635.
39. Kana BD, Mizrahi V (2010) Resuscitation-promoting factors as lytic enzymes for bacterial growth and signaling. FEMS Immunol Med Microbiol 58: 39–50.
40. Russell-Goldman E, Xu J, Wang X, Chan J, Tufariello JAM (2008) A mycobacterium tuberculosis rpf double-knockout strain exhibits profound defects in reactivation from chronic tuberculosis and innate immunity phenotypes. Infect Immun 76: 4269–4281.
41. Kondratieva T, Rubakova E, Kana BD, Biketov S, Potapov V, et al. (2011) Mycobacterium tuberculosis attenuated by multiple deletions of rpf genes effectively protects mice against TB infection. Tuberculosis 91: 219–223.
42. Ladel CH, Blum C, Dreher A, Reifenberg K, Kopf M, et al. (1997) Lethal tuberculosis in interleukin-6-deficient mutant mice. Infect Immun 65: 4843–4849.
43. Leal IS, Smedegård B, Andersen P, Appelberg R (1999) Interleukin-6 and interleukin-12 participate in induction of a type 1 protective T-cell response during vaccination with a tuberculosis subunit vaccine. Infect Immun 67: 5747–5754.
44. MacMicking JD, North RJ, LaCourse R, Mudgett JS, Shah SK, et al. (1997) Identification of nitric oxide synthase as a protective locus against tuberculosis. Proc Natl Acad Sci U S A 94: 5243–5248.
45. Chan J, Xing Y, Magliozzo R, Bloom B (1992) Killing of virulent mycobacterium tuberculosis by reactive nitrogen intermediates produced by activated murine macrophages. J Exp Med 175: 1111–1122.
46. Ehrt S, Schnappinger D, Bekiranov S, Drenkow J, Shi S, et al. (2001) Reprogramming of the macrophage transcriptome in response to interferon-γ and mycobacterium tuberculosis. J Exp Med 194: 1123–1140.
47. McCune Jr RM, Tompsett R, McDermott W (1956) The fate of mycobacterium tuberculosis in mouse tissues as determined by the microbial enumeration technique: II. the conversion of tuberculous infection to the latent state by the administration of pyrazinamide and a companion drug. J Exp Med 104: 763–802.
48. Kashino SS, Ovendale P, Izzo A, Campos-Neto A (2006) Unique model of dormant infection for tuberculosis vaccine development. Clin Vaccine Immunol 13: 1014–1021.
49. Kashino SS, Napolitano DR, Skobe Z, Campos-Neto A (2008) Guinea pig model of mycobacterium tuberculosis latent/dormant infection. Microb Infect 10: 1469–1476.
50. Diedrich CR, Mattila JT, Klein E, Janssen C, Phuah J, et al. (2010) Reactivation of latent tuberculosis in cynomolgus macaques infected with SIV is associated with early peripheral T cell depletion and not virus load. PLoS One 5: e9611.
51. Flynn JAL, Scanga CA, Tanaka KE, Chan J (1998) Effects of aminoguanidine on latent murine tuberculosis. J Immunol 160: 1796–1803.
52. Traver D, Winzeler A, Stern HM, Mayhall EA, Langenau DM, et al. (2004) Effects of lethal irradiation in zebrafish and rescue by hematopoietic cell transplantation. Blood 104: 1298–1305.
53. Orme I (1988) Characteristics and specificity of acquired immunologic memory to mycobacterium tuberculosis infection. J Immunol 140: 3589–3593.
54. Kaprelyants A, Kell D (1992) Rapid assessment of bacterial viability and vitality by rhodamine 123 and flow cytometry. J Appl Microbiol 72: 410–422.
55. Cosma CL, Swaim LE, Volkman HE, Ramakrishnan L, Davis JM (2006) Zebrafish and frog models of mycobacterium marinum infection. Curr Protoc Microbiol Chapter 10: Unit 10B.
56. Traver D, Paw BH, Poss KD, Penberthy WT, Lin S, et al. (2003) Transplantation and in vivo imaging of multilineage engraftment in zebrafish bloodless mutants. Nat Immunol 4: 1238–1246.

Mycobacterium marinum **causes a latent infection that can be reactivated by gamma irradiation in adult zebrafish.**

Supplementary Figures

Mataleena Parikka[1*], Milka M. Hammarén[1], Sanna-Kaisa E. Harjula, Nicholas J.A. Halfpenny, Kaisa E. Oksanen, Marika J. Lahtinen, Elina T. Pajula, Antti Iivanainen, Marko Pesu, Mika Rämet

[1]Equal contribution

*Email: mataleena.parikka@uta.fi

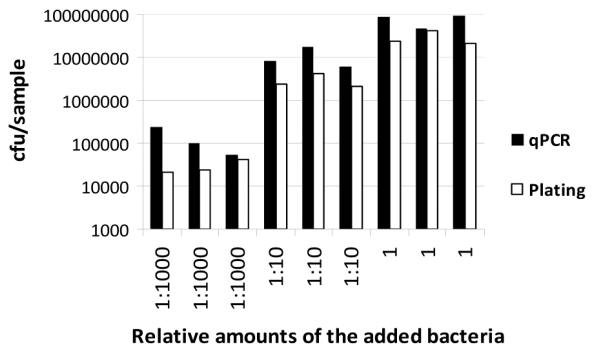

Figure S1

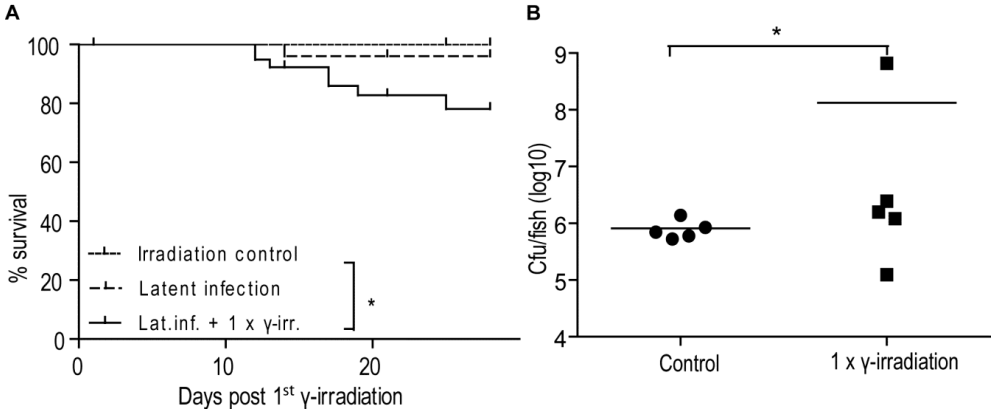

Figure S2

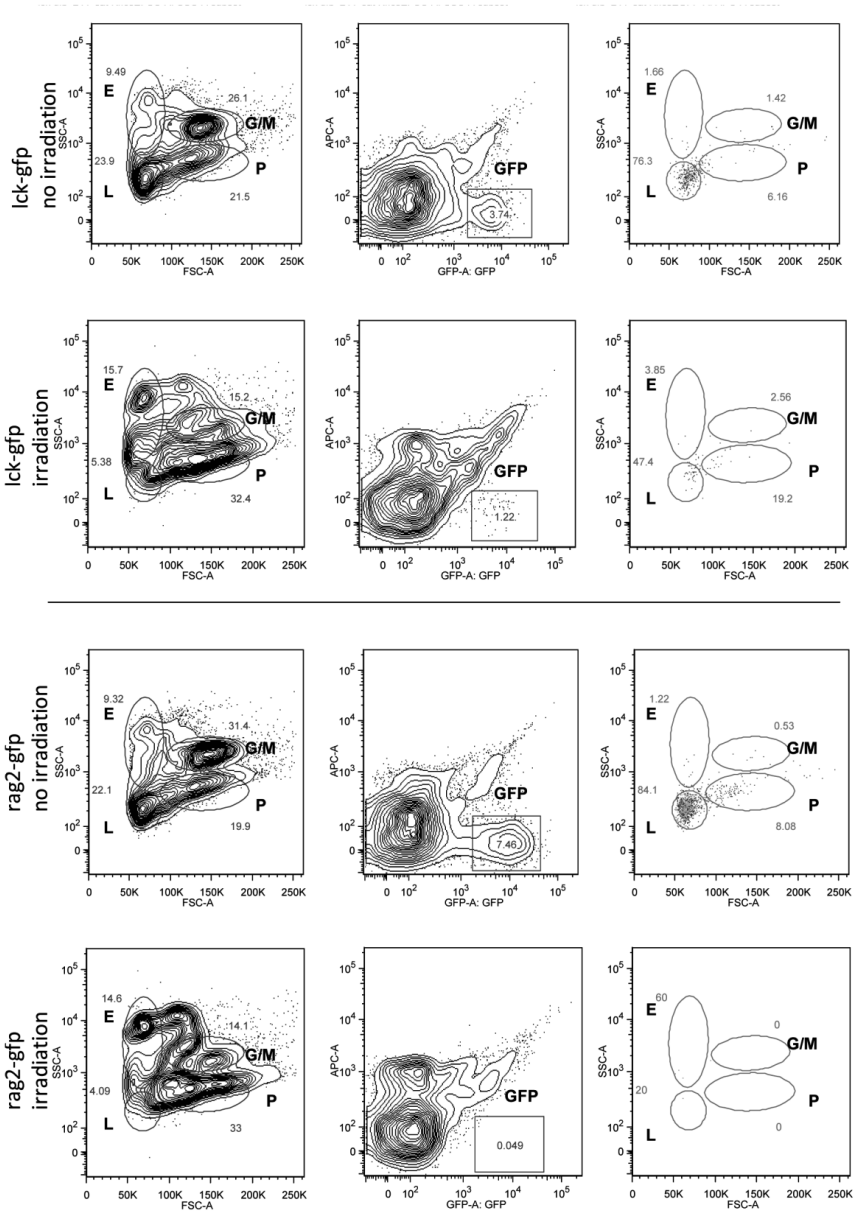
lck-gfp
no irradiation
lck-gfp
irradiation
rag2-gfp
no irradiation
rag2-gfp
irradiation
E
G/M
P
L
GFP
SSC-A
FSC-A
APC-A
GFP-A: GFP
9.49
26.1
23.9
21.5
3.74
1.66
1.42
76.3
6.16
15.7
15.2
5.38
32.4
1.22
3.85
2.56
47.4
19.2
9.32
31.4
22.1
19.9
7.46
1.22
0.53
84.1
8.08
14.6
14.1
4.09
33
0.049
60
0
20
0

Figure S3

PUBLICATION II

Interleukin 10 mutant zebrafish have an enhanced _interferon gamma_ response and improved survival against a _Mycobacterium marinum_ infection

Harjula S-KE, Ojanen MJT, Taavitsainen S, Nykter M, Rämet M.

Scientific Reports. 2018. 8(1):10360.
doi: 10.1038/s41598-018-28511-w.

SCIENTIFIC REPORTS

OPEN

Interleukin 10 mutant zebrafish have an enhanced *interferon gamma* response and improved survival against a *Mycobacterium marinum* infection

Received: 22 August 2017
Accepted: 20 June 2018
Published online: 09 July 2018

Sanna-Kaisa E. Harjula[1], Markus J. T. Ojanen[1,2], Sinja Taavitsainen[3], Matti Nykter[3] & Mika Rämet[1,4,5,6]

Tuberculosis ranks as one of the world's deadliest infectious diseases causing more than a million casualties annually. IL10 inhibits the function of Th1 type cells, and IL10 deficiency has been associated with an improved resistance against *Mycobacterium tuberculosis* infection in a mouse model. Here, we utilized *M. marinum* infection in the zebrafish (*Danio rerio*) as a model for studying Il10 in the host response against mycobacteria. Unchallenged, nonsense *il10*$^{e46/e46}$ mutant zebrafish were fertile and phenotypically normal. Following a chronic mycobacterial infection, *il10*$^{e46/e46}$ mutants showed enhanced survival compared to the controls. This was associated with an increased expression of the Th cell marker *cd4-1* and a shift towards a Th1 type immune response, which was demonstrated by the upregulated expression of *tbx21* and *ifng1*, as well as the down-regulation of *gata3*. In addition, at 8 weeks post infection *il10*$^{e46/e46}$ mutant zebrafish had reduced expression levels of proinflammatory cytokines *tnfb* and *il1b*, presumably indicating slower progress of the infection. Altogether, our data show that Il10 can weaken the immune defense against *M. marinum* infection in zebrafish by restricting *ifng1* response. Importantly, our findings support the relevance of *M. marinum* infection in zebrafish as a model for tuberculosis.

Annually more than 10 million new tuberculosis cases are estimated to emerge, leading to over a million casualties[1]. The immune defense against the pathogen which causes tuberculosis, *Mycobacterium tuberculosis*, requires the elaborate collaboration of both the innate and adaptive immunity, as is demonstrated by the increased disease susceptibility in recipients of TNF-antagonist as well as in HIV-positive individuals[1–3]. Accordingly, deficient, but also excessive, macrophage mediated TNF production as well as the lack of T helper (Th) 1 type cell responses compromise the host's ability to resist a mycobacterial infection and accelerate the disease pathogenesis[4–7].

IL10 is an anti-inflammatory cytokine that was originally identified as a protein secreted by Th2 cells able to inhibit cytokine production in Th1 cells[8,9]. Later, it was discovered that several other cell types, including both immune and nonimmune cells, produce IL10[10]. Genome-wide association studies in humans have linked *IL10* polymorphisms to susceptibility and resistance towards tuberculosis, although the results vary depending on the polymorphism studied and the study subjects[11,12]. Furthermore, *in vivo* mouse studies have shown that IL10 impairs the immune defense against *M. tuberculosis* by impeding host immunity at an early[13,14], but also during later stages of an infection[15]. In these studies, the lack of functional IL10 signaling resulted in enhanced protection

[1]Laboratory of Experimental Immunology, BioMediTech Institute and Faculty of Medicine and Life Sciences, University of Tampere, Tampere, Finland. [2]Laboratory of Immunoregulation, BioMediTech Institute and Faculty of Medicine and Life Sciences, University of Tampere, Tampere, Finland. [3]Laboratory of Computational Biology, BioMediTech Institute and Faculty of Medicine and Life Sciences, University of Tampere, Tampere, Finland. [4]Department of Pediatrics, Tampere University Hospital, Tampere, Finland. [5]Department of Children and Adolescents, Oulu University Hospital, Oulu, Finland. [6]PEDEGO Research Unit and Medical Research Center Oulu, University of Oulu, Oulu, Finland. Correspondence and requests for materials should be addressed to M.R. (email: mika.ramet@uta.fi)

against mycobacteria and was attributed to an increased Th1 response[13–16]. As a consequence, for example, macrophages were more capable of presenting *M. tuberculosis* antigens and recruiting inflammatory cells[13,14]. Enhanced protection was demonstrated by a lower bacterial burden in the lungs and spleen[13–15] and improved survival of the mice[15]. While IL10 deficiency or receptor blockade has been associated with an enhanced protection against mycobacteria in mice, it has also been reported that the lack of IL10 can eventually lead to harmful lung inflammation and to the progression of a mycobacterial disease in the mouse model[16].

The zebrafish is a small teleost, which is constantly gaining popularity as a model organism. The cellular components of the zebrafish immune system, such as mononuclear phagocytes[17], dendritic cells[18], T cells and B cells[19–23] and eosinophils[24] have been described and they resemble those of humans. To date, specific transcription factors expressed by different zebrafish Th as well as Treg cells have also been identified and characterized[25,26]. Previously, lymphocyte marker gene expression has been used to characterize immune response in adult zebrafish[27] and for example *foxp3a* has been validated as a Treg marker[28]. As for the humoral components of the zebrafish immune system, the mammalian homologs of the complement system[29], as well as the immunoglobulin isotypes IgD, IgM and the bony fish specific immunoglobulin Z/T[30] have been found. Overall, the zebrafish is a suitable model for immunological research (reviewed in[31]).

Mycobacterium marinum is a natural pathogen of the zebrafish and a close relative of *Mycobacterium tuberculosis*[32]. Comparably to *M. tuberculosis*, *M. marinum* infects macrophages[33,34] and eventually causes a systemic disease in zebrafish, which shares pathological and histological features with human tuberculosis[35–37]. A *M. marinum* infection model in zebrafish larvae has been widely used to study the innate immune response in a mycobacterial infection, and it enables the real-time visualization and rapid screening of potential tuberculosis drugs[38–40]. Furthermore, the *M. marinum* infection model in adult zebrafish allows studying the adaptive response[35–37].

Zebrafish *il10* has a mammalian-like gene organization and conserved IL10 signature motif[41,42]. Furthermore, Grayfer and Belosevic[43] have found IL10 receptor 1 in zebrafish and in goldfish (*Carassius Auratus* L.). Among their analyses, an alignment of these protein sequences with those of other vertebrates, the expression measurements in different tissues and immune cell populations at mRNA level and *in vitro* binding studies of recombinant goldfish IL10 receptor 1 and IL10 proteins, indicated conservation of the IL10 system throughout evolution. In order to study the role of Il10 in the immune defense against mycobacteria, we have here characterized an $il10^{e46/e46}$ mutant zebrafish strain in relation to a *M. marinum* infection. Also, we aim to gain more information about *M. marinum* infection in zebrafish as a model for human tuberculosis.

Results

A nonsense $il10^{e46}$ mutation creates an early stop codon in the zebrafish *il10* gene. In order to study Il10 in the host response against mycobacteria the zebrafish line e46, carrying a nonsense *il10* mutation, was obtained from the Wellcome Trust Sanger Institute[44]. In the $il10^{e46}$ mutant zebrafish a specific adenosine (A) to thymidine (T) point mutation results in a stop codon (TAA) after the first 27 amino acids in the translated region of exon 1 (Fig. 1a). As nonsense mediated decay degrades mRNA molecules producing non-functional proteins[45], we first studied if the $il10^{e46}$ mutation affects the levels of the *il10* mRNA, and quantified the expression of *il10* in different organs of the abdominal cavity by quantitative PCR (qPCR) (Fig. 1b). However, in any of the studied tissues *il10* mRNA expression did not differ between $il10^{e46/e46}$ mutants and wild type (WT) zebrafish, suggesting that the effects of the mutation are only evident at the translational level. In fact, signal peptide prediction using SignalP 4.1 Server[46] revealed that only five amino acids remain in the truncated protein, which consequently prevents the normal function of Il10 in the fish carrying the homozygous $il10^{e46}$ mutation (Fig. 1a).

Unchallenged $il10^{e46/e46}$ zebrafish are phenotypically normal and have similar blood cell populations and cytokine expression profiles compared to WT fish. IL10 knock-out (KO) mice have growth defects and suffer from chronic intestinal inflammation leading to 30% mortality before 3 months of age[47,48]. Like IL10 KO mouse strains, $il10^{e46/e46}$ zebrafish are fertile and can be maintained by spawning homozygous mutant siblings[47]. However, in contrast to mice, $il10^{e46/e46}$ mutant fish are phenotypically normal and do not have increased mortality compared to WT zebrafish. Our flow-cytometric analysis of the blood cell populations in kidney blood cell isolates revealed no differences in live cell, lymphocyte, myeloid cell or blood cell precursor cell counts in unchallenged $il10^{e46/e46}$ zebrafish compared to the WT control fish (Fig. 2a,b).

Colitis in IL10 KO mice is attributed to the increased production of inflammatory mediators such as TNF and IL1b as well as to a hyper-activated Th1 response[47,49,50]. In order to study signs of inflammation and T cell homeostasis in unchallenged $il10^{e46/e46}$ zebrafish, we extracted RNA from different adult zebrafish tissues and measured the expression levels of selected proinflammatory cytokines (*il1b*, *tnfa* and *tnfb)*, Th cell cytokines *(ifng1* and *il4*) as well as T cell markers *cd4-1* and *cd8a)* and a B cell marker *IgM* (Supplementary Fig. S1). In contrast to the IL10 KO mice, qPCR analysis from the liver and spleen revealed no differences in the relative expression levels of the studied inflammatory markers *tnfa*, *tnfb* and *il1b* between $il10^{e46/e46}$ and WT fish. The expression levels of the Th1 cytokine *ifng1* and the Th2 cytokine *il4* were also comparable between the fish groups. In addition, no differences in the mRNA expression of the T cell marker genes *cd8a* and *cd4-1*, between $il10^{e46/e46}$ and WT fish, were observed. The expression of *IgM* in the liver of $il10^{e46/e46}$ fish was decreased compared to controls ($P = 0.029$). Collectively, these data indicate that the $il10^{e46/e46}$ mutant zebrafish have no apparent immune abnormalities under unchallenged conditions.

In order to study in more detail the possible inflammation in the intestine of the Il10 deficient zebrafish, we collected the intestine from 1-year-old WT and $il10^{e46/e46}$ fish and measured the expression levels of several inflammatory cytokines and immune cell markers (Supplementary Fig. S2a). No difference in the expression of the inflammatory cytokines (*il1b, tnfa* and *tnfb)*, T lymphocyte markers (*cd4-1* and *cd8a)*, B lymphocyte marker *IgM*, Th2 and Treg markers, *(gata3* and *foxp3a*, respectively), or in Th1 and Th2 hallmark cytokines (*ifng1* and *il4*,

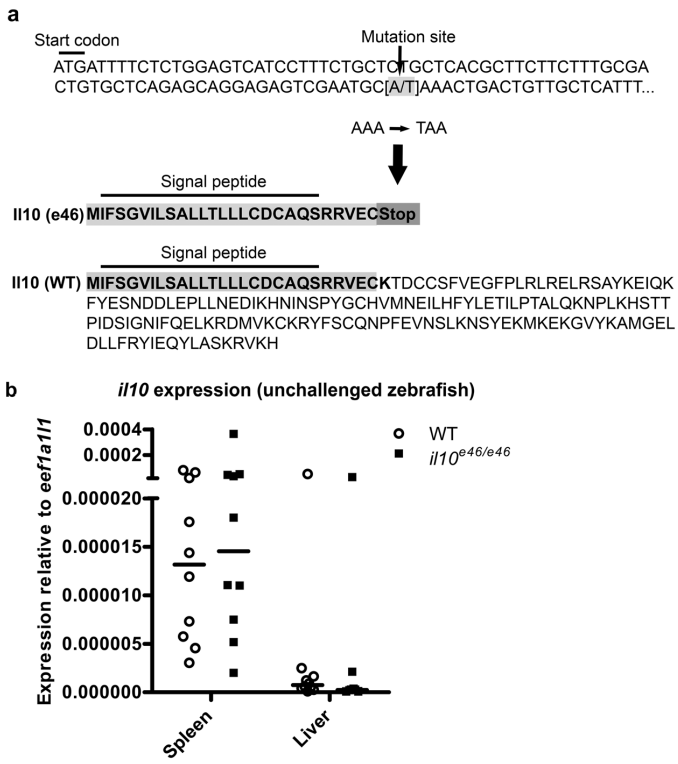

Figure 1. *il10*^{e46} point mutation in the exon 1 of the *il10* results in a premature stop codon but does not alter *il10* expression. (**a**) A schematic presentation of the *il10*^{e46} mutation; a adenosine (A) to thymidine (T) point mutation results in a stop codon (TAA) after the first 27 amino acids in exon 1. (**b**) Relative *il10* expression was measured with qPCR in unchallenged *il10*$^{e46/e46}$ mutant and WT zebrafish, spleen and liver from the same individuals ($n = 10$ in both groups) and is presented as a scatter dot blot and median. Note the divided *y* axis. Gene expressions were normalized to the expression of *eef1a1l1*. A two-tailed Mann-Whitney test was used for the statistical comparison of differences between *il10*$^{e46/e46}$ zebrafish and WT controls.

or in *il10)* was observed between WT and *il10*$^{e46/e46}$ fish. The expression of Th1 cell marker *tbx21* was higher in WT fish compared to *il10*$^{e46/e46}$ mutants ($P = 0.023$) but this is unlikely a sign towards colitis in *il10*$^{e46/e46}$ mutants. Furthermore, the visual appearance of WT and *il10*$^{e46/e46}$ intestine was similar with identifiable intestinal bulb, mid-intestine and posterior-intestine (Supplementary Fig. S2b).

Survival of adult *il10*$^{e46/e46}$ mutants is improved in a low-dose *M. marinum* infection. In mice, the absence of functional IL10 signaling leads to the improved control of a *M. tuberculosis* infection, and consequently, to better survival[13,15]. Other studies have, however, associated IL10 deficiency to increased inflammation leading to reduced survival[16]. To study the role of Il10 in the immune defense against a *M. marinum* infection in zebrafish, we first infected *il10*$^{e46/e46}$ and WT embryos into the yolk at 0–6 hours post fertilization and followed the survival of the larvae for seven days (Fig. 3a). After three days, mortality was observed in both of the groups resulting in ca. 70% mortality at the end of the follow-up with no significant difference between *il10*$^{e46/e46}$ and WT larvae.

Next, we injected a low-dose of *M. marinum* into the abdominal cavity of adult *il10*$^{e46/e46}$ and WT zebrafish and followed the survival of the fish for 20 weeks (Fig. 3b). During the first 8 weeks, we observed ca. 20% mortality in both of the fish groups, which was similar to our previously reported results from a low-dose mycobacterial infection[35,51]. However, from week eight onwards the mortality of the WT fish increased compared to the *il10*$^{e46/e46}$ mutants with an endpoint survival of 44% and 63%, respectively ($P = 0.037$).

In order to differentiate between resistance and tolerance against a *M. marinum* infection, we collected abdominal organ block samples from infected fish during the course of a mycobacterial infection. The samples were taken at 1 day post infection (dpi), 6 dpi, 4 weeks post infection (wpi) and 8/9 wpi, and bacterial amounts were analyzed. In our qPCR based bacterial quantification, detectable amounts of *M. marinum* in the infected zebrafish were primarily observed for the first time at the 6 dpi time point (Fig. 3c). At 6 dpi, but also at 4 wpi, no differences in *M. marinum* counts between *il10*$^{e46/e46}$ mutants and WT zebrafish were observed (at 6 dpi; bacterial copy number median 65,000 vs 74,000, at 4 wpi; median 126,000 vs 90,000, Fig. 3c). However, at 8/9wpi there was a smaller bacterial amount in the *il10*$^{e46/e46}$ fish compared to the WT fish (median 86,000 vs 645,000, $P = 0.039$).

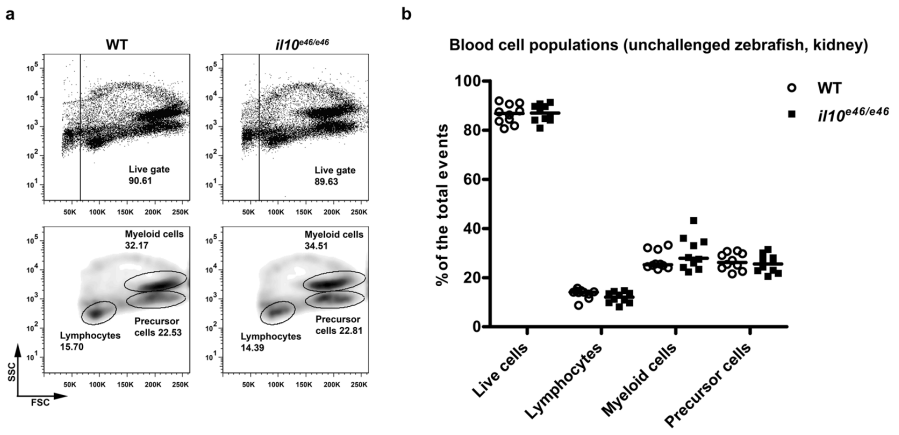

Figure 2. Unchallenged *il10*$^{e46/e46}$ zebrafish have kidney blood cell populations similar to those of WT control fish. (**a**,**b**) The relative proportions of live cells, lymphocytes, myeloid cells and precursor cells were determined with flow cytometry in *il10*$^{e46/e46}$ mutant zebrafish and in WT fish ($n = 10$ in both groups) based on granularity (SSC) and cell size (FSC). Representative flow cytometry plots are shown in panel (a). Gated populations are outlined, and the cell counts inside the gates are given as the percentages of the total viable cell population. The median of the relative proportions of different blood cell populations is presented as a scatter plot in panel (b). A two-tailed Mann-Whitney test was used for the statistical comparison of differences between *il10*$^{e46/e46}$ zebrafish and WT controls.

In addition, bacterial counts in *il10*$^{e46/e46}$ fish remained stable between 4 and 8/9 weeks, whereas there was a clear increase in bacteria in WT fish (median 65,000 vs 645,000, $P < 0.001$) (Fig. 3c). A Ziehl-Neelsen staining of formalin fixed and paraffin embedded zebrafish confirmed the presence of mycobacteria in both infected *il10*$^{e46/e46}$ and WT fish at 4 and 9 wpi (Fig. 3d). The histopathological analysis did not reveal any differences in granuloma morphology or in their tissue distribution (Supplementary Fig. S3). In conclusion *il10*$^{e46/e46}$ mutant zebrafish showed improved survival but no apparent changes in histopathology. In addition, there was a decrease in bacterial burden of *il10*$^{e46/e46}$ mutants at 8/9 wpi fish indicating enhanced resistance rather than a higher tolerance against low dose *M. marinum* infection.

***il10*$^{e46/e46}$ mutant zebrafish have an enhanced *ifng1* response in a low-dose mycobacterial infection.** To study the mechanisms underlying enhanced survival in *il10*$^{e46/e46}$ mutant zebrafish against a low-dose *M. marinum* infection we quantified the expression of selected cytokines and immune cell markers and conducted a flow cytometric analysis in the zebrafish kidney blood cells at different time points post infection (Figs 4–8). The expression levels of the studied genes in the kidney and abdominal organ block samples of unchallenged WT and *il10*$^{e46/e46}$ fish were similar. However, the relative *IgM* expression in the *il10*$^{e46/e46}$ mutant kidney was increased 2.5-fold compared to WT zebrafish ($P = 0.004$) but otherwise the mutants did not show any differences compared to WT.

First, we quantified the expression of *il10, tnfa*, *tnfb*, and *il1b* in the abdominal organ blocks of zebrafish at early time points during an infection (Fig. 4). Until 6 dpi, *M. marinum* infection did not alter the expression of *tnfb* or *il1b* either in *il10*$^{e46/e46}$ mutants or in WT fish compared to corresponding PBS injected controls. However, similarly to previous reports about the upregulation of *Il10* upon immunogenic stimulation[52,53], *il10* was significantly upregulated in the *il10*$^{e46/e46}$ mutants at 6 dpi in comparison to PBS controls ($P = 0.009$). WT fish, in turn, had a slight reduction in *tnfa* expression at 1 dpi compared to PBS injected fish ($P = 0.045$). As in unchallenged zebrafish, we did not see any differences in the expression levels of the cytokine genes between the *il10*$^{e46/e46}$ mutants and WT fish at 1 dpi or 6 dpi. At these early time points, expression levels of the T cell markers *cd4-1* (CD4 + cells) or *cd8a* (CD8 + cells) or the B cell marker *IgM* did not differ between *il10*$^{e46/e46}$ and WT fish either (Supplementary Fig. S4). These data indicate that a low-dose mycobacterial infection does not cause acute systemic inflammation in zebrafish and that the *il10*$^{e46/e46}$ zebrafish have a transcriptional innate cytokine response similar to the WT controls in the low-dose infection.

In order to study the role of Il10 later in a *M. marinum* infection, we conducted a flow cytometric analysis in the zebrafish kidney blood cells at 4 and 8 wpi and analyzed the relative amounts of lymphocyte, precursor cell and myeloid cell populations in *il10*$^{e46/e46}$ mutants and WT controls (Fig. 5). There were no differences in the relative lymphocyte or precursor cell counts between the groups. However, the relative proportion of myeloid cells was significantly lower in WT fish compared to the *il10*$^{e46/e46}$ mutants (median 21.6% vs. 26.2%, $P = 0.014$). Of note, the total live cell numbers were also lower in the WT controls compared to *il10*$^{e46/e46}$ mutant fish at 8 wpi ($P < 0.001$). Furthermore, in the WT control group the median of the relative myeloid cell count was 14.5% lower compared to the median of unchallenged fish at 8 wpi ($P = 0.001$).

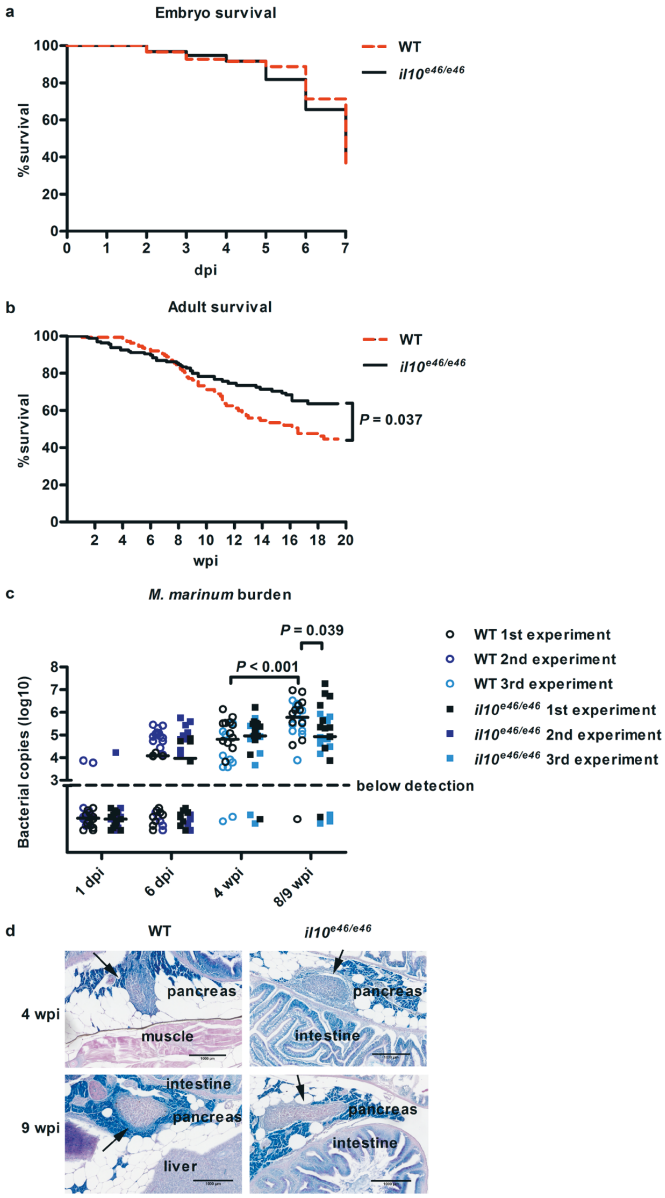

Figure 3. Adult *il10*$^{e46/e46}$ zebrafish have enhanced survival compared to WT controls in a low-dose *M. marinum* infection. (**a**) *il10*$^{e46/e46}$ ($n = 158$) and WT ($n = 181$) zebrafish larvae were microinjected before 6 hours post fertilization with *M. marinum* (3–29 CFU) and their survival was monitored for 7 days. The experiment was done six times and the data presented here is collected from one representative experiment. (**b**) The survival of adult *il10*$^{e46/e46}$ ($n = 172$) and WT ($n = 149$) zebrafish was monitored for 16–20 weeks after a low-dose (2–156 CFU) mycobacterial infection. The data were collected from four experiments. (**c**) The *M. marinum* burden in abdominal organ blocks (including kidney in the first and the second experiment, without kidney in the third experiment) of adult *il10*$^{e46/e46}$ mutant zebrafish ($n = 22$–27) and WT controls ($n = 22$–30 fish) was quantified with qPCR at 4 and 8/9 weeks post a low-dose infection (1–18 CFU). The bacterial load is presented as a scatter dot plot and as the median of total bacterial copies ($\log_{10}$). The data were collected from three experiments. (**d**) *M. marinum* granulomas were detected with Ziehl-Neelsen staining ($n = 4$ in both groups at both time points) at 4 and 9 weeks post a low-dose infection (2–9 CFU). Representative individuals from each group are shown. Granulomas are indicated with arrows. For panels (a) and (b) a log-rank (Mantel-Cox) and for panel (c) A two-tailed Mann-Whitney test was used for the statistical comparison of differences.

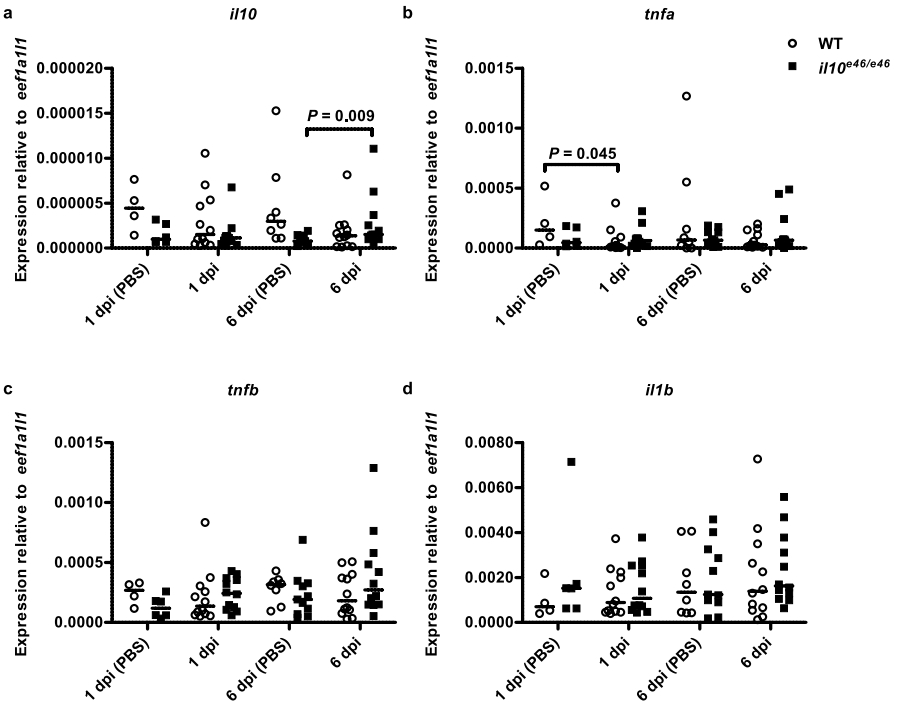

Figure 4. Nonfunctional *il10* does not increase the expression of proinflammatory cytokines at the early stages of a low-dose (2–9 CFU) mycobacterial infection in zebrafish. (**a–d**) The relative expression levels of *il10* and proinflammatory cytokine genes (*il1b*, *tnfa* and *tnfb*) were measured in the abdominal organ blocks (including kidney) of $il10^{e46/e46}$ mutant fish ($n = 6–12$) and WT controls ($n = 5–12$) at 1 dpi and 6 dpi and are presented as a scatter dot plot and median. Note the different scales of the *y* axes. Gene expressions were normalized to the expression of *eef1a1l1*. The data were collected from a single experiment. A two-tailed Mann-Whitney test was used for the statistical comparison of differences.

To obtain more quantitative data on T and B lymphocytes in $il10^{e46/e46}$ mutant and WT fish at 4 and 8 wpi, we next extracted RNA from the unsorted kidney cell samples used for the flow cytometry and determined relative expression levels of *il10*, the T cell markers *cd4-1* and *cd8a* as well as the B cell marker *IgM* (Fig. 6). No differences in the relative *il10* expression levels between the $il10^{e46/e46}$ mutant and the WT groups were observed. Interestingly, a qPCR analysis showed approximately 34.3% higher relative expression of *cd4-1* in $il10^{e46/e46}$ mutants compared to WT control fish at 4wpi ($P = 0.052$, NS) and a significantly higher expression at 8 wpi ($P = 0.017$). No differences in the kidney blood cell *cd8a* nor the B lymphocyte marker *IgM* expression were detected between $il10^{e46/e46}$ and WT zebrafish at 4 and 8 wpi. Notably, however, *cd8a* expression was significantly lower in $il10^{e46/e46}$ abdominal organ blocks compared to WT controls at 4 wpi ($P = 0.032$) (Fig. 6). Abdominal organ blocks did not have statistically significant differences in their *cd4-1* or *IgM* expression levels between $il10^{e46/e46}$ mutants and WT fish, although a trend towards the upregulation of *cd4-1* was seen at 4 wpi ($P = 0.053$, NS, Fig. 6). Altogether, the upregulated *cd4-1* expression in the $il10^{e46/e46}$ mutant kidneys is a possible consequence of an enhanced Th cell response in the infected $il10^{e46/e46}$ zebrafish.

In addition to the effects of *Il10* in regulating the production of proinflammatory cytokines in mice, human *IL10* is known to suppress the activation of Th cells by inhibiting the production of IFNG and IL4[54]. Hence, we quantified the relative expression of the Th1, Th2 and Treg cell transcription factors, *tbx21*, *gata3* and *foxp3a*, respectively, as well as the canonical Th1 and Th2 cell cytokine genes *ifng1* and *il4* in the kidney blood cells (Fig. 7). Indicative of an enhanced Th1 type immune response, our qPCR analysis showed that $il10^{e46/e46}$ mutant fish had higher relative expression levels of *tbx21* at 8wpi ($P = 0.042$), whereas the expression of *gata3* was lower compared to WT controls at the same time point ($P = 0.033$). Additionally, expression of the Th1 type cytokine gene *ifng1* was upregulated in $il10^{e46/e46}$ fish compared to WT zebrafish 8 wpi ($P = 0.025$). The expression of the canonical Th2 cytokine gene *il4* was instead similar in both $il10^{e46/e46}$ and WT fish the unsorted kidney cells at 4 and 8 wpi. Nor were any differences seen in the expression levels of *foxp3a* between the groups at either of the time points, suggesting a similar transcriptional Treg cell response in both mutants and WT fish during an infection. Mutation in *il10* can also cause differential tissue and cell type specific regulation of Th type gene expression since upregulation of *il4* was observed in the abdominal organ blocks of the $il10^{e46/e46}$ mutants compared to WT zebrafish at 9 wpi ($P = 0.023$, Fig. 7).

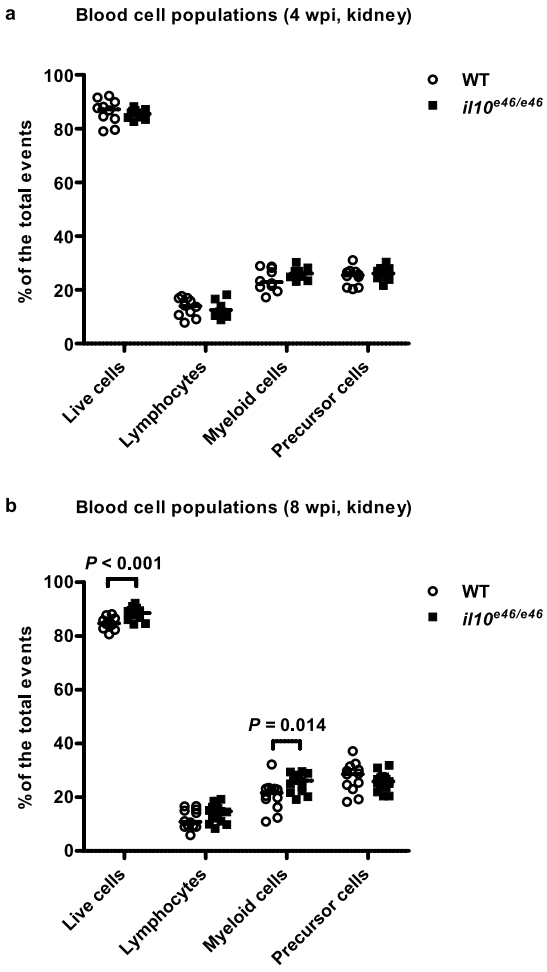

Figure 5. *il10*$^{e46/e46}$ mutation associates with a higher proportion of myeloid cells at 8 weeks post a low-dose (1–18 CFU) *M. marinum* infection. (**a**,**b**) The relative proportions of live cells, lymphocytes, precursor cells and myeloid cells were determined with flow cytometry from the kidneys of *il10*$^{e46/e46}$ mutants ($n = 10–15$) and WT control fish ($n = 10–12$) at 4 and 8 wpi based on granularity (SSC) and cell size (FSC). The data were collected from a single experiment and are presented as a scatter dot plot and median. A two-tailed Mann-Whitney test was used for the statistical comparison of differences between *il10*$^{e46/e46}$ zebrafish and WT controls.

A mycobacterial infection elicits the host's immune cells to produce humoral effectors such as complement components, reactive oxygen and nitrogen intermediates as well as proinflammatory cytokines to fight the infection[55]. In general, the magnitude of this response can be used to assess the severity of the prevalent bacterial disease. To compare the expression of mediators of inflammation in *il10*$^{e46/e46}$ mutants and WT fish in a chronic *M. marinum* infection, we quantified the expression of *tnfa*, *tnfb* and *il1b* in the kidney blood cells at 4 and 8 wpi (Fig. 8). qPCR results showed that *il10*$^{e46/e46}$ mutants had significantly lower expression levels of *tnfb* ($P = 0.048$) and *il1b* ($P = 0.029$) compared to WT fish at 8 wpi. No differences were observed in the expression of *tnfa* between *il10*$^{e46/e46}$ mutants and WT fish. Similar results were seen in the abdominal organ blocks as the relative expression of *il1b* was downregulated in *il10*$^{e46/e46}$ mutant fish compared to WT controls ($P = 0.043$, Fig. 8). Together, the elevated *tbx21* and *ifng1* expressions as well as the reduced expression of *gata3* in the *il10*$^{e46/e46}$ mutants indicate that a nonsense mutation in *il10* leads to a Th1 cell type immune response in zebrafish. In addition, this Th1 cell response associates with lower *tnfb* and *il1b* expression presumably indicating the slower progress of a mycobacterial infection as the expression of these cytokines have been shown to associate with the bacterial burden during the reactivation of *M. marinum* infection[56].

The *il10*$^{e46/e46}$ mutants are produced by ENU mutagenesis and thus likely contain also other mutations in their background in addition to the *e46* mutation. To address this, we outcrossed *il10*$^{e46/e46}$ mutants to wild type AB

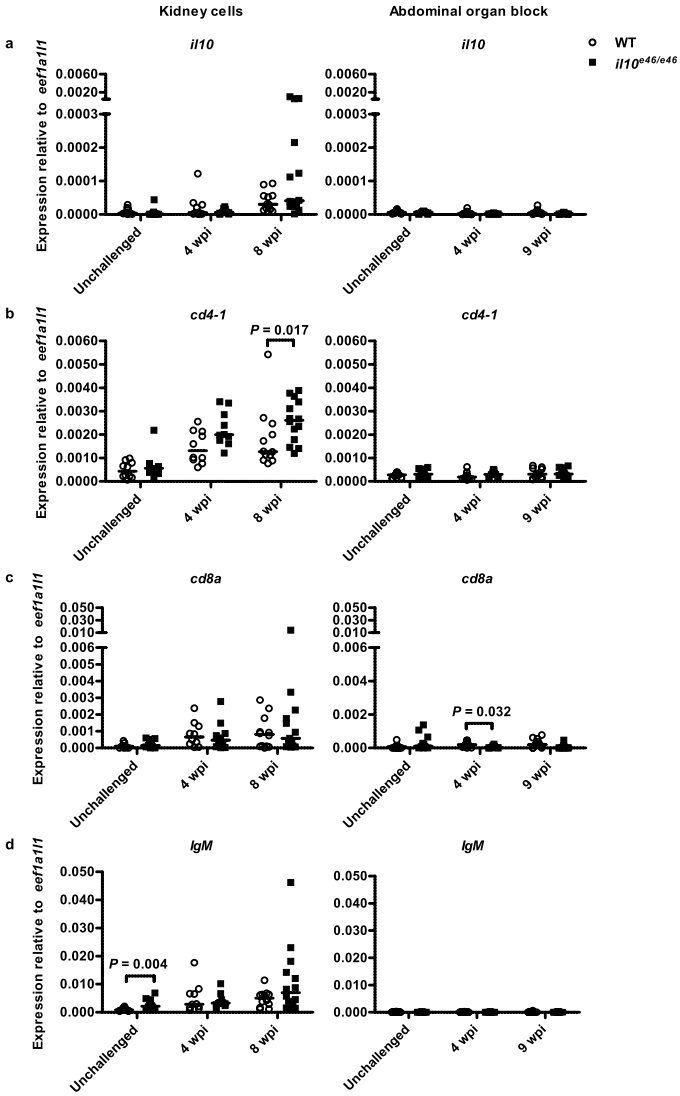

Figure 6. *il10*$^{e46/e46}$ mutant zebrafish have an elevated Th cell marker, *cd4-1*, expression level at 8 weeks post a *M. marinum* infection. (**a**–**d**) The relative expressions of *il10* and lymphocyte markers (*cd4-1, cd8a* and *IgM*) in kidneys of unchallenged *il10*$^{e46/e46}$ mutants ($n = 9$–10) and WT control fish ($n = 9$–10) and in the unsorted kidney cell populations of *il10*$^{e46/e46}$ mutants ($n = 10$–14) and WT control fish ($n = 10$–12) at 4 and 8 weeks post a low-dose (1–18 CFU) infection (on the left) as well as in the abdominal organ blocks (including kidney) of unchallenged *il10*$^{e46/e46}$ mutants ($n = 12$) and WT control fish ($n = 11$–12) and at 4 and 9 weeks post a low-dose (2–9 CFU) infection ($n = 9$–12 and $n = 11$–12, respectively) (on the right) were measured with qPCR. Data are presented as a scatter dot plot and median. Note the different scales of the *y* axes and the divided *y* axis in panels a and c. Gene expressions were normalized to the expression of *eef1a1l1*. Each dataset was collected from a single experiment. A two-tailed Mann-Whitney was used for the statistical comparison of differences.

zebrafish and incrossed their heterozygous progeny. Thereafter, we infected ungenotyped offspring of the heterozygous *il10*$^{e46/+}$ mutants with a low-dose of *M. marinum* and collected zebrafish kidneys for gene expression analysis (*cd4-1*, *tbx21*, *gata3 and ifng1*) 8 wpi. Also in this setting, *ifng1* expression was enhanced in *il10*$^{e46/e46}$ compared to controls (Fig. 9). We did not see significant differences in the expression levels of *cd4-1*, *tbx21* or *gata3*. However, the elevated *ifng1* expression further supports the notion that a nonsense mutation in *il10* leads to a Th1 cell type immune response in zebrafish.

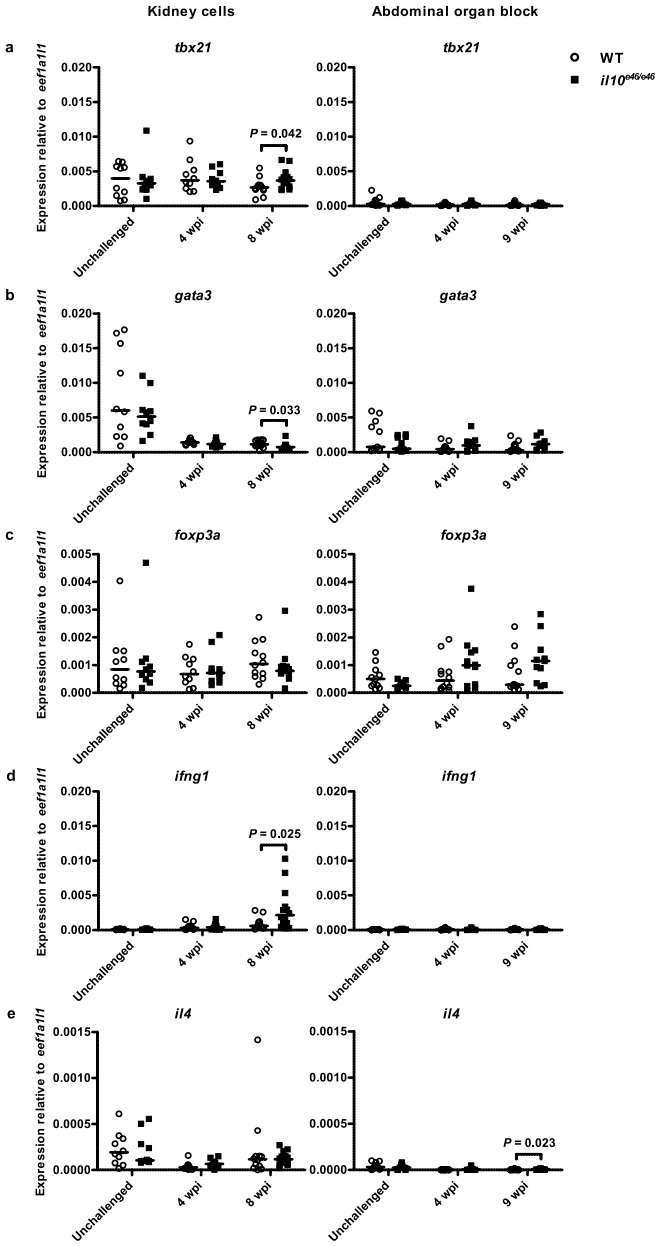

Figure 7. *il10*$^{e46/e46}$ mutant zebrafish have an enhanced Th1 cell mediated immune response in a mycobacterial infection. (**a**–**e**) The relative expressions of Cd4 + lymphocyte transcription factors (*tbx21*, *gata3*, *foxp3a*) and Th cell cytokines (*ifng1* and *il4*) in kidneys of unchallenged *il10*$^{e46/e46}$ mutants ($n = 10$) and WT control fish ($n = 10$) and in the unsorted kidney cell populations of *il10*$^{e46/e46}$ mutants ($n = 10$–14) and WT control fish ($n = 10$–12) at 4 and 8 weeks post a low-dose (1–18 CFU) infection (on the left) as well as in the abdominal organ blocks (including kidney) of unchallenged *il10*$^{e46/e46}$ mutants ($n = 12$) and WT control fish ($n = 11$–12) and at 4 and 9 weeks post a low-dose (2–9 CFU) infection ($n = 12$ and $n = 12$, respectively) (on the right) were measured with qPCR. Data are presented as a scatter dot plot and median. Gene expressions were normalized to the expression of *eef1a1l1*. Each dataset was collected from a single experiment. A two-tailed Mann-Whitney was used for the statistical comparison of differences.

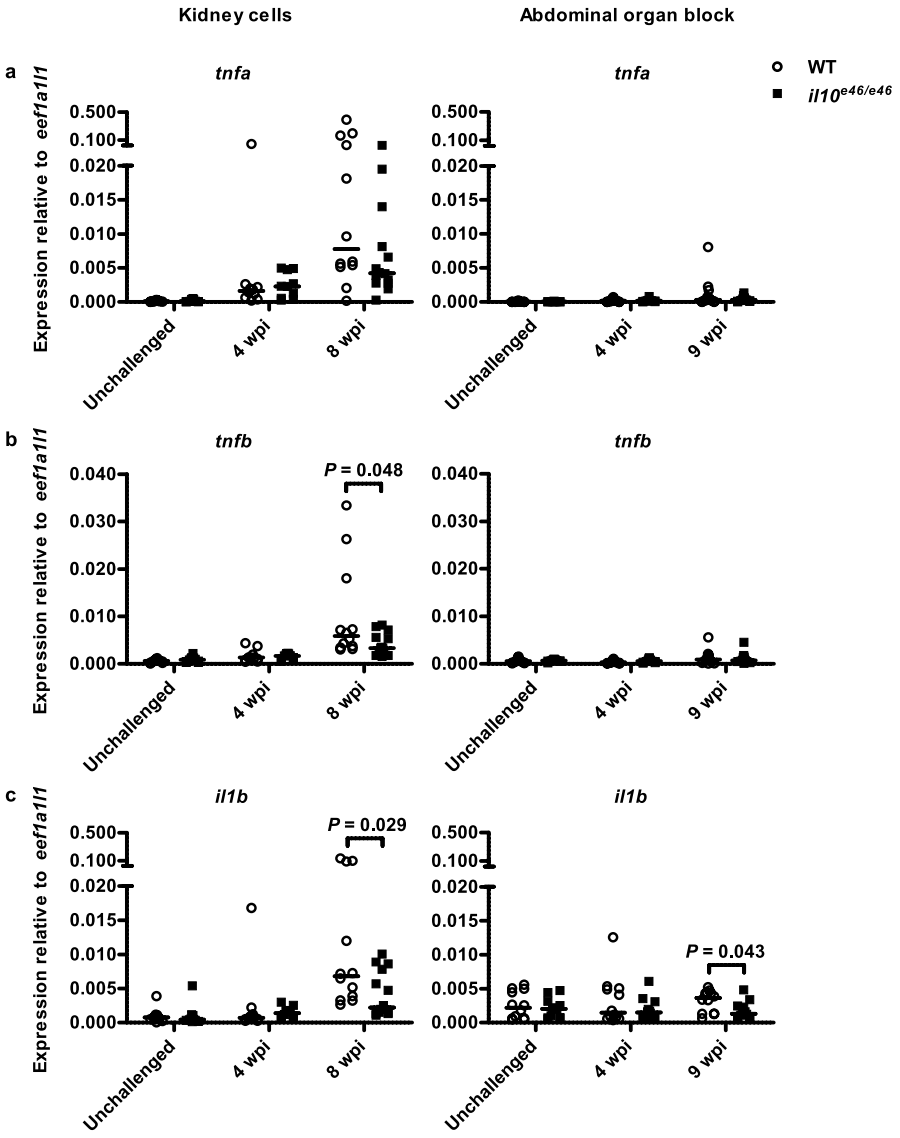

Figure 8. *il10*$^{e46/e46}$ mutant zebrafish have reduced inflammation in a chronic mycobacterial infection. (**a**–**c**) The relative expression of selected proinflammatory cytokines (*il1b*, *tnfa*, *tnfb*) in kidneys of unchallenged *il10*$^{e46/e46}$ mutants ($n = 10$) and WT control fish ($n = 10$) and in the unsorted kidney cell populations of *il10*$^{e46/e46}$ mutants ($n = 10$–14) and WT control fish ($n = 10$–12) at 4 and 8 weeks post a low-dose (1–18 CFU) infection (on the left) as well as in the abdominal organ blocks (including kidney) of unchallenged *il10*$^{e46/e46}$ mutants ($n = 12$) and WT control fish ($n = 12$) and at 4 and 9 weeks post a low-dose (2–9 CFU) infection ($n = 12$ and $n = 12$, respectively) (on the right) were measured with qPCR. Data are presented as a scatter dot plot and median. Note the different scales of the *y* axes and the divided *y* axis in panel a. Gene expressions were normalized to the expression of *eef1a1l1*. Each dataset was collected from a single experiment. A two-tailed Mann-Whitney was used for the statistical comparison of differences.

To further evaluate if there are significant co-segregating mutations, we extracted the DNA from the abdominal organ blocks of the offspring of the heterozygous *il10*$^{e46/+}$ mutants and performed whole genome sequencing. We compared the sequence of the coding regions of *il10*$^{e46/e46}$ mutants and WT fish to the GRCz11 reference genome and to the sequence of WT AB zebrafish. The putative mutations found in the analysis are shown in the

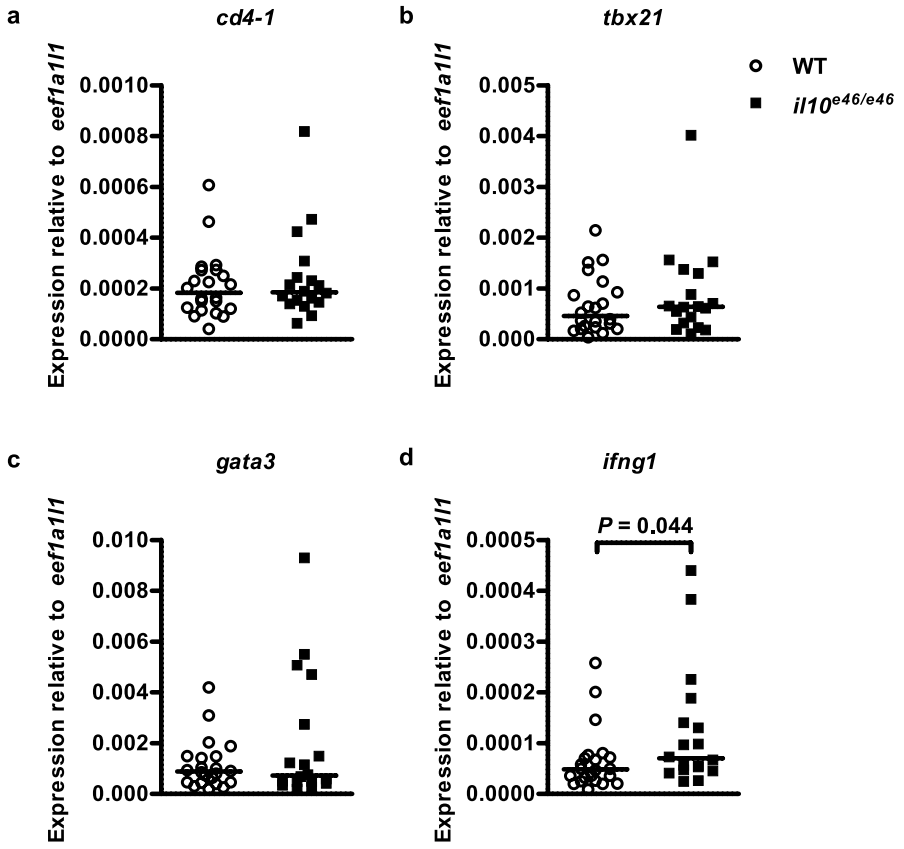

Figure 9. *il10*$^{e46/e46}$ mutant progeny of *il10*$^{e46/+}$ zebrafish have an elevated *ifng1* expression level in a *M. marinum* infection. (**a**–**d**) *il10*$^{e46/e46}$ mutants were outcrossed to wild type AB zebrafish and their heterozygous progeny was incrossed. The ungenotyped offspring of *il10*$^{e46/+}$ fish was infected with a low-dose (8–17 CFU) of *M. marinum*. The relative expression of lymphocyte marker (*cd4-1*), Cd4 + lymphocyte transcription factors (*tbx21*, *gata3*) and Th1 cytokine (*ifng1*) was measured in the kidneys of *il10*$^{e46/e46}$ ($n = 18$) and WT ($n = 22$) zebrafish at 8 wpi. Note the different scales of the *y* axes. Gene expressions were normalized to the expression of *eef1a1l1*. The data were collected from a single experiment. A two-tailed Mann-Whitney was used for the statistical comparison of differences.

Supplementary Table S1. 57 mutations with a mutant allele fraction equal to or greater than 25% caused either a stop codon or a frameshift (Supplementary Table S2). One of these mutant alleles in gene *si:dkey-19a16.2* had a 100% allele fraction in both *il10*$^{e46/e46}$ mutants and WT zebrafish indicating that it is homozygous in both. The allele fraction of 17 mutations shown in the Supplementary Table S2 differed significantly ($P < 0.05$) between *il10*$^{e46/e46}$ and WT zebrafish (Supplementary Table S3). As expected, *e46* allele had 100% fraction in *il10*$^{e46/e46}$ sample and 0% fraction in WT sample. Noteworthy, there were no other mutations that would cause either a nonsense or a frameshift mutation in the chromosome 11 (Supplementary Table S2). This indicates that none of these types of mutations are likely to be co-segregating with the *e46* mutation. The role of the other detected mutations in the immunity or other phenotypes remains to be evaluated.

Discussion

The exact mechanisms of the immune defense against *M. tuberculosis* are in many ways still unknown, although disease progression has been studied in human samples, as well as with various model organisms *in vivo* (reviewed in[57]). Although spontaneous latency occurs in *M. tuberculosis* infected maqaque[58] and rabbit[59,60], these models raise serious ethical concerns. On the other hand, a *M. tuberculosis* infection in mouse is a well-established model for tuberculosis, but accomplishing a latent disease requires either a prior Bacillus Calmette-Guérin vaccination to boost the host's immune response or a period of antibiotic treatment post infection in order to prevent an acute infection[61]. To study mycobacterial pathogenesis in the context of a natural host-pathogen interaction, a *M. marinum* infection in several fish species such as medaka[62], goldfish[43,63,64] and zebrafish[35–37] is used to model tuberculosis (reviewed in[65]).

Compared to other fish models, the zebrafish *M. marinum* infection has its benefits due to fast disease progression as well as the small size of the host[43,62–64]. In addition, a mycobacterial infection in adult zebrafish spontaneously reaches a latent state that can be reactivated with an immuno-suppressive treatment[35].

IL10 KO mice develop an age-related enterocolitis, demonstrated by symptoms such as weight loss, diarrhea and abnormal gut morphology[50]. More specifically, the lack of IL10 leads to the excess production of proinflammatory cytokines, such as IL1b and TNF, as well as increased Th1 activation leading to the over-production of IFNG[47,50]. Interestingly, unchallenged *il10*$^{e46/e46}$ zebrafish did not show any detectable signs of auto-immunity before the age of 10 months; the maximum age of the zebrafish used in the study. This is in line with the observed similar expression levels of the proinflammatory cytokine genes *tnfa*, *tnfb* and *il1b*, as well as the hallmark Th1 cytokine gene *ifng1* in all of the studied tissues in *il10*$^{e46/e46}$ mutants compared to WT control fish. Furthermore, no difference was observed in the relative expression levels of the T cell markers *cd8a* and *cd4-1* or in our flow cytometric analysis of lymphocyte counts. In addition, Treg cells have been shown to be required in maintaining peripheral tolerance to prevent autoimmunity[66–68] and recently, Sugimoto *et al*. have studied zebrafish colitis by using *foxp3a* mutant zebrafish[28]. While they found the inflammatory phenotype in these mutants, it did not lead to death as quickly as the corresponding genotype in mice. Consequently, they suggested that this may be due to the milder immune cell effector responses in aquatic vertebrates, including fish, which in turn may contribute to the ability of scarless regeneration of fish. Moreover, also in fish the microbes of the environment affect commensal bacteria, which in turn can explain the differences in enterocolitis between mice and fish[69]. It has also been suggested that fish maintenance in constant water circulation systems (similar to ones we have used) can prevent development of intestinal inflammation to some extent[70]. Noteworthy, in our studies, *foxp3a* expression was not altered in *il10*$^{e46/e46}$ mutants. Since IL10 has been shown to maintain the *FOXP3* expression in Treg cells in mice and humans, it points to a compensatory mechanism in fish[71]. Furthermore, Brugman *et al*. have speculated that there could be other immune mediators in addition to *il1b* and *il10* which contribute to the development of enterocolitis in zebrafish[70]. Of note, we did observe increased *IgM* expression in the kidney as well as decreased *IgM* expression in the liver of *il10*$^{e46/e46}$ zebrafish. Increased expression is in line with the previously reported higher serum immunoglobulin levels in IL10 deficient mice[48,50] whereas decreased expression of *IgM* in the liver supports studies demonstrating carp IL10 in enhancing IgM + B cell proliferation[72]. Together these results indicate that, in contrast to IL10 KO mice, unchallenged *il10*$^{e46/e46}$ mutant zebrafish have neither an overt inflammatory phenotype nor an inherently over-activated T cell response.

IL10 has been widely studied for its potent role in tuberculosis. Interestingly, mouse models of tuberculosis have not only reported that the lack of IL10 is beneficial to the host in a mycobacterial infection, but also that an IL10 deficiency can have detrimental effects on immunological control. For example, CBA/J background mice, which are susceptible to tuberculosis and whose IL10 function has been blocked, as well as *Il10*$^{-/-}$ mice, survived longer than control mice[14,15], whereas *Il10*$^{-/-}$ mice with the C57BL/6 J background were all dead after ca. 27 weeks, while all the WT controls survived[16]. Among other things, these contradictory results have been attributed to differences in mouse and bacterial strains and to variation between mouse phenotypes (e.g. gut flora)[73]. Here, we first used zebrafish embryos in the context of a mycobacterial infection to specifically study the innate immune response prior to the development of the adaptive immunity. In our embryonic *M. marinum* infection, the mortality of *il10*$^{e46/e46}$ mutant zebrafish larvae did not differ significantly from the WT controls. This suggests that in our model a nonsense mutation in the *il10* gene does not improve, or compromise, resistance against mycobacteria during the early innate immune response. Accordingly, mouse models of tuberculosis have indicated that IL10 deficient mice show no mortality until ca. 14 wpi[16] indicating a significant adaptive immune component in infection control. Using different injection route might lead to different outcome since the bacteria is able to proliferate in the yolk sac before it spreads into the different tissues[74]. However, Carvalho *et al*. have showed that the infection of *M. marinum* into the yolk sac leads to the formation of initial stages of granulomas, similar to ones that form when the caudal vein infection route is used[38]. The yolk sac infection method was also validated by showing that the decrease in the myeloid cell count lead to increased, and use of antibiotics to decreased *M. marinum* burden in the larvae[38]. Thus, since yolk sac infection is time-effective, it was chosen for the current study.

Next, we infected adult zebrafish with a low-dose of *M. marinum* and followed the fish for an average of 18.5 weeks. Curiously, the mortality of adult *il10*$^{e46/e46}$ zebrafish was on average significantly lower compared to their WT controls. The impaired survival of WT zebrafish compared to *il10*$^{e46/e46}$ mutants may be due to their inability to reach latency or a higher tendency for spontaneous reactivation. In fact, the function of IL10 has been linked to the reactivation of a chronic pulmonary *M. tuberculosis* infection in transgenic mice, which produce increased amounts of IL10[75]. In the study by Turner *et al*., the over-production of IL10 associated with a significantly increased bacterial burden as well as with decreased expression of *Tnf* and *Il12p40* as signs of reactivation. Mechanistically, the higher susceptibility to mycobacterial reactivation in WT fish could be a consequence of an unfavorable inflammatory TNF/IL10 balance in the tuberculous granuloma as was previously reported *in silico*[76].

In our low-dose infection model, we have previously demonstrated that a proinflammatory phenotype leading to an enhanced immediate immune response can associate with a decreased bacterial burden later in an infection at 9 wpi[51]. In addition, an appropriate TNF level has been shown to be important for tuberculosis immunity, as both the deficient and excessive production of TNF are linked to accelerated pathogenesis[7]. Here, we saw that, as in unchallenged zebrafish, the expression of the proinflammatory cytokine genes *tnfa*, *il1b* and *tnfb* in *il10*$^{e46/e46}$ mutant fish was at the same level compared to WT controls at 1 and 6 dpi. Furthermore, at these early time points after a low-dose *M. marinum* infection, the expression of *il1b* and *tnfb* was not upregulated compared to the fish injected with PBS. This is consistent with our previous studies[35] and with mouse studies in which TNF levels are not elevated in the serum or lungs of IL10 deficient mice before 14 and 15 dpi, respectively[13]. Expectedly, we did not see any changes or significant induction of the lymphocyte markers *cd4*, *cd8* or *IgM* at 1 or 6 dpi. This is in line with the onset of the adaptive immune response only after two weeks post the mycobacterial infection[55,77].

The immune response against tuberculosis requires an interplay between several of the host's immune cells, the most important being macrophages, dendritic cells and CD4 + T lymphocytes[78]. Our flow cytometric analyses at 4 and 8 wpi exhibited similar lymphocyte amounts in *il10*$^{e46/e46}$ mutant zebrafish compared to WT controls. Interestingly, however, *il10*$^{e46/e46}$ mutant fish had significantly higher relative amounts of kidney myeloid cells compared to WT zebrafish at 8 wpi and further studies are warranted to understand the downstream effects of the lack of Il10 leading to increased myeloid cell counts after a mycobacterial infection. Although we could not detect any differences in total lymphocyte amounts between *il10*$^{e46/e46}$ and WT zebrafish, our qPCR analysis on the unsorted kidney cell samples showed a trend of elevated *cd4-1* expression in *il10*$^{e46/e46}$ mutant fish compared to WT controls at 4 wpi and a significantly higher expression at 8 wpi. This may also be due to some other cell types than lymphocytes, such as dendritic cells and macrophages. However, this result is similar to IL10 deficient mice, in which elevated CD4 + T cell amounts are observed at different time points after an infection, and may imply an enhanced Th response in *il10*$^{e46/e46}$ mutants[14,15].

Th1 cells are important in attacking intracellular pathogens such as *M. tuberculosis*[4–6]. In tuberculosis, IFNG produced by Th1 cells activates macrophages, which results in the stimulation of phagocytosis, phagosome maturation, the production of reactive nitrogen intermediates and antigen presentation[79]. Furthermore, a *M. tuberculosis* infection in *Il10* deficient mice has also been shown to lead to the enhanced production of IFNG by T cells[13–15]. *il10*$^{e46/e46}$ mutant zebrafish had enhanced expression levels of the Th1 marker, *tbx21*, and decreased expression levels of the Th2 marker, *gata3*, at 8wpi. In addition, the Th1 cytokine *ifng1* was upregulated at 8 wpi in *il10*$^{e46/e46}$ mutants further suggesting a shift towards a Th1 cell mediated response. The upregulation of *ifng1* in *il10*$^{e46/e46}$ compared to WT control fish was also seen in the siblings from a heterozygous *il10*$^{e46/+}$ incross. This further confirms the enhanced production of *ifng1*, likely from Th1 cells, in the absence of Il10[14,15]. However, since the whole genome sequencing revealed also other mutant alleles causing a stop codon or frameshift in addition to the *e46* allele, we cannot exclude the possibility that these mutations contribute to our results. Noteworthy, with the allele fragment cut-off of 25% there were no stop codon or frameshift causing mutations in the chromosome 11 where *il10* is located. In other words, our analysis suggests no significant co-segregating damaging mutations.

It has been previously shown that Th2 type response (*gata3*/*tbx21* ratio) after four weeks of a *M. marinum* infection is associated with a low bacterial burden in the wild type AB fish[27]. In this study, adult wild type AB zebrafish were infected with a low-dose of *M. marinum* and were divided into three subgroups based on the bacterial burden at different time points. In the subgroup of the lowest bacterial burden, a Th2 type marker gene expression bias was observed. However, also Th1 response is induced (as indicated by elevated *ifng1* expression also in this current study) in response to *M. marinum* infection[35]. Thus, for the optimal immune response both Th1 and Th2 types of responses are apparently required. Our current data indicate that lack of Il10 results in enhanced *ifng1* expression and in better survival.

Although the role of IL10 in the host defense against *M. tuberculosis* is unambiguous, *in vivo* studies have concluded that in the absence of functional IL10 signaling, the Th1 response is hyper-activated resulting in improved resistance against a mycobacterial infection[13,15,73]. Consistent with this, our results show that a nonsense mutation in the zebrafish *il10* leads to improved survival after a *M. marinum* infection, and associates with an enhanced Th1 response against mycobacteria. The higher Th1/Th2 ratio in the chronically infected *il10*$^{e46/e46}$ mutant zebrafish is reflected by elevated *ifng1* and *tbx21* expression levels as well as decreased *gata3* mRNA levels at 8 wpi. We did not detect differences in the expression of the proinflammatory cytokine genes *tnfa*, *il1b* and *tnfb* between unchallenged *il10*$^{e46/e46}$ mutants and WT fish at the early stages of a *M. marinum* infection at 1 and 6 dpi. Taken together, these results suggest that the lack of Il10 does not enhance the early proinflammatory response after a *M. marinum* inoculate, but instead they highlight the importance of the Th1 response in resistance against a mycobacterial infection. Furthermore, our study validates the use of the zebrafish model of a *M. marinum* infection in tuberculosis studies.

Methods

Zebrafish lines and maintenance. Four to ten months old zebrafish were used in the adult experiments. The *il10* mutation carrying zebrafish line e46 was obtained from Wellcome Trust Sanger Institute (Hinxton UK)[44]. In addition, wild type AB zebrafish from the Tampere Zebrafish Core Facility were used in whole genome sequencing experiment. Unchallenged fish were maintained in a standard flowthrough system (Aquatic Habitats, Florida, USA) with an automated light/dark cycle of 14 h and 10 h and fed with SDS 400 food (Special Diets Services, Essex, UK) twice and with in-house cultured *Artemia nauplia* once a day. During the time when gene expression measurements in the intestine, infection experiment with outcrossed e46 line and the whole genome sequencing were done, the fish were fed with GEMMA Micro 500 food (Skretting, Stavanger, Norway) once a day. The genotypes of the fish were confirmed by Sanger sequencing performed by our faculty's sequencing facility. Homozygous fish and wild type (WT) siblings were spawn as separate groups and maintained separately for the experiments. *M. marinum* infected fish were maintained in a standard flowthrough system (Aqua Schwarz GMbH, Göttingen, Germany) in the aforementioned light/dark cycle and fed with SDS 400 food twice a day. Infected fish were monitored daily and humane endpoint criteria defined in animal experiment permits were applied. The Animal Experiment Board of Finland has approved the zebrafish housing, care, and all of the experiments (permits ESAVI/10079/04.10.06/2015, ESAVI/10823/04.10.07/2016 and ESAVI/2464/04.10.07/2017). The same ethical regulations as for all other vertebrate model animals are applied for zebrafish and all methods of this article were performed in accordance with relevant guidelines and regulations.

qPCR. Both RNA and DNA were extracted from kidney, spleen, liver, abdominal organ blocks (+/−kidney, which is the main hematopoietic tissue in zebrafish) and kidney blood cells with TRIreagent (Molecular Research Center, Ohio, USA) following the manufacturer's coextraction protocol. The quality of the RNA was validated from several abdominal organ block (including kidney) samples of with 1.5% agarose (Bioline, London, United Kingdom) gel electrophoresis. The RNA samples were treated with the RapidOut DNA Removal Kit (Thermo

Fischer Scientific, Waltham, USA) to remove genomic DNA. For the RNA samples, reverse transcription was done with the SensiFAST™ cDNA synthesis kit (BioLine, London, UK) and the relative gene expression levels of target genes were determined from cDNA with quantitative PCR (qPCR) using the PowerUp™ SYBR® master mix (Thermo Fischer Scientific). The qPCR primer sequences and the ZFIN identification codes for the analyzed genes are given in Supplementary Table S4. The expression levels of the target genes were calculated relative to the expression of *eef1a1l1*[80] using $2^{-\Delta Ct}$ method. Total DNA was used to quantify the *M. marinum* colony forming units (CFU) with qPCR using SensiFAST™ SYBR® No-ROX (Bioline)[35]. The detection limit of this method was considered 1,000 CFU. qPCR was performed with a CFX96 qPCR machine (Bio-Rad, California, USA) and the data was analyzed with the Bio-Rad CFX Manager software v1.6 (Bio-Rad). Genomic DNA contamination was controlled by including no reverse transcriptase controls to the cDNA synthesis and to the following qPCR reaction from randomly selected RNA samples. The specificity of the qPCR for each amplified region was validated with a melt curve analysis and with a 1.5% agarose gel electrophoresis from a series of selected samples.

Imaging of zebrafish intestine. The intestine of *il10*$^{e46/e46}$ mutants and WT zebrafish was imaged with Nikon SMZ745T microscope and DS-Vi1 camera (Nikon, Minato, Tokyo, Japan). The scale bar was measured with NIS-Elements D 4.2 software (Nikon).

Flow cytometry. Flow cytometry was performed as described previously[19,51]. In short, adult zebrafish were euthanized with 0.04% 3-amino benzoic acid ethyl ester and their kidneys were isolated and suspended in PBS with 0.5% fetal bovine serum (Gibco/Invitrogen, California, USA). Relative amounts of lymphocytes, blood cell precursors and myeloid cells in unchallenged and infected zebrafish were determined with a FACSCanto II (Becton, Dickinson, New Jersey, USA) and the data were analyzed with the FlowJo program (v7.5; Tree Star, Inc, Oregon, USA). After flow-cytometry, the remaining kidney cell suspensions from the *M. marinum* infected zebrafish were pelleted with 1,000 g for 1 min at + 4 °C, washed with 500 µl of PBS, centrifuged at 10,000 g for 1 min at + 4 °C, resuspended in 700 µl of TRIreagent (Molecular Research Center, Ohio, USA) and stored at −20 °C until RNA extraction. The remaining abdominal organ block (excluding kidney) from the infected fish were also collected and stored at −80 °C until DNA extractions. Throughout the article these remaining organs (without kidney) from flow cytometry are referred the abdominal organ block. In other experiments, abdominal organ block refers to all the organs isolated from the abdominal cavity (including kidney).

Experimental *M. marinum* infections. *M. marinum* (ATCC 927) was cultured and inoculated as described previously[35]. However, here *M. marinum* was suspended in phosphate buffered saline (PBS) rather than in potassium chloride prior to infections. In the zebrafish embryos, PBS with 2% polyvinylpyrrolidone-40 and 0.3 mg/ml phenol red (Sigma-Aldrich, Missouri, USA) was used as a mycobacterial carrier solution. A volume of 1 nl was injected 0–6 hours post fertilization into the yolk sac with aluminosilicate capillary needles (Sutter instrument Co., California, USA) using a micromanipulator (Narishige International, London UK) and a PV830 Pneumatic PicoPump (World Precision Instruments, Sarasota, Florida, USA) and visualized with a Stemi 2000 microscope (Carl Zeiss MicroImaging GmbH, Göttingen, Germany). Survival was followed daily by inspecting the larvae under a microscope. For the adult zebrafish infections, fish were anesthetized with 0.02% 3-amino benzoic acid ethyl ester, and 5 µl of *M. marinum* with 0.3 mg/ml phenol red (Sigma-Aldrich, Missouri, USA) was injected into the abdominal cavity with a 30 gauge Omnican 100 insulin needle (Braun, Melsungen, Germany). The *M. marinum* amounts (CFU) used in both the embryonic and adult infections were verified by plating bacterial inoculates on 7H10 agar (Becton Dickinson, New Jersey, USA) plates.

Ziehl-Neelsen staining. The presence of *M. marinum* in infected adult zebrafish was verified with Ziehl-Neelsen staining from paraffin embedded tissue sections as described previously[35,81]. Visualization of stained sections was performed using an Objective Imaging Surveyor virtual slide scanner (Objective Imaging, Cambridge, United Kingdom) and the scanned sections were digitized with a 20 × Plan Apochromatic microscope objective at a resolution of 0.4 µm/pixel. The image data were converted to JPEG2000 format as described previously[82]. The granulomas were counted and classified according to Myllymäki *et al.*[56].

Whole genome sequencing. The DNA samples extracted from the offspring of the heterozygous *il10*$^{e46/+}$ mutants and wild type AB fish was used for the whole genome sequencing. In each sample DNA of ten fish was pooled together. The RNA removal, Kapa Hyper Plus -library preparation and the whole genome sequencing were conducted at the Institute for Molecular Medicine Finland FIMM Technology Centre, Helsinki, Finland. The DNA libraries were sequenced with the 150 bp paired-end sequencing on the Illumina NovaSeq 6000 platform with a sequencing depth of >110 gigabases/sample.

Whole genome sequence alignment and quality control. Paired-end reads were processed prior to alignment to remove sequencing adapters and low-quality bases at the read tails. Adapters were trimmed using cutadapt-1.11[83] in paired mode. Low-quality bases at read ends with a smoothed base quality <25 were trimmed using an in-house algorithm. After quality control, the paired-end reads were aligned against the GRCz11 zebrafish reference genome using Bowtie-2.3.0[84]. Optical and PCR duplicates were removed using samblaster-0.1.24[85].

Mutation analysis from the whole genome sequencing data. Mutations were called from the *il10*$^{e46/e46}$ mutant and WT zebrafish using an in-house pipeline. This was done by identifying variants with an alternate allele fraction of at least 20% and at least 5 supporting reads. The allele fraction was also required to be 20 times higher than the alternate allele fraction of the mutation in the AB zebrafish. Mutations and their protein-level effects were annotated using ANNOVAR[86]. Frameshift and stop-gain mutations were curated using Integrative Genomics Viewer (IGV)[87].

Statistical analyses. Web-based ClinCalc program (http://clincalc.com/Stats/SampleSize.aspx) was used for all of the sample size calculations. Based on our previous adult zebrafish survival experiments with a low-dose *M. marinum* infection, we estimated the end-point mortality difference between WT and *il10*$^{e46/e46}$ zebrafish to be 40%. With a 80% statistical power, a minimum group size of 22 was determined for the survival experiments. In order to estimate the bacterial quantification sample size for the current research, our previously published *M. marinum* quantification with 0.5 unit difference (log10 scale, standard deviation 0.5) between study groups[51] was used as a guideline. Using the desired 80% power this difference accounted for a group size of 16 fish for the bacterial quantification.

Statistical analyses of the results, except the whole genome sequencing data, were performed with the Prism program, version 5.02 (GraphPad Software, Inc, California, USA). The statistical significance from the survival experiments was determined with a log-rank (Mantel-Cox) test and from the flow cytometry and qPCR experiments with a nonparametric Mann-Whitney analysis. When analyzing the whole genome sequencing data, *P* values for each mutation were calculated between the *il10*$^{e46/e46}$ mutants and WT fish using Fisher's exact test. *P* values of <0.05 were considered significant.

Data availability. The datasets generated and analyzed during the current study are available from the corresponding author on reasonable request. The whole genome sequencing data is available at European Nucleotide Archive (https://www.ebi.ac.uk/ena/; ERP number: ERP109293).

References

1. World Health Organization. Global tuberculosis report 2016. http://www.who.int/tb/publications/global_report/en/ (2016).
2. Havlir, D. V. & Barnes, P. F. Tuberculosis in patients with human immunodeficiency virus infection. *N. Engl. J. Med.* **340**, 367–373 (1999).
3. Harris, J. & Keane, J. How tumour necrosis factor blockers interfere with tuberculosis immunity. *Clin. Exp. Immunol.* **161**, 1–9 (2010).
4. Flynn, J. L. *et al*. An essential role for interferon gamma in resistance to *Mycobacterium tuberculosis* infection. *J. Exp. Med*. **178**, 2249–2254 (1993).
5. Cooper, A. M., Magram, J., Ferrante, J. & Orme, I. M. Interleukin 12 (IL-12) is crucial to the development of protective immunity in mice intravenously infected with *Mycobacterium tuberculosis*. *J. Exp. Med.* **186**, 39–45 (1997).
6. Cooper, A. M. *et al*. Disseminated tuberculosis in interferon gamma gene-disrupted mice. *J. Exp. Med.* **178**, 2243–2247 (1993).
7. Roca, F. J. & Ramakrishnan, L. TNF dually mediates resistance and susceptibility to mycobacteria via mitochondrial reactive oxygen species. *Cell* **153**, 521–534 (2013).
8. Fiorentino, D. F., Bond, M. W. & Mosmann, T. R. Two types of mouse T helper cell. IV. Th2 clones secrete a factor that inhibits cytokine production by Th1 clones. *J. Exp. Med.* **170**, 2081–2095 (1989).
9. Moore, K. W. *et al*. Homology of cytokine synthesis inhibitory factor (IL-10) to the Epstein-Barr virus gene BCRFI. *Science* **248**, 1230–1234 (1990).
10. Mosser, D. M. & Zhang, X. Interleukin-10: new perspectives on an old cytokine. *Immunol. Rev.* **226**, 205–218 (2008).
11. Pacheco, A. G., Cardoso, C. C. & Moraes, M. O. IFNG+874T/A, IL10 −1082G/A and TNF −308G/A polymorphisms in association with tuberculosis susceptibility: a meta-analysis study. *Hum. Genet.* **123**, 477–484 (2008).
12. Delgado, J. C., Baena, A., Thim, S. & Goldfeld, A. E. Ethnic-specific genetic associations with pulmonary tuberculosis. *J. Infect. Dis.* **186**, 1463–1468 (2002).
13. Redford, P. S. *et al*. Enhanced protection to *Mycobacterium tuberculosis* infection in IL-10-deficient mice is accompanied by early and enhanced Th1 responses in the lung. *Eur. J. Immunol.* **40**, 2200–2210 (2010).
14. Cyktor, J. C. *et al*. IL-10 inhibits mature fibrotic granuloma formation during *Mycobacterium tuberculosis* infection. *J. Immunol.* **190**, 2778–2790 (2013).
15. Beamer, G. L. *et al*. Interleukin-10 promotes *Mycobacterium tuberculosis* disease progression in CBA/J mice. *J. Immunol.* **181**, 5545–5550 (2008).
16. Higgins, D. M. *et al*. Lack of IL-10 alters inflammatory and immune responses during pulmonary *Mycobacterium tuberculosis* infection. *Tuberculosis (Edinb)* **89**, 149–157 (2009).
17. Wittamer, V., Bertrand, J. Y., Gutschow, P. W. & Traver, D. Characterization of the mononuclear phagocyte system in zebrafish. *Blood* **117**, 7126–7135 (2011).
18. Lin, A. F. *et al*. The DC-SIGN of zebrafish: insights into the existence of a CD209 homologue in a lower vertebrate and its involvement in adaptive immunity. *J. Immunol.* **183**, 7398–7410 (2009).
19. Langenau, D. M. *et al*. *In vivo* tracking of T cell development, ablation, and engraftment in transgenic zebrafish. *Proc. Natl. Acad. Sci. USA* **101**, 7369–7374 (2004).
20. Willett, C. E., Zapata, A. G., Hopkins, N. & Steiner, L. A. Expression of zebrafish rag genes during early development identifies the thymus. *Dev. Biol.* **182**, 331–341 (1997).
21. Yoon, S. *et al*. First demonstration of antigen induced cytokine expression by CD4-1+lymphocytes in a poikilotherm: Studies in zebrafish (*Danio rerio*). *Plos One* **10**, e0126378, https://doi.org/10.1371/journal.pone.0126378 (2015).
22. Danilova, N. & Steiner, L. A. B cells develop in the zebrafish pancreas. *Proc. Natl. Acad. Sci. USA* **99**, 13711–13716 (2002).
23. Page, D. M. *et al*. An evolutionarily conserved program of B-cell development and activation in zebrafish. *Blood* **122**, e1–11 (2013).
24. Balla, K. M. *et al*. Eosinophils in the zebrafish: prospective isolation, characterization, and eosinophilia induction by helminth determinants. *Blood* **116**, 3944–3954 (2010).
25. Dee, C. T. *et al*. CD4-Transgenic zebrafish reveal tissue-resident Th2- and regulatory T cell–like populations and diverse mononuclear phagocytes. *J. Immunol.* **197**, 3520–3530 (2016).
26. Mitra, S., Alnabulsi, A., Secombes, C. J. & Bird, S. Identification and characterization of the transcription factors involved in T-cell development, t-bet, stat6 and foxp3, within the zebrafish, *Danio rerio*. *FEBS J.* **277**, 128-147 (2010).
27. Hammarén, M. M. *et al*. Adequate Th2-type response associates with restricted bacterial growth in latent mycobacterial infection of zebrafish. *Plos Pathog.* **10**, e1004190, https://doi.org/10.1371/journal.ppat.1004190 (2014).
28. Sugimoto, K., Hui, S. P., Sheng, D. Z., Nakayama, M. & Kikuchi, K. Zebrafish FOXP3 is required for the maintenance of immune tolerance. *Dev. Comp. Immunol.* **73**, 156–162 (2017).
29. Zhang, S. & Cui, P. Complement system in zebrafish. *Dev. Comp. Immunol.* **46**, 3–10 (2014).
30. Zimmerman, A. M., Moustafa, F. M., Romanowski, K. E. & Steiner, L. A. Zebrafish immunoglobulin IgD: unusual exon usage and quantitative expression profiles with IgM and IgZ/T heavy chain isotypes. *Mol. Immunol.* **48**, 2220–2223 (2011).
31. Lohi, O., Parikka, M. & Ramet, M. The zebrafish as a model for paediatric diseases. *Acta Paediatr.* **102**, 104–110 (2013).
32. Stinear, T. P. *et al*. Insights from the complete genome sequence of *Mycobacterium marinum* on the evolution of *Mycobacterium tuberculosis*. *Genome Res.* **18**, 729–741 (2008).

33. El-Etr, S. H., Yan, L. & Cirillo, J. D. Fish monocytes as a model for mycobacterial host-pathogen interactions. *Infect. Immun.* **69**, 7310–7317 (2001).
34. Barker, L. P., George, K. M., Falkow, S. & Small, P. L. Differential trafficking of live and dead *Mycobacterium marinum* organisms in macrophages. *Infect. Immun.* **65**, 1497–1504 (1997).
35. Parikka, M. *et al*. *Mycobacterium marinum* causes a latent infection that can be reactivated by gamma irradiation in adult zebrafish. *Plos Pathog.* **8**, e1002944, https://doi.org/10.1371/journal.ppat.1002944 (2012).
36. Prouty, M. G., Correa, N. E., Barker, L. P., Jagadeeswaran, P. & Klose, K. E. Zebrafish-*Mycobacterium marinum* model for mycobacterial pathogenesis. *FEMS Microbiol. Lett.* **225**, 177–182 (2003).
37. Swaim, L. E. *et al*. *Mycobacterium marinum* infection of adult zebrafish causes caseating granulomatous tuberculosis and is moderated by adaptive immunity. *Infect. Immun.* **74**, 6108–6117 (2006).
38. Carvalho, R. *et al*. A high-throughput screen for tuberculosis progression. *Plos One* **6**, e16779, https://doi.org/10.1371/journal.pone.0016779 (2011).
39. Dalton, J. P. *et al*. Screening of anti-mycobacterial compounds in a naturally infected zebrafish larvae model. *J. Antimicrob. Chemother.* **72**, 421–427 (2017).
40. Davis, J. M. *et al*. Real-time visualization of mycobacterium-macrophage interactions leading to initiation of granuloma formation in zebrafish embryos. *Immunity* **17**, 693–702 (2002).
41. Piazzon, M. C., Lutfalla, G. & Forlenza, M. IL10, A tale of an evolutionarily conserved cytokine across vertebrates. *Crit. Rev. Immunol.* **36**, 99–129 (2016).
42. Zhang, D. C., Shao, Y. Q., Huang, Y. Q. & Jiang, S. G. Cloning, characterization and expression analysis of *interleukin-10* from the zebrafish (*Danio rerion*). *J. Biochem. Mol. Biol.* **38**, 571–576 (2005).
43. Grayfer, L. & Belosevic, M. Identification and molecular characterization of the *interleukin-10* receptor 1 of the zebrafish (*Danio rerio*) and the goldfish (*Carassius auratus* L.). *Dev. Comp. Immunol.* **36**, 408–417 (2012).
44. Kettleborough, R. N. *et al*. A systematic genome-wide analysis of zebrafish protein-coding gene function. *Nature* **496**, 494–497 (2013).
45. Nickless, A., Bailis, J. M. & You, Z. Control of gene expression through the nonsense-mediated RNA decay pathway. *Cell. Biosci.* **7**, 7; https://doi.org/10.1186/s13578-017-0153-7 eCollection2017 (2017).
46. Petersen, T. N., Brunak, S., von Heijne, G. & Nielsen, H. SignalP 4.0: discriminating signal peptides from transmembrane regions. *Nat. Methods* **8**, 785–786 (2011).
47. Bristol, I. J., Mahler, M. & Leiter, E. H. Interleukin-10 gene targeted mutation. *JAX notes* (1997).
48. Kuhn, R., Lohler, J., Rennick, D., Rajewsky, K. & Muller, W. Interleukin-10-deficient mice develop chronic enterocolitis. *Cell* **75**, 263–274 (1993).
49. Keubler, L. M., Buettner, M., Hager, C. & Bleich, A. A Multihit Model: Colitis Lessons from the Interleukin-10-deficient Mouse. *Inflamm. Bowel Dis.* **21**, 1967–1975 (2015).
50. Gomes-Santos, A. C. *et al*. New insights into the immunological changes in IL-10-deficient mice during the course of spontaneous inflammation in the gut mucosa. *Clin. Dev. Immunol.* **2012**, 560817, https://doi.org/10.1155/2012/560817 (2012).
51. Ojanen, M. J. *et al*. The proprotein convertase subtilisin/kexin furinA regulates zebrafish host response against *Mycobacterium marinum*. *Infect. Immun.* **83**, 1431–1442 (2015).
52. Barsig, J. *et al*. Lipopolysaccharide-induced interleukin-10 in mice: role of endogenous tumor necrosis factor-alpha. *Eur. J. Immunol.* **25**, 2888–2893 (1995).
53. Verbon, A. *et al*. Serum concentrations of cytokines in patients with active tuberculosis (TB) and after treatment. *Clin. Exp. Immunol.* **115**, 110–113 (1999).
54. Del Prete, G. *et al*. Human IL-10 is produced by both type 1 helper (Th1) and type 2 helper (Th2) T cell clones and inhibits their antigen-specific proliferation and cytokine production. *J. Immunol.* **150**, 353–360 (1993).
55. van Crevel, R., Ottenhoff, T. H. & van der Meer, J. W. Innate immunity to *Mycobacterium tuberculosis*. *Clin. Microbiol. Rev.* **15**, 294–309 (2002).
56. Myllymäki, H., Niskanen, M., Luukinen, H., Parikka, M. & Ramet, M. Identification of protective postexposure mycobacterial vaccine antigens using an immunosuppression-based reactivation model in the zebrafish. *Dis. Model. Mech*. **11**, https://doi.org/10.1242/dmm.033175 (2018).
57. Myllymäki, H., Niskanen, M., Oksanen, K. E. & Rämet, M. Animal models in tuberculosis research – where is the beef? *Expert Opinion on Drug Discovery* **10**, 871–883 (2015).
58. Lin, P. L. *et al*. Quantitative comparison of active and latent tuberculosis in the cynomolgus macaque model. *Infect. Immun.* **77**, 4631–4642 (2009).
59. Subbian, S. *et al*. Spontaneous latency in a rabbit model of pulmonary tuberculosis. *Am. J. Pathol.* **181**, 1711–1724 (2012).
60. Subbian, S. *et al*. Molecular immunologic correlates of spontaneous latency in a rabbit model of pulmonary tuberculosis. *Cell. Commun. Signal.* **11**, 16, https://doi.org/10.1186/1478-811X-11-16 (2013).
61. Shi, C., Shi, J. & Xu, Z. A review of murine models of latent tuberculosis infection. *Scand. J. Infect. Dis.* **43**, 848–856 (2011).
62. Broussard, G. W. & Ennis, D. G. *Mycobacterium marinum* produces long-term chronic infections in medaka: a new animal model for studying human tuberculosis. *Comp. Biochem. Physiol. C. Toxicol. Pharmacol.* **145**, 45–54 (2007).
63. Ruley, K. M. *et al*. Identification of *Mycobacterium marinum* virulence genes using signature-tagged mutagenesis and the goldfish model of mycobacterial pathogenesis. *FEMS Microbiol. Lett.* **232**, 75–81 (2004).
64. Talaat, A. M., Reimschuessel, R., Wasserman, S. S. & Trucksis, M. Goldfish, *Carassius auratus*, a novel animal model for the study of *Mycobacterium marinum* pathogenesis. *Infect. Immun.* **66**, 2938–2942 (1998).
65. Myllymäki, H., Bäuerlein, C. A. & Rämet, M. The zebrafish breathes new life into the study of tuberculosis. *Front. Immunol.* **7**, 196, https://doi.org/10.3389/fimmu.2016.00196 (2016).
66. Sakaguchi, S. Regulatory T cells: history and perspective. *Methods Mol. Biol.* **707**, 3–17 (2011).
67. Sakaguchi, S. Regulatory T cells: key controllers of immunologic self-tolerance. *Cell* **101**, 455–458 (2000).
68. Pesu, M. *et al*. T-cell-expressed proprotein convertase furin is essential for maintenance of peripheral immune tolerance. *Nature* **455**, 246–250 (2008).
69. Brugman, S. The zebrafish as a model to study intestinal inflammation. *Dev. Comp. Immunol.* **64**, 82–92 (2016).
70. Brugman, S. *et al*. Oxazolone-induced enterocolitis in zebrafish depends on the composition of the intestinal microbiota. *Gastroenterology* **137**, 1757.e1, https://doi.org/10.1053/j.gastro.2009.07.069 (2009).
71. Paul, G., Khare, V. & Gasche, C. Inflamed gut mucosa: downstream of interleukin-10. *Eur. J. Clin. Invest.* **42**, 95–109 (2012).
72. Piazzon, M. C., Savelkoul, H. S., Pietretti, D., Wiegertjes, G. F. & Forlenza, M. Carp Il10 has anti-inflammatory activities on phagocytes, promotes proliferation of memory T cells, and regulates B cell differentiation and antibody secretion. *J. Immunol.* **194**, 187–199 (2015).
73. Redford, P. S., Murray, P. J. & O'Garra, A. The role of IL-10 in immune regulation during *M. tuberculosis* infection. *Mucosal Immunol.* **4**, 261–270 (2011).
74. Benard, E. L. *et al*. Infection of zebrafish embryos with intracellular bacterial pathogens. *J. Vis. Exp*. **61**, https://doi.org/10.3791/3781 (2012).
75. Turner, J. *et al*. *In vivo* IL-10 production reactivates chronic pulmonary tuberculosis in C57BL/6 mice. *J. Immunol.* **169**, 6343–6351 (2002).

76. Cilfone, N. A., Perry, C. R., Kirschner, D. E. & Linderman, J. J. Multi-scale modeling predicts a balance of tumor necrosis factor-alpha and interleukin-10 controls the granuloma environment during *Mycobacterium tuberculosis* infection. *Plos One* **8**, e68680, https://doi.org/10.1371/journal.pone.0068680 (2013).
77. Cooper, A. M. Cell-mediated immune responses in tuberculosis. *Annu. Rev. Immunol.* **27**, 393–422 (2009).
78. Korb, V. C., Chuturgoon, A. A. & Moodley, D. *Mycobacterium tuberculosis*: Manipulator of protective immunity. *Int. J. Mol. Sci.* **17**, 131, https://doi.org/10.3390/ijms17030131 (2016).
79. Lyadova, I. V. & Panteleev, A. V. Th1 and Th17 cells in tuberculosis: Protection, pathology, and biomarkers. *Mediators Inflamm.* **2015**, 854507, https://doi.org/10.1155/2015/854507 (2015).
80. Tang, R., Dodd, A., Lai, D., McNabb, W. C. & Love, D. R. Validation of zebrafish (*Danio rerio)* reference genes for quantitative real-time RT-PCR normalization. *Acta Biochim. Biophys. Sin. (Shanghai)* **39**, 384–390 (2007).
81. Oksanen, K. E. *et al.* An adult zebrafish model for preclinical tuberculosis vaccine development. *Vaccine* **31**, 5202–5209 (2013).
82. Tuominen, V. J. & Isola, J. The application of JPEG2000 in virtual microscopy. *J. Digit. Imaging* **22**, 250–258 (2009).
83. Martin, M. Cutadapt removes adapter sequences from high-throughput sequencing reads. *EMBnet.journal* **17**, 12 (2011).
84. Langmead, B. & Salzberg, S. L. Fast gapped-read alignment with Bowtie 2. *Nat. Methods* **9**, 357–359 (2012).
85. Faust, G. G. & Hall, I. M. SAMBLASTER: fast duplicate marking and structural variant read extraction. *Bioinformatics* **30**, 2503–2505 (2014).
86. Wang, K., Li, M. & Hakonarson, H. ANNOVAR: functional annotation of genetic variants from high-throughput sequencing data. *Nucleic Acids Res.* **38**, e164, https://doi.org/10.1093/nar/gkq603 (2010).
87. Robinson, J. T. *et al*. Integrative genomics viewer. *Nat. Biotechnol.* **29**, 24–26 (2011).

Acknowledgements

This study was financially supported by the Academy of Finland (M.R., 277495), the Sigrid Juselius Foundation (M.R.), the Jane and Aatos Erkko Foundation (M.R.), the Competitive State Research Financing of the Expert Responsibility Area of Tampere University Hospital (M.R.), Competitive State Research Financing of the Expert Responsibility area of Oulu University Hospital (M.R.) and the Tampere Tuberculosis Foundation (M.R., S.-K.H.), the Emil Aaltonen Foundation (S.-K.H), Foundation of the Finnish Anti-Tuberculosis Association (S.-K.H.), the City of Tampere Science Foundation (S.-K.H), the Väinö and Laina Kivi Foundation (S.-K.H.), the Finnish Cultural Foundation, the Central Foundation (S.-K.H.), the Finnish Concordia Fund (S.-K.H.), Orion Research Foundation sr (S.-K.H) and University of Tampere Doctoral Programme in Biomedicine and Biotechnology (M.O.). We thank the Tampere Zebrafish Core Facility, partly funded by Biocenter Finland, for maintaining and providing the zebrafish, Hannaleena Piippo, Jenna Ilomäki, Leena Mäkinen, Tuula Myllymäki and Sami Leino for technical assistance, Marko Pesu, Mataleena Parikka and Hannu Turpeinen for scientific advice and support, Heini Huhtala for the statistical advice and Helen Cooper for proof-reading this manuscript.

Author Contributions

S.-K.H., M.O., M.N. and M.R. designed the experiments. S.-K.H., M.O., S.T. and M.R. wrote the paper. S.-K.H. and M.O. performed the experiments. S.-K.H., M.O., S. T and M.N. analyzed the data. All authors reviewed and approved the manuscript.

Additional Information

Supplementary information accompanies this paper at https://doi.org/10.1038/s41598-018-28511-w.

Competing Interests: The authors declare no competing interests.

Publisher's note: Springer Nature remains neutral with regard to jurisdictional claims in published maps and institutional affiliations.

interleukin 10 mutant zebrafish have an enhanced *interferon gamma* response and improved survival against a *Mycobacterium marinum* infection

Sanna-Kaisa E. Harjula, Markus J.T. Ojanen, Sinja Taavitsainen, Matti Nykter, Mika Rämet*

***Corresponding author:** Correspondence to Mika Rämet, phone: 358-50-4336276, Email: mika.ramet@uta.fi

Supplementary Figures

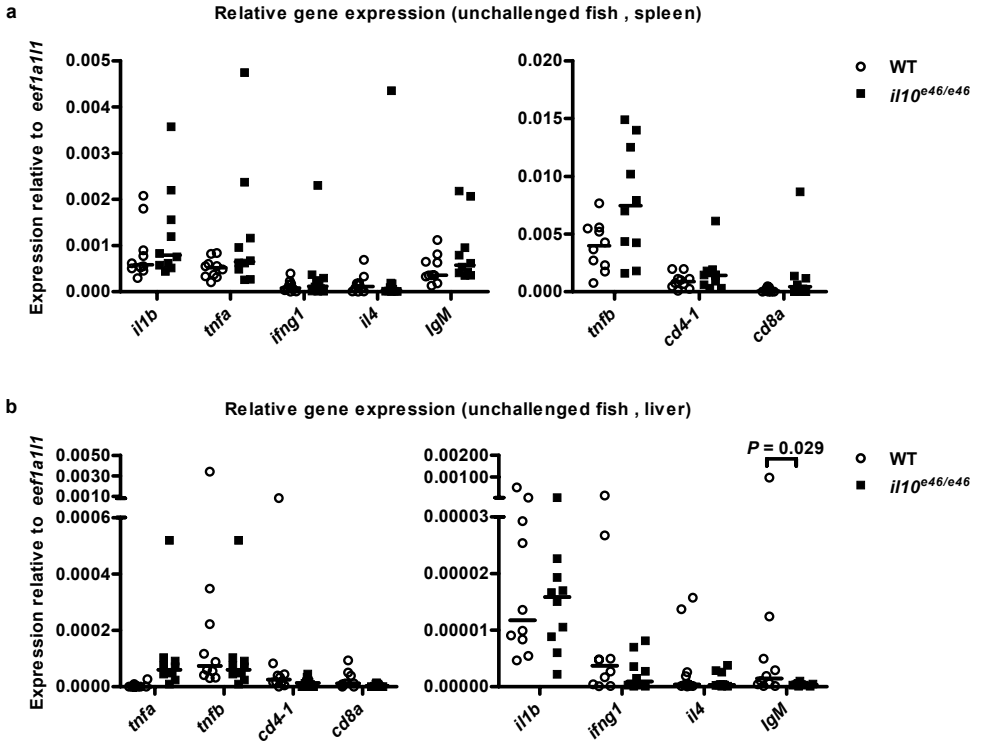

Supplementary Figure S1

Unchallenged *il10*$^{e46/e46}$ zebrafish have similar expression profiles of lymphocyte markers and cytokines as WT control fish in the spleen and liver **(a - b)**. The relative expression of selected proinflammatory cytokines (*il1b*, *tnfa*, *tnfb*), Th cell cytokines *(ifng1* and *il4*), T cell markers *(cd4 and cd8)* as well as a B cell marker (*IgM*) in *il10*$^{e46/e46}$ mutant zebrafish and WT controls in spleen and liver from the same individuals (n = 10 in both groups) were quantified with qPCR and are represented as scatter dot plot and median. Note the different scales of the y axes and the divided y axis in panel b. Gene expressions were normalized to the expression of *eef1a1l1*. A two-tailed Mann-Whitney test was used for the statistical comparison of differences between *il10*$^{e46/e46}$ zebrafish and WT controls.

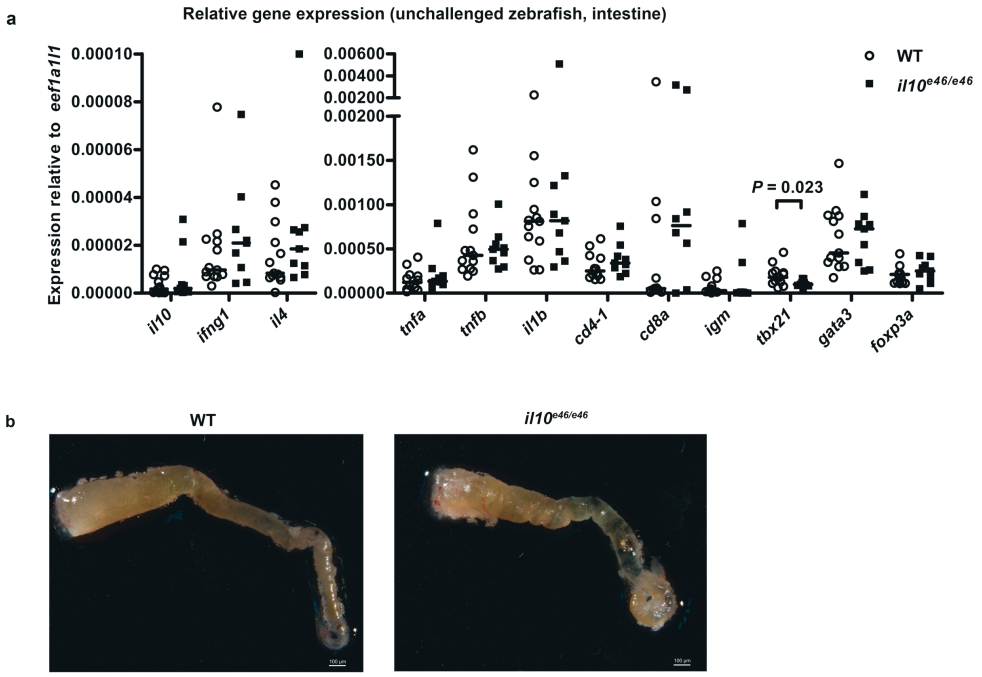

Supplementary Figure S2

Unchallenged *il10*$^{e46/e46}$ zebrafish have similar expression profiles of lymphocyte markers and cytokines as WT control fish in the intestine. **(a)** The relative expression of *il10*, selected proinflammatory cytokines (*il1b*, *tnfa*, *tnfb*), Th cell cytokines (*ifng1* and *il4*), T cell markers *(cd4-1 and cd8a*), a B cell marker (*IgM*) as well as Cd4+ lymphocyte transcription factors (*tbx21, gata3*, *foxp3a*) in *il10*$^{e46/e46}$ mutant zebrafish (n = 9) and WT controls (n = 13) in intestine were quantified with qPCR and are represented as scatter dot plot and median. Note the different scales of the y axes and the divided y axis. Gene expressions were normalized to the expression of *eef1a1l1*. A two-tailed Mann-Whitney test was used for the statistical comparison of differences between *il10*$^{e46/e46}$ zebrafish and WT controls. **(b)** The visual appearance of *il10*$^{e46/e46}$ mutant and WT control zebrafish intestine was studied by microscopy (n = 3 in both groups). A representative image from each group is shown.

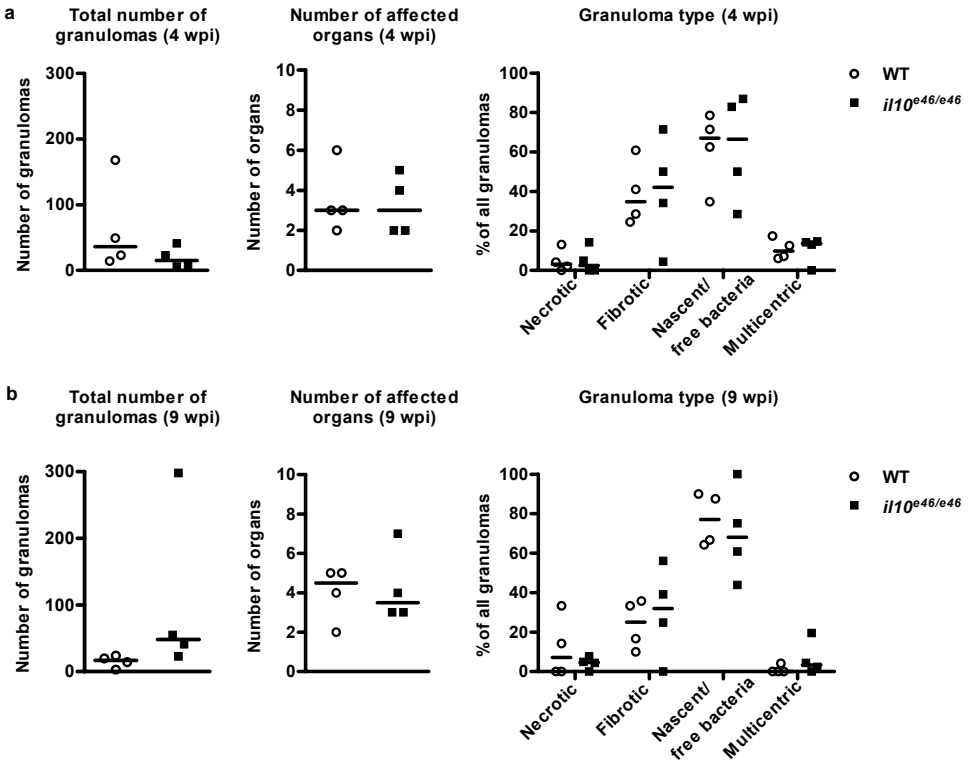

Supplementary Figure S3

There are no differences in the quantity or quality of granulomas between *il10*$^{e46/e46}$ zebrafish and WT controls in histological analysis. **(a-b)** The number of *M. marinum* granulomas were counted and the affected organs and the type of granulomas were identified in *il10*$^{e46/e46}$ zebrafish and WT controls from Ziehl-Neelsen stained sections (n = 4 in both groups at both time points) at 4 and 9 weeks post a low-dose infection (2 - 9 CFU). The granulomas were placed in one or several of the following categories: necrotic, fibrotic, multicentric, and nascent granuloma/a site of free bacteria. A two-tailed Mann-Whitney test was used for the statistical comparison of differences between *il10*$^{e46/e46}$ zebrafish and WT controls.

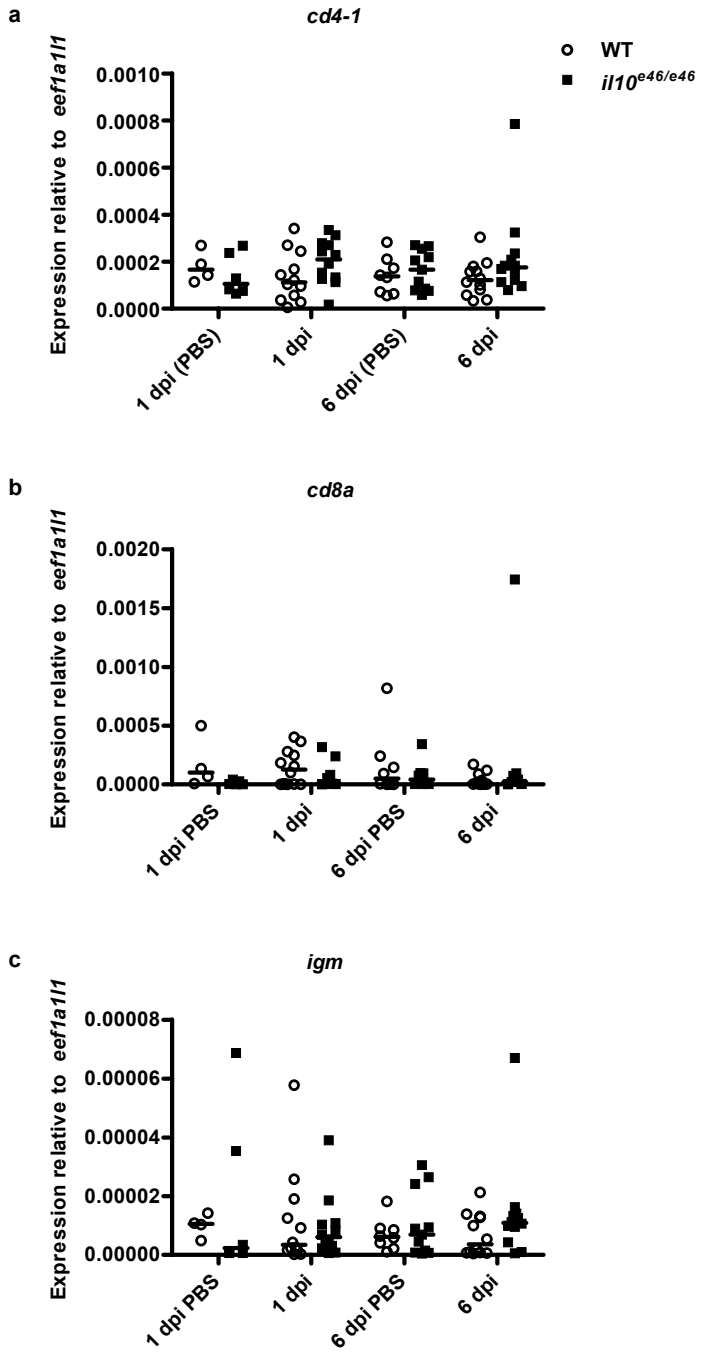
a
cd4-1
WT
il10e46/e46
Expression relative to eef1a1l1
0.0010
0.0008
0.0006
0.0004
0.0002
0.0000
1 dpi (PBS)
1 dpi
6 dpi (PBS)
6 dpi
b
cd8a
Expression relative to eef1a1l1
0.0020
0.0015
0.0010
0.0005
0.0000
1 dpi PBS
1 dpi
6 dpi PBS
6 dpi
c
igm
Expression relative to eef1a1l1
0.00008
0.00006
0.00004
0.00002
0.00000
1 dpi PBS
1 dpi
6 dpi PBS
6 dpi

Supplementary Figure S4

il10$^{e46/e46}$ mutation does not affect the expression levels of lymphocyte markers at the early stages of a low-dose mycobacterial infection. **(a - c)** The relative expression levels of T cell markers (*cd4-1* and *cd8a*) as well as the B cell marker *IgM* were measured in the abdominal organ blocks (including kidney) of *il10*$^{e46/e46}$ mutant fish (n = 4 - 12) and WT controls (n = 5 - 12) at 1 dpi and 6 days post a low-dose (2 - 9 CFU) infection and are presented as a scatter dot plot and median. Note the different scales on the y axes. Gene expressions were normalized to the expression of *eef1a1l1*. The data were collected from a single experiment. In panels a - c a two-tailed Mann-Whitney test was used for the statistical comparison of differences.

Supplementary Tables S1-S3 are provided as separate files.

Supplementary Table S1

All mutations found in the whole genome sequencing analysis. P values were calculated with Fisher's exact test, $P < 0.05$ was considered significant.

Supplementary Table S2

Stop codon or frameshift causing mutations found in the whole genome sequencing analysis. Mutations with allele fraction of ≥ 25 % in either of the groups are shown here. P values were calculated with Fisher's exact test, $P < 0.05$ was considered significant.

Supplementary Table S3

Stop codon or frameshift causing mutations found in the whole genome sequencing analysis that differ significantly between *il10*$^{e46/e46}$ and WT zebrafish. P values were calculated with Fisher's exact test, $P < 0.05$ was considered significant.

Supplementary Table S4

qPCR primers used for gene expression analysis

Gene[1]	ZFIN ID	Human gene ortholog (HGNC)	Sequence 5' - 3'	Reference
eef1a1l1 (ef1a)	ZDB-GENE-990415-52	*EEF1A1*	F CTGGAGGCCAGCTCAAACAT	(80)
			R ATCAAGAAGAGTAGTACCGCTAGCATTAC	
il10	ZDB-GENE-051111-1	*IL10*	F GCTCTGCTCACGCTTCTTC	(51)
			R TGGTTCCAAGTCATCGTTG	
tnfa	ZDB-GENE-050317-1	*TNF*	F GGGCAATCAACAAGATGGAAG	(35)
			R GCAGCTGATGTGCAAAGACAC	
tnfb	ZDB-GENE-050601-2	*TNF*	F GCATGTGATGAAGCCAAACG	-
			R GATTGTCCTGAAGGGTCACC	
il1b	ZDB-GENE-040702-2	*IL1B*	F TGGACTTCGCAGCACAAAATG	(88)
			R GTTCACTTCACGCTCTTGGATG	
cd4-1	ZDB-GENE-100922-280	*CD4*	F TAAAGCACAAGAAAGCCATG	-
			R TACTCTGCGGGTTCCTGTTG	
cd8a	ZDB-GENE-060210-2	*CD8A*	F GGAGTACCAGATCCAGTAACACAC	-
			R AACCTCCGACCAGAGATGTG	
IgM	ZDB-GENE-030925-46	*IGHM*	F AGATCCAATACAAAGATACTATGC	(21)
			R TGGTGAAATGGAATTGTGG	
tbx21	ZDB-GENE-080104-3	*TBX21*	F GGCCTACCAGAATGCAGACA	(27)
			R GGTGCGTACAGCGTGTCATA	
gata3	ZDB-GENE-990415-82	*GATA3*	F GGATGGCACC GGTC ACTATT	(27)
			R CAGCAGACAGCCTCCGTTT	
foxp3a	ZDB-GENE-061116-2	*FOXP3*	F CAAAAGCAGAGTGCCAGTGG	(27)
			R CGCATAAGCAC CGATTCTGC	
ifng1	ZDB-GENE-040629-1	*IFNG*	F CTTTCCAGGCAAGAGTGCAGA	(89)
			R TCAGCTCAAACAAAGCCTTTCG	
il4	ZDB-GENE-100204-1	*IL4*	F CCAGAGTGTGAATGGGATCC	-
			R TTTCCAGTCCCGGTATATGC	

[1] Zebrafish gene names and qPCR primer sequences are listed accompanied with the ZFIN identification codes and the names of the orthologous genes in humans. HGNC, HUGO Gene Nomenclature Committee.

Supplementary References

88. Pressley, M. E., Phelan, P. E.,3rd, Witten, P. E., Mellon, M. T. & Kim, C. H. Pathogenesis and inflammatory response to *Edwardsiella tarda* infection in the zebrafish. *Dev. Comp. Immunol.* **29**, 501-513 (2005).

89. Vojtech, L. N., Sanders, G. E., Conway, C., Ostland, V. & Hansen, J. D. Host immune response and acute disease in a zebrafish model of *Francisella pathogenesis*. *Infect. Immun.* **77**, 914-925 (2009).

interleukin 10 **mutant zebrafish have an enhanced** ***interferon gamma*** **response and improved survival against a** ***Mycobacterium marinum*** **infection**

Sanna-Kaisa E. Harjula, Markus J.T. Ojanen, Sinja Taavitsainen, Matti Nykter, Mika Rämet*

Supplementary Table S2

Stop codon or frameshift causing mutations found in the whole genome sequencing analysis.

Mutations with allele fraction of ≥ 25 % in either of the groups are shown here. *P* values were calculated with Fisher's exact test, $P < 0.05$ was considered significant.

Chromosome	Position	Reference sequence	Mutated sequence	Gene	Mutation effect	Allele fraction in *il10*$^{e46/e46}$	Total reads in *il10*$^{e46/e46}$	Allele fraction in WT	Total reads in WT	*P value*
Allele fraction 100 % in *il10*$^{e46/e46}$										
chr11	21138119	A	T	*il10*	Stopgain p.K28X	100.0 %	9	0.0 %	12	0.000
chr22	6078391	A	C	*si:dkey-19a16.2*	Stopgain p.Y52X	100.0 %	21	100.0 %	61	1.000
Allele fraction ≥ 50 and < 100 % in *il10*$^{e46/e46}$										
chr20	25568916	CT	C	*cyp2p7*	Frameshift p.S43fs	75.4 %	65	79.0 %	62	0.676
chr24	16547360	A	T	*sema5a*	Stopgain p.K31X	73.0 %	37	74.5 %	47	1.000
chr20	46261469	C	CAT	*taar14j*	Frameshift p.S260fs	64.7 %	17	66.7 %	18	1.000
chr3	13440882	CTTCCT	C	*si:dkey-117i10.1*	Frameshift p.T24fs	64.3 %	28	19.4 %	36	0.000
chr17	16450701	G	GCC	*efcab11*	Frameshift p.A124fs	61.5 %	26	60.0 %	25	1.000
chr24	9977936	TGA	T	*zgc:171977*	Frameshift p.L390fs	58.8 %	34	60.0 %	30	1.000
chr8	25858331	A	AT	*opn7c*	Frameshift p.M399fs	55.6 %	36	64.5 %	31	0.618
chr2	51656679	AT	A	*abhd4*	Frameshift p.I332fs	52.0 %	50	79.2 %	72	0.003
chr1	47416639	G	A	*gja5b*	Stopgain p.R68X	50.0 %	70	47.6 %	63	0.863
chr15	38019260	C	G	*si:ch73-380l3.2*	Stopgain p.Y130X	50.0 %	40	33.9 %	59	0.144
Allele fraction ≥ 25 and < 50 % in *il10*$^{e46/e46}$										
chr6	23117185	G	A	*ten1*	Stopgain p.Q35X	48.1 %	27	51.9 %	27	1.000
chr22	6099168	T	A	*zgc:171887*	Stopgain p.L270X	47.4 %	19	72.4 %	29	0.127
chr5	54416778	G	C	*coq4*	Stopgain p.Y272X	45.2 %	42	64.4 %	59	0.068
chr17	11391712	ATGTT	A	*arid4a*	Frameshift p.N1188fs	44.4 %	36	30.0 %	50	0.181
chr10	25055	T	TGTGTGCGTGC	*riox2*	Frameshift p.V307fs	44.2 %	86	37.3 %	102	0.372
chr10	35009853	G	GGTTAACAC	*exosc8*	Stopgain p.G239_G240delinsGX	42.1 %	19	36.4 %	22	0.757
chr2	118346	G	GA	*znfl2a*	Frameshift p.Q305fs	40.3 %	67	21.8 %	55	0.033
chr19	7106900	TATCCC	T	*psmb8a*	Frameshift p.L155fs	39.0 %	41	47.5 %	40	0.505
chr25	35664623	CT	C	*lrrk2*	Frameshift p.K16fs	38.9 %	36	56.8 %	37	0.162
chr7	39668850	G	GC	*zgc:158564*	Frameshift p.G6fs	38.0 %	50	40.0 %	45	1.000
chr14	5816714	G	A	*kazald2*	Stopgain p.Q24X	37.3 %	75	44.2 %	86	0.424
chr3	4536062	A	T	*ftr43*	Stopgain p.Y435X	36.7 %	49	42.2 %	45	0.674
chr19	20415113	A	AG	*tbc1d5*	Frameshift p.P499fs	36.4 %	22	44.4 %	36	0.593
chr19	20415118	ATGAC	A	*tbc1d5*	Frameshift p.P496fs	36.4 %	22	42.1 %	38	0.787

chr21	39187384	GTT	G	*cryba1b*	Frameshift p.R28fs	36.4 %	22	3.0 %	33	0.002
chr17	19506128	C	T	*slc22a15*	Stopgain p.R226X	34.4 %	32	50.0 %	34	0.223
chr7	5156566	C	A	*zgc:195075*	Stopgain p.E232X	33.8 %	68	55.1 %	78	0.012
chr5	11413501	C	T	*zgc:112294*	Stopgain p.Q220X	33.3 %	60	58.2 %	55	0.009
chr16	42487920	C	T	*herpud2*	Stopgain p.Q164X	32.4 %	68	51.9 %	79	0.020
chr6	8072865	C	CA	*palm3*	Frameshift p.S359fs	31.8 %	22	10.0 %	20	0.135
chr19	646131	G	A	*slc6a18*	Stopgain p.Q613X	31.1 %	74	56.8 %	74	0.003
chr23	36178138	C	A	*hoxc1a*	Stopgain p.S12X	31.0 %	29	28.2 %	39	1.000
chr7	58130525	ATG	A	*ank2b*	Frameshift	30.5 %	59	36.4 %	55	0.555
chr19	19738811	G	GA	*hoxa11a*	Frameshift p.E298fs	30.0 %	40	43.1 %	58	0.210
chr2	47811514	GT	G	*mbnl1*	Frameshift p.F282fs	29.8 %	57	26.1 %	88	0.705
chr15	43923860	G	GGTGTGT	*naalad2*	Stopgain p.E264delinsGVX	29.5 %	44	18.2 %	33	0.295
chr25	3360318	A	AC	*chchd3b*	Frameshift p.T145fs	29.4 %	34	41.2 %	34	0.447
chr20	39399318	C	T	*pimr136*	Stopgain p.Q495X	29.4 %	34	35.2 %	54	0.646
chr16	20014268	TATTGTCTGA	T	*ahr1a*	Frameshift p.I652fs	29.0 %	31	59.3 %	27	0.033
chr15	44188370	C	CGA	*zgc:165514*	Frameshift p.D209fs	28.1 %	57	33.9 %	62	0.555
chr20	776081	A	AACACACACAC	*myo6a*	Frameshift p.X1289delinsX	27.8 %	72	32.1 %	84	0.602
chr7	73453601	T	A	*cbln8*	Stopgain p.L26X	26.7 %	30	37.8 %	37	0.435
chr14	7519685	T	TA	*gfra3*	Frameshift p.X459delinsX	26.7 %	30	33.3 %	30	0.779
chr4	76500798	T	A	*ms4a17a.17*	Stopgain p.Y160X	26.5 %	68	24.0 %	75	0.847
chr4	72217012	G	T	*zgc:165515*	Stopgain p.E67X	26.3 %	38	9.3 %	54	0.044
chr6	49771733	C	T	*ctsz*	Stopgain p.Q32X	25.9 %	27	67.9 %	28	0.003
chr10	24771	G	GGTGT	*riox2*	Frameshift p.Q245fs	25.5 %	137	26.9 %	119	0.887
chr23	25942120	T	TA	*pkig*	Frameshift p.X78delinsX	25.0 %	40	43.9 %	41	0.102
chr21	45334440	GGTGTGT	G	*tcf7*	Frameshift p.G331fs	25.0 %	80	16.5 %	97	0.191

Allele fraction < 25 % il10$^{e46/e46}$ and > 25 % in WT

chr19	316892	C	CATCTG	*ctss1*	Frameshift p.T238fs	22.1 %	77	44.0 %	91	0.003
chr8	16587853	CT	C	*calr*	Frameshift p.K216fs	20.3 %	64	30.6 %	134	0.172
chr2	41936758	G	T	*ebi3*	Stopgain p.Y270X	16.3 %	43	39.3 %	61	0.016
chr8	16587873	T	A	*calr*	Stopgain p.K210X	12.3 %	65	28.6 %	126	0.011
chr1	31846955	C	A	*nt5c2b*	Stopgain p.E45X	9.1 %	11	50.0 %	16	0.042
chr25	19706102	GCTTTACAGCTGTTTTGAC	G	*mxg*	Frameshift p.A241fs	7.1 %	14	44.8 %	29	0.016

interleukin 10 **mutant zebrafish have an enhanced** ***interferon gamma*** **response and improved survival against a** ***Mycobacterium marinum*** **infection**

Sanna-Kaisa E. Harjula, Markus J.T. Ojanen, Sinja Taavitsainen, Matti Nykter, Mika Rämet*

Supplementary Table S3

Stop codon or frameshift causing mutations found in the whole genome sequencing analysis that differ significantly between ***il10*** $^{e46/e46}$ **and WT zebrafish**

Mutations with allele fraction of ≥ 25 % in either of the groups are shown here. *P* values were calculated with Fisher's exact test, $P < 0.05$ was considered significant.

Chromosome	Position	Reference sequence	Mutated sequence	Gene	Mutation effect	Allele fraction in *il10* $^{e46/e46}$	Total reads in *il10* $^{e46/e46}$	Allele fraction in WT	Total reads in WT	*P value*
chr11	21138119	A	T	*il10*	Stopgain p.K28X	100.0 %	9	0.0 %	12	0.000
chr3	13440882	CTTCCT	C	*si:dkey-117i10.1*	Frameshift p.T24fs	64.3 %	28	19.4 %	36	0.000
chr21	39187384	GTT	G	*cryba1b*	Frameshift p.R28fs	36.4 %	22	3.0 %	33	0.002
chr2	51656679	AT	A	*abhd4*	Frameshift p.I332fs	52.0 %	50	79.2 %	72	0.003
chr19	646131	G	A	*slc6a18*	Stopgain p.Q613X	31.1 %	74	56.8 %	74	0.003
chr6	49771733	C	T	*ctsz*	Stopgain p.Q32X	25.9 %	27	67.9 %	28	0.003
chr19	316892	C	CATCTG	*ctss1*	Frameshift p.T238fs	22.1 %	77	44.0 %	91	0.003
chr5	11413501	C	T	*zgc:112294*	Stopgain p.Q220X	33.3 %	60	58.2 %	55	0.009
chr8	16587873	T	A	*calr*	Stopgain p.K210X	12.3 %	65	28.6 %	126	0.011
chr7	5156566	C	A	*zgc:195075*	Stopgain p.E232X	33.8 %	68	55.1 %	78	0.012
chr2	41936758	G	T	*ebi3*	Stopgain p.Y270X	16.3 %	43	39.3 %	61	0.016
chr25	19706102	GCTTTACAGCTGTTTTGAC	G	*mxg*	Frameshift p.A241fs	7.1 %	14	44.8 %	29	0.016
chr16	42487920	C	T	*herpud2*	Stopgain p.Q164X	32.4 %	68	51.9 %	79	0.020
chr2	118346	G	GA	*znfl2a*	Frameshift p.Q305fs	40.3 %	67	21.8 %	55	0.033
chr16	20014268	TATTGTCTGA	T	*ahr1a*	Frameshift p.I652fs	29.0 %	31	59.3 %	27	0.033
chr1	31846955	C	A	*nt5c2b*	Stopgain p.E45X	9.1 %	11	50.0 %	16	0.042
chr4	72217012	G	T	*zgc:165515*	Stopgain p.E67X	26.3 %	38	9.3 %	54	0.044

PUBLICATION III

Characterization of immune response against *Mycobacterium marinum* infection in the main hematopoietic organ of adult zebrafish (*Danio rerio)*

Harjula S-KE, Saralahti AK, Ojanen MJT, Rantapero T, Uusi-Mäkelä MIE, Nykter M, Lohi O, Parikka M, Rämet M.

Developmental and Comparative Immunology. 2020. 103:103523.
doi: 10.1016/j.dci.2019.103523.

Developmental and Comparative Immunology 103 (2020) 103523

Contents lists available at ScienceDirect

Developmental and Comparative Immunology

journal homepage: www.elsevier.com/locate/devcompimm

Characterization of immune response against *Mycobacterium marinum* infection in the main hematopoietic organ of adult zebrafish (*Danio rerio*)

Sanna-Kaisa E. Harjula[a], Anni K. Saralahti[a], Markus J.T. Ojanen[a,b], Tommi Rantapero[c], Meri I.E. Uusi-Mäkelä[a], Matti Nykter[c], Olli Lohi[d], Mataleena Parikka[e,f], Mika Rämet[a,g,h,i,*]

[a] *Laboratory of Experimental Immunology, BioMediTech, Faculty of Medicine and Health Technology, FI-33014, Tampere University, Finland*
[b] *Laboratory of Immunoregulation, BioMediTech, Faculty of Medicine and Health Technology, FI-33014, Tampere University, Finland*
[c] *Laboratory of Computational Biology, BioMediTech, Faculty of Medicine and Health Technology, FI-33014, Tampere University, Finland*
[d] *Tampere Center for Child Health Research, Tampere University and Tays Cancer Center, Tampere University Hospital, FI-33014, Tampere University, Finland*
[e] *Laboratory of Infection Biology, BioMediTech, Faculty of Medicine and Health Technology, FI-33014, Tampere University, Finland*
[f] *Oral and Maxillofacial Unit, Tampere University Hospital, P.O. Box 2000, FI-33521, Tampere, Finland*
[g] *Department of Pediatrics, Tampere University Hospital, P.O. Box 2000, FI-33521, Tampere, Finland*
[h] *PEDEGO Research Unit, Medical Research Center Oulu, P.O. Box 8000, FI-90014, University of Oulu, Finland*
[i] *Department of Children and Adolescents, Oulu University Hospital, P.O. Box 10, FI-90029, OYS, Finland*

ARTICLE INFO

Keywords:
Zebrafish
Mycobacterium marinum
Transcriptome analysis
Forward genetic screen

ABSTRACT

Tuberculosis remains a major global health challenge. To gain information about genes important for defense against tuberculosis, we used a well-established tuberculosis model; *Mycobacterium marinum* infection in adult zebrafish. To characterize the immunological response to mycobacterial infection at 14 days post infection, we performed a whole-genome level transcriptome analysis using cells from kidney, the main hematopoietic organ of adult zebrafish. Among the upregulated genes, those associated with immune signaling and regulation formed the largest category, whereas the largest group of downregulated genes had a metabolic role. We also performed a forward genetic screen in adult zebrafish and identified a fish line with severely impaired survival during chronic mycobacterial infection. Based on transcriptome analysis, these fish have decreased expression of several immunological genes. Taken together, these results give new information about the genes involved in the defense against mycobacterial infection in zebrafish.

1. Introduction

In 2017, approximately 10 million people worldwide developed tuberculosis, a pulmonary or disseminated infection caused by *Mycobacterium tuberculosis* (World Health Organization, 2018). Although *M. tuberculosis* infection can be cleared by innate immunity (Verrall et al., 2014), it more typically leads to a latent phase. According to current estimations, 23% of the world's population are asymptomatic carriers of the bacteria (World Health Organization, 2018). The currently available Bacillus Calmette-Guérin (BCG) tuberculosis vaccine protects infants from disseminated tuberculosis but is less effective against pulmonary disease in adults. This vaccine is also unable to prevent the reactivation of latent disease (Mangtani et al., 2014; Tang et al., 2016). Thus, BCG vaccination cannot prevent the spread of tuberculosis.

Based on genome-wide association studies (GWAS) and candidate gene studies in various human populations, as well as on animal studies, host genetics contributes to the susceptibility of developing active tuberculosis (Berg et al., 2016; Cooper et al., 1993, 1997; Filipe-Santos et al., 2006; Harjula et al., 2018a; Sullivan et al., 2005; Tobin et al., 2010; Yim and Selvaraj, 2010). Human polymorphisms in genes encoding human leukocyte antigens (HLA) (Dallmann-Sauer et al., 2018; Yim and Selvaraj, 2010), Interferon (IFN) gamma, Interleukin10 and various chemokines and their receptors (Yim and Selvaraj, 2010), to mention but a few, have been associated with tuberculosis susceptibility. For some of these genes, there is also experimental evidence

Abbreviations: BCG, Bacille Calmette-Guérin; CFU, colony forming unit; dpf, days post fertilization; dpi, days post infection; GWAS, genome-wide association study; hpi, hours post infection; RIN, RNA integrity number; TL, *Tüpfel long fin*; wpi, weeks post infection; WT, wild type

* Corresponding author. Faculty of Medicine and Health Technology, FI-33014, Tampere University, Finland.
E-mail addresses: sanna.harjula@tuni.fi (S.-K.E. Harjula), anni.saralahti@tuni.fi (A.K. Saralahti), markus.ojanen@tuni.fi (M.J.T. Ojanen), tommi.rantapero@tuni.fi (T. Rantapero), meri.uusi-makela@tuni.fi (M.I.E. Uusi-Mäkelä), matti.nykter@tuni.fi (M. Nykter), olli.lohi@tuni.fi (O. Lohi), mataleena.parikka@tuni.fi (M. Parikka), mika.ramet@tuni.fi (M. Rämet).

https://doi.org/10.1016/j.dci.2019.103523
Received 13 September 2019; Received in revised form 9 October 2019; Accepted 14 October 2019
Available online 15 October 2019

from animal models on their importance in disease resistance (Beamer et al., 2008; Cooper et al., 1993; Cyktor et al., 2013; Flynn et al., 1993; Harjula et al., 2018a; Higgins et al., 2009; Peters et al., 2001; Torraca et al., 2015).

During the last couple of decades, *Mycobacterium marinum* infection in both zebrafish embryos/larvae and adult zebrafish has become a widely used model of tuberculosis (Myllymäki et al., 2015, 2016). *M. marinum* is a natural zebrafish pathogen and, similarly to its close relative *M. tuberculosis* (Stinear et al., 2008), it infects macrophages (Barker et al., 1997; El-Etr et al., 2001) and can cause a latent or slowly progressive infection, which can be reactivated by immunosuppression (Harjula et al., 2018a; Myllymäki et al., 2018; Parikka et al., 2012). Also comparable to tuberculosis, *M. marinum* infection both in zebrafish larvae and adult zebrafish results in granuloma formation (Davis et al., 2002; Myllymäki et al., 2018; Parikka et al., 2012; Swaim et al., 2006). In fact, the notion that granuloma not only benefits the host but also gives the bacteria a good environment in which to survive and spread the disease, originates from zebrafish studies (Davis and Ramakrishnan, 2009; Volkman et al., 2004).

The host response to the *M. marinum* infection in zebrafish has been studied in several transcriptome analyses (Benard et al., 2016; Hegedüs et al., 2009; Kenyon et al., 2017; Meijer et al., 2005; Ojanen et al., 2019; Rotman et al., 2011; Rougeot et al., 2014, 2019; van der Sar et al., 2009; van der Vaart et al., 2012; Veneman et al., 2015). These studies show that the gene expression profile of *M. marinum* infected zebrafish changes as the infection progresses. Consequently, in zebrafish larvae infected at 1 day post fertilization (dpf), three stages of the transcriptional response have been recognized: early, mid and late phase (Benard et al., 2016). Characteristic of the early phase is a transcriptional response, including upregulation of genes involved in response to bacterium, proteolysis and cellular macromolecular complex assembly and a downregulation of protein folding-associated genes at 2 h post infection (hpi), concurrent with phagocytosis of the bacteria (Benard et al., 2014). During mid-phase, starting at 6 hpi, the number of the differentially regulated genes is low. This is followed by an increase in differentially expressed genes during late phase (4 and 5 days post infection, dpi) (Benard et al., 2016). According to the aforementioned studies, the exact response not only depends on the stage of the infection but also on the virulence of the *M. marinum* strain (Rotman et al., 2011; van der Sar et al., 2009).

In general for adult zebrafish, genes encoding for zinc-finger proteins, immune-related transcription factors and proteins related to apoptosis, among others, are upregulated at the early stages of the *M. marinum* infection (van der Sar et al., 2009). At later stages, genes encoding for immune-related transcription factors, cytokines, chemokine receptors, complement components, matrix metalloproteases and lysosomal proton transporters, among others, are induced independently of the virulence of the bacteria in the adult zebrafish (Meijer et al., 2005; van der Sar et al., 2009).

In the present study, we performed a genome-wide transcriptome analysis using cells from kidney, the main hematopoietic organ in zebrafish, at 14 days post *M. marinum* infection. In this manner, we focused the analysis predominantly on immune cells. Furthermore, the immune response of wild type (WT) zebrafish was compared to the immune response of a susceptible mutant fish line, identified from an ongoing forward genetic screen.

2. Materials and methods

2.1. Zebrafish lines and maintenance

3 to 15 month-old WT AB and TL (*Tüpfel long fin*, *gja5b*$^{t1/t1}$, *lof* $^{dt2/dt2}$) zebrafish (*Danio rerio*) lines from the Tampere Zebrafish Core Facility were used for the experiments. The *rag*$^{hu1999/hu1999}$ mutant fish obtained from the Zebrafish International Resource Center (ZIRC, University of Oregon, Eugene, Oregon, USA) at the age of 6–8 months were used as a positive control in the infection experiments.

The zebrafish were maintained according to standard protocols (Nüsslein-Volhard and Dahm, 2002). Briefly, the unchallenged zebrafish were kept in a standard flow-through system (Aquatic Habitats, Apopka, Florida, USA) with a light/dark cycle of 14/10 h and fed once a day with SDS 400 (Special Diet Services, Witham, Essex, UK) and once a day with in-house cultured *Artemia nauplia*. Alternatively, fish were fed once a day with GEMMA Micro 500 (Skretting, Stavanger, Norway). The *M. marinum* infected fish were kept in a standard flow-through unit (Aqua Schwarz GmbH, Göttingen, Germany) with the same light/dark cycle as the unchallenged fish and fed twice a day with SDS 400 or once a day with GEMMA Micro 500. Zebrafish embryos/larvae were maintained in embryonic medium (5 mM NaCL, 0.17 mM KCl, 0.33 mM CaCl2, 0.33 mM MgSO4, 10% methylene blue at 28.5 °C, fed with SDS100 (Special Diet Services) or GEMMA Micro 75 (Skretting) starting at 5 dpf and transferred to the flow-through system at 6 dpf.

The well-being of the fish was monitored daily and the humane endpoint criteria determined in the animal experiment permits were used. The Animal Experiment Board has approved the housing and care of the zebrafish and all the conducted experiments (permits ESAVI/4234/04.10.03/2012, ESAVI/6403/04.10.03/2012, ESAVI/10079/04.10.06/2015, ESAVI/2776/2019, ESAVI/10539/2019, LSLH-2007-7254/Ym-23 and ESAVI/10366/04.10.07/2016). Furthermore, the Finnish Act on the Protection of Animals Used for Scientific or Educational Purposes (497/2013) as well as the EU Directive on the Protection of Animals Used for Scientific Purposes (2010/63/EU) were applied during this study.

2.2. The gene-breaking Tol2 transposon based mutagenesis in zebrafish embryos

The gene-breaking transposon pGBT-RP2-1 (RP2) vector (Addgene plasmid # 31828; http://n2t.net/addgene:31828; RRID:Addgene_31828) and pT3TS-Tol2 vector (Addgene plasmid # 31831; http://n2t.net/addgene:31831; RRID:Addgene_31831) for the production of *tol2* mRNA were received as a generous gift from Professor Stephen C. Ekker's laboratory (Mayo Clinic, Rochester, Minnesota, USA) (Balciunas et al., 2006; Clark et al., 2011). Both plasmids were transformed into *E. coli* One Shot TOP10 cells (Invitrogen™, Thermo Fisher Scientific, Waltham, Massachusetts, USA). Plasmid DNA was extracted with QIAGEN Plasmid Plus Maxi Kit (Qiagen, Hilden, Germany) and sequenced to confirm successful transformation. In order to produce *tol2* mRNA, pT3TS-Tol2 plasmid was first linearized by digestion with FastDigest BamHI (Thermo Scientific, Thermo Fisher Scientific). Then, the linearized plasmid was used as a template for *in vitro* transcription performed with mMESSAGE mMACHINE Transcription Kit, (Invitrogen™, Thermo Fisher Scientific) according to the manufacturer's instructions. The zebrafish mutagenesis was conducted as previously described (Clark et al., 2011). Briefly, 12.5 pg of RP2 plasmid and *tol2* mRNA in 1x PBS with 0.6% phenol red (Sigma-Aldrich, Saint Louis, Missouri, USA) were injected into the cell of 1-cell stage WT AB zebrafish embryos with a borosilicate capillary needle (Sutter Instrument Co., Novato, California, USA) using a PV830 Pneumatic PicoPump (World Precision Instruments, Sarasota, Florida, USA) and a micromanipulator (Narishige International, London, UK). If the mutagenesis was successful, RP2 was randomly inserted into the zebrafish genome causing one or several mutations per fish (Clark et al., 2011). Mutation carrying embryos (the founder fish in the genetic screen, designated as F0) were selected based on the expression of *Green fluorescent protein* (*GFP*) under a Lumar V.12 fluorescence stereomicroscope (Carl Zeiss MicroImaging GmbH, Göttingen, Germany) or Nikon AZ100 Fluorescence Macroscope (Nikon, Minato, Tokyo, Japan) (Clark et al., 2011).

2.3. Generation of the mutant zebrafish lines

In order to produce zebrafish lines carrying unknown mutations, F0 founder fish were first crossed to TL. The fish in the resulting F1 generation carried various sets of mutations. These fish were named with a running number (also the final name of the subsequent resultant mutant zebrafish line) and crossed to TL. This resulted in an F2 generation consisting of fish heterozygous for the mutations. The F2 generation was then incrossed to produce an F3 generation with a theoretical Mendelian ratio of WT, heterozygous and homozygous fish for each mutation. Further fish generations were produced by incrossing the previous generation (until F5). In some cases, in order to maintain the line, the fish were again crossed to TL. For the *M. marinum* infection experiments on embryos, the F7 generation was utilized. Mutation carrying progeny in each generation were selected for based on *GFP* expression.

2.4. Experimental M. marinum infections

The culture of *M. marinum* strain ATCC 927 and the inoculation into adult zebrafish were done as described previously (Harjula et al., 2018a; Parikka et al., 2012). For these infections, the zebrafish were anesthetized with 0.02% 3-amino benzoic acid ethyl ester (Sigma-Aldrich). Following this, 5 μl of *M. marinum* suspended in 1x PBS with 0.3 mg/ml phenol red (Sigma-Aldrich) was injected into the abdominal cavity of the fish using a 30 gauge Omnican 100 insulin needle (Braun, Melsungen, Germany). The survival of the fish was followed for 12–14 weeks. During the screen, 2–10 mutant lines were included in one experiment together with the WT line and occasionally *rag*$^{hu1999/hu1999}$ mutants. For the lines showing increased or decreased susceptibility, the survival assay was performed at least three times in total.

For the zebrafish embryo infections, *M. marinum* was suspended in 1x PBS with 0.3 mg/ml phenol red (Sigma-Aldrich). At 1 dpf, zebrafish embryos were anesthetized with 0.02% 3-amino benzoic acid ethyl ester (Sigma-Aldrich) and 2 nl of bacterial solution was injected into the caudal vein with a borosilicate capillary needle using a PV830 Pneumatic PicoPump (World Precision Instruments) and a micromanipulator (Narishige International). The survival of the embryos was monitored once a day for seven days. The infection dose (colony forming units, CFU) in both adult and embryo survival assays was verified by plating injected bacterial suspension on 7H10 agar (Becton Dickinson and Company, Franklin Lakes, New Jersey, USA) plates.

2.5. Experimental Streptococcus pneumoniae infections

The culture of *Streptococcus pneumoniae* WT strain TIGR4 (T4), of serotype 4 and sequence type 205, and the inoculation into zebrafish embryos were done as described previously (Aaberge et al., 1995; Rounioja et al., 2012). Briefly, 5% lamb blood agar plates (Tammer-Tutkan maljat Oy, Tampere, Finland) were used to grow T4 in 37 °C and 5% CO_2 overnight. From the plate, T4 was suspended in 5 ml of Todd Hewitt broth (Becton, Dickinson and Company) and grown from OD_{620} 0.1 to OD_{620} of 0.4. After this, bacteria were suspended in 0.2 M KCl with 1% of 70 kDa Rhodamine Dextran (Invitrogen™, Thermo Fisher Scientific). At 2 dpf, zebrafish embryos were anesthetized with 0.02% 3-amino benzoic acid ethyl ester (Sigma-Aldrich) and 2 nl of the bacterial solution was microinjected into the blood circulation valley with a borosilicate capillary needle (Sutter Instrument Co.) using a PV830 Pneumatic PicoPump (World Precision Instruments) and a micromanipulator (Narishige International). The survival was followed once a day for five days. The infection dose (CFU) was verified by plating injected bacterial suspension on 5% lamb blood agar plates (Tammer-Tutkan maljat Oy).

2.6. RNA extraction and quality control

For the transcriptome analysis, the RNA was extracted from zebrafish kidney with the Qiagen RNeasy Mini Kit (Qiagen) according to the manufacturer's protocol. The removal of genomic DNA from the samples was done with the RapidOut DNA Removal Kit (Thermo Scientific, Thermo Fisher Scientific). The purity of the samples was checked with a NanoDrop™ 2000 Spectrophotometer (Thermo Scientific, Thermo Fisher Scientific) and the concentration was measured with a Qubit™ RNA BR Assay Kit (Invitrogen™, Thermo Fisher Scientific). The integrity of RNA was checked with a Fragment Analyzer (Advanced Analytical Technologies, Iowa, USA) using the Standard Sensitivity RNA Analysis Kit (Advanced Analytical Technologies) and the PROSize® 2.0 Data Analysis Software (Advanced Analytical Technologies). The samples with an RNA integrity number (RIN) ≥ 7.8 were chosen for the RNA sequencing.

2.7. Whole genome transcription analysis by RNA sequencing

The preparation of the cDNA library and the RNA sequencing were performed at Novogene, Hong Kong. The cDNA library of 250–300 bp was prepared with the 150 bp paired-end sequencing on the Illumina platform yielding > 20 million reads/sample.

2.8. RNA sequencing data analysis

The quality of the reads was inspected using FastQC (Andrews, 2010). The reads were aligned against the GRCz10 reference genome with STAR using default parameters (Dobin et al., 2013). The expressions of genes were quantified with FeatureCounts (Liao et al., 2014) using Ensembl GRCz10.91 as the reference gene set (Hubbard et al., 2002). The normalization of the raw expressions and the differential gene expression analysis were both conducted using R-package DESeq2 (Love et al., 2014).

To analyze the transcriptome data further, we included genes which were expressed ≥ |3|-fold between the groups and also had medians of ≥ |3|-fold. Gene ontology enrichment analysis was performed with The Gene Ontology Enrichment Analysis (GO Ontology Database released 1st of January 2019 and Panther Overrepresentation Test released 13th of November 2018) (Ashburner et al., 2000; Mi et al., 2017; The Gene Ontology Consortium, 2019) using the unranked list of upregulated or downregulated genes as the target list and the list of all the protein coding genes present in the RNA sequencing data as a background list. Classification of upregulated genes was based on the data available from Ensembl genome browser (Zerbino et al., 2018) versions 91 (version used for the data analysis) and 95, Reactome (Fabregat et al., 2018), The Zebrafish Information Network ZFIN (Howe et al., 2013), InterPro (Mitchell et al., 2019), The PROSITE database (Sigrist et al., 2013), Pfam 32.0 (El-Gebali et al., 2019), the NCBI Gene database (Gene, 2004), the NCBI BioSystems database (Geer et al., 2010) and the literature. Downregulated genes were classified according to the gene ontology data available in Ensembl, ZFIN and NCBI gene databases. If the gene did not have an official name/description, the preferred name of the gene from the NCBI database was used if available.

2.9. qPCR

Reverse transcription of the RNA samples was done using the SensiFAST™ cDNA synthesis kit (BioLine, London, UK). cDNA was then used for determining the relative gene expression levels of the target genes with quantitative PCR (qPCR) using PowerUp™ SYBR® master mix (Applied Biosystems™, Thermo Fisher Scientific). Supplementary Table 1 gives the sequences of the qPCR primers used and the Ensembl gene identification codes for the analyzed genes. $2^{-\Delta Ct}$ method was used for calculating the expression levels of target genes relative to the expression of *eef1a1l1* (Tang et al., 2007). *M. marinum* burden (CFU)

was quantified from the total DNA of the infected fish with qPCR using SensiFAST™ SYBR® No-ROX (Bioline) as previously described (Parikka et al., 2012), considering 100 CFU as the detection limit. DNA for the analysis was extracted from the abdominal organ blocks (excluding kidney) with TRI Reagent® (Molecular Research Center, Cincinnati, Ohio, USA) according to manufacturer's protocol. A CFX96 qPCR machine (Bio-Rad, California, USA) was used to perform qPCR and the Bio-Rad CFX Manager software v3.1 (Bio-Rad) to analyze the data. Random RNA samples with no reverse transcription and non-template controls were used in qPCR to control for genomic DNA and other contamination. A melt curve analysis and 1.5% TAE agarose gel electrophoresis was used to validate the specificity of the qPCR products. PCR products below the detection limit or the ones with incorrect melt curves were given a Ct value of 40 when the gene expression analysis was performed.

2.10. Statistical analysis and power calculations

Sample size calculations were conducted as described earlier (Harjula et al., 2018a). As for the *M. marinum* quantification, based on the high mortality of mutant463 zebrafish and our previous results (Myllymäki et al., 2018; Parikka et al., 2012), the difference between the groups was this time estimated to be 0.75 unit on the log10 scale resulting in the group size minimum of 7.

In the gene ontology enrichment analyses *P* values were calculated with Fisher's exact test and Bonferroni correction was used for multiple testing. Statistical analyses for other results were conducted with Prism, version 5.02 (GraphPad Software, Inc, California, USA). For the survival analyses a log-rank (Mantel-Cox) test was used. To test whether the bacterial count is increased in the mutant463 line compared to WT and whether the differences in gene expression detected by RNA sequencing are repeated when analyzed with qPCR, a nonparametric one-tailed Mann-Whitney test was used. *P* values of < 0.05 were considered significant.

2.11. Data management

The RNA-sequencing data discussed in this publication (Harjula et al., 2018b, 2018c) have been deposited in NCBI's Gene Expression Omnibus (Edgar et al., 2002) and are accessible through GEO Series accession numbers GSE118288 (https://www.ncbi.nlm.nih.gov/geo/query/acc.cgi?acc=GSE118288) for the WT data and GSE118350 (https://www.ncbi.nlm.nih.gov/geo/query/acc.cgi?acc=GSE118350) for the mutant463 data.

3. Results

3.1. A low-dose infection with M. marinum leads to induction of immune response and changes in expression of genes regulating metabolism in kidney derived cells in adult zebrafish

We have previously shown that a low-dose *M. marinum* infection into the abdominal cavity of adult zebrafish leads to a latent or slowly progressive infection, which can be used to model different phases of tuberculosis (Harjula et al., 2018a; Myllymäki et al., 2018; Parikka et al., 2012). In order to characterize the immune response to low-dose *M. marinum* infection in WT zebrafish, we infected 5–6 month-old zebrafish with 5–9 CFU of *M. marinum* and performed a whole-genome level transcriptome analysis from their kidneys. Since the kidney is the main hematopoietic organ in adult zebrafish (Davidson and Zon, 2004), it was selected to characterize the immunological response to the infection, particularly in immune cells. At 7, 14 and 28 days post infection (dpi), we collected kidneys for RNA extraction. From the fish collected at 14 dpi, we selected four males for each group for RNA sequencing. As a negative control, we used four 7 month-old unchallenged WT male fish. The yield from RNA sequencing was 23–28 million reads per sample and 90% of the reads were successfully mapped to the transcript database Ensembl GRCz10.91.

Table 1
Enriched processes from gene ontology analysis of the upregulated protein coding genes. The Gene Ontology Consortium Enrichment analysis was performed using upregulated genes as a target list and all the protein coding genes in the RNA sequencing data as a background list. *P* values were calculated with Fisher's exact test and Bonferroni correction was used for multiple testing. $P < 0.05$ was considered significant.

GO term	Description	*P* value
GO:0006952	defense response	1.05E-06
GO:0006955	immune response	1.48E-06
GO:1990266	neutrophil migration	1.53E-06
GO:0097530	granulocyte migration	2.57E-06
GO:0097529	myeloid leukocyte migration	4.58E-06
GO:0070098	chemokine-mediated signaling pathway	7.44E-06
GO:0050900	leukocyte migration	7.85E-06
GO:1990869	cellular response to chemokine	9.50E-06
GO:1990868	response to chemokine	9.50E-06
GO:0030593	neutrophil chemotaxis	2.86E-05
GO:0006954	inflammatory response	4.02E-05
GO:0071621	granulocyte chemotaxis	4.67E-05
GO:0060326	cell chemotaxis	8.22E-05
GO:0030595	leukocyte chemotaxis	8.75E-05
GO:0002376	immune system process	1.44E-04
GO:0009617	response to bacterium	1.72E-04
GO:0006959	humoral immune response	4.57E-04
GO:0019221	cytokine-mediated signaling pathway	1.15E-03
GO:0071345	cellular response to cytokine stimulus	1.37E-03
GO:0043207	response to external biotic stimulus	2.06E-03
GO:0051707	response to other organism	2.06E-03
GO:0009607	response to biotic stimulus	2.13E-03
GO:0061844	antimicrobial humoral immune response mediated by antimicrobial peptide	2.42E-03
GO:0034097	response to cytokine	5.04E-03
GO:0006950	response to stress	6.42E-03
GO:0019730	antimicrobial humoral response	6.53E-03
GO:0002440	production of molecular mediator of immune response	1.07E-02
GO:0002377	immunoglobulin production	1.07E-02
GO:0051704	multi-organism process	1.10E-02
GO:0006935	chemotaxis	1.54E-02
GO:0042330	taxis	2.26E-02
GO:0009605	response to external stimulus	2.33E-02
GO:0071222	cellular response to lipopolysaccharide	3.91E-02
GO:0071219	cellular response to molecule of bacterial origin	3.91E-02
GO:0071216	cellular response to biotic stimulus	4.36E-02

In transcriptome analysis, we found 201 protein coding genes to be differentially expressed at 14 days post a low-dose *M. marinum* infection compared to the unchallenged WT fish (Tables 1–3, Supplementary Tables 2–3). More specifically, 96 of the differentially expressed protein coding genes were upregulated and 105 downregulated. In addition, we identified 21 upregulated and 30 downregulated noncoding RNAs (Supplementary Tables 4 and 5). We performed Gene Ontology Consortium enrichment analysis for both the upregulated and downregulated protein coding genes. According to this analysis, all the significantly enriched biological processes ($P < 0.05$), among the analyzed 86 upregulated genes recognized by the tool, were related to immune response (Table 1). This emphasizes the feasibility of using kidney tissue to characterize the immune response to infection. Among the most enriched processes were inflammatory response, response to bacterium and chemotaxis (Table 1). Next, we divided all the upregulated genes into subgroups based on the data available the databases listed in Chapter 2.8., as well as on the existing literature (Fig. 1A, Tables 2 and 3). The categories included immune response (43 genes), lipid binding and metabolism (9 genes), other metabolic role (13 genes), other role (27 genes) and unknown role (4 genes) (Fig. 1A, Tables 2 and 3).

Downregulated protein coding genes are shown in Fig. 1B and Supplementary Tables 2–3. Among the analyzed 92 downregulated genes, many of the significantly ($P < 0.05$) enriched processes were

Table 2
Immune response -related protein coding genes induced in mycobacterial infection in adult zebrafish kidney at 14 dpi (days post infection). The table shows the fold change in expression in *M. marinum* infected zebrafish compared to the unchallenged fish ($n = 4$ in both groups). Fold change represents the fold change between the group medians. The table includes only the genes with at least two samples with ≥ 20 normalized reads after infection and the genes whose expression was induced at least 3.0-fold (calculated both with the DEseq-tool and from the medians).

Gene symbol	Gene name/description	Ensembl gene ID	Fold change (median)	Reference
Acute phase response and antimicrobial activity				
saa	*serum amyloid A*	ENSDARG00000045999	21.8	
hamp	*hepcidin antimicrobial peptide*	ENSDARG00000102175	20.5	
lygl2	*lysozyme g-like 2*	ENSDARG00000099562	7.4	Mohapatra et al., 2019
leap2	*liver-expressed antimicrobial peptide 2*	ENSDARG00000104654	3.3	
Neutrophil degranulation				
SERPINB8 (1 of many)	*zgc:173729*	ENSDARG00000057263	8.7	
plaub	*plasminogen activator, urokinase b*	ENSDARG00000039145	4.2	
cst14b.1	*cystatin 14b, tandem duplicate 1*	ENSDARG00000045980	3.2	
serpinb1l4	*serpin peptidase inhibitor, clade B (ovalbumin), member 1, like 4*	ENSDARG00000096888	3.1	
krt5	*keratin 5*	ENSDARG00000058371	3.0	
Inflammasome				
si:ch211-236p5.3	*NACHT, LRR and PYD domains-containing protein 3-like*	ENSDARG00000086418	13.3	Hu et al., 2017
si:ch211-233m11.1	*NACHT, LRR and PYD domains-containing protein 12*	ENSDARG00000074653	6.8	
fosab	*v-fos FBJ murine osteosarcoma viral oncogene homolog Ab*	ENSDARG00000031683	3.4	Chinenov et al., 2001; van Dam et al., 2001; Malik et al., 2017
Immune signaling and regulation				
chad	*chondroadherin*	ENSDARG00000045071	7.5	
ccl39.1	*chemokine (C–C motif) ligand 39, duplicate 1*	ENSDARG00000101041	7.3	
cxcl11.1	*chemokine (C-X-C motif) ligand 11, duplicate 1*	ENSDARG00000100662	6.0	
cxcl8a	*chemokine (C-X-C motif) ligand 8a*	ENSDARG00000104795	5.3	
si:dkey-117a8.4	*c3a anaphylatoxin chemotactic receptor-like*	ENSDARG00000097698	5.0	
ccl34b.8	*chemokine (C–C motif) ligand 34b, duplicate 8*	ENSDARG00000093098	4.0	
rxfp1	*relaxin family peptide receptor 1*	ENSDARG00000090071	3.9	Figueiredo et al., 2006
CABZ01001434.1		ENSDARG00000098602	3.8	
BX323596.1	*C-X-C motif chemokine 11-6-like*	ENSDARG00000101138	3.8	
cxcl11.8	*chemokine (C-X-C motif) ligand 11, duplicate 8*	ENSDARG00000095747	3.8	
bmp5	*bone morphogenetic protein 5*	ENSDARG00000101701	3.7	Shih et al., 2017; Rosendahl et al., 2002
selenou1b	*selenoprotein U1b*	ENSDARG00000087059	3.6	Guo et al., 2015; Avery et al., 2018
sox2	*SRY (sex determining region Y)-box 2*	ENSDARG00000070913	3.4	
egr3	*early growth response 3*	ENSDARG00000089156	3.3	Kenyon et al., 2017
Other role in innate immune response				
si:dkey-21e2.15	*mast cell protease 1A*	ENSDARG00000092788	5.9	
foxq1a	*forkhead box Q1a*	ENSDARG00000030896	5.5	Earley et al., 2018
p2ry11	*purinergic receptor P2Y, G-protein coupled, 11*	ENSDARG00000014929	3.8	Berchtold et al., 1999; Adrian et al., 2000
cyp21a2	*cytochrome P450, family 21, subfamily A, polypeptide 2*	ENSDARG00000037550	3.5	Poliani et al., 2010
MFAP4 (1 of many)	*microfibril-associated glycoprotein 4-like*	ENSDARG00000089667	3.1	Walton et al., 2015
Adaptive immune response				
RAC1	*ras-related C3 botulinum toxin substrate 1-like*	ENSDARG00000099506	64.5	
BX649608.2		ENSDARG00000102940	16.5	Mandel et al., 2012
ighv5-5	*immunoglobulin heavy variable 5-5*	ENSDARG00000096342	10.1	
ighv4-1	*immunoglobulin heavy variable 4-1*	ENSDARG00000096259	9.8	
CU896602.3		ENSDARG00000074999	7.0	
tmem176l.3b	*transmembrane protein 176l.3b*	ENSDARG00000096874	6.0	Louvet et al., 2005; Zuccolo et al., 2010
egr1	*early growth response 1*	ENSDARG00000037421	5.7	Gomez-Martin et al., 2010
si:dkey-234i14.12		ENSDARG00000097228	5.4	
unc119b	*unc-119 homolog b (C. elegans)*	ENSDARG00000044362	5.2	Gorska et al., 2004, 2009; Gorska and Alam 2012 Stephen et al., 2018
ighv13-2	*immunoglobulin heavy variable 13-2*	ENSDARG00000096372	5.1	
zgc:153659		ENSDARG00000039801	5.0	
igl3v1	*immunoglobulin light 3 variable 1*	ENSDARG00000093258	4.0	

associated with metabolism, in particular with lipid metabolism (Supplementary Table 2). Since the gene ontology tool did not recognize all the downregulated protein coding genes, they were also manually classified into different biological processes, based on the gene ontology data available. The resultant downregulated subgroups were: immune system (4 genes), lipid metabolism and transport (10 genes), other metabolic process (the largest category with 36 genes), other localization process (8 genes), signaling and regulation (9 genes), other process (10 genes) and an unknown process (28 genes) (Fig. 1B, Supplementary Table 3).

Of note, there was a clear expression of several blood cell and hemoglobin related genes in addition to known kidney expressed genes (Elmonem et al., 2018; Song et al., 2004; Walters et al., 2010) such as *chemokine (CXC motif), receptor 4b* (*cxcr4b*), *aminoleculinate, delta-,*

Table 3
Metabolic and other non-immunological protein coding genes induced in mycobacterial infection in adult zebrafish kidney at 14 dpi (days post infection). The table shows the fold change in expression in *M. marinum* infected zebrafish compared to unchallenged fish ($n = 4$ in both groups). Fold change represents the fold change between the group medians. The table includes only the genes with at least two samples with ≥ 20 normalized reads after infection and the genes whose expression was induced at least 3.0-fold (calculated both with the DEseq-tool and from the medians). The fold changes are presented as the quotient of medians when the divisor is zero.

Gene symbol	Gene name/description	Ensembl gene ID	Fold change (median)
Lipid binding and metabolism			
fabp6	*fatty acid binding protein 6, ileal (gastrotropin)*	ENSDARG00000044566	131.5
dpep1	*dipeptidase 1*	ENSDARG00000068181	16.8
scd	*stearoyl-CoA desaturase (delta-9-desaturase)*	ENSDARG00000033662	6.3
abhd5b	*abhydrolase domain containing 5b*	ENSDARG00000100388	5.3
alox5b.2	*arachidonate 5-lipoxygenase b, tandem duplicate 2*	ENSDARG00000043089	4.4
nceh1a	*neutral cholesterol ester hydrolase 1a*	ENSDARG00000020427	3.6
crabp1b	*cellular retinoic acid binding protein 1b*	ENSDARG00000035904	3.4
g0s2	*G0/G1 switch 2*	ENSDARG00000078859	3.3
rbp7b	*retinol binding protein 7b, cellular*	ENSDARG00000070486	3.0
Other metabolic role			
CR559945.2	*probable N-acetyltransferase CML5*	ENSDARG00000106491	13:0
TPO	*thyroid peroxidase*	ENSDARG00000033280	43.0
ca4b	*carbonic anhydrase IV b*	ENSDARG00000042293	11.5
tgm5l	*transglutaminase 5, like*	ENSDARG00000098837	10.5
arid6	*AT-rich interaction domain 6*	ENSDARG00000069988	6.3
tgm8	*transglutaminase 8*	ENSDARG00000097651	6.0
ca9	*carbonic anhydrase IX*	ENSDARG00000102300	5.8
lum	*lumican*	ENSDARG00000045580	5.6
hoxb5b	*homeobox B5b*	ENSDARG00000054030	4.1
si:dkey-203a12.9		ENSDARG00000104721	3.9
paplna	*papilin a, proteoglycan-like sulfated glycoprotein*	ENSDARG00000027867	3.7
si:ch211-243a20.3	*si:ch211-243a20.3*	ENSDARG00000092240	3.1
prrx1b	*paired related homeobox 1b*	ENSDARG00000042027	3.0
Other role			
si:dkey-7i4.24	*myosin heavy chain, clone 203*	ENSDARG00000096906	27.8
tnni2a.1	*troponin I type 2a (skeletal, fast), tandem duplicate 1*	ENSDARG00000045592	16.1
zgc:136930	*thread keratin gamma*	ENSDARG00000055192	13.6
myhb	*myosin, heavy chain b*	ENSDARG00000001993	8.8
tcnbb	*transcobalamin beta b*	ENSDARG00000091996	7.4
hspb11	*heat shock protein, alpha-crystallin-related, b11*	ENSDARG00000002204	7.4
mrap	*melanocortin 2 receptor accessory protein*	ENSDARG00000091992	6.7
scpp1	*secretory calcium-binding phosphoprotein 1*	ENSDARG00000090416	6.7
slco2a1	*solute carrier organic anion transporter family, member 2A1*	ENSDARG00000061896	5.6
CABZ01072043.1		ENSDARG00000102907	5.6
tmem196a	*transmembrane protein 196a*	ENSDARG00000013935	5.4
hpcal1	*hippocalcin-like 1*	ENSDARG00000022763	5.1
asic2	*acid-sensing (proton-gated) ion channel 2*	ENSDARG00000006849	5.0
krt17	*keratin 17*	ENSDARG00000094041	4.3
cthrc1a	*collagen triple helix repeat containing 1a*	ENSDARG00000087198	4.1
col12a1b	*collagen, type XII, alpha 1b*	ENSDARG00000019601	4.1
sh3glb2b	*SH3-domain GRB2-like endophilin B2b*	ENSDARG00000035470	4.0
mamdc2b	*MAM domain containing 2b*	ENSDARG00000073695	3.9
si:ch211-105c13.3		ENSDARG00000089441	3.8
krt15	*keratin 15*	ENSDARG00000036840	3.8
tspan34	*tetraspanin 34*	ENSDARG00000103951	3.7
apnl	*actinoporin-like protein*	ENSDARG00000090900	3.4
myoz3a	*myozenin 3a*	ENSDARG00000067701	3.3
FO834829.3		ENSDARG00000102718	3.3
im:7150988		ENSDARG00000098058	3.3
BX664721.3	*endonuclease domain-containing 1 protein-like*	ENSDARG00000073995	3.2
si:ch211-150d5.3	*von Willebrand factor A domain-containing protein 7-like*	ENSDARG00000093384	3.0
Unknown role			
FO704758.1		ENSDARG00000098478	6.3
CABZ01056516.1		ENSDARG00000102467	5.0
si:dkey-248g15.3		ENSDARG00000097959	4.2
si:ch211-113d11.8		ENSDARG00000105494	3.4

synthase 2 (*alas2*), *choride channel K* (*clcnk*) and *nephrosis 1, congenital, Finnish type (nephrin)* (*nphs1*) (Supplementary Fig. 1) as well as genes typically used as markers for different types of immune cells (Supplementary Fig. 2), indicating that the samples represent the kidney and different types of blood cells.

3.2. Innate immune response is dominant at 14 days post M. marinum infection

The largest group of the protein coding genes induced upon infection consisted of genes with a documented or predicted immunological role. To further examine the induced immune response, these genes were divided into subcategories comprising acute phase response and

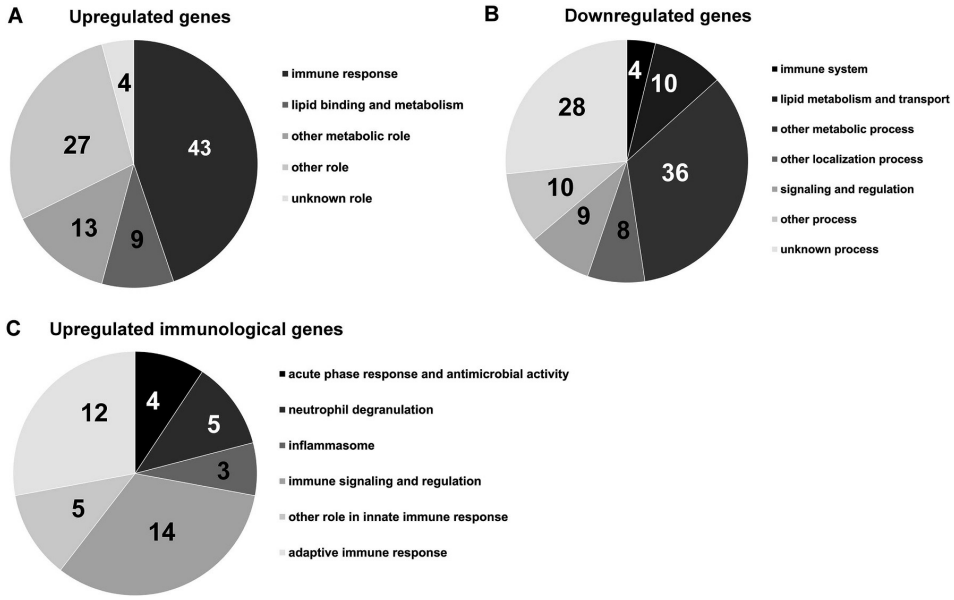

Fig. 1. Categorization of mycobacterium-responsive genes. Differentially expressed genes at 14 days post a low-dose (5–9 CFU, colony forming units) *M. marinum* infection were divided into categories based on their **roles** and/or the **biological processes** they participate in. **(A, C)** The upregulated genes were classified based on their roles as detailed in Materials and methods. **(B)** Downregulated genes were classified according to the gene ontology process data as detailed in Materials and methods. **(C)** Upregulated immunological genes were classified as in panel **(A)**.

antimicrobial activity (4 genes), neutrophil degranulation (5 genes), inflammasome (3 genes), immune signaling and regulation (14 genes), other role in innate immune response (5 genes) and adaptive immune response (12 genes) (Fig. 1C, Table 2). Most of these subcategories were related to innate immunity, highlighting that these responses still have an important role in the immune defense at 14 days post *M. marinum* infection and in the initiation of the adaptive immune response.

The innate immunity processes associated with defense response to bacteria were represented in our data. Acute phase protein coding gene *serum amyloid A* (*saa*) was induced together with three genes encoding proteins with antimicrobial activity: *hepcidin antimicrobial peptide* (*hamp*), *liver-expressed antimicrobial peptide 2* (*leap2*) and predicted *lysozyme g-like 2* (*lygl2*). Out of the other innate defense mechanisms, neutrophil degranulation was evidenced by the induction of five protein-coding genes.

An inflammatory response against pathogenic *M. tuberculosis* includes inflammasome activation (Wawrocki and Druszczynska, 2017). Three of the induced genes were associated with inflammasomes. These were: *si:ch211-236p5.3* encoding predicted NACHT, LRR and PYD domains-containing protein 3-like protein; *si:ch211-233m11.1* coding for a putative NOD-like receptor, NACHT, LRR and PYD domains-containing protein 12 (Hu et al., 2017; Vladimer et al., 2012); and *v-fos FBJ murine osteosarcoma viral oncogene homolog Ab* (*fosab*). The latter codes for an ortholog of a transcription factor that is a part of activator protein 1 (AP-1) protein complex (Chinenov and Kerppola, 2001; van Dam and Castellazzi, 2001) which participates in inflammasome activation (Malik and Kanneganti, 2017). Also related to inflammasome activation, another upregulated gene, *egr3*, codes for Early growth response 3 transcription factor that positively regulates *interleukin 1, beta,* (*il1b*) expression (Kenyon et al., 2017).

Some genes upregulated in our data, or their orthologs, are expressed in various innate immune cell types. These included genes expressed in macrophages (*forkhead box Q1a*, *foxq1a* (Earley et al., 2018) and one putative *microfibril-associated glycoprotein 4-like, MFAP4* variant (Walton et al., 2015)); dendritic cells (*purinergic receptor P2Y G-protein coupled, 11*, *p2ry11* (Berchtold et al., 1999) and putative *cytochrome P450, family 21, subfamily A, polypeptide 2*, *cyp21a2* (Poliani et al., 2010)); and mast cells (putative *mast cell protease 1A, si:dkey-21e2.15*). Related to cell migration, genes and putative genes encoding chemokines and chemokine-like proteins formed the largest subset of the genes with a postulated or documented role in immune signaling and regulation. On top of this, the human ortholog of upregulated signaling protein *relaxin family peptide receptor 1* (*rfxp1*), *LGR7*, has a reported role in leukocyte migration (Figueiredo et al., 2006).

In addition to the genes involved in innate immune response, twelve genes coding for proteins with a suggested or documented role in adaptive immunity were upregulated upon *M. marinum* infection. Four of these: predicted *CU896602.3*, *si:dkey-234i14.12*, *zgc:153659* and *immunoglobulin light 3 variable 1* (*igl3v1*), code for proteins having a postulated role in immunoglobulin production. Five potential genes (or their human orthologs) have suggested roles in T and B lymphocyte signaling and regulation: *early growth response 1* (*egr1*) (Gomez-Martin et al., 2010), *immunoglobulin heavy variable 4-1* (*ighv4-1*), *immunoglobulin heavy variable 5-5* (*ighv5-5*), *immunoglobulin heavy variable 13-2* (*ighv13-2*) and *RAC1* coding for a putative ras-related C3 botulinum toxin substrate 1-like protein.

3.3. M. marinum infection changes expression of metabolism associated genes

In addition to the immune system-related genes presented in Table 2, nine genes involved in lipid binding or lipid metabolism and 13 genes classed as 'other metabolic role' were induced (Table 3). Significantly, the most induced gene, *fatty acid binding protein 6* (*fabp6*) has a postulated role in lipid binding and metabolism. The upregulation of lipid metabolism associated genes due to *M. marinum* infection is supported by the literature, as the ability of *M. tuberculosis* to manipulate host metabolism and to use the host lipids for its pathogenic activities

and survival has been widely studied in a number of different research models (Barisch and Soldati, 2017; Korb et al., 2016; Stutz et al., 2018).

Involvement of lipid metabolism in the response to *M. marinum* is also apparent when analyzing the set of downregulated genes. This group included nine genes under the gene ontology term 'lipid metabolism', including 5 genes encoding apolipoproteins or predicted apolipoproteins and one, *apolipoprotein Bb, tandem duplicate 2* (*apobb.1*), especially associated with lipid transport. Among the most enriched processes of the downregulated genes were lipid localization, cellular lipid catabolic process and lipid transport (Supplementary Table 2). The downregulation of lipid catabolism and transport could be associated with the tendency of mycobacteria to manipulate the host to store the lipids inside the cell for the bacteria to use for its own purposes (Peyron et al., 2008; Russell et al., 2009; Stutz et al., 2018).

3.4. A forward genetic screen identifies a fish line with increased susceptibility to M. marinum infection

In order to identify genes that are important for defense against *M. marinum* infection in zebrafish, we conducted a forward genetic screen using gene-breaking transposon-based mutagenesis. 127 zebrafish lines, carrying a set of random mutations in F3–F5 inbred generations, were screened for altered susceptibility to *M. marinum* infection. To do this, we infected 3–15 month-old zebrafish from each mutant line with a low-dose (1–72 CFU) of *M. marinum* and followed the survival of the fish for 12–14 weeks. *rag1*$^{hu1999/hu1999}$ mutant fish, which have no functional T and B cells (Wienholds et al., 2002) were used as a positive control. During the screen, we identified 10 lines with impaired survival and one line with improved survival against *M. marinum* infection.

The most susceptible line, designated mutant463, showed drastically impaired survival (8% at the 14 weeks post infection, wpi endpoint) compared to the WT zebrafish (74%, $P < 0.0001$) (Fig. 2A). For reference, Fig. 2A also shows the survival rates of two mutant lines as compared to WT; mutant189 (endpoint survival 83%) and mutant229 (endpoint survival 68%). Supplementary Fig. 3A shows the survival of mutant463 fish prior to RNA extraction for the RNA sequencing experiment (survival at the 4 wpi endpoint of 38% in the mutant463 group vs. 100% in the WT group, $P = 0.002$). This survival was also similar to the mutant463 zebrafish survival kinetics observed during the screen. Buffer injection (PBS) did not cause any mortality among the mutant463 fish (Supplementary Fig. 3A). Infection with 220–328 CFU of *S. pneumoniae* (T4 serotype) resulted in a minor impairment to mutant463 embryo survival when compared to WT embryo survival (Supplementary Fig. 3B).

In our previous studies, high mortality after *M. marinum* infection associated with high bacterial burden (Harjula et al., 2018a; Myllymäki et al., 2018; Parikka et al., 2012). To clarify whether a defect in tolerance or resistance underlies the decreased survival of the mutant463 fish, we studied the *M. marinum* burden in the mutants and WT control zebrafish at 7 and 14 dpi (Fig. 2B). At 7 dpi, there was no difference in the bacterial count between mutant463 and WT fish (estimated copy number median 206 vs. 440 CFU, respectively), whereas at 14 dpi there was significantly higher bacterial burden in mutant463 fish compared to WT fish (copy number median 23,076 vs. 701 CFU, $P = 0.042$, respectively).

To further study whether the decreased survival and the increased mycobacterial burden in mutant463 fish is attributed to defects in the innate immune response, we performed a survival assay on WT and mutant463 zebrafish embryos, which rely solely on the innate immune system for protection against infection. We infected 32–198 CFU into the caudal vein of the embryos at 1 dpf and followed their survival for 7 days (Supplementary Fig. 3C). In contrast to the situation in adult fish, mutant463 embryos showed similar survival kinetics to WT embryos. This result suggests that the increased susceptibility of the mutant463 zebrafish line against a mycobacterial infection is due to defective adaptive rather than innate immunity.

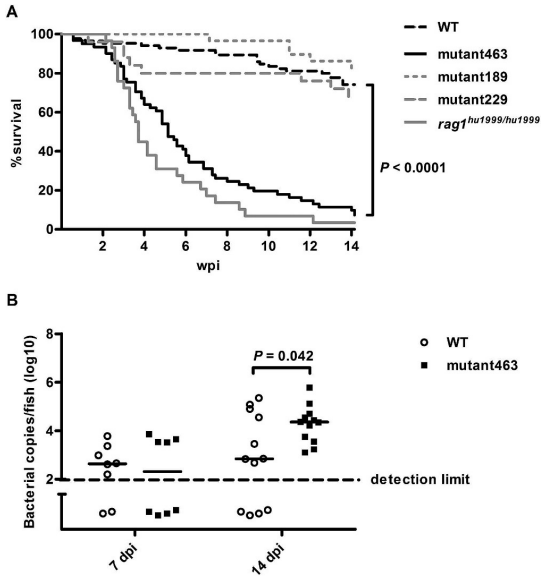

Fig. 2. Survival and bacterial burden of the mutant463 zebrafish after *M. marinum* infection. Adult mutant463 zebrafish have impaired survival and elevated bacterial burden after a low-dose *M. marinum* infection. **(A)** The survival of WT (wild type) ($n = 84$), *rag1*$^{hu1999/hu1999}$ ($n = 29$, a positive control) and three mutant zebrafish lines, mutant189 ($n = 29$), mutant229 ($n = 25$) and mutant463 ($n = 61$), was monitored for 14 weeks post a low-dose (2–35 CFU, colony forming units) *M. marinum* infection. The graphs represent the data from one (mutant189 and mutant229), two (*rag1*$^{hu1999/hu1999}$) or three (WT, mutant463) independent experiments. The survival data is presented as a Kaplan-Meier survival curve. wpi, weeks post infection **(B)** The *M. marinum* burden in the abdominal organ blocks (excluding kidney) of the low-dose (5–9) infected WT ($n = 8$–12) and mutant463 ($n = 8$–12) adult zebrafish was measured with qPCR at 7 and 14 dpi (days post infection). The bacterial count is presented as a scatter dot plot and as the median of total bacterial copies (log10). A log-rank (Mantel-Cox) test for panel (A) and a one-tailed Mann-Whitney test for panel (B) was used to perform the statistical comparison of differences.

3.5. The hypersusceptible mutant463 zebrafish have decreased expression of si:ch211-236p5.3 and unc119b involved in the innate and adaptive immune response

To further elucidate the reasons behind increased susceptibility of the mutant463 fish to mycobacterial infection, we analyzed the transcriptome of mutant463 zebrafish at 14 days post *M. marinum* infection and compared it to WT controls. Out of the 96 upregulated protein coding genes in WT fish, 27 had reduced expression in mutant463 compared to WT fish (Table 4). In addition, out of the 21 non-coding upregulated RNAs, 8 had reduced expression in the mutant463 zebrafish (Supplementary Table 6). None of the typical immune cell marker genes were clearly ($\geq$ 3-fold) downregulated in mutant463 zebrafish compared to WT (Supplementary Fig. 2). However, there were other protein coding genes with a potential immunological role and reduced expression in mutants. For selected genes, the RNA sequencing result was confirmed by qPCR at 7, 14 and 28 dpi (Fig. 3).

Among the genes with reduced expression in mutant463 fish were four genes with metabolic roles. One of these, *fabp6*, showed a 4.5-fold reduction at 14 dpi compared to WT fish in RNA sequencing and a 6.1-fold reduction at 28 dpi in qPCR ($P < 0.016$) (Fig. 3A). In addition to its roles in lipid binding and metabolism, Fabp6 is a bile acid binding protein (Capaldi et al., 2009). Bile acid mediates inflammation through different mechanisms in the liver (Li et al., 2017) and attenuates

Table 4
The protein coding genes downregulated in mycobacterial infection in mutant463 zebrafish kidney compared to WT (wild type) at 14 dpi (days post infection). The table shows the fold change in expression of the genes upregulated in mycobacterial infection between mutant463 and WT zebrafish ($n = 4$ in both groups). Fold change represents the fold change between the group medians. The table includes only the genes with at least two samples with ≥20 normalized reads in the WT group and whose expression was reduced at least 3.0-fold (calculated both with the DEseq-tool and from the medians). The fold changes are presented as the quotient of medians when the divisor is zero.

Gene symbol	Gene name/description	Ensembl gene ID	Fold change (median)
Immune response			
si:ch211-236p5.3	*NACHT, LRR and PYD domains-containing protein 3-like*	ENSDARG00000086418	−20:0
unc119b	*unc-119 homolog b (C. elegans)*	ENSDARG00000044362	−23.9
plaub	*plasminogen activator, urokinase b*	ENSDARG00000039145	−12.5
chad	*chondroadherin*	ENSDARG00000045071	−7.5
leap2	*liver-expressed antimicrobial peptide 2*	ENSDARG00000104654	−4.5
si:dkey-21e2.15	*mast cell protease 1A*	ENSDARG00000092788	−4.2
ighv5-5	*immunoglobulin heavy variable 5-5*	ENSDARG00000096342	−3.0
Metabolism			
TPO	*thyroid peroxidase*	ENSDARG00000033280	−43
CR559945.2	*probable N-acetyltransferase CML5*	ENSDARG00000106491	−13
hoxb5b	*homeobox B5b*	ENSDARG00000054030	−4.6
fabp6	*fatty acid binding protein 6, ileal (gastrotropin)*	ENSDARG00000044566	−4.5
Other role			
si:ch211-150d5.3	*von Willebrand factor A domain-containing protein 7-like*	ENSDARG00000093384	−24
myhb	*myosin, heavy chain b*	ENSDARG00000001993	−22
tmem196a	*transmembrane protein 196a*	ENSDARG00000013935	−21.6
mamdc2b	*MAM domain containing 2b*	ENSDARG00000073695	−20.8
tspan34	*tetraspanin 34*	ENSDARG00000103951	−16
tnni2a.1	*troponin I type 2a (skeletal, fast), tandem duplicate 1*	ENSDARG00000045592	−14.8
myoz3a	*myozenin 3a*	ENSDARG00000067701	−13.1
scpp1	*secretory calcium-binding phosphoprotein 1*	ENSDARG00000090416	−8.0
slco2a1	*solute carrier organic anion transporter family, member 2A1*	ENSDARG00000061896	−4.5
tcnbb	*transcobalamin beta b*	ENSDARG00000091996	−4.4
lum	*lumican*	ENSDARG00000045580	−4.3
BX664721.3	*endonuclease domain-containing 1 protein-like*	ENSDARG00000073995	−4.1
krt15	*keratin 15*	ENSDARG00000036840	−3.5
FO834829.3		ENSDARG00000102718	−3
Unknown role			
FO704758.1		ENSDARG00000098478	−33.3
CABZ01056516.1		ENSDARG00000102467	−6.4

inflammation through its receptors in the kidney (Herman-Edelstein et al., 2018). *fabp6* as well as another lipid metabolism associated gene *stearoyl-CoA desaturase (delta-9-desaturase)* (*scd*) were significantly induced upon *M. marinum* infection also when measured by qPCR. *fabp6* was induced 131.5-fold in RNA sequencing at 14 dpi and in qPCR; 14.9-fold at 7 dpi ($P = 0.007$) and 25.1-fold at 14 dpi ($P = 0.015$) (Fig. 3A). *scd* was induced 6.3-fold in RNA sequencing at 14 dpi and 2.1-fold ($P = 0.007$) in qPCR at 14 dpi (Fig. 3B).

Out of the 27 protein coding genes with reduced expression in mutant463 fish, 7 have a documented or predicted role in innate immunity (Table 4). For example, the expression of predicted *NACHT, LRR and PYD domains-containing protein 3-like* (*si:ch211-236p5.3*) was almost completely absent in mutant463 zebrafish upon *M. marinum* infection, whereas it was induced by infection in WT fish (13.3-fold induction in RNA sequencing). The diminished expression of this gene in mutant463 compared to WT fish was also seen in qPCR analysis with larger sample sizes (Fig. 3C) at 14 dpi (1848.4-fold reduction, $P < 0.0001$) and at 28 dpi (493.7-fold reduction, $P = 0.0002$). This gene and its paralogs have been predicted to code for a component of the inflammasome and to have a role in intracellular microbial recognition and immune activation.

Two of the genes with reduced expression have a role in adaptive immunity (Table 4). While *ighv5-5* (3.0-fold reduction) has a predicted role in the B cell receptor signaling pathway and in the positive regulation of B cell activation, *unc-119 homolog b (C. elegans)* (*unc119b*) is a zebrafish ortholog for the human gene coding for Unc-119 lipid binding chaperone (*UNC119*), which has been shown to be essential for T cell activation (Gorska et al., 2004; Stephen et al., 2018). *unc119b* showed 23.9-fold reduction in RNA sequencing and in qPCR showed the following; 11.4-fold reduction at 7 dpi ($P = 0.019$), 8.4-fold reduction at 14 dpi ($P = 0.003$) and 76.0-fold reduction at 28 dpi ($P = 0.0002$) (Fig. 3D).

4. Discussion

The transcriptional responses to mycobacterial infection are an outcome of the dynamic interplay between the host and the pathogen. Thus, it is implicit that the gene expression profile over the duration of *M. marinum* infection in zebrafish depends on the type of cells analyzed as well as the time-point of the analysis, the host and bacterial strains and the bacterial dosage, particularly when the analysis is carried out at the whole organismal level (Benard et al., 2016; Kenyon et al., 2017; Ojanen et al., 2019; Rougeot et al., 2014; van der Sar et al., 2009). Here, we utilized a zebrafish *M. marinum* infection model to study response to infection at the transcriptional level, using kidney samples to obtain a focused view of transcriptional changes in hematopoietic cells. Since head kidney is the main hematopoietic organ of zebrafish, it contains immune precursor cells. In our previous studies we have reported the presence of granulomas (Oksanen et al., 2013; Parikka et al., 2012) in adult zebrafish kidney. Therefore our data can give information about the interaction between the mature host immune cells and bacteria in addition to the production of immune cells during infection. As expected, the expression of many genes involved in the innate immune response were induced, such as genes involved in bacterial elimination, immune cell migration and neutrophil degranulation.

Activation of an inflammasome is a typical response to intracellular

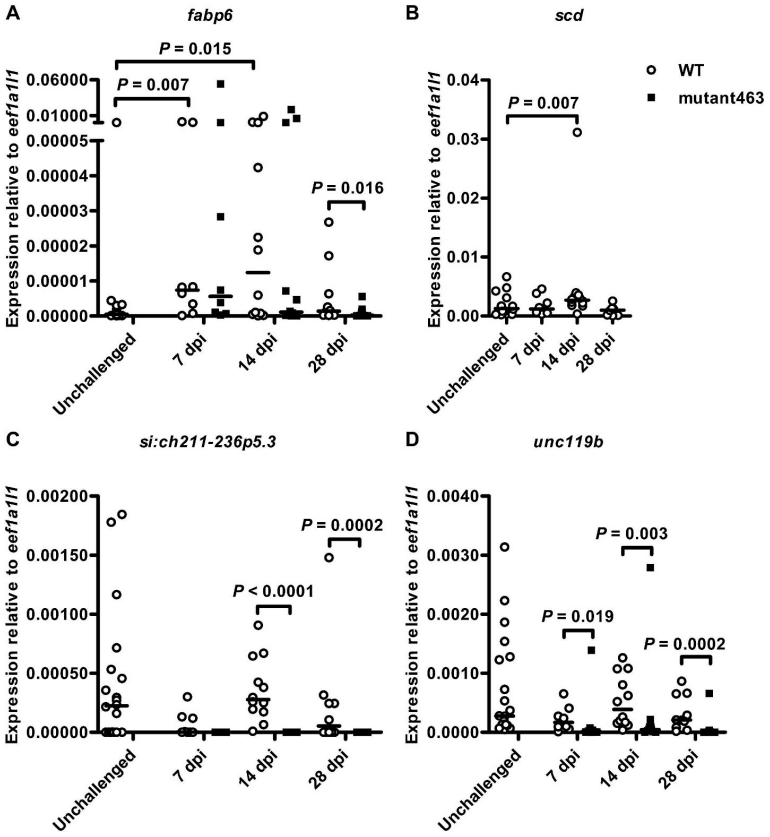

Fig. 3. The expression of selected genes following *M. marinum* infection. Hypersusceptible mutant463 zebrafish have decreased expression levels of the postulated inflammasome-related gene *si:ch211-236p5.3* and potentially T cell -related *unc119b* at various time-points during *M. marinum* (5–9 CFU, colony forming units) infection. **(A-D)** The relative expression levels of genes upregulated during mycobacterial infection in WT (wild type) (*scd*) and downregulated in mutant463 compared to WT (*fabp6*, si:*ch211-236p5.3* and *unc119b*) according to the transcriptome analysis were measured with qPCR from the kidney samples of unchallenged WT (n = 20) as well as WT (n = 8–12) and mutant463 (n = 8–14) zebrafish at 7, 14 and 28 dpi (days post infection). Data are presented as a scatter dot plot and median. Note the different scales of y-axes and the divided y-axis in panel (A). The expression of *eef1a1l1* was used to normalize the measured gene expressions. Data was collected from one experiment. A one-tailed Mann-Whitney test was used to perform the statistical comparison of differences. dpi, days post infection.

microbes (Mitchell and Isberg, 2017). Kenyon et al. (2017) used transcriptome analysis in neutrophils from zebrafish larvae at 3 dpi, to show differential expression of genes encoding inflammasome components (Kenyon et al., 2017). Our new data in adult zebrafish also revealed the upregulation of several genes associated with inflammasome function. Of note, one of the genes with substantially reduced expression in the hypersusceptible mutant463 fish was an inflammasome-associated gene, predicted *NACHT, LRR and PYD domains-containing protein 3-like* (*si:ch211-236p5.3*). There was no measurable expression of *si:ch211-236p5.3* detected by RNA sequencing post *M. marinum* infection and *si:ch211-236p5.3* expression was detected only in one fish out of 34 by qPCR. Conclusive data about the significance of this gene as well as other inflammasome components requires the phenotypic analysis of mutant fish lines. As such, the importance of inflammasome activation, as a defense mechanism against mycobacteria in zebrafish, remains to be determined.

Based on the known role of adaptive immunity in the defense against tuberculosis (O'Garra et al., 2013), our analysis, like previous corresponding studies (Meijer et al., 2005; van der Sar et al., 2009), also showed induction of genes coding for proteins that potentially participate in adaptive immune response, particularly in T cell function. Kidney is not a secondary lymphoid organ of zebrafish and therefore antigen presentation and lymphocyte activation do not typically occur in kidney (Renshaw and Trede, 2012). However, several genes with postulated roles in these processes were upregulated in our data, possibly as a result of granuloma formation in kidney and related presence of antigen presenting cells and lymphocytes. This is supported, for example, by a notion that genes related to neutrophil degranulation were among the upregulated genes. Alternatively the upregulation is related to the other possible functions of these genes. Based on the literature, two predicted genes upregulated in our data and having possible roles related to adaptive immunity are *transmembrane protein 176l.3b* (*tmem176l.3b*), and a member of the Claudin 1 -protein family, *BX649608.2*. The rat gene *Tmem176b* has been shown to be upregulated in inactive and immature antigen presenting cells in rats with allografts (Louvet et al., 2005) and conserved genes encoding the proteins of this family have also been found in zebrafish (Zuccolo et al., 2010). Therefore, *tmem176l.3b* could have an adaptive immunity related function also in zebrafish. Claudin 1 expression has been reported in human T and B lymphocytes and also in monocytes (Mandel et al., 2012), suggesting a potential immunological role for *BX649608.2*. Our analysis also revealed the upregulation of genes participating in B cell activation and immunoglobulin production. In line with these results, and related to the function of adaptive immune cells, Th2 type response has been suggested to have an important role in resistance against *M. marinum* in adult zebrafish (Hammarén et al., 2014).

One of the adaptive immune genes induced in WT zebrafish but with impaired expression in the hypersusceptible mutant463 line was *unc119b*. The human ortholog *UNC119* has been linked to T cell lymphopenia (Gorska and Alam, 2012), having been found to activate Lymphocyte-specific protein tyrosine kinase (LCK) and Proto-oncogene tyrosine-protein kinase Fyn (FYN) (Gorska et al., 2004). Thus, UNC119 is involved in T cell receptor (TCR) signaling and is essential for immune synapse formation (Gorska et al., 2004, 2009). On top of this, Stephen et al. (2018) recently showed that UNC119 binds LCK and further described the mechanisms by which UNC119 participates in the

immune synapse and in the initiation of T cell signaling by affecting the membrane localization of LCK (Stephen et al., 2018). They also proposed a new role for ciliary machinery in maintaining activated LCK at the immune synapse (Stephen et al., 2018). Since the $CD4^+$ T cells are indispensable in the immune defense against tuberculosis (Jasenosky et al., 2015), the increased susceptibility of mutant463 fish to *M. marinum* infection could be due to Unc119b deficiency. However, there are no clear differences in the expression of the genes coding for the most common T cell markers, *cd4-1*, *cd8a*, *lck*, *rag1*, *rag2* but instead, there is a 2.3-fold reduction in the eosinophil marker *gata2a*. In addition to T cell activation, UNC119 also plays a role in eosinophil survival (Cen et al., 2003). Since eosinophils have an ability to present antigens to $CD4^+$ Th cells in response to *Mycobacterium tuberculosis* purified protein derivate (Farhan et al., 2016), the defects in mycobacterial response in the mutant463 fish could derive from the complex effects of *unc119b* repression both in T cell signaling and eosinophil survival.

As mentioned above, the ability of *M. tuberculosis* to benefit from host lipids has been widely studied (Wilburn et al., 2018). Defects in certain host metabolic genes have been shown to affect the survival of the bacteria and the disease outcome (Kumar et al., 2010). Several genes involved in lipid metabolism, binding and transport were differentially expressed in our transcriptome data describing *M. marinum* infection in zebrafish. This has also been reported previously by others (Benard et al., 2016; Kenyon et al., 2017; Meijer et al., 2005; Ojanen et al., 2019; Rougeot et al., 2019; van der Sar et al., 2009). Two upregulated genes in our data code for lipid binding proteins *retinol binding protein 7b, cellular* (*rbp7b*) and *cellular retinoic acid binding protein 1b* (*crabp1b*). The mouse ortholog of *rbp7*, has been linked to abnormal levels of vitamin A (Piantedosi et al., 2005) and *crabp1b* has postulated roles in retinoic acid biosynthesis, signaling, binding and catabolism. Vitamin A and retinoic acid in turn have antimicrobial activity against *M. tuberculosis* (Wheelwright et al., 2014) and enhance autophagy in macrophages during intracellular bacterial infection (Coleman et al., 2018). An *in vitro* study in human macrophages infected with *M. tuberculosis* showed that a set of host genes involved in autophagy affect the survival of the bacteria inside macrophages (Kumar et al., 2010).

Some other genes which, according to our data, are upregulated during *M. marinum* infection and encode proteins associated to lipid metabolism, have reported or possible immunological functions. *dipeptidase 1* (*dpep1*), for example, has a potential role in leukotriene synthesis. Leukotriene B_4 is a known chemoattractant (Samuelsson, 1983) and an excess of leukotriene B_4 has been shown to lead to hyperinflammation and susceptibility to tuberculosis in zebrafish larvae (Tobin et al., 2012). On the other hand, from a genetic screen by Ramakrishnan's group, a deficiency in the leukotriene B_4 synthesis pathway in zebrafish larvae has been reported to cause an anti-inflammatory state, resulting in increased mycobacterial susceptibility (Tobin et al., 2010). Moreover, the human ortholog of another upregulated gene in our data, *Arachidonate 5-lipoxygenase b, tandem duplicate 2* (*alox5b.2*) encodes a protein which participates in leukotriene B_4 synthesis (Rådmark et al., 2015). Liu et al. (2013) showed that downregulation of *alox5b.2* leads to a reduced migration of leukocytes to a tail fin amputation site (Liu et al., 2013). Related to cell migration, Ramakrishnan's group has also recognized a role in macrophage migration for *cathepsin L.1* (*ctsl.1*) in zebrafish larvae during *M. marinum* infection (Berg et al., 2016).

Head kidney is also a part of endocrine system in teleosts (Geven and Klaren, 2017) and a key thyroid signaling organ (Quesada-García et al., 2014). Accordingly, *thyroid peroxidase* (*TPO*) was among most highly induced genes in our study (Table 3). In addition, *relaxin family peptide receptor 1* (*rxfp1*) and *melanocortin 2 receptor accessory protein* (*mrap)* with postulated roles in hormone-mediated signaling and in peptide hormone binding, respectively, were among the upregulated genes (Tables 2 and 3). Of note, *TPO* is downregulated in mutant463 compared to WT (Table 4). Out of the downregulated genes, *glycoprotein hormone beta 5* (*gphb5*) has a postulated role in the regulation of thyroid hormone mediated signaling pathway and *CABZ01111515.1* in thyroid hormone transport (Supplementary Table 3).

Our analysis also revealed differential expression of muscle-related genes in the kidney. The following muscle-related genes: *myosin, heavy chain b* (*myhb*); *troponin I type 2a (skeletal, fast); tandem duplicate 1* (*tnni2a.1*) and *myozenin 3a* (*myoz3a*); whilst upregulated in WT fish infected with *M. marinum*, were downregulated compared to WT in the hypersusceptible mutant463 at 14 dpi. The downregulation of muscle-related genes in selected neutrophil populations, during *M. marinum* infection in zebrafish, has been shown in a transcriptome analysis by Kenyon et al. (2017). Their results are thus suggestive of other immunological roles for muscle-related genes. The differential expression of genes traditionally associated with muscle function during infection, has also been shown in several other transcriptome level analyses in zebrafish (Meijer et al., 2005; Ojanen et al., 2019; van der Sar et al., 2009) as well as in a study in *Drosophila melanogaster* (Apidianakis et al., 2005). Moreover, expression of such genes has been shown in the macrophages, neutrophils and lymphocytes of zebrafish larvae (Rougeot et al., 2019). It has also been shown that, after exercise, the same functional gene networks are found in both human skeletal muscle and blood neutrophils (Broadbent et al., 2017).

5. Conclusions

In this study, we report a whole-genome level transcriptome analysis using adult zebrafish kidney cells at 14 days post a *M. marinum* infection. Kidney is the main hematopoietic organ of zebrafish and thus informative for studying immune response. Our results show that, at this time-point, the innate immune response is dominant. Furthermore, through a forward genetic screen, we identified a line with impaired resistance against *M. marinum*. The importance of immune responsive genes for resistance against mycobacterial disease can be studied using reverse genetics utilizing for example Clustered Regularly Interspaced Short Palindromic Repeats (CRISPR)/CRISPR-associated (Cas) -based mutagenesis. In this way, it is possible to solve which genes and pathways are most critical to harness for therapeutic strategies against mycobacterial diseases.

Declaration of competing interest

None.

Funding sources

This study was financially supported by the Academy of Finland (M.R., 277495, M.P. 316324), the Sigrid Juselius Foundation (M.R., M.P.), the Jane and Aatos Erkko Foundation (M.R., M.P.), the Competitive State Research Financing of the Expert Responsibility Area of Tampere University Hospital (M.R., M.P.), Competitive State Research Financing of the Expert Responsibility area of Oulu University Hospital (M.R.), the Tampere Tuberculosis Foundation (M.R., S.-K.H., M.P.), the University of Tampere Foundation (S.-K.H), the Emil Aaltonen Foundation (A.S., S.-K.H), Foundation of the Finnish Anti-Tuberculosis Association (S.-K.H.), the City of Tampere Science Foundation (A.S., S.-K.H), the Väinö and Laina Kivi Foundation (S.-K.H.), the Finnish Cultural Foundation, the Central Fund (S.-K.H.), the Finnish Concordia Fund (S.-K.H.), Orion Research Foundation (S.-K.H), the Academy of Finland PROFI4-project (S.-K.H.), the Finnish Society for Study of Infectious Diseases (S.-K.H.), Tampere University Doctoral Programme in Medicine and Life Sciences (A.S., M.O., M.U., T.R.), the Finnish Cultural Foundation, the Pirkanmaa Regional Fund (A.S.), the Maud Kuistila Memorial Foundation (A.S.) and the Oskar Öflunds Stiftelse (A.S.).

Acknowledgements

We thank Stephen C. Ekker's Laboratory (Maya Clinic, Rochester,

USA) for the pGBT-RP2-1 and pT3TS-Tol2 plasmids and advice. We also thank the Tampere Zebrafish Core Facility, partly funded by Biocenter Finland, for maintaining and providing the zebrafish, Hannaleena Piippo, Jenna Ilomäki, Leena Mäkinen, Tuula Myllymäki, Mirja Niskanen, Heather Baird, Nicholas Halfpenny, Sofia Vesterkvist, Essi Mäkinen, Jenni Jouppila, Matilda Salminen, Annemari Uusimäki, Riikka Penttinen, Carina Bäuerlein and Janey Barron for technical assistance, Tampere Imaging Facility (BioMediTech, Faculty of Medicine and Health Technology, Tampere University), Heini Huhtala for the statistical advice and Jack George for proof-reading the manuscript.

Appendix A. Supplementary data

Supplementary data to this article can be found online at https://doi.org/10.1016/j.dci.2019.103523.

References

Aaberge, I.S., Eng, J., Lermark, G., Lovik, M., 1995. Virulence of *Streptococcus pneumoniae* in mice: a standardized method for preparation and frozen storage of the experimental bacterial inoculum. Microb. Pathog. 18, 141–152.

Adrian, K., Bernhard, M.K., Breitinger, H.G., Ogilvie, A., 2000. Expression of purinergic receptors (ionotropic P2X1-7 and metabotropic P2Y1-11) during myeloid differentiation of HL60 cells. Biochim. Biophys. Acta 1492, 127–138.

Andrews, S., 2010. FastQC: a quality control tool for high throughput sequence data. Available online at: http://www.bioinformatics.babraham.ac.uk/projects/fastqc/.

Apidianakis, Y., Mindrinos, M.N., Xiao, W., Lau, G.W., Baldini, R.L., Davis, R.W., Rahme, L.G., 2005. Profiling early infection responses: *Pseudomonas aeruginosa* eludes host defenses by suppressing antimicrobial peptide gene expression. Proc. Natl. Acad. Sci. U.S.A. 102, 2573–2578.

Ashburner, M., Ball, C.A., Blake, J.A., Botstein, D., Butler, H., Cherry, J.M., Davis, A.P., Dolinski, K., Dwight, S.S., Eppig, J.T., Harris, M.A., Hill, D.P., Issel-Tarver, L., Kasarskis, A., Lewis, S., Matese, J.C., Richardson, J.E., Ringwald, M., Rubin, G.M., Sherlock, G., 2000. Gene ontology: tool for the unification of biology. The Gene Ontology Consortium. Nat. Genet. 25, 25–29.

Avery, J.C., Hoffmann, P.R., 2018. Selenium, selenoproteins, and immunity. Nutrients 10. https://doi.org/10.3390/nu10091203.

Balciunas, D., Wangesteen, K.J., Wilber, A., Bell, J., Geurts, A., Sivasubbu, S., Wang, X., Hackett, P.B., Largaespada, D.A., McIvor, R.S., Ekker, S.C., 2006. Harnessing a high cargo-capacity transposon for genetic applications in vertebrates. PLoS Genet. 2, e169.

Barisch, C., Soldati, T., 2017. Breaking fat! How mycobacteria and other intracellular pathogens manipulate host lipid droplets. Biochimie 141, 54–61.

Barker, L.P., George, K.M., Falkow, S., Small, P.L., 1997. Differential trafficking of live and dead *Mycobacterium marinum* organisms in macrophages. Infect. Immun. 65, 1497–1504.

Beamer, G.L., Flaherty, D.K., Assogba, B.D., Stromberg, P., Gonzalez-Juarrero, M., de Waal Malefyt, R., Vesosky, B., Turner, J., 2008. Interleukin-10 promotes *Mycobacterium tuberculosis* disease progression in CBA/J mice. J. Immunol. 181, 5545–5550.

Benard, E.L., Roobol, S.J., Spaink, H.P., Meijer, A.H., 2014. Phagocytosis of mycobacteria by zebrafish macrophages is dependent on the scavenger receptor Marco, a key control factor of pro-inflammatory signalling. Dev. Comp. Immunol. 47, 223–233.

Benard, E.L., Rougeot, J., Racz, P.I., Spaink, H.P., Meijer, A.H., 2016. Transcriptomic approaches in the zebrafish model for tuberculosis-Insights into host- and pathogen-specific determinants of the innate immune response. Adv. Genet. 95, 217–251.

Berchtold, S., Ogilvie, A.L., Bogdan, C., Muhl-Zurbes, P., Ogilvie, A., Schuler, G., Steinkasserer, A., 1999. Human monocyte derived dendritic cells express functional P2X and P2Y receptors as well as ecto-nucleotidases. FEBS Lett. 458, 424–428.

Berg, R.D., Levitte, S., O'Sullivan, M.P., O'Leary, S.M., Cambier, C.J., Cameron, J., Takaki, K.K., Moens, C.B., Tobin, D.M., Keane, J., Ramakrishnan, L., 2016. Lysosomal disorders drive susceptibility to tuberculosis by compromising macrophage migration. Cell 165, 139–152.

Broadbent, J., Sampson, D., Sabapathy, S., Haseler, L.J., Wagner, K.H., Bulmer, A.C., Peake, J.M., Neubauer, O., 2017. Gene networks in skeletal muscle following endurance exercise are coexpressed in blood neutrophils and linked with blood inflammation markers. J. Appl. Physiol. 122, 752–766 1985.

Capaldi, S., Saccomani, G., Fessas, D., Signorelli, M., Perduca, M., Monaco, H.L., 2009. The X-ray structure of zebrafish (*Danio rerio*) ileal bile acid-binding protein reveals the presence of binding sites on the surface of the protein molecule. J. Mol. Biol. 385, 99–116.

Cen, O., Gorska, M.M., Stafford, S.J., Sur, S., Alam, R., 2003. Identification of UNC119 as a novel activator of SRC-type tyrosine kinases. J. Biol. Chem. 278, 8837–8845.

Chinenov, Y., Kerppola, T.K., 2001. Close encounters of many kinds: fos-Jun interactions that mediate transcription regulatory specificity. Oncogene 20, 2438–2452.

Clark, K.J., Balciunas, D., Pogoda, H.M., Ding, Y., Westcot, S.E., Bedell, V.M., Greenwood, T.M., Urban, M.D., Skuster, K.J., Petzold, A.M., Ni, J., Nielsen, A.L., Patowary, A., Scaria, V., Sivasubbu, S., Xu, X., Hammerschmidt, M., Ekker, S.C., 2011. *In vivo* protein trapping produces a functional expression codex of the vertebrate proteome. Nat. Methods 8, 506–515.

Coleman, M.M., Basdeo, S.A., Coleman, A.M., Cheallaigh, C.N., Peral de Castro, C., McLaughlin, A.M., Dunne, P.J., Harris, J., Keane, J., 2018. *All-trans* retinoic acid augments autophagy during intracellular bacterial infection. Am. J. Respir. Cell Mol. Biol. 59, 548–556.

Cooper, A.M., Magram, J., Ferrante, J., Orme, I.M., 1997. Interleukin 12 (IL-12) is crucial to the development of protective immunity in mice intravenously infected with *Mycobacterium tuberculosis*. J. Exp. Med. 186, 39–45.

Cooper, A.M., Dalton, D.K., Stewart, T.A., Griffin, J.P., Russell, D.G., Orme, I.M., 1993. Disseminated tuberculosis in *interferon gamma* gene-disrupted mice. J. Exp. Med. 178, 2243–2247.

Cyktor, J.C., Carruthers, B., Kominsky, R.A., Beamer, G.L., Stromberg, P., Turner, J., 2013. IL-10 inhibits mature fibrotic granuloma formation during *Mycobacterium tuberculosis* infection. J. Immunol. 190, 2778–2790.

Dallmann-Sauer, M., Correa-Macedo, W., Schurr, E., 2018. Human genetics of mycobacterial disease. Mamm. Genome 29, 523–538.

Davidson, A.J., Zon, L.I., 2004. The 'definitive' (and 'primitive') guide to zebrafish hematopoiesis. Oncogene 23, 7233–7246.

Davis, J.M., Clay, H., Lewis, J.L., Ghori, N., Herbomel, P., Ramakrishnan, L., 2002. Real-time visualization of mycobacterium-macrophage interactions leading to initiation of granuloma formation in zebrafish embryos. Immunity 17, 693–702.

Davis, J.M., Ramakrishnan, L., 2009. The role of the granuloma in expansion and dissemination of early tuberculous infection. Cell 136, 37–49.

Dobin, A., Davis, C.A., Schlesinger, F., Drenkow, J., Zaleski, C., Jha, S., Batut, P., Chaisson, M., Gingeras, T.R., 2013. STAR: ultrafast universal RNA-seq aligner. Bioinformatics 29, 15–21.

Earley, A.M., Dixon, C.T., Shiau, C.E., 2018. Genetic analysis of zebrafish homologs of human *FOXQ1*, *foxq1a* and *foxq1b*, in innate immune cell development and bacterial host response. PLoS One 13, e0194207.

Edgar, R., Domrachev, M., Lash, A.E., 2002. Gene Expression Omnibus: NCBI gene expression and hybridization array data repository. Nucleic Acids Res. 30, 207–210.

El-Etr, S.H., Yan, L., Cirillo, J.D., 2001. Fish monocytes as a model for mycobacterial host-pathogen interactions. Infect. Immun. 69, 7310–7317.

El-Gebali, S., Mistry, J., Bateman, A., Eddy, S.R., Luciani, A., Potter, S.C., Qureshi, M., Richardson, L.J., Salazar, G.A., Smart, A., Sonnhammer, E.L.L., Hirsh, L., Paladin, L., Piovesan, D., Tosatto, S.C.E., Finn, R.D., 2019. The Pfam protein families database in 2019. Nucleic Acids Res. 47, D427–D432.

Elmonem, M.A., Berlingerio, S.P., van den Heuvel, L.P., de Witte, P.A., Lowe, M., Levtchenko, E.N., 2018. Genetic renal diseases: the emerging role of zebrafish models. Cells 7. https://doi.org/10.3390/cells7090130.

Fabregat, A., Jupe, S., Matthews, L., Sidiropoulos, K., Gillespie, M., Garapati, P., Haw, R., Jassal, B., Korninger, F., May, B., Milacic, M., Roca, C.D., Rothfels, K., Sevilla, C., Shamovsky, V., Shorser, S., Varusai, T., Viteri, G., Weiser, J., Wu, G., Stein, L., Hermjakob, H., D'Eustachio, P., 2018. The reactome pathway knowledgebase. Nucleic Acids Res. 46, D649–D655.

Farhan, R.K., Vickers, M.A., Ghaemmaghami, A.M., Hall, A.M., Barker, R.N., Walsh, G.M., 2016. Effective antigen presentation to helper T cells by human eosinophils. Immunology 149, 413–422.

Figueiredo, K.A., Mui, A.L., Nelson, C.C., Cox, M.E., 2006. Relaxin stimulates leukocyte adhesion and migration through a relaxin receptor LGR7-dependent mechanism. J. Biol. Chem. 281, 3030–3039.

Filipe-Santos, O., Bustamante, J., Chapgier, A., Vogt, G., de Beaucoudrey, L., Feinberg, J., Jouanguy, E., Boisson-Dupuis, S., Fieschi, C., Picard, C., Casanova, J.L., 2006. Inborn errors of IL-12/23- and IFN-gamma-mediated immunity: molecular, cellular, and clinical features. Semin. Immunol. 18, 347–361.

Flynn, J.L., Chan, J., Triebold, K.J., Dalton, D.K., Stewart, T.A., Bloom, B.R., 1993. An essential role for interferon gamma in resistance to *Mycobacterium tuberculosis* infection. J. Exp. Med. 178, 2249–2254.

Geer, L.Y., Marchler-Bauer, A., Geer, R.C., Han, L., He, J., He, S., Liu, C., Shi, W., Bryant, S.H., 2010. The NCBI BioSystems database. Nucleic Acids Res. 38, 492.

Gene, 2004. National Library of Medicine (US). National Center for Biotechnology Information, Bethesda (MD) 2019. https://www.ncbi.nlm.nih.gov/gene/, Accessed date: 14 April 2019.

Geven, E.J.W., Klaren, P.H.M., 2017. The teleost head kidney: integrating thyroid and immune signaling. Dev. Comp. Immunol. 66, 73–83.

Gomez-Martin, D., Diaz-Zamudio, M., Galindo-Campos, M., Alcocer-Varela, J., 2010. Early growth response transcription factors and the modulation of immune response: implications towards autoimmunity. Autoimmun. Rev. 9, 454–458.

Gorska, M.M., Alam, R., 2012. A mutation in the human *Uncoordinated 119* gene impairs TCR signaling and is associated with CD4 lymphopenia. Blood 119, 1399–1406.

Gorska, M.M., Liang, Q., Karim, Z., Alam, R., 2009. Uncoordinated 119 protein controls trafficking of Lck via the Rab11 endosome and is critical for immunological synapse formation. J. Immunol. 183, 1675–1684.

Gorska, M.M., Stafford, S.J., Cen, O., Sur, S., Alam, R., 2004. Unc119, a novel activator of Lck/Fyn, is essential for T cell activation. J. Exp. Med. 199, 369–379.

Guo, F., He, H., Fu, Z.C., Huang, S., Chen, T., Papasian, C.J., Morse, L.R., Xu, Y., Battaglino, R.A., Yang, X.F., Jiang, Z., Xin, H.B., Fu, M., 2015. Adipocyte-derived PAMM suppresses macrophage inflammation by inhibiting MAPK signalling. Biochem. J. 472, 309–318.

Hammarén, M.M., Oksanen, K.E., Nisula, H.M., Luukinen, B.V., Pesu, M., Rämet, M., Parikka, M., 2014. Adequate Th2-type response associates with restricted bacterial growth in latent mycobacterial infection of zebrafish. PLoS Pathog. 10, e1004190.

Harjula, S.E., Ojanen, M.J.T., Taavitsainen, S., Nykter, M., Rämet, M., 2018a. *Interleukin 10* mutant zebrafish have an enhanced interferon gamma response and improved survival against a *Mycobacterium marinum* infection. Sci. Rep. 8, 1036.

Harjula, S.E., Saralahti, A.K., Ojanen, M.J., Rantapero, T., Uusi-Mäkelä, M.I., Nykter, M., Lohi, O., Parikka, M., Rämet, M., 2018b. Characterization of the immune response to

Mycobacterium marinum infection in zebrafish. In: NCBI's Gene Expression Omnibus, . https://www.ncbi.nlm.nih.gov/geo/query/acc.cgi?acc=GSE118288.
Harjula, S.E., Saralahti, A.K., Ojanen, M.J., Rantapero, T., Uusi-Mäkelä, M.I., Nykter, M., Lohi, O., Parikka, M., Rämet, M., 2018c. Characterization of the immune response to *Mycobacterium marinum* infection in zebrafish [mutant 463]. In: NCBI's Gene Expression Omnibus, . https://www.ncbi.nlm.nih.gov/geo/query/acc.cgi?acc=GSE118350.
Hegedüs, Z., Zakrzewska, A., Agoston, V.C., Ordas, A., Racz, P., Mink, M., Spaink, H.P., Meijer, A.H., 2009. Deep sequencing of the zebrafish transcriptome response to mycobacterium infection. Mol. Immunol. 46, 2918–2930.
Herman-Edelstein, M., Weinstein, T., Levi, M., 2018. Bile acid receptors and the kidney. Curr. Opin. Nephrol. Hypertens. 27, 56–62.
Higgins, D.M., Sanchez-Campillo, J., Rosas-Taraco, A.G., Lee, E.J., Orme, I.M., Gonzalez-Juarrero, M., 2009. Lack of IL-10 alters inflammatory and immune responses during pulmonary *Mycobacterium tuberculosis* infection. Tuberculosis 89, 149–157.
Howe, D.G., Bradford, Y.M., Conlin, T., Eagle, A.E., Fashena, D., Frazer, K., Knight, J., Mani, P., Martin, R., Moxon, S.A., Paddock, H., Pich, C., Ramachandran, S., Ruef, B.J., Ruzicka, L., Schaper, K., Shao, X., Singer, A., Sprunger, B., Van Slyke, C.E., Westerfield, M., 2013. ZFIN, the Zebrafish Model Organism Database: increased support for mutants and transgenics. Nucleic Acids Res. 41, 854.
Hu, Y.W., Wu, X.M., Ren, S.S., Cao, L., Nie, P., Chang, M.X., 2017. NOD1 deficiency impairs CD44a/Lck as well as PI3K/Akt pathway. Sci. Rep. 7, 297.
Hubbard, T., Barker, D., Birney, E., Cameron, G., Chen, Y., Clark, L., Cox, T., Cuff, J., Curwen, V., Down, T., Durbin, R., Eyras, E., Gilbert, J., Hammond, M., Huminiecki, L., Kasprzyk, A., Lehvaslaiho, H., Lijnzaad, P., Melsopp, C., Mongin, E., Pettett, R., Pocock, M., Potter, S., Rust, A., Schmidt, E., Searle, S., Slater, G., Smith, J., Spooner, W., Stabenau, A., Stalker, J., Stupka, E., Ureta-Vidal, A., Vastrik, I., Clamp, M., 2002. The Ensembl genome database project. Nucleic Acids Res. 30, 38–41.
Jasenosky, L.D., Scriba, T.J., Hanekom, W.A., Goldfeld, A.E., 2015. T cells and adaptive immunity to *Mycobacterium tuberculosis* in humans. Immunol. Rev. 264, 74–87.
Kenyon, A., Gavriouchkina, D., Zorman, J., Napolitani, G., Cerundolo, V., Sauka-Spengler, T., 2017. Active nuclear transcriptome analysis reveals inflammasome-dependent mechanism for early neutrophil response to *Mycobacterium marinum*. Sci. Rep. 7, 650.
Korb, V.C., Chuturgoon, A.A., Moodley, D., 2016. *Mycobacterium tuberculosis*: manipulator of protective immunity. Int. J. Mol. Sci. 17, 131.
Kumar, D., Nath, L., Kamal, M.A., Varshney, A., Jain, A., Singh, S., Rao, K.V., 2010. Genome-wide analysis of the host intracellular network that regulates survival of *Mycobacterium tuberculosis*. Cell 140, 731–743.
Li, M., Cai, S.Y., Boyer, J.L., 2017. Mechanisms of bile acid mediated inflammation in the liver. Mol. Asp. Med. 56, 45–53.
Liao, Y., Smyth, G.K., Shi, W., 2014. featureCounts: an efficient general purpose program for assigning sequence reads to genomic features. Bioinformatics 30, 923–930.
Liu, Y.J., Fan, H.B., Jin, Y., Ren, C.G., Jia, X.E., Wang, L., Chen, Y., Dong, M., Zhu, K.Y., Dong, Z.W., Ye, B.X., Zhong, Z., Deng, M., Liu, T.X., Ren, R., 2013. Cannabinoid receptor 2 suppresses leukocyte inflammatory migration by modulating the JNK/c-Jun/Alox5 pathway. J. Biol. Chem. 288, 13551–13562.
Louvet, C., Chiffoleau, E., Heslan, M., Tesson, L., Heslan, J.M., Brion, R., Beriou, G., Guillonneau, C., Khalife, J., Anegon, I., Cuturi, M.C., 2005. Identification of a new member of the CD20/FcepsilonRIbeta family overexpressed in tolerated allografts. Am. J. Transplant. 5, 2143–2153.
Love, M.I., Huber, W., Anders, S., 2014. Moderated estimation of fold change and dispersion for RNA-seq data with DESeq2. Genome Biol. 15, 55–58.
Malik, A., Kanneganti, T.D., 2017. Inflammasome activation and assembly at a glance. J. Cell Sci. 130, 3955–3963.
Mandel, I., Paperna, T., Glass-Marmor, L., Volkowich, A., Badarny, S., Schwartz, I., Vardi, P., Koren, I., Miller, A., 2012. Tight junction proteins expression and modulation in immune cells and multiple sclerosis. J. Cell Mol. Med. 16, 765–775.
Mangtani, P., Abubakar, I., Ariti, C., Beynon, R., Pimpin, L., Fine, P.E., Rodrigues, L.C., Smith, P.G., Lipman, M., Whiting, P.F., Sterne, J.A., 2014. Protection by BCG vaccine against tuberculosis: a systematic review of randomized controlled trials. Clin. Infect. Dis. 58, 470–480.
Meijer, A.H., Verbeek, F.J., Salas-Vidal, E., Corredor-Adamez, M., Bussman, J., van der Sar, A.M., Otto, G.W., Geisler, R., Spaink, H.P., 2005. Transcriptome profiling of adult zebrafish at the late stage of chronic tuberculosis due to *Mycobacterium marinum* infection. Mol. Immunol. 42, 1185–1203.
Mi, H., Huang, X., Muruganujan, A., Tang, H., Mills, C., Kang, D., Thomas, P.D., 2017. PANTHER version 11: expanded annotation data from Gene Ontology and Reactome pathways, and data analysis tool enhancements. Nucleic Acids Res. 45, D18–D189.
Mitchell, A.L., Attwood, T.K., Babbitt, P.C., Blum, M., Bork, P., Bridge, A., Brown, S.D., Chang, H.Y., El-Gebali, S., Fraser, M.I., Gough, J., Haft, D.R., Huang, H., Letunic, I., Lopez, R., Luciani, A., Madeira, F., Marchler-Bauer, A., Mi, H., Natale, D.A., Necci, M., Nuka, G., Orengo, C., Pandurangan, A.P., Paysan-Lafosse, T., Pesseat, S., Potter, S.C., Qureshi, M.A., Rawlings, N.D., Redaschi, N., Richardson, L.J., Rivoire, C., Salazar, G.A., Sangrador-Vegas, A., Sigrist, C.J.A., Sillitoe, I., Sutton, G.G., Thanki, N., Thomas, P.D., Tosatto, S.C.E., Yong, S.Y., Finn, R.D., 2019. InterPro in 2019: improving coverage, classification and access to protein sequence annotations. Nucleic Acids Res. 47, D351–D360.
Mitchell, G., Isberg, R.R., 2017. Innate immunity to intracellular pathogens: balancing microbial elimination and inflammation. Cell Host Microbe 22, 166–175.
Mohapatra, A., Parida, S., Mohanty, J., Sahoo, P.K., 2019. Identification and functional characterization of a g-type lysozyme gene of *Labeo rohita*, an Indian major carp species. Dev. Comp. Immunol. 92, 87–98.
Myllymäki, H., Bäuerlein, C.A., Rämet, M., 2016. The zebrafish breathes new Life into the study of tuberculosis. Front. Immunol. 7, 196.
Myllymäki, H., Niskanen, M., Luukinen, H., Parikka, M., Rämet, M., 2018. Identification of protective postexposure mycobacterial vaccine antigens using an immunosuppression-based reactivation model in the zebrafish. Dis. Model Mech. 11. https://doi.org/10.1242/dmm.033175.
Myllymäki, H., Niskanen, M., Oksanen, K.E., Rämet, M., 2015. Animal models in tuberculosis research – where is the beef? Expert Opin. Drug Discov. 10, 871–883.
Nüsslein-Volhard, C., Dahm, R., 2002. Zebrafish. Oxford University Press, Oxford, New York.
O'Garra, A., Redford, P.S., McNab, F.W., Bloom, C.I., Wilkinson, R.J., Berry, M.P., 2013. The immune response in tuberculosis. Annu. Rev. Immunol. 31, 475–527.
Ojanen, M.J.T., Uusi-Mäkelä, M.I.E., Harjula, S.E., Saralahti, A.K., Oksanen, K.E., Kähkönen, N., Määttä, J.A.E., Hytönen, V.P., Pesu, M., Rämet, M., 2019. Intelectin 3 is dispensable for resistance against a mycobacterial infection in zebrafish (Danio rerio). Sci. Rep. 9, 995.
Oksanen, K.E., Halfpenny, N.J., Sherwood, E., Harjula, S.K., Hammarén, M.M., Ahava, M.J., Pajula, E.T., Lahtinen, M.J., Parikka, M., Rämet, M., 2013. An adult zebrafish model for preclinical tuberculosis vaccine development. Vaccine 31, 5202–5209.
Parikka, M., Hammarén, M.M., Harjula, S.K., Halfpenny, N.J., Oksanen, K.E., Lahtinen, M.J., Pajula, E.T., Iivanainen, A., Pesu, M., Rämet, M., 2012. *Mycobacterium marinum* causes a latent infection that can be reactivated by gamma irradiation in adult zebrafish. PLoS Pathog. 8, e1002944.
Peters, W., Scott, H.M., Chambers, H.F., Flynn, J.L., Charo, I.F., Ernst, J.D., 2001. Chemokine receptor 2 serves an early and essential role in resistance to *Mycobacterium tuberculosis*. Proc. Natl. Acad. Sci. U.S.A. 98, 7958–7963.
Peyron, P., Vaubourgeix, J., Poquet, Y., Levillain, F., Botanch, C., Bardou, F., Daffe, M., Emile, J.F., Marchou, B., Cardona, P.J., de Chastellier, C., Altare, F., 2008. Foamy macrophages from tuberculous patients' granulomas constitute a nutrient-rich reservoir for *M. tuberculosis* persistence. PLoS Pathog. 4, e1000204.
Piantedosi, R., Ghyselinck, N., Blaner, W.S., Vogel, S., 2005. Cellular retinol-binding protein type III is needed for retinoid incorporation into milk. J. Biol. Chem. 280, 24286–24292.
Poliani, P.L., Kisand, K., Marrella, V., Ravanini, M., Notarangelo, L.D., Villa, A., Peterson, P., Facchetti, F., 2010. Human peripheral lymphoid tissues contain autoimmune regulator-expressing dendritic cells. Am. J. Pathol. 176, 1104–1112.
Quesada-García, A., Valdehita, A., Kropf, C., Casanova-Nakayama, A., Segner, H., Navas, J.M., 2014. Thyroid signaling in immune organs and cells of the teleost fish rainbow trout (*Oncorhynchus mykis*). Fish Shellfish Immunol. 38, 166–174.
Rådmark, O., Werz, O., Steinhilber, D., Samuelsson, B., 2015. 5-Lipoxygenase, a key enzyme for leukotriene biosynthesis in health and disease. Biochim. Biophys. Acta 1851, 331–339.
Renshaw, S.A., Trede, N.S., 2012. A model 450 million years in the making: zebrafish and vertebrate immunity. Dis. Model Mech. 5, 38–47.
Rosendahl, A., Pardali, E., Speletas, M., Ten Dijke, P., Heldin, C.H., Sideras, P., 2002. Activation of bone morphogenetic protein/Smad signaling in bronchial epithelial cells during airway inflammation. Am. J. Respir. Cell Mol. Biol. 27, 160–169.
Rotman, J., van Gils, W., Butler, D., Spaink, H.P., Meijer, A.H., 2011. Rapid screening of innate immune gene expression in zebrafish using reverse transcription - multiplex ligation-dependent probe amplification. BMC Res. Notes 4, 19–196.
Rougeot, J., Torraca, V., Zakrzewska, A., Kanwal, Z., Jansen, H.J., Sommer, F., Spaink, H.P., Meijer, A.H., 2019. RNAseq profiling of leukocyte populations in zebrafish larvae reveals a *cxcl11* chemokine gene as a marker of macrophage polarization during mycobacterial infection. Front. Immunol. 10, 832.
Rougeot, J., Zakrzewska, A., Kanwal, Z., Jansen, H.J., Spaink, H.P., Meijer, A.H., 2014. RNA sequencing of FACS-sorted immune cell populations from zebrafish infection models to identify cell specific responses to intracellular pathogens. Methods Mol. Biol. 1197, 261–274.
Rounioja, S., Saralahti, A., Rantala, L., Parikka, M., Henriques-Normark, B., Silvennoinen, O., Rämet, M., 2012. Defense of zebrafish embryos against *Streptococcus pneumoniae* infection is dependent on the phagocytic activity of leukocytes. Dev. Comp. Immunol. 36, 342–348.
Russell, D.G., Cardona, P.J., Kim, M.J., Allain, S., Altare, F., 2009. Foamy macrophages and the progression of the human tuberculosis granuloma. Nat. Immunol. 10, 943–948.
Samuelsson, B., 1983. Leukotrienes: mediators of immediate hypersensitivity reactions and inflammation. Science 220, 568–575.
Shih, H.Y., Hsu, S.Y., Ouyang, P., Lin, S.J., Chou, T.Y., Chiang, M.C., Cheng, Y.C., 2017. Bmp5 regulates neural crest cell survival and proliferation via two different signaling pathways. Stem Cells 35, 1003–1014.
Sigrist, C.J., de Castro, E., Cerutti, L., Cuche, B.A., Hulo, N., Bridge, A., Bougueleret, L., Xenarios, I., 2013. New and continuing developments at PROSITE. Nucleic Acids Res. 41, 344.
Song, H.D., Sun, X.J., Deng, M., Zhang, G.W., Zhou, Y., Wu, X.Y., Sheng, Y., Chen, Y., Ruan, Z., Jiang, C.L., Fan, H.Y., Zon, L.I., Kanki, J.P., Liu, T.X., Look, A.T., Chen, Z., 2004. Hematopoietic gene expression profile in zebrafish kidney marrow. Proc. Natl. Acad. Sci. U.S.A. 101, 16240–16245.
Stephen, L.A., ElMaghloob, Y., McIlwraith, M.J., Yelland, T., Castro Sanchez, P., Roda-Navarro, P., Ismail, S., 2018. The ciliary machinery is repurposed for T cell immune synapse trafficking of LCK. Dev. Cell 47, 12–132 e4.
Stinear, T.P., Seemann, T., Harrison, P.F., Jenkin, G.A., Davies, J.K., Johnson, P.D., Abdellah, Z., Arrowsmith, C., Chillingworth, T., Churcher, C., Clarke, K., Cronin, A., Davis, P., Goodhead, I., Holroyd, N., Jagels, K., Lord, A., Moule, S., Mungall, K., Norbertczak, H., Quail, M.A., Rabbinowitsch, E., Walker, D., White, B., Whitehead, S., Small, P.L., Brosch, R., Ramakrishnan, L., Fischbach, M.A., Parkhill, J., Cole, S.T., 2008. Insights from the complete genome sequence of *Mycobacterium marinum* on the evolution of *Mycobacterium tuberculosis*. Genome Res. 18, 729–741.
Stutz, M.D., Clark, M.P., Doerflinger, M., Pellegrini, M., 2018. *Mycobacterium tuberculosis*: rewiring host cell signaling to promote infection. J. Leukoc. Biol. 103, 259–268.
Sullivan, B.M., Jobe, O., Lazarevic, V., Vasquez, K., Bronson, R., Glimcher, L.H., Kramnik,

I., 2005. Increased susceptibility of mice lacking T-bet to infection with *Mycobacterium tuberculosis* correlates with increased IL-10 and decreased IFN-gamma production. J. Immunol. 175, 4593–4602.
Swaim, L.E., Connolly, L.E., Volkman, H.E., Humbert, O., Born, D.E., Ramakrishnan, L., 2006. *Mycobacterium marinum* infection of adult zebrafish causes caseating granulomatous tuberculosis and is moderated by adaptive immunity. Infect. Immun. 74, 6108–6117.
Tang, J., Yam, W.C., Chen, Z., 2016. *Mycobacterium tuberculosis* infection and vaccine development. Tuberculosis 98, 30–41.
Tang, R., Dodd, A., Lai, D., McNabb, W.C., Love, D.R., 2007. Validation of zebrafish (*Danio rerio*) reference genes for quantitative real-time RT-PCR normalization. Acta Biochim. Biophys. Sin. 39, 384–390.
The Gene Ontology Consortium, 2019. The gene ontology Resource: 20 years and still GOing strong. Nucleic Acids Res. 47, D33–D338.
Tobin, D.M., Vary Jr., J.C., Ray, J.P., Walsh, G.S., Dunstan, S.J., Bang, N.D., Hagge, D.A., Khadge, S., King, M.C., Hawn, T.R., Moens, C.B., Ramakrishnan, L., 2010. The *lta4h* locus modulates susceptibility to mycobacterial infection in zebrafish and humans. Cell 140, 717–730.
Tobin, D.M., Roca, F.J., Oh, S.F., McFarland, R., Vickery, T.W., Ray, J.P., Ko, D.C., Zou, Y., Bang, N.D., Chau, T.T., Vary, J.C., Hawn, T.R., Dunstan, S.J., Farrar, J.J., Thwaites, G.E., King, M.C., Serhan, C.N., Ramakrishnan, L., 2012. Host genotype-specific therapies can optimize the inflammatory response to mycobacterial infections. Cell 148, 434–446.
Torraca, V., Cui, C., Boland, R., Bebelman, J.P., van der Sar, A.M., Smit, M.J., Siderius, M., Spaink, H.P., Meijer, A.H., 2015. The CXCR3-CXCL11 signaling axis mediates macrophage recruitment and dissemination of mycobacterial infection. Dis. Model Mech. 8, 253–269.
van Dam, H., Castellazzi, M., 2001. Distinct roles of Jun : fos and Jun : ATF dimers in oncogenesis. Oncogene 20, 2453–2464.
van der Sar, A.M., Spaink, H.P., Zakrzewska, A., Bitter, W., Meijer, A.H., 2009. Specificity of the zebrafish host transcriptome response to acute and chronic mycobacterial infection and the role of innate and adaptive immune components. Mol. Immunol. 46, 2317–2332.
van der Vaart, M., Spaink, H.P., Meijer, A.H., 2012. Pathogen recognition and activation of the innate immune response in zebrafish. Adv. Hematol. 2012, 159807.
Veneman, W.J., de Sonneville, J., van der Kolk, K.J., Ordas, A., Al-Ars, Z., Meijer, A.H., Spaink, H.P., 2015. Analysis of RNAseq datasets from a comparative infectious disease zebrafish model using GeneTiles bioinformatics. Immunogenetics 67, 135–147.
Verrall, A.J., Netea, M.G., Alisjahbana, B., Hill, P.C., van Crevel, R., 2014. Early clearance of *Mycobacterium tuberculosis*: a new frontier in prevention. Immunology 141, 506–513.
Vladimer, G.I., Weng, D., Paquette, S.W., Vanaja, S.K., Rathinam, V.A., Aune, M.H., Conlon, J.E., Burbage, J.J., Proulx, M.K., Liu, Q., Reed, G., Mecsas, J.C., Iwakura, Y., Bertin, J., Goguen, J.D., Fitzgerald, K.A., Lien, E., 2012. The NLRP12 inflammasome recognizes *Yersinia pestis*. Immunity 37, 96–107.
Volkman, H.E., Clay, H., Beery, D., Chang, J.C., Sherman, D.R., Ramakrishnan, L., 2004. Tuberculous granuloma formation is enhanced by a mycobacterium virulence determinant. PLoS Biol. 2, e367.
Walters, K.B., Green, J.M., Surfus, J.C., Yoo, S.K., Huttenlocher, A., 2010. Live imaging of neutrophil motility in a zebrafish model of WHIM syndrome. Blood 116, 2803–2811.
Walton, E.M., Cronan, M.R., Beerman, R.W., Tobin, D.M., 2015. The macrophage-specific promoter *mfap4* allows live, long-term analysis of macrophage behavior during mycobacterial infection in zebrafish. PLoS One 10, e0138949.
Wawrocki, S., Druszczynska, M., 2017. Inflammasomes in *Mycobacterium tuberculosis*-driven immunity. Can. J. Infect Dis. Med. Microbiol. 2309478 2017.
Wheelwright, M., Kim, E.W., Inkeles, M.S., De Leon, A., Pellegrini, M., Krutzik, S.R., Liu, P.T., 2014. All-trans retinoic acid-triggered antimicrobial activity against *Mycobacterium tuberculosis* is dependent on NPC2. J. Immunol. 192, 2280–2290.
Wienholds, E., Schulte-Merker, S., Walderich, B., Plasterk, R.H., 2002. Target-selected inactivation of the zebrafish *rag1* gene. Science 297, 99–102.
Wilburn, K.M., Fieweger, R.A., VanderVen, B.C., 2018. Cholesterol and fatty acids grease the wheels of *Mycobacterium tuberculosis* pathogenesis. Pathog. Dis. 76. https://doi.org/10.1093/femspd/fty021.
World Health Organization, 2018. Global tuberculosis report 2018. https://www.who.int/tb/publications/global_report/en/, Accessed date: 12 September 2019.
Yim, J.J., Selvaraj, P., 2010. Genetic susceptibility in tuberculosis. Respirology 15, 241–256.
Zerbino, D.R., Achuthan, P., Akanni, W., Amode, M.R., Barrell, D., Bhai, J., Billis, K., Cummins, C., Gall, A., Giron, C.G., Gil, L., Gordon, L., Haggerty, L., Haskell, E., Hourlier, T., Izuogu, O.G., Janacek, S.H., Juettemann, T., To, J.K., Laird, M.R., Lavidas, I., Liu, Z., Loveland, J.E., Maurel, T., McLaren, W., Moore, B., Mudge, J., Murphy, D.N., Newman, V., Nuhn, M., Ogeh, D., Ong, C.K., Parker, A., Patricio, M., Riat, H.S., Schuilenburg, H., Sheppard, D., Sparrow, H., Taylor, K., Thormann, A., Vullo, A., Walts, B., Zadissa, A., Frankish, A., Hunt, S.E., Kostadima, M., Langridge, N., Martin, F.J., Muffato, M., Perry, E., Ruffier, M., Staines, D.M., Trevanion, S.J., Aken, B.L., Cunningham, F., Yates, A., Flicek, P., 2018. Ensemble 2018. Nucleic Acids Res. 46, D754–D761.
Zuccolo, J., Bau, J., Childs, S.J., Goss, G.G., Sensen, C.W., Deans, J.P., 2010. Phylogenetic analysis of the *MS4A* and *TMEM176* gene families. PLoS One 5, e9369.

Characterization of immune response against *Mycobacterium marinum* infection in the main hematopoietic organ of adult zebrafish (*Danio rerio*)

Sanna-Kaisa E. Harjula, Anni K. Saralahti, Markus J.T. Ojanen, Tommi Rantapero, Meri I.E. Uusi-Mäkelä, Matti Nykter, Olli Lohi, Mataleena Parikka, Mika Rämet*

***Corresponding author:** Correspondence to Mika Rämet, E-mail: mika.ramet@tuni.fi, Faculty of Medicine and Health Technology, FI-33014 Tampere University, Finland

Appendix A. Supplementary material

Supplementary Figures

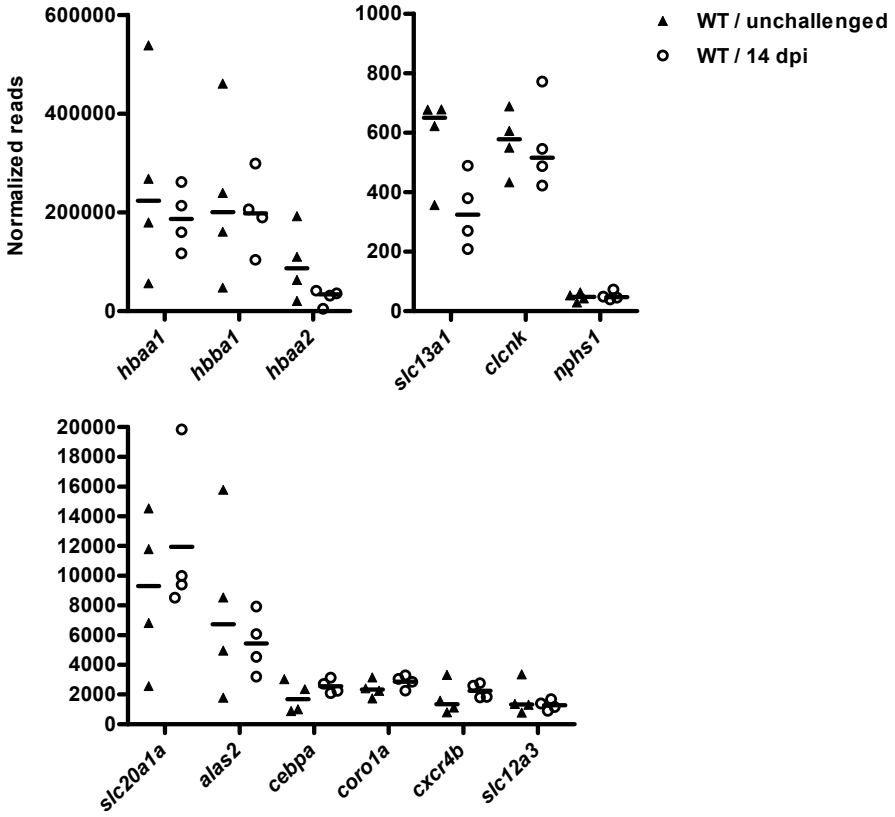

Supplementary Figure 1 The expression of selected genes in the zebrafish kidney. The whole-genome level transcriptome analysis revealed expression of several genes known to be expressed in kidney and blood cells. Normalized read counts in unchallenged adult WT (wild type) zebrafish and at 14 days post a low-dose (5–9 CFU, colony forming units) infection (n = 4 in both groups) are presented as a scatter dot plot and median. Note the different scales of the y-axes.

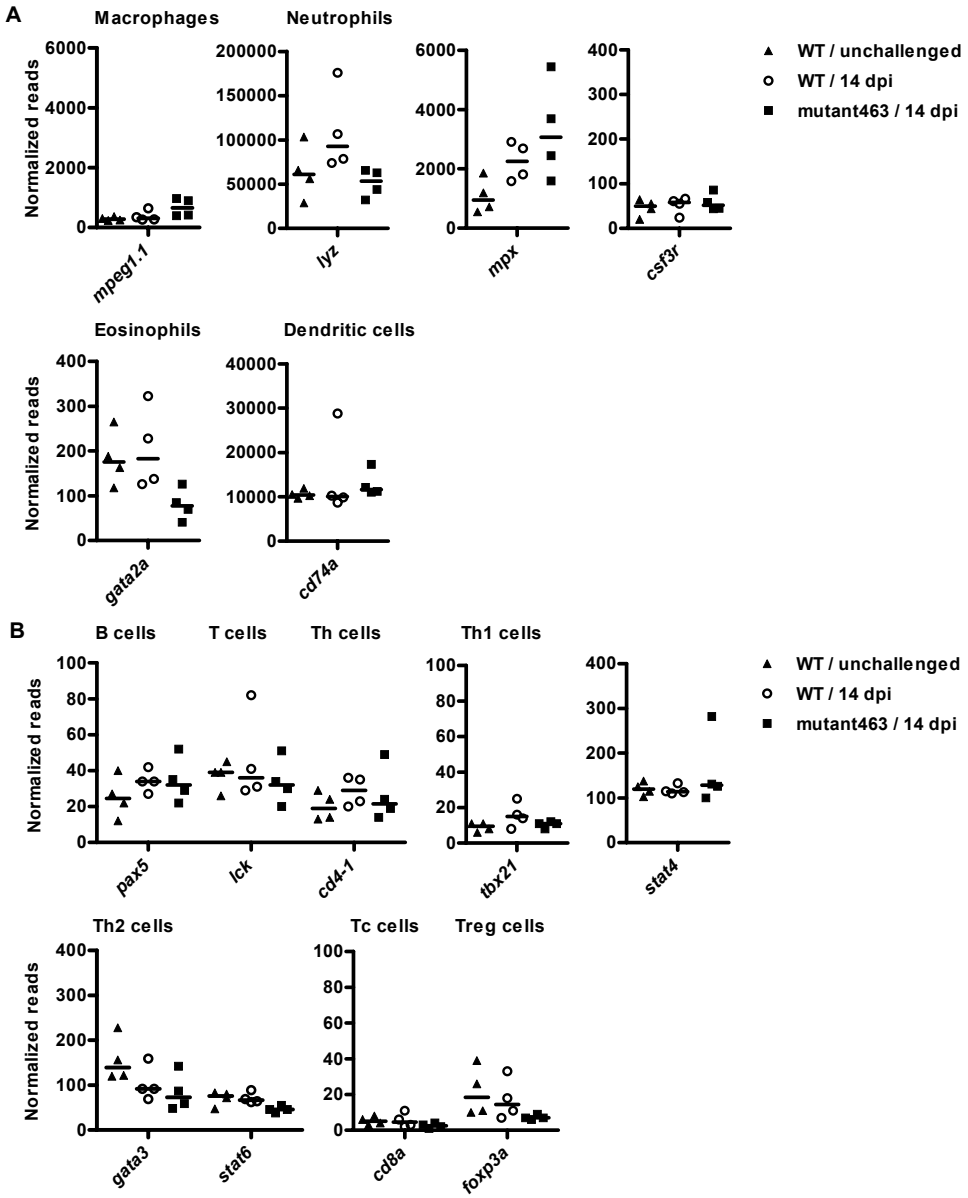

Supplementary Figure 2 The expression of selected immune cell markers in zebrafish kidney. The whole-genome level transcriptome analysis revealed no significant differences in the expression of **(A)** innate or **(B)** adaptive immune cell markers between adult WT (wild type) zebrafish at 14 days post a low-dose (5–9 CFU, colony forming units) infection and unchallenged WT zebrafish or

between the WT and mutant463 zebrafish at 14 dpi (n = 4 in each group). The normalized read counts are presented as a scatter dot plot and median. Note the different scales of the y-axes.

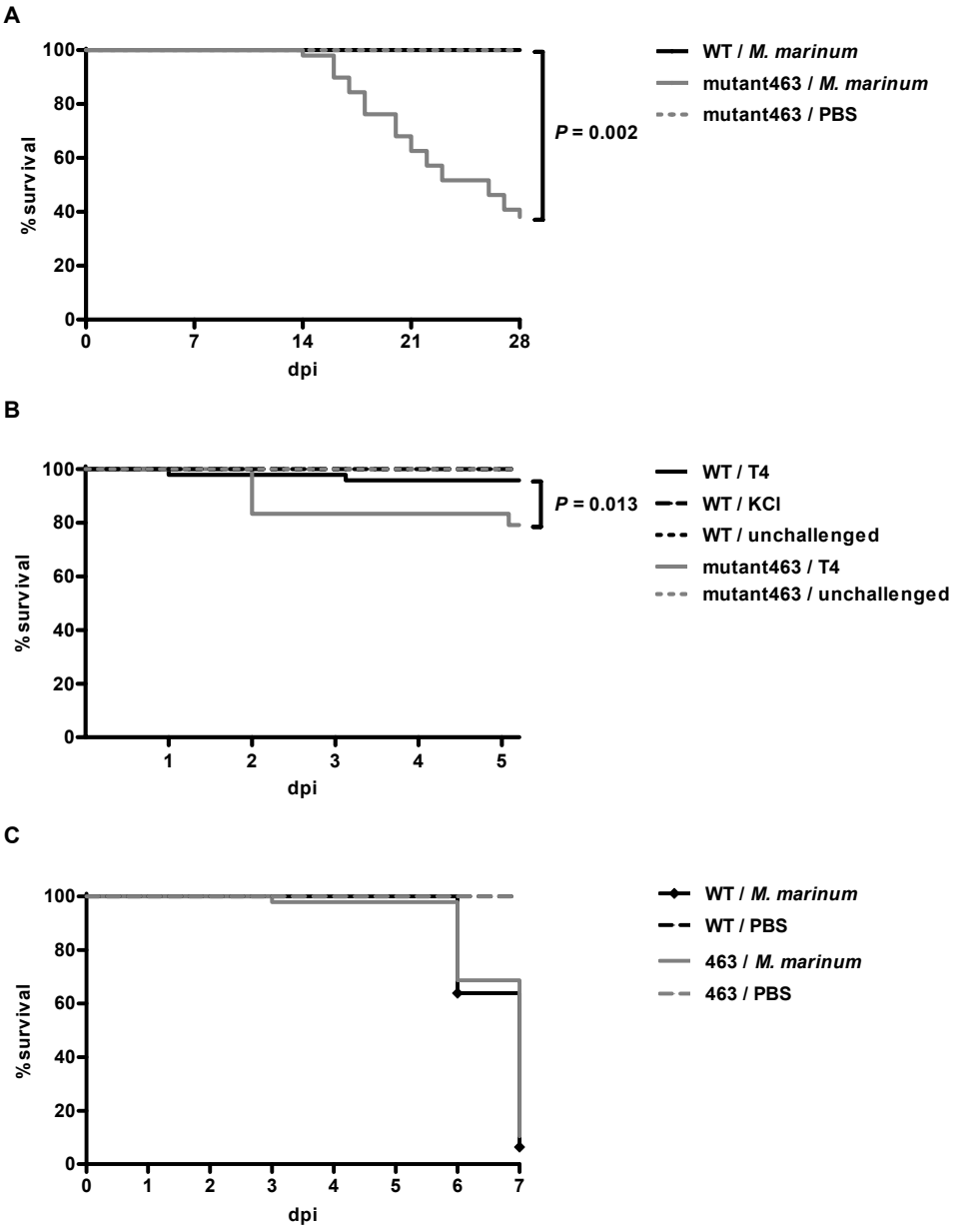

Supplementary Figure 3 The survival of zebrafish after *M. marinum* and *S. pneumoniae* challenge. **(A)** The survival phenotype of the *M. marinum* infected mutant463 fish during the RNA sequencing experiment is consistent with the phenotype detected in the screen. mutant463 adult zebrafish ($n = 58$) and WT (wild-type) controls ($n = 30$) were followed for four weeks post a low-dose infection (5–9

CFU, colony forming units). mutant463 zebrafish (n = 17) injected with PBS were included as controls. **(B)** mutant463 embryos showed only mildly impaired survival compared to WT in a *S. pneumoniae* infection. mutant463 and WT (wild type) (n = 24 and n = 48, respectively) embryos were infected with 220–328 CFU (colony forming units) of *S. pneumoniae* (T4 serotype) at 2 dpf (days post fertilization). WT embryos injected with 0.2 M KCl (n = 24) and unchallenged mutant463 and WT embryos (n = 12) were included as controls. **(C)** The survival of mutant463 embryos is not impaired in *M. marinum* infection compared to WT embryos. mutant463 zebrafish embryos (n = 48) and WT (wild type) embryos (n = 94) were infected with 32–198 CFU of *M. marinum* into the caudal vein at 1 dpf (days post fertilization). mutant463 and WT embryos injected with PBS (n = 22 and n = 57, respectively) were included as controls. The graphs in panels (A) and (B) represent data from one experiment and the graph in panel (C) from two experiments. The survival data is presented as a Kaplan-Meier survival curve. A log-rank (Mantel-Cox) test was used to perform the statistical comparison of differences. dpi, days post infection.

Supplementary Tables

Supplementary Table 1 qPCR primers used for gene expression analysis.

Gene	Ensembl gene ID	Human ortholog (HGNC)	Sequence 5'-3'	Reference
eef1a1l1 (ef1a)	ENSDARG00000020850	-	**F** CTGGAGGCCAGCTCAAACAT **R** ATCAAGAAGAGTAGTACCGCTAGCATTAC	(Tang et al., 2007)
fabp6	ENSDARG00000044566	*FABP6*	**F** CTGCAAACTGATCGGTATCC **R** GCTCTCTTTGCCTACGATGA	-
scd	ENSDARG00000033662	*SCD*	**F** ATGGCCTTCCAGAATGACAT **R** CTAGTTTGCGTCCTCTCTCG	-
unc119b	ENSDARG00000044362	*UNC119*	**F** CATCCCCATCAATAACTTCC **R** CTCACGAATGAGATCCTCAG	-
si:ch211-236p5.3	ENSDARG00000086418	-	**F** GGACAAGCTCAACATGGATA **R** CTGCTTCATTGTCACAAGTG	-

[1] Zebrafish gene names and qPCR primer sequences are listed accompanied with the Ensembl identification codes and the names of the orthologous genes in humans. HGNC, HUGO Gene Nomenclature Committee.

Supplementary Table 2 Enriched processes from gene ontology analysis, downregulated protein coding genes. The Gene Ontology Consortium Enrichment analysis was performed using downregulated genes as a target and all the protein genes in the RNA sequencing data as a background list. *P* values were calculated with Fisher's exact test and Bonferroni correction was used for multiple testing. $P < 0.05$ was considered significant.

GO term	Description	*P* value
GO:0065005	protein-lipid complex assembly	9.70E-08
GO:0010873	positive regulation of cholesterol esterification	9.70E-08
GO:0010872	regulation of cholesterol esterification	9.70E-08
GO:0045940	positive regulation of steroid metabolic process	9.70E-08
GO:0034380	high-density lipoprotein particle assembly	9.70E-08
GO:0034377	plasma lipoprotein particle assembly	9.70E-08
GO:0071827	plasma lipoprotein particle organization	1.49E-07
GO:0071825	protein-lipid complex subunit organization	1.49E-07
GO:0034372	very-low-density lipoprotein particle remodeling	1.49E-07
GO:0034370	triglyceride-rich lipoprotein particle remodeling	1.49E-07
GO:0034369	plasma lipoprotein particle remodeling	1.49E-07
GO:0034368	protein-lipid complex remodeling	1.49E-07
GO:0097006	regulation of plasma lipoprotein particle levels	1.49E-07
GO:0043691	reverse cholesterol transport	1.49E-07
GO:0034367	protein-containing complex remodeling	2.23E-07
GO:0019433	triglyceride catabolic process	2.23E-07
GO:0019218	regulation of steroid metabolic process	3.25E-07
GO:0033700	phospholipid efflux	3.25E-07
GO:0033344	cholesterol efflux	8.86E-07
GO:0032374	regulation of cholesterol transport	8.86E-07
GO:0032371	regulation of sterol transport	8.86E-07
GO:0046464	acylglycerol catabolic process	8.86E-07
GO:0046461	neutral lipid catabolic process	8.86E-07
GO:0046889	positive regulation of lipid biosynthetic process	1.19E-06
GO:0006695	cholesterol biosynthetic process	1.59E-06
GO:0032368	regulation of lipid transport	1.59E-06
GO:1902653	secondary alcohol biosynthetic process	2.08E-06
GO:0045834	positive regulation of lipid metabolic process	3.46E-06
GO:0042632	cholesterol homeostasis	6.87E-06
GO:0055092	sterol homeostasis	6.87E-06
GO:1905952	regulation of lipid localization	6.87E-06
GO:0006641	triglyceride metabolic process	1.54E-05
GO:0046503	glycerolipid catabolic process	1.54E-05
GO:0030301	cholesterol transport	2.21E-05
GO:0015918	sterol transport	2.63E-05

GO:0046890	regulation of lipid biosynthetic process	4.30E-05
GO:0016126	sterol biosynthetic process	4.30E-05
GO:0006639	acylglycerol metabolic process	1.34E-04
GO:0006638	neutral lipid metabolic process	1.34E-04
GO:0008203	cholesterol metabolic process	1.95E-04
GO:0055088	lipid homeostasis	2.19E-04
GO:1902652	secondary alcohol metabolic process	2.47E-04
GO:0015850	organic hydroxy compound transport	4.75E-04
GO:0019216	regulation of lipid metabolic process	5.26E-04
GO:0016125	sterol metabolic process	7.07E-04
GO:0006694	steroid biosynthetic process	9.36E-04
GO:0015914	phospholipid transport	2.55E-03
GO:0015748	organophosphate ester transport	3.43E-03
GO:0046165	alcohol biosynthetic process	3.68E-03
GO:0006869	lipid transport	4.76E-03
GO:0010876	lipid localization	5.53E-03
GO:0008202	steroid metabolic process	5.94E-03
GO:0016042	lipid catabolic process	8.68E-03
GO:0042157	lipoprotein metabolic process	1.31E-02
GO:0044242	cellular lipid catabolic process	1.31E-02
GO:1901617	organic hydroxy compound biosynthetic process	2.36E-02
GO:0006032	chitin catabolic process	2.59E-02
GO:0006030	chitin metabolic process	4.71E-02

Supplementary Table 3 The protein coding genes downregulated in mycobacterial infection in adult zebrafish kidney at 14 dpi (days post infection). The table shows the fold change in expression in *M. marinum* (5–9 CFU, colony forming units) infected zebrafish compared to unchallenged fish (n = 4 in both groups). Fold change represents the fold change between the group medians. The table includes only the genes with at least two samples with ≥ 20 normalized reads in the unchallenged control group and the genes whose expression was reduced at least 3.0-fold (calculated both with the DEseq-tool and from the medians). The fold changes are presented as the quotient of medians when the divisor is zero.

Gene symbol	Gene name/description	Ensembl gene ID	Fold change (median)
Immune system			
ptx3b	*pentraxin 3, long b*	ENSDARG00000079515	-6.0
masp1	*mannan-binding lectin serine peptidase 1*	ENSDARG00000068726	-5.6
enpp1	*ectonucleotide pyrophosphatase/ phosphodiesterase 1*	ENSDARG00000005789	-4.0
pdgfrb	*platelet-derived growth factor receptor, beta polypeptide*	ENSDARG00000100897	-3.2
Lipid metabolism and transport			
apoa4b.2	*apolipoprotein A-IV b, tandem duplicate 2*	ENSDARG00000020866	-26.4
apoa4b.1	*apolipoprotein A-IV b, tandem duplicate 1*	ENSDARG00000040298	-19.2
apoea	*apolipoprotein Ea*	ENSDARG00000102004	-15.1
apoa4b.2	*apolipoprotein A-IV b, tandem duplicate 2*	ENSDARG00000094929	-15.1
apobb.1	*apolipoprotein Bb, tandem duplicate 1*	ENSDARG00000022767	-14.4
zgc:162608	*zgc:162608*	ENSDARG00000069375	-14.0
tmem86b	*transmembrane protein 86B*	ENSDARG00000038296	-11.3
pla2g12b	*phospholipase A2, group XIIB*	ENSDARG00000015662	-7.5
apoa1a	*apolipoprotein A-Ia*	ENSDARG00000012076	-7.1
sccpdha	*saccharopine dehydrogenase a*	ENSDARG00000075766	-4.4
Other metabolic process			
chia.3	*chitinase, acidic.3*	ENSDARG00000009612	-73.4
chia.1	*chitinase, acidic.1*	ENSDARG00000100635	-67.4
chia.2	*chitinase, acidic.2*	ENSDARG00000099185	-49.4
CSDC2 (1 of many)	*cold shock domain containing C2, RNA binding b*	ENSDARG00000100167	-41.0
zgc:153968	*zgc:153968*	ENSDARG00000061858	-33.0
cyp2x8	*cytochrome P450, family 2, subfamily X, polypeptide 8*	ENSDARG00000043997	-18.8
si:ch211-284e20.8	*fetuin-B*	ENSDARG00000070918	-17.5
ahr1a	*aryl hydrocarbon receptor 1a*	ENSDARG00000020046	-10.0
sp5a	*sp5 transcription factor a*	ENSDARG00000076571	-8.7

tdrd12	*tudor domain containing 12*	ENSDARG00000075217	-7.3
urahb	*urate (5-hydroxyiso-) hydrolase b*	ENSDARG00000089331	-7.1
mep1b	*meprin A, beta*	ENSDARG00000037533	-6.2
acsl5	*acyl-CoA synthetase long-chain family member 5*	ENSDARG00000075931	-6.1
aco1	*aconitase 1, soluble*	ENSDARG00000026376	-5.9
tfap2e	*transcription factor AP-2 epsilon*	ENSDARG00000008861	-5.5
selenop2	*selenoprotein P2*	ENSDARG00000079727	-5.4
tdo2b	*tryptophan 2,3-dioxygenase b*	ENSDARG00000023176	-4.8
F7	*coagulation factor VII, like*	ENSDARG00000100782	-4.7
b3gnt7	*UDP-GlcNAc:betaGal beta-1,3-N-acetylglucosaminyltransferase 7*	ENSDARG00000038489	-4.5
aldh3a2b	*aldehyde dehydrogenase 3 family, member A2b*	ENSDARG00000029381	-4.4
fbxo15	*F-box protein 15*	ENSDARG00000016897	-4.1
pias4b	*protein inhibitor of activated STAT, 4b*	ENSDARG00000042215	-4.1
ft1	*alpha(1,3)fucosyltransferase gene 1*	ENSDARG00000059056	-4.0
galnt9	*polypeptide N-acetylgalactosaminyltransferase 9*	ENSDARG00000006832	-3.9
gpx3	*glutathione peroxidase 3*	ENSDARG00000043342	-3.9
cremb	*CAMP responsive element modulator b*	ENSDARG00000102899	-3.7
ENSDARG00000104218	*CABZ01056821.1*	ENSDARG00000104218	-3.5
tbxtb	*T-box transcription factor Tb*	ENSDARG00000039806	-3.5
hnf4b	*hepatic nuclear factor 4, beta*	ENSDARG00000104742	-3.5
nme4	*NME/NM23 nucleoside diphosphate kinase 4*	ENSDARG00000088390	-3.5
si:dkey-91i10.3	*sterol 26-hydroxylase, mitochondrial*	ENSDARG00000057262	-3.4
ldhbb	*lactate dehydrogenase Bb*	ENSDARG00000071076	-3.3
asb11	*ankyrin repeat and SOCS box containing 11*	ENSDARG00000056561	-3.3
ripply2	*ripply transcriptional repressor 2*	ENSDARG00000070535	-3.1
inhbab	*inhibin subunit beta Ab*	ENSDARG00000024759	-3.1
si:dkeyp-118b1.2	*si:dkeyp-118b1.2*	ENSDARG00000079131	-3.0

Other localization process

sst1.1	*somatostatin 1, tandem duplicate 1*	ENSDARG00000040799	-19.7
aqp8a.2	*aquaporin 8a, tandem duplicate 2*	ENSDARG00000071592	-10.0
CABZ01111515.1	*CABZ01111515.1*	ENSDARG00000098922	-7.2
slc15a1b	*solute carrier family 15 (oligopeptide transporter), member 1b*	ENSDARG00000044528	-5.5
si:dkey-192p21.6	*si:dkey-192p21.6*	ENSDARG00000091212	-4.2
shisa9b	*shisa family member 9b*	ENSDARG00000052642	-3.8
aqp3b	*aquaporin 3b*	ENSDARG00000069518	-3.2
syt9a	*synaptotagmin IXa*	ENSDARG00000003994	-3.1

Signaling and regulation

myl7	*myosin, light chain 7, regulatory*	ENSDARG00000019096	-12:0
opn8b	*opsin 8, group member b*	ENSDARG00000079045	-10.3
zgc:172079	*zgc:172079*	ENSDARG00000105644	-8.8

gphb5	*glycoprotein hormone beta 5*	ENSDARG00000027472	-7.7
rgs7a	*regulator of G protein signaling 7a*	ENSDARG00000016584	-4.9
gna15.3	*guanine nucleotide binding protein (G protein), alpha 15 (Gq class), tandem duplicate 3*	ENSDARG00000056654	-4.6
lurap1	*leucine rich adaptor protein 1*	ENSDARG00000044406	-4.5
tbxa2r	*thromboxane A2 receptor*	ENSDARG00000104717	-3.3
pid1	*phosphotyrosine interaction domain containing 1*	ENSDARG00000098984	-3.1
Other process			
fabp1b.1	*fatty acid binding protein 1b, tandem duplicate 1*	ENSDARG00000059227	-45.8
zgc:172053	*zgc:172053*	ENSDARG00000038321	-25.7
zgc:171534	*zgc:171534*	ENSDARG00000105265	-4.6
cnnm4b	*cyclin and CBS domain divalent metal cation transport mediator 4b*	ENSDARG00000074309	-4.5
SYNDIG1	*synapse differentiation inducing 1*	ENSDARG00000100751	-4.3
tnni4b.1	*troponin I4b, tandem duplicate 1*	ENSDARG00000092999	-4.1
ccdc170	*coiled-coil domain containing 170*	ENSDARG00000016161	-4.1
CABZ01057159.1	*CABZ01057159.1*	ENSDARG00000102894	-3.4
chtopb	*chromatin target of PRMT1b*	ENSDARG00000070430	-3.1
zgc:174904	*zgc:174904*	ENSDARG00000059049	-3.1
Unknown process			
LO018612.1		ENSDARG00000102208	-45:0
si:dkey-182g1.6	*si:dkey-182g1.6*	ENSDARG00000055831	-11:0
FO393424.3	*transmembrane and immunoglobulin domain-containing protein 1-like*	ENSDARG00000108332	-10:0
si:ch211-125e6.5	*ladderlectin-like*	ENSDARG00000069381	-82.0
si:dkey-207m2.4	*si:dkey-207m2.4*	ENSDARG00000100654	-52.7
si:ch211-133n4.10	*si:ch211-133n4.10*	ENSDARG00000063613	-45.0
si:ch211-225b7.5	*si:ch211-225b7.5*	ENSDARG00000097453	-30.7
wu:fa56d06		ENSDARG00000103342	-26.5
zgc:194887	*zgc:194887*	ENSDARG00000098586	-23.0
si:ch211-230g14.6	*si:ch211-230g14.6*	ENSDARG00000103737	-19.5
si:ch211-155m12.1	*si:ch211-155m12.1*	ENSDARG00000101642	-10.7
tdrd6	*tudor domain containing 6*	ENSDARG00000070052	-10.3
si:ch211-251f6.6	*fish-egg lectin-like*	ENSDARG00000053448	-7.8
igfals	*insulin-like growth factor binding protein, acid labile subunit*	ENSDARG00000037836	-5.6
si:ch211-264f5.2	*si:ch211-264f5.2*	ENSDARG00000078547	-5.6
vwa3a	*von Willebrand factor A domain containing 3A*	ENSDARG00000087210	-5.4
si:ch211-130h14.4	*si:ch211-130h14.4*	ENSDARG00000094016	-4.6
si:ch211-152c8.5	*protein phosphatase 1 regulatory subunit 3G*	ENSDARG00000104576	-4.4
si:ch211-222n4.2	*coiled-coil domain containing 74B*	ENSDARG00000093026	-4.1
CABZ01011067.1	*CABZ01011067.1*	ENSDARG00000105027	-3.6

si:ch73-364h19.1	*si:ch73-364h19.1*	ENSDARG00000097523	-3.5
si:dkey-253d23.8	*zinc finger protein 347-like*	ENSDARG00000094427	-3.4
si:ch73-90k17.1	*si:ch73-90k17.1*	ENSDARG00000095463	-3.3
si:ch211-277c7.7	*si:ch211-277c7.7*	ENSDARG00000105348	-3.3
zgc:171687	*zgc:171687*	ENSDARG00000038682	-3.3
cbln13	*cerebellin 13*	ENSDARG00000026904	-3.2
si:ch211-198b3.4	*UPF0573 protein C2orf70 homolog*	ENSDARG00000089110	-3.1
otop2	*otopetrin 2*	ENSDARG00000006522	-3.1

Supplementary Table 4 The non-coding RNAs induced in mycobacterial infection in adult zebrafish kidney at 14 dpi (days post infection). The table shows the fold change in expression in *M. marinum* infected zebrafish compared to unchallenged fish (n = 4 in both groups). Fold change represents the fold change between the group medians. The table includes only the genes with at least two samples with ≥ 20 normalized reads after infection and the genes whose expression was induced at least 3.0-fold (calculated both with the DEseq-tool and from the medians). The fold changes are presented as the quotient of medians when the divisor is zero.

Gene symbol	Biotype	Ensembl gene ID	Fold change (median)
SNORD59	snoRNA	ENSDARG00000081030	27:0
snoU83B	snoRNA	ENSDARG00000083950	26:0
dre-mir-1388	miRNA	ENSDARG00000082246	24:0
SNORA81	snoRNA	ENSDARG00000083986	20:0
CABZ01056516.2	lincRNA	ENSDARG00000108320	19:0
5S_rRNA	rRNA	ENSDARG00000100330	13:0
CABZ01056628.2	lincRNA	ENSDARG00000108742	10:0
FQ790226.1	lincRNA	ENSDARG00000107569	23.0
FO834836.1	lincRNA	ENSDARG00000107210	17.5
CR388132.1	lincRNA	ENSDARG00000097728	13.0
SNORD101	snoRNA	ENSDARG00000081654	11.2
CR352342.2	lincRNA	ENSDARG00000106620	9.0
Vault	misc_RNA	ENSDARG00000084089	6.9
SNORA27	snoRNA	ENSDARG00000084628	6.3
CU459094.3	antisense_RNA	ENSDARG00000095666	6.3
BX957297.2	lincRNA	ENSDARG00000105608	6.1
SNORA35	snoRNA	ENSDARG00000080450	5.8
CABZ01067313.1	lincRNA	ENSDARG00000107603	3.5
ccl34a.4	processed_transcript	ENSDARG00000090873	3.2
U4	snRNA	ENSDARG00000087328	3.0
snoZ30	snoRNA	ENSDARG00000081799	3.0

Supplementary Table 5. The non-coding RNAs downregulated in mycobacterial infection in adult zebrafish kidney at 14 dpi (days post infection). The table shows the fold change in expression in *M. marinum* infected zebrafish compared to unchallenged fish (n = 4 in both groups). Fold change represents the fold change between the group medians. The table includes only the genes with at least two samples with ≥ 20 normalized reads in the unchallenged control group and the genes whose expression was reduced at least 3.0-fold (calculated both with the DEseq-tool and from the medians). The fold changes are presented as the quotient of medians when the divisor is zero.

Gene symbol	Biotype	Ensembl gene ID	Fold change (median)
5S_rRNA	rRNA	ENSDARG00000109195	-26:0
SNORD52	snoRNA	ENSDARG00000084989	-23:0
CABZ01081671.1	lincRNA	ENSDARG00000107132	-22:0
5S_rRNA	rRNA	ENSDARG00000106985	-22:0
5S_rRNA	rRNA	ENSDARG00000108508	-18:0
BX004770.1	processed_transcript	ENSDARG00000093939	-17:0
5S_rRNA	rRNA	ENSDARG00000100831	-12:0
FO834903.1	lincRNA	ENSDARG00000106392	-164.1
CT027832.1	lincRNA	ENSDARG00000108416	-16.9
AL772209.1	lincRNA	ENSDARG00000108851	-8.6
CABZ01043956.2	lincRNA	ENSDARG00000106895	-7.8
FP103005.1	antisense_RNA	ENSDARG00000099852	-7.3
BX005229.1	lincRNA	ENSDARG00000105987	-7.3
BX469930.1	lincRNA	ENSDARG00000092358	-6.0
CU633740.1	lincRNA	ENSDARG00000106006	-5.6
SNORA21	snoRNA	ENSDARG00000080533	-5.3
CR376741.1	processed_transcript	ENSDARG00000095393	-5.3
SNORD49	snoRNA	ENSDARG00000104121	-5.0
BX957270.2	lincRNA	ENSDARG00000107325	-4.6
CU855854.1	antisense_RNA	ENSDARG00000096846	-4.5
dre-let-7b	miRNA	ENSDARG00000081807	-4.4
AL954359.1	processed_transcript	ENSDARG00000093646	-4.0
FO904843.1	lincRNA	ENSDARG00000107094	-3.9
CR749763.5	processed_transcript	ENSDARG00000093983	-3.9
CABZ01005013.1	lincRNA	ENSDARG00000107311	-3.9
AL928901.2	lincRNA	ENSDARG00000108929	-3.8
AL845369.2	processed_transcript	ENSDARG00000095523	-3.6
AL954359.2	processed_transcript	ENSDARG00000094423	-3.3
BX640520.3	processed_transcript	ENSDARG00000095363	-3.2
AL845314.1	lincRNA	ENSDARG00000108104	-3.1

Supplementary Table 6. The non-coding RNAs downregulated in mycobacterial infection in mutant463 zebrafish kidney compared to WT (wild type) at 14 dpi (days post infection). The table shows the fold change in expression of genes upregulated in mycobacterial infection between mutant463 and WT zebrafish ($n = 4$ in both groups). Fold change represents the fold change between the group medians. The table includes only the genes with at least two samples with ≥ 20 normalized reads in the WT group and the genes whose expression was reduced at least 3.0-fold (calculated both with the DEseq-tool and from the medians). The fold changes are presented as the quotient of medians when the divisor is zero.

Gene symbol	Biotype	Ensembl gene ID	Fold change (median)
SNORA81	snoRNA	ENSDARG00000083986	-20:0
CR388132.1	lincRNA	ENSDARG00000097728	-13:0
U4	snRNA	ENSDARG00000087328	-11:0
FQ790226.1	lincRNA	ENSDARG00000107569	-115.0
CABZ01056516.2	lincRNA	ENSDARG00000108320	-7.6
CABZ01067313.1	lincRNA	ENSDARG00000107603	-5.8
BX957297.2	lincRNA	ENSDARG00000105608	-3.1
CR352342.2	lincRNA	ENSDARG00000106620	-3.0